MASTERS BY RESEARCH

The influence of hydroclimatic and chemical variability on legacy contamination from historical metal mines.

Jones, Colin

Award date:
2020

Awarding institution:
Bangor University

The influence of hydroclimatic and chemical variability on legacy contamination from historical metal mines.

Colin Edward Jones

2019

Research Project

Bangor University

MScRES – Environmental Sciences

November 2019 University number: 500174854

Declaration and Consent

Details of the Work

I hereby agree to deposit the following item in the digital repository maintained by Bangor University and/or in any other repository authorized for use by Bangor University.

Author Name: Colin Edward Jones

Title: The influence of hydroclimatic and chemical variability on legacy contamination and associated remediation systems.

Supervisor/Department: Dr Graham Bird/School of natural sciences

Funding body (if any): N/A

Qualification/Degree obtained: MScRes Environmental sciences

This item is a product of my own research endeavours and is covered by the agreement below in which the item is referred to as "the Work". It is identical in content to that deposited in the Library, subject to point 4 below.

Non-exclusive Rights

Rights granted to the digital repository through this agreement are entirely non-exclusive. I am free to publish the Work in its present version or future versions elsewhere.

I agree that Bangor University may electronically store, copy or translate the Work to any approved medium or format for the purpose of future preservation and accessibility. Bangor University is not under any obligation to reproduce or display the Work in the same formats or resolutions in which it was originally deposited.

Bangor University Digital Repository

I understand that work deposited in the digital repository will be accessible to a wide variety of people and institutions, including automated agents and search engines via the World Wide Web.

I understand that once the Work is deposited, the item and its metadata may be incorporated into public access catalogues or services, national databases of electronic theses and dissertations such as the British Library's EThOS or any service provided by the National Library of Wales.

Statement 1:

This work has not previously been accepted in substance for any degree and is not being concurrently submitted in candidature for any degree unless as agreed by the University for approved dual awards.

Signed  (candidate)

Date 30/09/2019

Statement 2:

This thesis is the result of my own investigations, except where otherwise stated. Where correction services have been used, the extent and nature of the correction is clearly marked in a footnote(s).

All other sources are acknowledged by footnotes and/or a bibliography.

Signed  (candidate)

Date 30/09/2019

Statement 3:

I hereby give consent for my thesis, if accepted, to be available for photocopying, for inter-library loan and for electronic repositories, and for the title and summary to be made available to outside organisations.

Signed  (candidate)

Date 30/09/2019

Statement 4:

Choose one of the following options

a)	I agree to deposit an electronic copy of my thesis (the Work) in the Bangor University (BU) Institutional Digital Repository, the British Library ETHOS system, and/or in any other repository authorized for use by Bangor University and where necessary have gained the required permissions for the use of third party material.	x
b)	I agree to deposit an electronic copy of my thesis (the Work) in the Bangor University (BU) Institutional Digital Repository, the British Library ETHOS system, and/or in any other repository authorized for use by Bangor University when the approved **bar on access** has been lifted.	
c)	I agree to submit my thesis (the Work) electronically via Bangor University's e-submission system, however I **opt-out** of the electronic deposit to the Bangor University (BU) Institutional Digital Repository, the British Library ETHOS system, and/or in any other repository authorized for use by Bangor University, due to lack of permissions for use of third party material.	

Options B should only be used if a bar on access has been approved by the University.

In addition to the above I also agree to the following:

1. That I am the author or have the authority of the author(s) to make this agreement and do hereby give Bangor University the right to make available the Work in the way described above.

2. That the electronic copy of the Work deposited in the digital repository and covered by this agreement, is identical in content to the paper copy of the Work deposited in the Bangor University Library, subject to point 4 below.

3. That I have exercised reasonable care to ensure that the Work is original and, to the best of my knowledge, does not breach any laws – including those relating to defamation, libel and copyright.

4. That I have, in instances where the intellectual property of other authors or copyright holders is included in the Work, and where appropriate, gained explicit permission for the inclusion of that material in the Work, and in the electronic form of the Work as accessed through the open access digital repository, *or* that I have identified and removed that material for which adequate and appropriate permission has not been obtained and which will be inaccessible via the digital repository.

5. That Bangor University does not hold any obligation to take legal action on behalf of the Depositor, or other rights holders, in the event of a breach of intellectual property rights, or any other right, in the material deposited.

6. That I will indemnify and keep indemnified Bangor University and the National Library of Wales from and against any loss, liability, claim or damage, including without limitation any related legal fees and court costs (on a full indemnity bases), related to any breach by myself of any term of this agreement.

Signature:  Date : 30/09/2019.

Acknowledgements

Acknowledgements of guidance by Dr Graham Bird. Bangor University Thoday laboratory for carrying out general analysis of water quality parameters and anion analysis. Synlab UK Ltd. For the use of ICP-OES.

Abstract

Historic mining processes were inefficient and unregulated, leading to a legacy of pollution in fluvial systems in formerly mined areas of the UK. Wales is no exception, the Water Framework Directive (WFD) and Natural Resources Wales (NRW) identified 50 sites of concern requiring remediation in the Metal Mines Strategy for Wales (MMSW) which are demonstrating legacy pollution of Potentially Harmful Elements (PHEs) and are failing water quality standards. In 2016 NRW stated that they are aiming to achieve good ecological status by 2027 using remediation techniques at 50 metal mine sites. The 50 mines have been identified as the worst polluters inputting 200 tonnes of Zn, 32 tonnes of Cu, 15 tonnes of Pb and 600 Kg of Cd to environment on annual basis. To achieve this accurate assessment of water quality variation and remediation requirements would be required. Previous studies on water quality impacts from legacy metal mines have only evaluated data of short-term snapshot metal concentrations or fluxes and associated hydro-climatic conditions. This paper will aim to evaluate the temporal variability of water quality in response to hydro-climatic controls at a range of monitoring resolutions and evaluate the potential effectiveness of current and future mine water treatment schemes. The study will use the mine sites of Parc mine and Cwm Rheidol mine. The study utilized remote data loggers to monitor hydroclimatic and chemical conditions at each mine site supplemented by analysis of anion and cations via ICP-OES and ion chromatography to assess PHEs and define temporal and spatial variation in water quality. Hourly monitoring highlighted the potential for underestimated PHEs loads demonstrating an increased PHE load of 36.1% in comparison to weekly monitoring. This was due to diel cycling that was identified at Parc mine exemplifying increased PHE concentrations during night-time periods. The study found Zn and Cd to be the primary cause for concern at both mine sites, failing water quality standards with concentrations that exceed guidelines defined by the WFD (The Water Framework Directive, 2015). The current passive remediation system in place at Cwm Rheidol was found to be 75.9% effective for Zn, the effectiveness varied temporally with changes in discharge. The study identified hydroclimatic variability to have a significant effect on water quality. The study highlights the requirement of high-resolution hourly monitoring to aid accurate load calculations to enable identification of the correct remediation system to manage PHE concentration reduction in light of a temporally varied PHE load.

Contents

Figures

Chapter 1 - Introduction

Chapter 2 - Trace metals and the fluvial environment

Tables

Chapter 1 – Introduction

1.1 Geology and trace metal deposits

1.1.1 Global-scale processes

Trace metals are deposited on a global scale by processes often associated with tectonic activity. The spatial relationship of tectonic processes and metalliferous deposits is significant, with most major ore deposits found proximal to areas of current or past tectonic forces and magmatism (Evans, A. M., 1987; Skinner and Porter, 2007). Metalliferous ore deposits are commonly formed at plate boundaries in faults and fractures. The tectonic setting of the ore deposit will govern what metals are present within a deposit (Figure 1.1) (Skinner and Porter, 2007). Tectonic plate boundaries are subject to processes such as mountain building Orogenies at divergent boundaries, rifting at divergent boundaries and displacement at transform boundaries (Figure 1.1) these processes have the capability of producing metalliferous ores from hydrothermal circulation processes (Figure 1.2). Ores can also be produced with intrusive magmatic deposits (Figure 1.1), intrusive magmatic deposits such as plutons have the capability to generate hydrothermal circulation depositing metalliferous ores (Skinner and Porter, 2007).

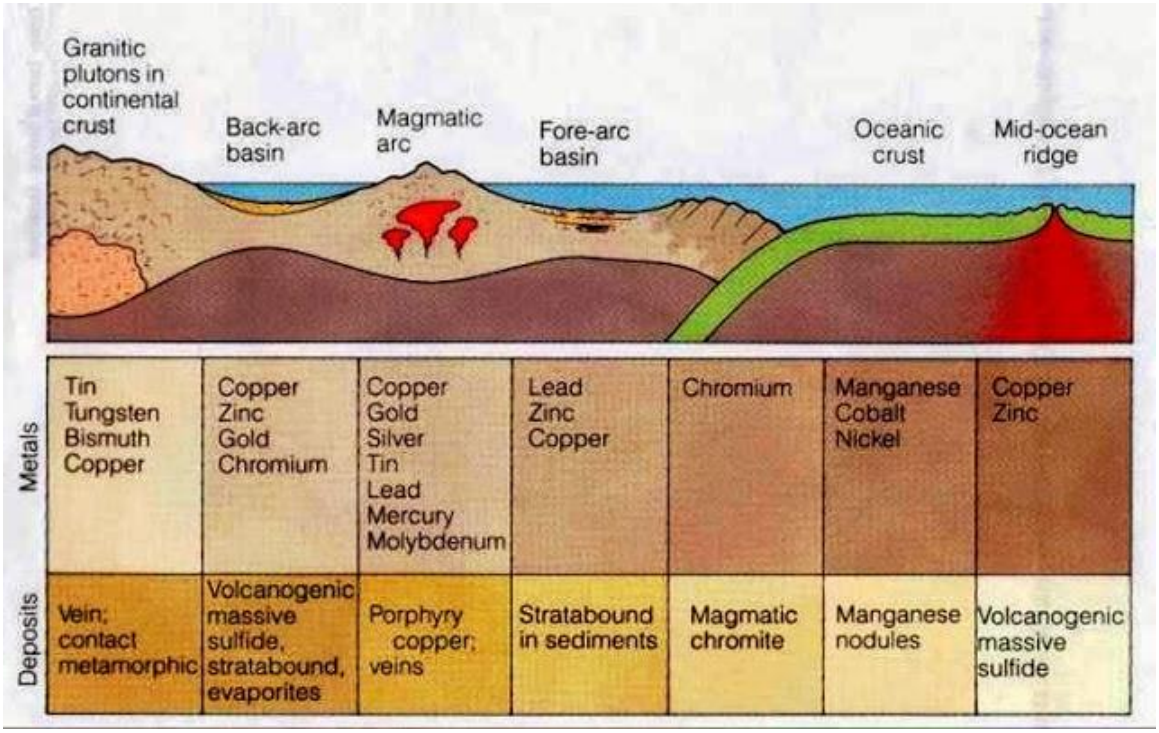

Figure 1.1. Tectonic settings of metalliferous ore deposits (Skinner and Porter, 2007).

Hydrothermal circulation of meteoric and surface waters can lead to ore deposition in fractures and faults (Figure 1.2) where hydrothermal circulation occurs, the metalliferous mineral deposits that are deposited in the fractures and faults are known as lodes (Gleeson *et al.,* 2001; Burnham, 2007).

Hydrothermal processes 'concentrate' solid particulate minerals, the minerals present in the ore deposit are dependent on the country rocks and what minerals have been 'concentrated' from the

surrounding country rocks (Sheppard, 1977; Gleeson *et al.,* 2001). Hydrothermal processes are essentially endothermic process driven by endogenic geothermal heat. Heat from magmatism at tectonic boundaries, mantle hotspots and decaying radioactive isotopes are the drivers of hydrothermal circulation and there for are the primary control on mineral deposition of metalliferous ores (Burnham, 2007). Metals are either formed in epithermal - near surface processes (<5m depth) or by mesothermal processes (>5 meters depth) (Figure 1.2).

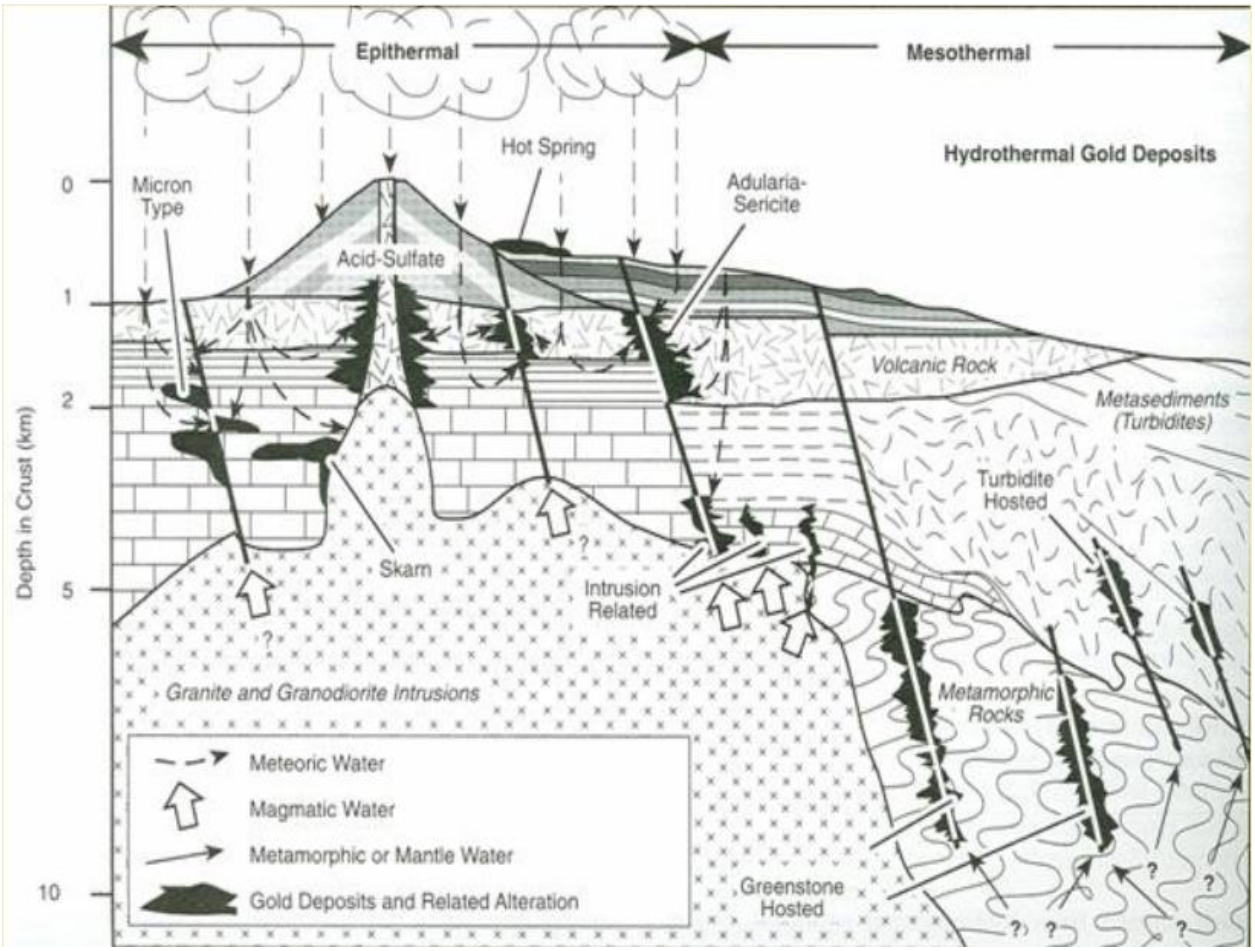

Figure 1.2. – Hydrothermal circulation with ground waters and meteoric waters (Burnham 2007).

Superficial surface deposits of metals can also occur, known as placer deposits, which are essentially hydrothermal deposited lodes that have been weathered, eroded and redistributed in a fluvial system (Camm and Hosking, 1985; Jarsjö *et al.,* 2017). Due to the nature of the type of deposit, metals are generally deposited where reductions in energy occur within a fluvial system, the metals effectively drop out of transport in these areas over time where they collect into a placer deposit (Camm and Hosking, 1985).

1.1.2 The UK context

The majority of mineralisation in Wales that has produced metalliferous ores is due to mountain building episodes during the dismemberment of Pangea and the closing of the Iapetus Ocean (Cooper *et al.,* 2000). The age of the majority of mineralization in Wales spans from ~550 to 290 Ma (Haggerty *et al.,* 1996; Cooper *et al.,* 2000). In Wales, two main Orogenies took place due to the closure of the Iapetus Ocean; known

as the Caledonian Orogeny and the Variscan Orogeny (Cooper *et al.,* 2000). The Caledonian Orogeny caused greatest deformation and mineralisation within the Mid and North Wales regions and the Variscan orogeny was focused in the south Wales region (Cooper *et al.,* 2000).

The Caledonian Orogeny's late stage hydrothermal mineralisation has resulted in deposition of metalliferous ores in Mid and North wales (Cooper *et al.,* 2000). The metal-bearing ores, deposited in lodes, have been extracted since the Bronze Age. Metals such as Au, Ag, Pb, Zn and Cu have been exploited in Wales (Johnston, 2002). Wales has experienced several stages of mineralisation resulting in different types of ore deposits and they are spatially dived into several ore fields (Figure 1.3). The areas of Parc Mine and Cwm Rheidol Mine will be the field sites used in this study they are located in differing ore fields of the Lower Palaeozoic (Cooper *et al.,* 2000).

There has been a substantial amount of research pertaining to the geological history of Wales and it has extensively elucidated the processes resulting in the formation of mineral veins/lodes in Wales (Cooper *et al.,* 2000). Previous work has developed an in depth understanding of the history and depositional environments of the mineral lodes in Wales, which enables spatial understanding of how minerals are distributed within Wales (Cooper *et al.,* 2000; Palumbo-Roe and Colman, 2010). From research pertaining the geological history of wales in relation to mineralisation, it can be identified that the majority of the metalliferous minerals present in Wales were produced during the late stage of the Caledonian Orogeny, producing areas of mineralisation known as the ore fields of the Central Wales Orefield and the Llanrwst Orefield (Cooper *et al.,* 2000).

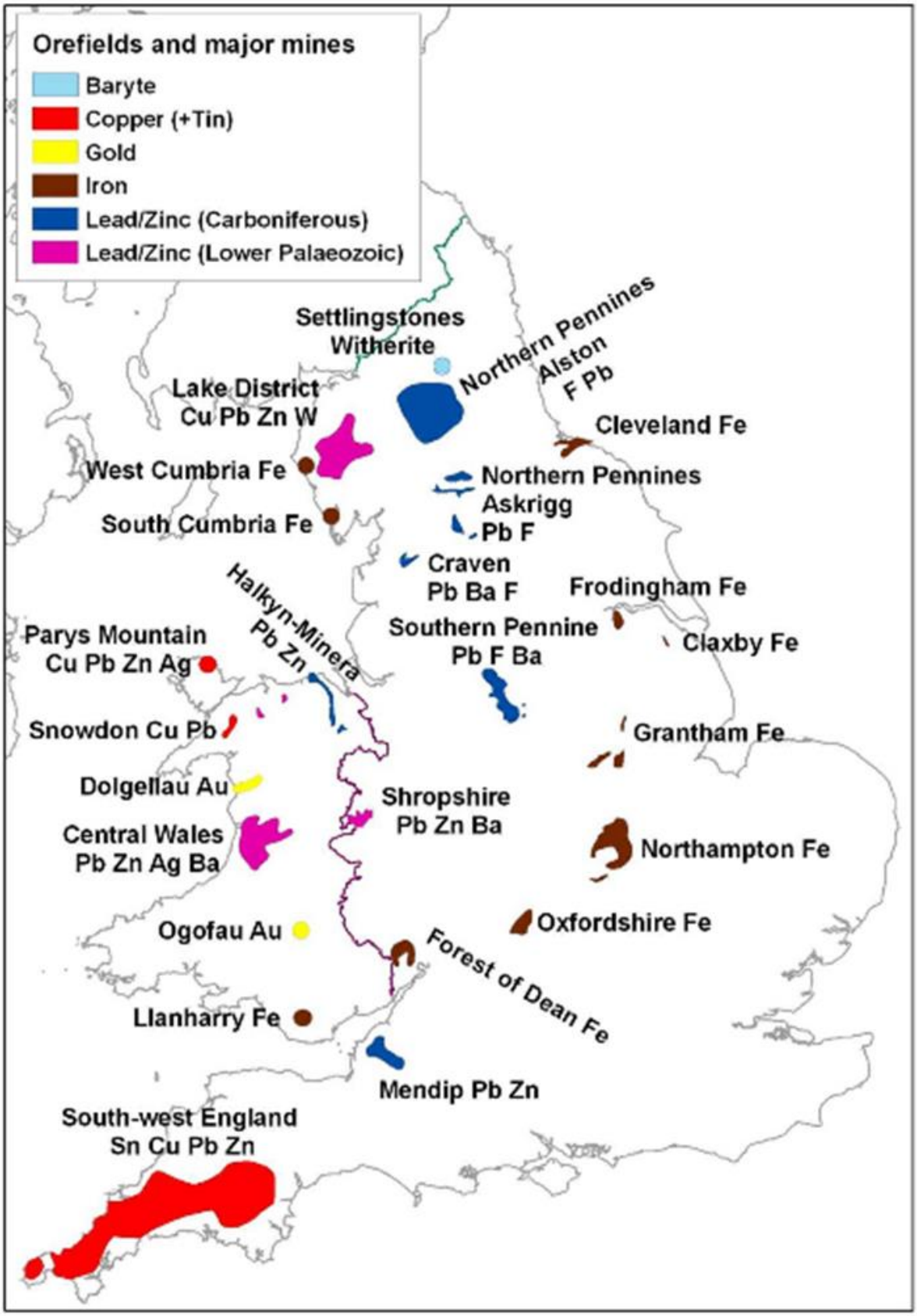

Figure 1.3. Location of Ore fields and the principal metals associated (Palumbo-Roe and Colman, 2010).

1.2. Historic mining and trace metal pollution

1.2.1 Global issues

Globally, metal mining has taken place since the pre-Roman era, dating back to at least 4000 years BP (Evans, A. M., 1987; Cooper *et al.,* 2000). Mining and mineral trading became a key feature of early civilised economies, driving technological advancements of metal recovery (Carvalho, 2017). By the Roman era, the Roman Empire was extracting large quantities of potentially harmful elements (PHEs) such as Pb, Cu and Zn to improve living standards and sustain a high living standard (Nriagu, 1996). The occurrence of historically inefficient and unregulated mining practices over millennia, in addition to any current mining processes, has left a legacy of pollution in in formerly-mined and currently-mined river catchments around the world (Davies, 1987; Milton *et al.,* 2002; Environment Agency Wales, 2002; Natural Resources Wales, 2016). Consequently, there has been work identifying contamination due to the legacy of historical metal mining (Davies, 1987; Gao and Bradshaw, 1995; Milton *et al.,* 2002). Since 1900, mining of not only trace metals, but all mining, has increased significantly on a global scale, mining and extraction of ores and industrial minerals has increased 8-fold since 1900 and global Gross Domestic Product (GDP) has increased 27-fold (Carvalho, 2017) (Figure 1.4). With mining regulations regarding contaminate release only being introduced in the late 1990s, the majority of mining that has taken place on a global scale has been carried out unregulated (Figure 1.4) (Environment Agency Wales, 2002; Carvalho, 2017).

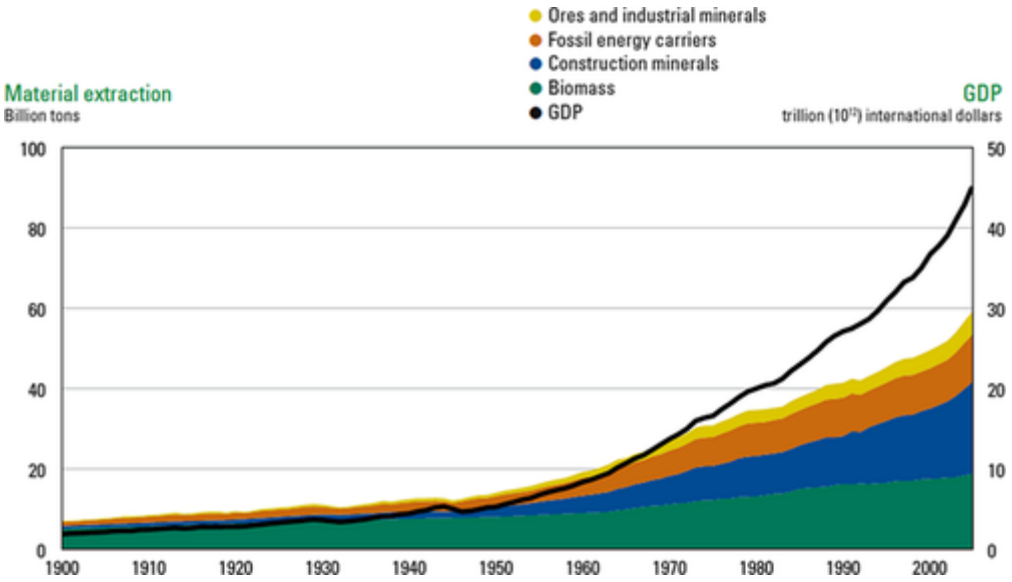

Figure 1.4. Increases of extracted material and Gross Domestic product since 1900 (Carvalho, 2017).

1.2.2 UK

The UK is no exception to early metal mining, for example, at Parys Mountain mine, which was once one of the largest producers of Cu in Europe. Copper has been extracted on the site since the Roman era and extraction on an industrial scale began during the mid-18th century (SKM, 2011). By the late-18th century Parys Mountain mine was dominating the world market for Cu production, however, due to the discovery of economic deposits aboard mining ceased during the early 20th century and no mining has taken place for the

last 100 years (Younger, and Potter, 2012). The situation of overseas economic mine deposits has left a legacy of mines including Pb mines.

Lead was worked extensively during the 13th and 14th century and decreased significantly in the 15th century due to the Black Death (Environment Agency Wales, 2002). Mining of Pb in the UK took place in various locations across the UK and in Wales primary deposits were in the Central Welsh and Llanrwst Orefield's. The primary production period of Pb mining took place 1750 – 1900 (Davies, 1987). This was largely due to the advancements in technology that occurred during the 17th century and saw the development free draining adits, water pumps and later explosives (Environment Agency Wales, 2002). During the late 19th century Zn mining in Wales peaked due to increased demand of the industrial revolution, contributing to 43% of the UK total between 1845 and 1938 (Environment Agency Wales, 2002). At the end of the 19th century large economic deposits of Pb and Cu were discovered in Spain, South America and Australia which were cheaper to import than production in the UK. The UK metal mining industry began to decline at the beginning of the 20th century due to overseas deposits and the decline in the price of Zn in 1921, by the 1920s the majority of metal mining in the UK has ceased with the exception of mining and exploration of precious metals such as gold (Davies, 1987; Cooper *et al.,* 2000; Johnston, 2002; Environment Agency Wales, 2002).

1.3. Environmental impacts

1.3.1 Current environmental impacts

There has been a legacy of mining pollution since the discovery of fire which led to the small-scale pollution in cave environments, since the discovery of fire and mining in ancient times there has been links between PHE pollution and anthropogenic activities (Nriagu, 1996). Mining processes have caused pollution to the secondary environment causing increased PHE levels in soils, aquatic systems and the atmosphere by the release of PHEs (Davies, 1987; Johnston, 2002; Johnston *et al.,* 2008; Foulds *et al.,* 2014). Processes of contamination occur during and post mining, within the UK and many parts of the world, pollution problems from mining are from legacy mining sites (Bird, 2016). Records of historical PHE pollution in the atmosphere from smelting processes have been recorded in various natural deposits particularly in bogs, aquatic sediments and ice sheets (Nriagu, 1979; Nriagu, 1996). Records from polar ice sheets hold the greatest details of PHE pollution due to their rapid accretion rate (Nriagu, 1996).

PHEs can be released to the environment from point sources of mines, entering the surface drainage network as dissolved or sediment fluxes and are deposited in alluvial systems (Bird, 2016). The PHEs released from legacy mining have potential to be hazardous to human health, flora and fauna causing problems such as increased cancer risk, skin lesion, cardiovascular disease, respiratory disorders and hearing loss (Furlow, 2014; Abraham et al., 2018). Legacy mining sites are of concern due to related PHE contamination. Legacy mine sites were not subject to mining regulation to ensure preservation of a pristine environment, whilst they were active leaving, this has led to the problem of legacy of mining pollution (Abraham et al., 2018).

There are many examples of mining contamination from historical mining across the globe, in Australia it has been reported that there is significant levels of mercury and arsenic in soils that can be attributed to historic gold mining (Abraham et al., 2018).

Historic mining sites that have left a legacy of PHEs that are still of a great concern due to the previously stored toxic sediment that can be remobilized. Remobilized sediments can impact on lowland ecosystems allowing for the potential introduction of toxic PHEs to the food chain and ground waters (Singer et al., 2013).

The introduction of new contaminants into aquatic systems is still a major concern as legacy mining sites are still acting as point sources contamination (Gao and Bradshaw, 1995; Bird, 2016). Historic mining sites have left a 'geochemical footprint' of contamination in fluvial environments and alluvial sediments (Macklin et al., 1994). Legacy pollution has left PHE in the environment due to processes including acid mine drainage (AMD), acid rock drainage (ARD), leaching and erosion of particulate waste. The geochemical footprint of legacy mining pollutants stored in sediments can be used as chronological record of contamination and the spatial extent of these sediments can also be achieved due to the geochemical footprint that is left behind (Vale et al., 2016).

1.3.2 Future environmental impacts

The increased potential of extreme weather events due to current and future climate change highlights the significance legacy mining sites due to their potential to cause future contamination due to remobilization of contaminated sediments. Release mechanisms to the environment of PHE contamination can be geogenic and anthropogenic (Bird *et al.,* 2014; Di Bonito *et al.,* 2019). Inputs to fluvial and alluvial systems from historic mine sites include AMD/ARD, circum neutral mine drainage, release of PHE rich slurries and tailings dam failures (Nriagu, 1996; Johnston *et al.,* 2008). Climate change can cause hydro-climatic conditions to become more varied and extreme (Brooks *et al.,* 2010; Hosseini *et al.,* 2017). Mining processes have the potential to be exuberated by climate change by altering hydroclimatic variables within a groundwater and fluvial systems which will inevitably reintroduce legacy contamination and increase the rate of release from current mining activities of PHEs from processes such as flooding. Flooding is a short-term hydro-climatic affect that can remobilize contaminated sediment and can reduce the water quality of fluvial system in question, flooding events are becoming more frequent due to climate change (Foulds *et al.,* 2014). The implications of future climate change have the potential to alter mine specific pH which will alter PHE loading upon a fluvial system (Brooks et al., 2010; Anawar, 2013). In combination of altered site-specific pH and an increased flow it can be said that climate change will have a dramatic effect of PHE loading in fluvial systems (Foulds *et al.,* 2014). These implications will need to be examined to be accounted for in future remediation schemes of PHE mining sites. There has been increased research to identify areas in need of remediation to achieve good ecological status defined by WFD (Johnston, 2002; Environment Agency Wales, 2002; Palmer, 2006; Johnston *et al.,* 2008; Natural Resources Wales, 2013; Natural Resources Wales, 2016).

1.4. Remediation

1.4.1 Global Remediation Strategy

There is environmental damage from metalliferous mining operations across North America, Europe and the rest of the word. Remediation is required primarily for legacy mining operations, modern mining processes have less impact on the environment due to emplaced laws and controls to minimise contamination levels released, legacy mines have operated prior to regulations and they have not emplaced procedures to reduce contamination this has left them sources of contamination to date. Globally remediation has looked at various processes including soil amendment, phytoremediation and innovative passive and active treatment systems. Low cost permanent remediation solutions such as passive systems are favoured on a global scale. (Dybowska *et al.,* 2006)

1.4.2 Remediation strategy – Wales

The need for remediation of metal mine sites in Wales was Identified by the Coal Authority and the National Rivers Authority in 1994 this led to the introduction of two remediation schemes in 1998 at Cwmbrwyno and Van mines, they were successful but short lived due to the lack of available funding (Johnston, 2002). Due to this the Environment Agency (EA) Wales obtained funding from the National Assembly for Wales and went on to produce the Metal Mines Strategy for Wales (MMSW) with the aim of identifying priority sites requiring remediation and approaching their stakeholders to improve the potential of future remediation at metal mine sites of high importance. To define the priority sites the EA used the Database of Metal Mines in Wales produced by the National rivers authority in 1996 that included 204 sites across Wales, the strategy involved defining the sites by their ecological and archaeological importance (Johnston, 2002). The aim of the MMSW is to improve water bodies to a good ecological status defined by the water framework directive (WFD) (Law, 2018).

The EA identified 50 contaminated mine sites in Wales that are of the greatest concern during the formulation MMSW, the county of Ceredigion encompassed 38 of the mine sites (Figure 1.5) that fell below the standards of good ecological status defined by The WFD (Johnston, 2002). The MMSW is an initiative that collaborates with stakeholders of areas of environmental concern with the aim of performing remediation on the sites to ascertain a good ecological status to reduce risk to human health and the local ecology. The introduction of the WFD was implemented in 2003 to ensure to improvement of water quality of the UK fluvial system by control of pollutants entering the system (Law, 2018).

In 2008 a report by the Coal Authority and SEPA identified that the problem of contaminated mines was being addressed but that to achieve success in reaching the criteria of the WFD a catchment view approach must be taken to deal with the point sources through an array of remedial measures (Johnston *et al.,* 2008).

By 2013 work had been carried out on over 90 water bodies in Wales by Natural Resources Wales (NRW) formerly the EA, to access and identify the reasons and the point sources of contamination that failed

the WFD. NRW are continuing work to prioritise the mine sites of the greatest pollution, with some of the sites identified, remediation processes have been initiated, sites including Cwm Rheidol, Frongoch Mine and Upper Teifi Mines and further research at Nant y Mwyn Mine, Dylife Mine and Parys Mountain Mine have received some form of remediation (Natural Resources Wales, 2013).

A remediation pilot trail at Cwm Rheidol mine in the form of a passive treatment trail in the form of a compost-bioreactor known as a vertical flow pond (VFP) has been carried out (Natural Resources Wales, 2013). Research pertaining its effectiveness at a low resolution has been carried out by Williams (2014).

In 2016 NRW stated that they are aiming to achieve good ecological status by 2027 using remediation techniques at 50 identified metal mine sites across Wales (Natural Resources Wales, 2016), they are looking to achieve this by carrying out the program outlined in the MMSW (Environment Agency Wales, 2002).

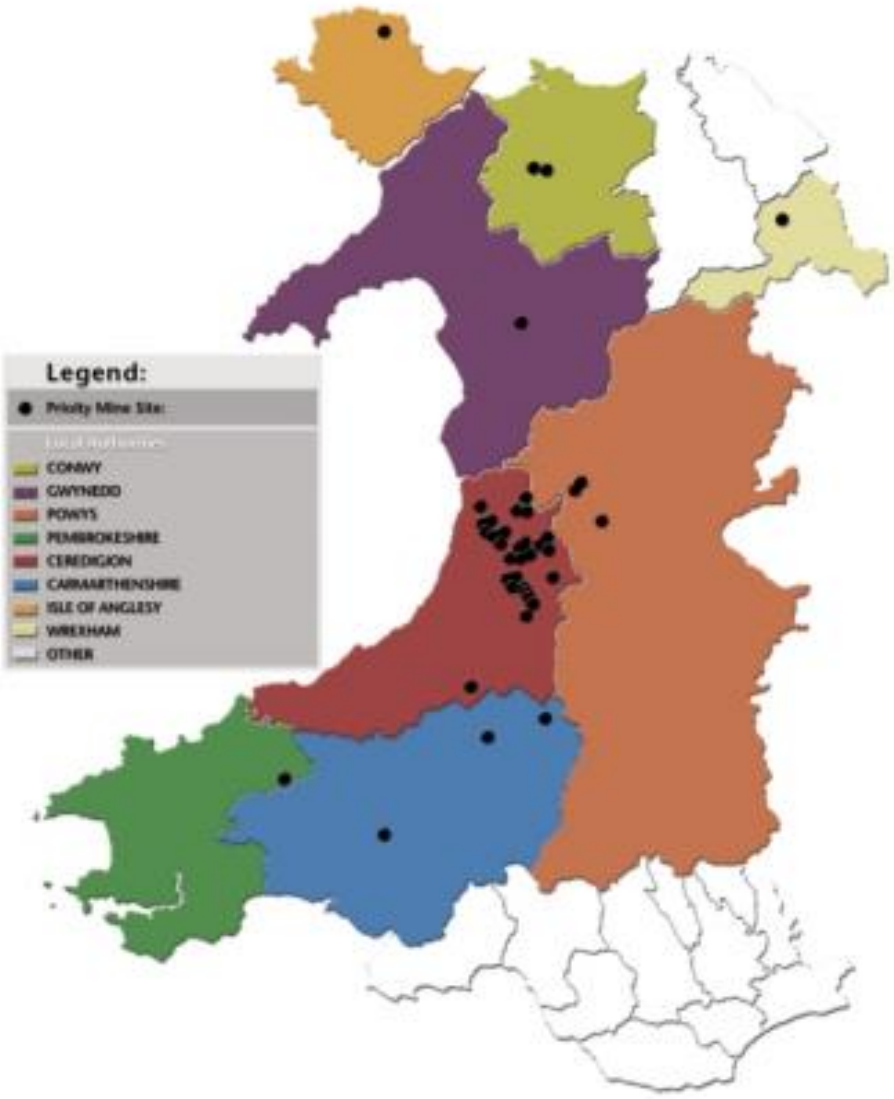

Figure 1.5. Location of the top 50 legacy mine sites causing environmental pollution from metalliferous contaminants (Environment Agency Wales, 2002).

1.5 Study aims

Previous studies on water quality impacts from legacy metal mines have largely only evaluated data of short-term snapshot PHE concentrations or loads and associated hydro-climatic conditions e.g. (Pettine *et al.,* 1994; Gao and Bradshaw, 1995; Kim *et al.,* 2007; Potter *et al.,* 2013; Bhat *et al.,* 2014). There has been relatively little work to study PHE loads and how they are affected by hydro-climatic conditions over short term temporal scales at high-resolution (Nimick *et al.,* 2007). In recent years there has been research pertaining active and passive treatment systems for treating rivers with prolific pollution from metal mining (Jarvis *et al.,* 2015; Morgan *et al.,* 2017). However, there has also been less work carried out to ascertain suitable remediation for metalliferous point sources in relation to potentially variable hydro-climatic conditions and water chemistry.

This study will aim to evaluate the temporal variability of water quality in response to hydro-climatic controls and evaluate the potential effectiveness of future mine water treatment schemes at two sites of contrasting geochemical and geological conditions: Cwm Rheidol Mine (pyrite-rich, low pH) and Parc mine (carbonate-rich, circum-neutral pH). Parc mine is identified as an area for further research and Cwm Rheidol mine is identified as an area for remediation (Johnston, 2002). Later to the MMSW, NRW have only trailed remediation on some of the top 10 sites identified at risk this includes Cwm Rheidol near Aberystwyth in which pilot remediation schemes have taken place, Parc Mine in Llanrwst is yet to receive attention. Now that NRW have confirmed they would like to achieve remediation targets by 2027 remediation works will be required to be carried out across North Wales at affected sites to achieve good ecological status (Natural Resources Wales, 2016). The need for further research at both sites to assess to current state of the water quality and the future requirements of any remedial actions are required (Natural Resources Wales, 2016). The study will identify temporal spatial variation of water quality at legacy metal mine sites and will address the following research questions:

Research question 1. Evaluate the temporal and spatial variability of water quality in response to hydro-climatic variability.

Possible outcomes – Cwm Rheidol mine and Parc mine

H^0: There will be no affect to water quality in response to hydroclimatic controls at Parc mine and Cwm Rheidol mine.

H^1: There will be an effect to the water quality in response to hydroclimatic controls at Parc mine and Cwm Rheidol mine.

Research question 2. The project will ascertain if there is any ineffectiveness of the passive remediation treatment scheme at Cwm Rheidol and ascertain if Parc mine receiving no recent remediation is justified, aiding the evaluation of the potential effectiveness of future mine water treatment schemes.

Possible outcome – Cwm Rheidol mine

H^0: The passive remediation scheme at Cwm Rheidol mine has no effect on the improvement of water to the standards of the WFD quality of the Afon Rheidol.

H^1: The passive remediation scheme at Cwm Rheidol mine has an effect on the improvement of water to the standards of the WFD quality of the Afon Rheidol.

Possible outcome – Parc mine

H^0: The contamination at Parc mine is causing an effect to water quality to fail standards defined by the WFD (The Water Framework Directive, 2015) and does require urgent remediation.

H^1: The contamination at Parc mine is not causing an effect to water quality and is within standards defined by the WFD (The Water Framework Directive, 2015) and does not require urgent remediation.

1.6 Research objectives

The study will look to answer the research questions by completing the following objectives:

- Undertake synoptic sampling of waters to establish temporal variation of water chemistry over a range of timescales to identify temporal water quality variation.
- Monitor hydrological conditions at the time of sampling to identify relationships between water quality variation and hydrological variables.
- Quantify PHE fluxes (loads) and geochemical enrichment factors for PHE content in mine waters and recipient streams at regular intervals to establish variation and compare with hydro-climatic variation.
- Establish the variability in the percentage PHE removal by mine water treatment over a range of discharge conditions to identify any periods of ineffective PHE removal.
- Establish what metalliferous pollutants need to be remediated at each site and aid identification other contaminants at other similar legacy mine sites.
- Identify differences in water quality variation between the two mine sites to establish if differing environments can affect water quality variation.
- To use the data to highlight future potential hazards caused by hydro-climatic variability at legacy mine sites.
- Gain an understanding of the required actions for remediation from the hydro-climatic, chemical and PHE variability data.
- High-resolution monitoring to identify short term temporal effects to water quality caused by varying hydro-climatic conditions which will highlight the efficiency of the trail VFP remediation at cwm Rheidol.

Chapter 2: Trace metals and the fluvial environment

2.1 Introduction

Trace metals also referred to as heavy metals, have been defined by their crustal abundance and specific gravity (Hu and Gao, 2008; Srivastava and Majumder, 2008; Ackova, 2018). Davies (1980) defines trace metals as <6g cm^{-3}, Srivastava and Majumder (2008) define trace metals as <5 g cm^{-3} and Ackova (2018) defined trace metals as a density <4g cm^{-3}. Coordination chemistry can also be used as a way of defining trace metals, trace metals can be sub-divided into non-essential trace metals and toxic trace metals (Srivastava and Majumder, 2008). Metals considered toxic trace metals include lead (Pb), zinc (Zn) and cadmium (Cd) (Ackova, 2018). Toxic trace metals can enter the fluvial environment from range of natural and anthropogenic processes (Nriagu, 1979; Nriagu, 1988; Charlesworth *et al.,* 1996).

Potentially harmful elements (PHEs) refers to trace metals which have potential concern for human and aquatic life (Bird *et al.,* 2009). Areas that exceed quality guidelines of PHEs are of a particular concern for human health (The Water Framework Directive, 2015). Recent decades have seen an increase in the release of PHEs to the environment they are considered the most prolific environmental contaminants (Bini and Wahsha,2014). The extraction processes of metalliferous ores have been found to be a primary contributor to PHEs to the environment during recent decades (Bird *et al.,* 2009), although geogenic processes can contribute PHEs to the environment also (Bird *et al.,* 2014).

2.2 Toxicity of PHEs

Populations can be exposed to PHEs from various pathways including oral bioaccesibility from consumption of contaminated waters, ingestion of dust particle including household and road dusts (Marinho Reis *et al.,* 2018) and consumption of contaminated food sources (Antoniadis *et al.,* 2017). PHEs can pose a risk to human health when consumed in drinking water (Chowdhury *et al.,* 2016). Ground waters and surface waters, as well as soils and sediments, are influenced geogenic and anthropogenic PHE sources, with one of the primary anthropogenic sources being mining (Martin *et al.,* 2016). PHE contaminated ground waters can be a water source for domestic needs creating a pathway of human expose to PHEs from mining (Bird *et al.,* 2009). PHEs are also detrimental to aquatic life (Yi *et al.,* 2011) benthic invertebrates (Clements, 1994) and plant life (Ackova, 2018). Plants have been found to exemplify sensitive effects to PHE toxicity (Ackova, 2018).

2.2.1 Zinc

Zinc is required for human and animal health and deficiencies in Zn can lead to negative health effects and high-level exposures to Zn in humans and animals have been found to cause respiratory and gastrointestinal problems, although effects are minimal and require only basic medical attention (Walsh *et*

al., 1994). There has also been links to asthma, skin diseases and cancer in association with Zn (Chowdhury *et al.,* 2016). It has also been reported that intake of Zn ~15mg per day can reduce negative health effects of PHEs such as As (Chowdhury *et al.,* 2016). Zinc is an essential element for plants and ~300-400 mg kg^{-1} per day is typical for a toxicity limit for plants. Zinc toxicity in plants can reduce root growth, slow the development of the plant and alter metabolic processes. Zinc toxicity also has the potential to cause chlorosis (Ackova, 2018)

2.2.2 Cadmium

Cadmium is toxic for all living organisms, Inorganic Cd is a known carcinogen, Cd is also related to kidney damage (Chowdhury *et al.,* 2016). It is an easily transportable element in the fluvial system and is distributed to all living organisms in areas of high toxicity (Ackova, 2018). Cadmium has also been linked to health problems such as asthma, ulcers and other skin diseases and renal failure (Chowdhury *et al.,* 2016). Cadmium is of concern for public health. Plant uptake of essential trace metals is hindered with toxicity of Cd. Cadmium toxicity in plants is demonstrated as chlorosis, browning of roots and eventual death of the plant. Cadmium can also reduce the efficiency of enzyme activity within a plant (Ackova, 2018)

2.2.3 Lead

Lead can be detrimental to human health causing affects to the central nervous system, renal, hematopoietic, cardiovascular, gastrointestinal, musculoskeletal, endocrinological, reproductive, neurological and immune systems (Chowdhury *et al.,* 2016). Low level exposures of Pb can affect brain development leading to permanently altered functions (Chowdhury *et al.,* 2016). Research by Karuppannan and Kawo (2018) has also linked Pb exposure with symptoms of asthma, ulcers, skin diseases, renal failure. Pb is a PHE for plants also and can cause a range of negative health effects on plant species increased levels of Pb can cause phytotoxicity that causes negative affects to the morphology, germination, photosynthetic rates, water content and enzyme rates. These affects are exemplified at their greatest at high concentrations of Pb (Ackova, 2018). The primary effect of Pb is on reduced enzyme activity that can lead to oxidative stress in plants (Ackova, 2018).

2.3 Water chemistry

Ion analysis via graphical interpretations of piper plots enables water quality and potential origin to be identified by identifying anthropogenic inputs that have taken place and influenced water quality (Bikundia and Mohan, 2014). Piper trilinear diagrams represent a way of analysing cation and anion content of mine water and recipient stream water (Figure 2.1) and are a useful means of identifying water quality of water bodies including lakes, marine, river and streams (Figure 2.2). (Bikundia and Mohan, 2014; Karuppannan and Kawo, 2018).

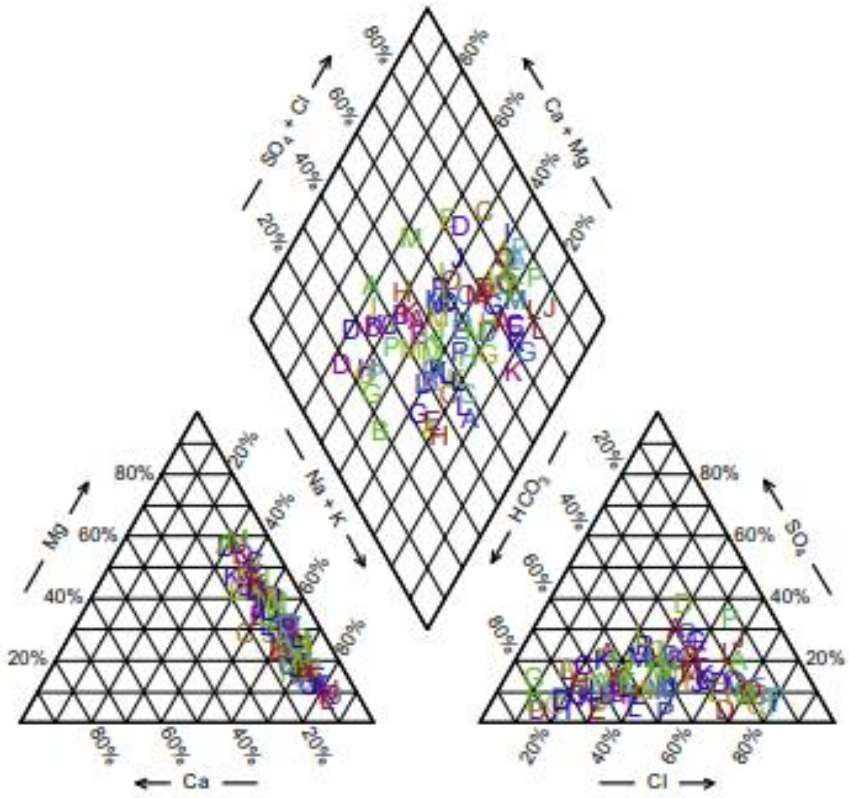

Figure 2.1. Cation and anion analysis using piper diagrams to define water quality (Bikundia and Mohan, 2014).

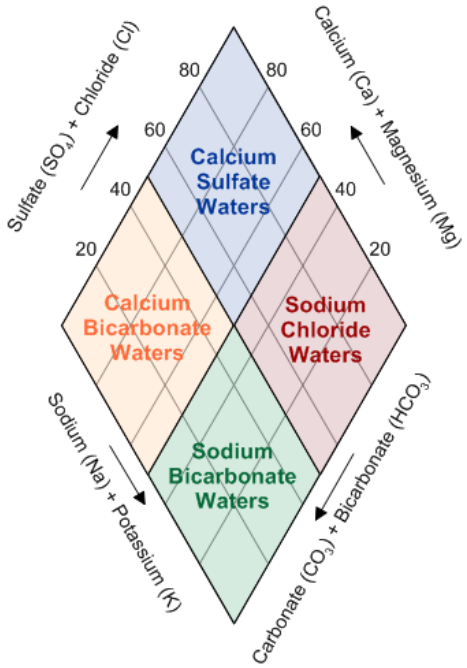

Figure 2.2. Water Chemistry exemplified via a trilinear plot, calcium sulphate areas are found in areas with mine drainage or gypsum rich groundwater. Calcium bicarbonate rich water is present in shallow fresh ground water, sodium chloride waters are waters of marine or ancient origin and sodium bicarbonate water are present in deep ground water (Golden software, 2018).

2.3.1 Anions

Major anions include bicarbonate (HCO_3^-), sulphate (SO_4^{2-}), chloride (Cl^-), nitrate (NO_3^-), and fluoride (F^-). Waters containing high Cl^- can use a pollution index to be used as a tracer for ground water contaminants, chloride is of the least reactive anions contained within groundwaters (Bikundia and Mohan, 2014). Bicarbonate can be formed at circumneutral pH, CO_2 is able to dissolve carbonate minerals and CO_2 can dissolve into water to produce Bicarbonate. The dissolution of carbonate minerals can also release Ca^{2+}, Mg^{2+} and HC03-. Sulphate occurs as a naturally occurring element on Earth, it is therefore present in all water sources globally, there are several natural sources of SO_4^{2-} in the environment they include sulphide minerals, gypsum and anhydrite. Sulphate has the potential to effect gastro-intestinal systems at high concentration and effects can be greater when in combination of Mg^{2+} and Na+ (Bikundia and Mohan, 2014). High concentrations of NO_3^- in ground and mine waters that are consume can cause problems such as blue baby disease in young children, respiratory and nervous system disorders (Majumdar, 2003). The primary source of contamination of groundwaters is via fertilisation of agricultural lands (Bikundia and Mohan, 2014). High F^- concentrations can also be harmful to health with high concentrations causing problems such as dental and skeletal fluorosis (Rao and Mamatha, 2004; Bikundia and Mohan, 2014).

2.3.2 Cations

There are several major cations that can indicate a waters quality, they include calcium (Ca), magnesium (Mg), sodium (Na) and potassium (K), all traces elements and metals are cations also, of the major cations Ca, Mg and Na are of primary concern with Ca and Mg affecting water hardness and Na affecting salinity of a water body. High Ca and Mg can be indicative of areas with basic volcanology and basaltic aquifers. High Na can also occur in areas due to cation exchange processes with Ca (Karuppannan and Kawo, 2018). Sodium has no health-based guideline defined by the World Health Organisation (WHO) but is rather defined by taste at 200 mg/l. Magnesium is considered an essential trace element and can also affect the extent hardness of water, increases of Ca and Mg can increase the corrosivity of water (World Health Organization, 2011).

2.4 Sources of PHEs

There are a range of natural geogenic PHE loading and anthropogenic contamination processes that introduce PHEs to the fluvial system environment (Figure 2.3).

2.4.1 Geogenic PHE loading

Aquatic systems and sediments that contain elevated levels of trace PHEs can be derived from natural processes such as ARD in areas of sulphide-enriched bedrock and bedrock weathering. Geogenic PHE loading is a result of chemical speciation, leaching and physical weathering of naturally occurring trace elements in bedrock and soils (Rivera *et al.,* 2016). Areas of geogenic contamination can be as harmful to the environment as anthropogenically induced contaminated areas (Rivera *et al.,* 2016). An example of geogenic contamination found increased PHE concentrations in local organisms in close proximity of naturally

enriched rocks and sediments of the Magdalena Bay, Mexico (Shea *et al.,* 2016). Work carried by Bird *et al.* (2014) on the Harlech dome area of Wales identified As as a geogenic contaminate in the area of Coed y Brenin and the Afon Mawddach due the presence of a porphyry Cu deposit rather than point sources from gold mining that took place during the 19th and 20th centuries (Bird *et al.,* 2014). Overall, there has been less work to identify geogenic sources of contamination than anthropogenic sources of contamination.

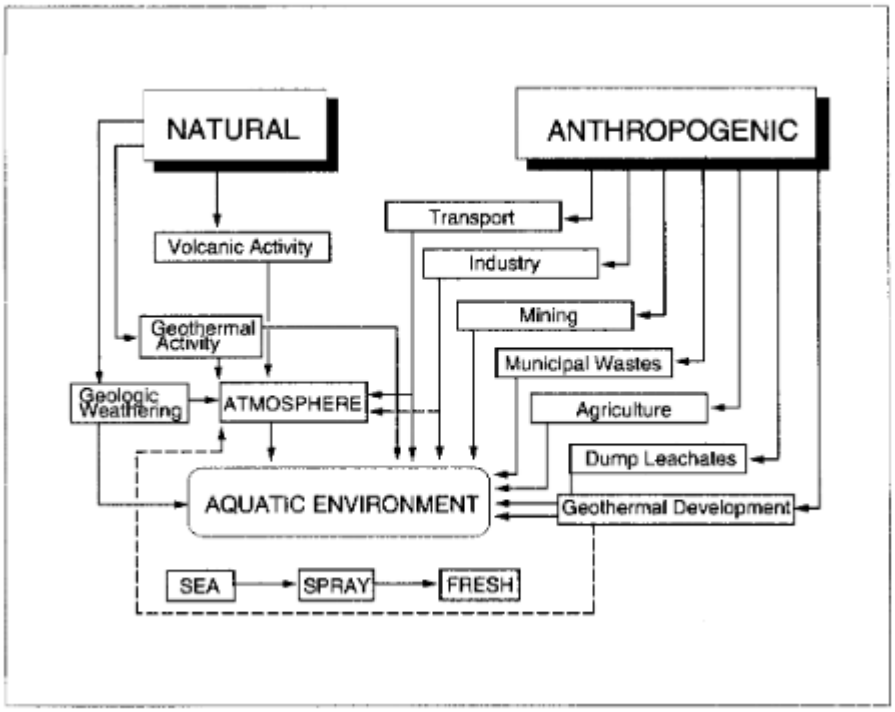

Figure 2.3. Sources to PHEs to the aquatic environment (Charlesworth *et al.,* 1996).

2.4.2 Anthropogenic sources

There is a wide variety of anthropogenic sources of PHE contamination to the secondary environment, including mining, transport, industrial processes, agricultural processes and geothermal energy development (Figure 2.3) (Wang *et al.,* 2004). Due to the amount of human-induced change there currently is upon Earth, which began at the start of the human civilization, it has now been suggested that the term 'Anthropocene' can be used to describe these changes that define a new epoch (Zalasiewicz *et al.,* 2010). Human activity has introduced significant quantities of chemical substances into aquatic systems and sedimentary environments these have been recognised as 'anthropogenic anomalies' (Galuszka and Migaszewski, 2011). Environmental contamination from anthropogenic sources is a primary issue for environmental studies looking at PHEs and their effects. The identification of natural geogenic and human anthropogenic sources of PHEs enables identification of anthropogenic anomalies. There is also the possibility of previously anthropogenically produced stored contaminants within the fluvial system to be remobilized, reintroducing contaminates into the environment (Foulds *et al.,* 2014). The current state of the environment is a result of natural geogenic and anthropogenic sources of contamination (Galuszka and Migaszewski, 2011).

2.4.3 Identifying geogenic background concentrations and quantifying anthropogenic contamination

The origin of work on measuring background concentrations of elements within the Earth's crust was initiated in the 1950s as means of identifying areas of mineral resources for exploitation. Later it become apparent that mineral exploration surveys are an invaluable tool in recognising localised geochemical anomalies, localised geochemical anomalies can be indicative of anthropogenic contamination or natural enrichment of bedrock. Methods for quantifying background concentrations have been identified by several researchers (Matschullat *et al.,* 2000; Reimann and de Caritat, 2000; Reimann and de Caritat, 2005; Reimann and Garrett, 2005). Past research, originating in 1970s, has defined background concentrations and used these in the quantification of Enrichment Factors (EF). This method has been found to be an ineffective way to distinguish between geogenic PHE loading and anthropogenic contamination (Reimann and de Caritat, 2005).

EF calculations are a method that compares element concentrations in a sample media against reference elements that are at a level considered background concentrations due to their abundance, they include silicon and aluminium (the two most abundant elements in the crust) and are measured against Clarke or shale values (Reimann and de Caritat, 2005). Clarke values are estimated average concentrations of 90 elements occurring naturally in the Earth's crust (Clarke, 1924), they have later been compiled by Reimann et al. (1998) to produce a comprehensive range of geochemical background and enrichment values, Clarke values are useful in remediation, toxicological and geochemical baseline studies (Reimann *et al.,* 1998). Other EF calculations look at the ratio between atmospheric and crustal concentrations to calculate enrichment (Hernández-Mena *et al.,* 2011) and some calculations use basal sediment averages to represent baseline conditions for enrichment calculations (Corella *et al.,* 2018). The selection of background media (bedrock, soils or waters) and the chosen reference element for EF calculations can result in varied enrichment values for an area in question (Bern *et al.,* 2019), it is therefore important to ensure that the correct media and elements are chosen for each considered environment to ensure a true enrichment value is obtained. Values generally range between 1 – >10, 1 is considered enrichment from crustal sources and a value of >10 would indicate an enrichment of anthropogenic origin. Equation 2.1 exemplifies the calculation:

$$\mathrm{EF} = \frac{\mathrm{Ae} * \mathrm{Bc}}{\mathrm{Ac} * \mathrm{Be}} \quad \text{(Equation 2.1)}$$

Where Ae is the concentration of the element in question in the sample (bedrock, soil or water).

Where Be is the Concentration of reference element in the sample (bedrock, soil or water).

Where Ac is the Clarke value, uncontaminated soil or water concentration of the element in question.

Where Bc is the Clarke value, uncontaminated soil or water concentration of the reference element.

EFs cannot apply as a way to distinguish between geogenic PHE loading and anthropogenic sources of contamination, EFs in fact indicate differentiation between the solubility of elements (Reimann and de

Caritat, 2000). Highly soluble elements such as Cd and Cu appear to have high EFs due to the nature of the equation (Reimann and de Caritat, 2000). EFs can also be affected by differing bedrock geology, atmospheric dust and geogenic mineral deposits, ensuring that concentrations for comparison are of a similar media to ensure accurate enrichment calculations (Reimann and de Caritat, 2000; Reimann and Garrett, 2005; Reimann and de Caritat, 2005). Raw data from geochemical surveys is the most reliable method of identifying background concentrations and localised anthropogenic contamination (Reimann and de Caritat, 2000; Reimann and de Caritat, 2005).

Background concentrations from geochemical surveys are dependent upon the scale and location of an area in question. Surveys of the crust over a large spatial scale can provide a baseline of PHEs concentrations. Background concentrations calculated from large scale surveys will be the result of the combination geogenic and anthropogenic activities, due to the low resolution of large-scale surveys which would encompass a range of contaminated sites and natural areas (Portier, 2001; Reimann and de Caritat, 2005). The data from large scale surveys can also be used as a means of calculating average concentrations of crustal elements to provide a reliable source for environmental quality guidelines (Galuszka and Migaszewski, 2011). Although large scale surveys may be able to identify a continental scale baseline, they are inadequate at helping to identify localised geogenic loading and anthropogenic contaminations. Local scale surveying and mapping of PHE concentrations, that are spatially higher resolution surveys, will identify localised anthropogenic and geogenic contamination, and can be compared to regional scale baseline surveys to identify geogenic loading and anthropogenic contamination (Reimann and Garrett, 2005).

Other means of geochemical calculation exist to identify anthropogenic contamination. Contamination Factor (CF) is a comparison of mean elemental concentrations within a sample against pre-industrial values for that element. Clarke values and Pre-industrious values appear to have a correlation (Hakanson, 1980). There are numerous studies that have looked at anthropogenic contamination from mining sites (Davies, 1987; Gao and Bradshaw, 1995; Reimann and de Caritat, 2000; Reimann and Garrett, 2005; Reimann and de Caritat, 2005; Singer *et al.,* 2013; Bird, 2016; Marsay, 2018).

2.5 Mining sources of PHE loads

There are various processes involved in PHE release to the environment from areas of PHE mining (Figure 2.4). Potentially harmful elements can be released to the environment in solute loads (AMD, ARD and leaching of mine spoil) or particulate loads (erosion of spoil, tailings dam failures and release of PHE rich slurries). Potentially harmful elements load release and subsequent contamination of the proximal environment can exemplify temporal and spatial variability in PHE solute and particulate loads concentrations (section 2.7).

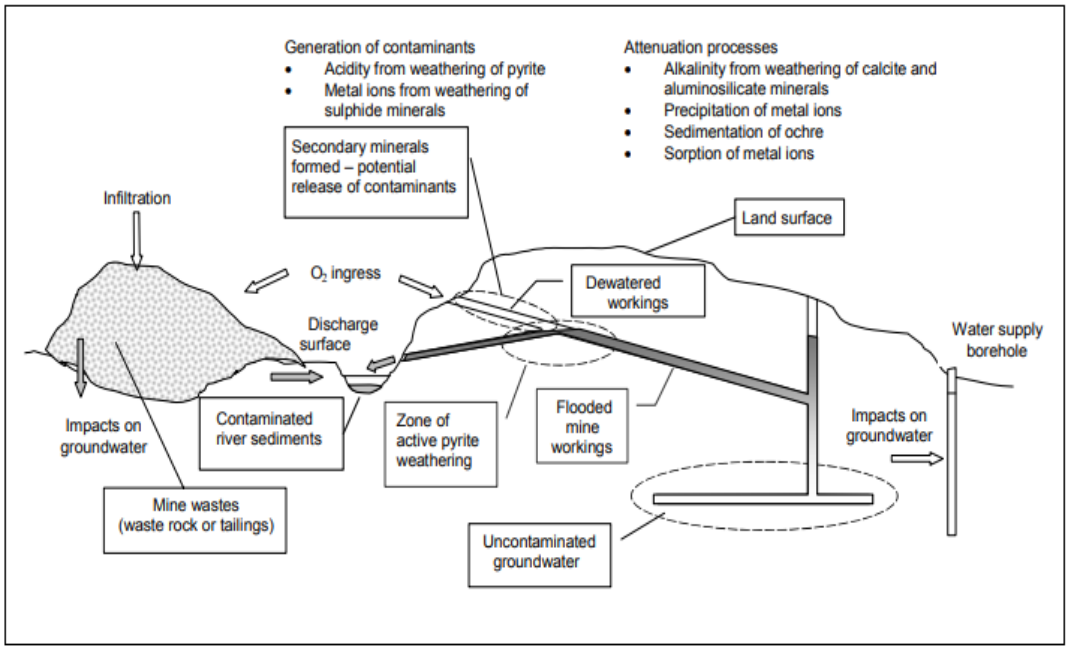

Figure 2.4. – Sources and pathways of mine water contamination (Johnston *et al.,* 2008)**.**

2.5.1 Leaching

Leachates from mine workings and mine waste have the capability to infiltrate and contaminate groundwaters. Leaching can be exacerbated by flood events and the hydroclimatic factors of river flow will directly affect the rate of leaching, leaching outputs of AMD and ARD can be from mining point sources and mine tailings dumps (Gao and Bradshaw, 1995).

AMD and ARD leaching process have the potential to enter fluvial and ground waters, tailings that interact with groundwater aquifers, the intersection that is between saturated and unsaturated zones provides means for leachates of PHEs to enter ground water aquifers. Areas in which tailings and ground waters are in contact with oxidation zones allow for areas where leachates will be highest due to oxidation of sulphides (Figure 2.5) (Brown and Hosseinipour, 1991).

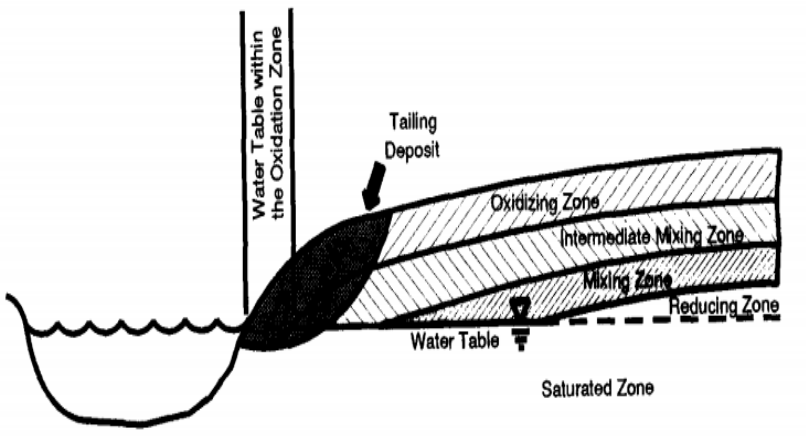

Figure 2.5. Interactions between leachates of tailings, fluvial systems and groundwaters (Brown and Hosseinipour, 1991).

There has been extensive research pertaining to leaching in mining environments (Shu and Bradshaw, 1995; Gao and Bradshaw, 1995; Zhu *et al.,* 1999; Lim *et al.,* 2009; Zheng *et al.,* 2012; He Xuwen *et al.,* 2015; Tuovinen *et al.,* 2018). Studies have found the most prolific PHEs in leachates such as highly soluble elements, As and Cd, exemplifying lower concentrations in leachates than less soluble elements such as Pb and Zn due to concentrations of these less soluble trace elements being present in higher concentrations in bedrock and soil sources (Gao and Bradshaw, 1995; Haggerty *et al.,* 1995; Shu and Bradshaw, 1995; Davies, *et al.,* 2016). Studies have found leachates from tailings can be reduced by covering the tailings with an inert substrate and that if capping if performed first substantial reductions in PHE loads from the leachates of mine tailings can be achieved (Gao and Bradshaw, 1995; Shu and Bradshaw, 1995). It is also possible reduce leachates from mine tailings using plants (Zhu *et al.,* 1999), but greatest results of leachates reductions can be achieved by a combination of planting and capping mine tailings.

2.5.2 Acid Mine Drainage (AMD) and Acid Rock Drainage (ARD)

AMD and ARD are result of sulphide oxidation (Equation 2.2) (Equation 2.3). Given their chalcophile nature, mineralized PHEs deposits commonly, although not exclusively, feature PHEs as sulphide minerals (lead sulphide- PbS – galena, zinc sulphide – ZnS – sphalerite, iron sulphide – FeS2- pyrite). Pyrite is an abundant element in non-ferrous ore deposits but is thought of as a gangue mineral in non-ferrous PHE deposits. AMD occurs due to atmospheric exposure at mine sites within drained mines and tailings, allowing oxygen present in the air and water to react with sulphide minerals such as pyrite (FeS_2) (Equation 2.2). ARD is the geogenic counterpart, the same chemical processes occur but due to natural geogenic uplift and erosion processes exposing mineral deposits rather than anthropogenic mining process exploiting mineral deposits (Marsay, 2018).

$$2FeS_2 + 2H_2O + 7O_2 \rightarrow 2Fe_{2+} + 4SO_4 + 4H_{+(aq)} \quad \text{(Equation 2.2)}$$

Pyrite+water+oxygen = iron(II)+sulphate+acid

AMD and ARD sulphide oxidation cause lowering of pH by releasing H^+ ions this increases the acidity of the mine water. Ferrous iron Fe2+ can then be oxidised to produce ferric Fe3+ (Equation 2.3). This is catalysed by *Thiobacillus ferrooxidans*, an Fe-oxidizing bacterium it plays a key role in accelerating oxidation of Fe and reduction of sulphur compounds (Leduc, 1994).

$$4Fe_{2+} + O_2 + 4H_+ \rightarrow 4Fe_{3+} + 2H_2O \quad \text{(Equation 2.3)}$$

Ferric iron (Fe^{3+}) and water produce Fe oxyhydroxides by hydrolysis which precipitate out of solution along with other coprecipitated minerals (Equation 2.4). Ferric Fe is a strong oxidizer and allows for further oxidation of ferrous Fe^{2+} which produces more H^+ ions and increases the acidity to a greater to extent in a cyclic nature, this allows for dissolution of other less reactive PHE ores including PbS - lead sulphide (Marsay, 2018).

$$Fe_{3+} + 3H_2O \rightarrow Fe(OH)_3 + 3H_3^+ \quad \text{(Equation 2.4)}$$

AMD and ARD increases PHE loading of point sources by reducing acidity and increasing solubility of PHEs, AMD and ARD has increased PHE loading on fluvial systems that fail water quality guidelines (Pozo-Antonio *et al.,* 2014; Marsay, 2018).

2.5.3 Circum – Neutral mine Drainage

Circum neutral pH mine water discharge occurs at mining sites with a carbonate-rich underlying geology and/or with a mineral deposit containing relatively small quantities of pyrite, and significantly reduces a mines potential to produce AMD (Warrender, and Pearce, 2007; Bearcock *et al.,* 2010; Palumbo-Roe and Colman, 2010; Marsay, 2018). Weathering of sulphide minerals such as sphalerite and galena in circum neutral water can release soluble cations, the chemical process for the dissolution of sphalerite – ZnS, (Equation 2.5) (Warrender, *et al.,* 2011). Sulphides are released by leaching sulphides produced in the dissolution of sulphide minerals.

$$ZnS_{(s)} + 2O_{2(aq)} \rightarrow Zn_{2+} + SO_4^{2-} \text{ (Equation 2.5)}$$

Circum-neutral mine waters demonstrate a sulphate-rich and Fe-poor aquatic environment and are defined by increased concentrations of PHE ions such as Zn, Cd and Cu due to their solubility at a wide pH spectrum (Warrender, *et al.,* 2011). Due to PHE ions solubility at circum neutral mine water sites such as Parc mine and at many other sites in North and mid wales recipient water catchments are often exceeding water quality standards define by the Water Framework Directive (WFD) (Environment Agency Wales, 2002). Circum-neutral mine drainage has been a problem in Wales, Studies have looked at Parc mine to define the current environment pollution at the mine site from leaching and erosion on the spoil heap that have received remediation during 1970s (Gao and Bradshaw, 1995; Davies, *et al.,* 2016).

2.5.4 Erosion

Erosion of particulate waste is of concern to water quality, erosion of tailings can cause a river to become heavily contaminated with particulate waste (Davies, 1987; Macklin and Klimek, 1992; Yi *et al.,* 2011; Singer *et al.,* 2013) Erosion can be exuberated by flood events, the hydroclimatic factors of river flow and stage will directly affect the rate erosion, increasing turbidity. Erosional outputs of wastes from mining are point sources of PHE contamination (Gao and Bradshaw, 1995).

Erosion of tailings can cause release of PHEs, erosion is an important factor in PHE release to the environment. Erosion of tailings is particularly of concern in areas with most erratic climates. Erosion of mine tailings can take place due to hydraulic processes and aeolian processes, both of which have the potential to distribute PHEs on a regional scale (Boussen *et al.,* 2010).

2.5.5 Tailings dam failures and PHE rich slurries

Tailings dam failures are a frequent occurrence in mine sites, they can cause loss of life, modelling has shown has been carried out of tailings dam failures to prevent future disasters (Wang *et al.,* 2018). Within Europe the primary cause of tailings dam failures and the release of PHE rich slurries is precipitation, seismic

liquefaction is also a driver of tailings failures elsewhere in the world. Generally, the majority, ~90% of dam failures occur at active mines and ~10% occur at legacy mine sites within Europe (Rico *et al.,* 2008).

2.6 Hydro-climatic factors and mine water chemistry

Hydro-climatic factors influence the rate and efficiency of PHE release mechanisms and due to this water quality of the recipient fluvial systems due to PHE loading proximal to PHE mining sites. Hydroclimatic variables include temperature, O_2 in gas and dissolved phases, point source and recipient stream velocity and flow, these hydroclimatic variables are influenced by conditions such as rainfall events, snowmelt, drought, atmospheric pressure and atmospheric temperature (Charlesworth *et al.,* 1996; Jarvie *et al.,* 2000; Environment Agency Wales, 2002; Brooks *et al.,* 2010; Palumbo-Roe and Colman, 2010; Anawar, 2013; Foulds *et al.,* 2014; Hosseini *et al.,* 2017). Changes in hydroclimatic variables occur temporally and can alter chemical properties that include:

2.6.1 Turbidity

Turbidity is a measure of particulates in water. Particulate PHEs are produced as a result of oxidation, hydrolysis and precipitation that take place as a result of AMD and ARD processes, ferric Fe^{3+} can be produced as a result (Marsay, 2018). Precipitation of ferric Fe can also cause other PHEs to coprecipitate. Increased turbidity in mine water can be due to precipitation that generally occurs as it is exposed to the atmosphere as it leaves a mining point source (Lawler *et al.,* 2006; Mativenga *et al.,* 2018). Increased turbidity can be an indicator of increased PHE load.

2.6.2 pH

pH has a direct effect on the solubility of mining contaminants low pH values can increase the solubility of PHE mine contaminants such as Pb, Zn, Cu, Al and Cd (Environment Agency Wales, 2002). As pH values raise above 3.5, precipitation of PHE contaminates can take place. At low pH <3.5, it allows for *Thiobacillus ferrooxidans* to be highly efficient which further lower pH ensuring PHEs are kept in solution (Leduc, 1994). As the pH increases when mine water leaves a mine due to mixing with river water precipitation of PHEs can occur. Values of pH correlate to the solubility of PHEs, increases in pH reduced the solubility of PHEs (Figure 2.6) (Jickells, 1997).

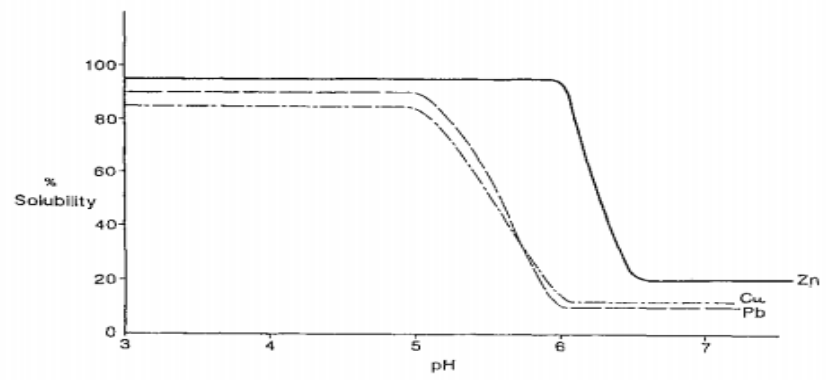

Figure 2.6. Relationship of PHE solubility and pH (Jickells, 1997).

2.6.3 Electrical conductivity

Electrical conductivity (EC) identifies how well water provides the transfer of electrical charge. The greater the amount of dissolve ions in a solution the higher the EC. EC can be used as indication of the total dissolved solids in a solution. EC there is controlled by the pH of the mine water generally the with decreased pH of mine water there is an increased PHE load of PHEs that will be indicated by the EC (The Water Framework Directive, 2015).

2.6.4 Redox potential

Redox potential (Eh) identifies the oxidising or reducing potential waters by analysing the extent of equilibrium, positive redox potential will indicate increased oxidation potential and a negative potential will indicate an increased reduction potential (Macpherson and Towsend, 1998). Redox potential is a measure of a water's potential to gain or lose electrons, excess electrons produce a negative charge and excess protons produce a positive charge. Oxidation states of water indicate whether there is an excess or lack of electrons.

2.6.4.1 Redox potential, pH and its influence on speciation

PHEs in a fluvial system are present in particulate or solute forms, with the majority of a PHE fluxes to a riverine environment in a particulate form, speciation can describe the delineation of solute and particulate PHEs (Pettersson *et al.,* 1993; Pettine *et al.,* 1994; Gao and Bradshaw, 1995; Zheng *et al.,* 2012). In aquatic systems PHEs are combined with inorganic and organic particles which then demonstrate a PHE complex. The amount of free and dissolved ions in water can define the speciation of a fluvial body. Speciation can define the amount of PHEs in complexed and adsorbed forms (Vega and Weng, 2013). Organic matter and ferrous oxides have the potential to reduce PHEs, while manganese oxides can oxidise PHEs. Solubility of PHEs is an important factor along with Eh, pH controls solubility and is often examined with Eh to define water environments (Figure 2.7) (Macpherson and Towsend, 1998).

Redox and pH are primary properties controlling the extent of release of PHEs to the environment. Release of PHEs has been found to coincide with the release of Fe-Mg oxyhydroxides, low pH and reducing redox environments have been found to be favourable for the release of Fe-Mg oxyhydroxides and the subsequent coprecipitation of PHEs (Cao *et al.,* 2001). PHEs release that correlates with the release of Fe-Mg oxyhydroxides is due to adsorption leading to coprecipitation. PHEs in the exchangeable fraction can conversely decrease due to lowering of pH and redox (Cao *et al.,* 2001).

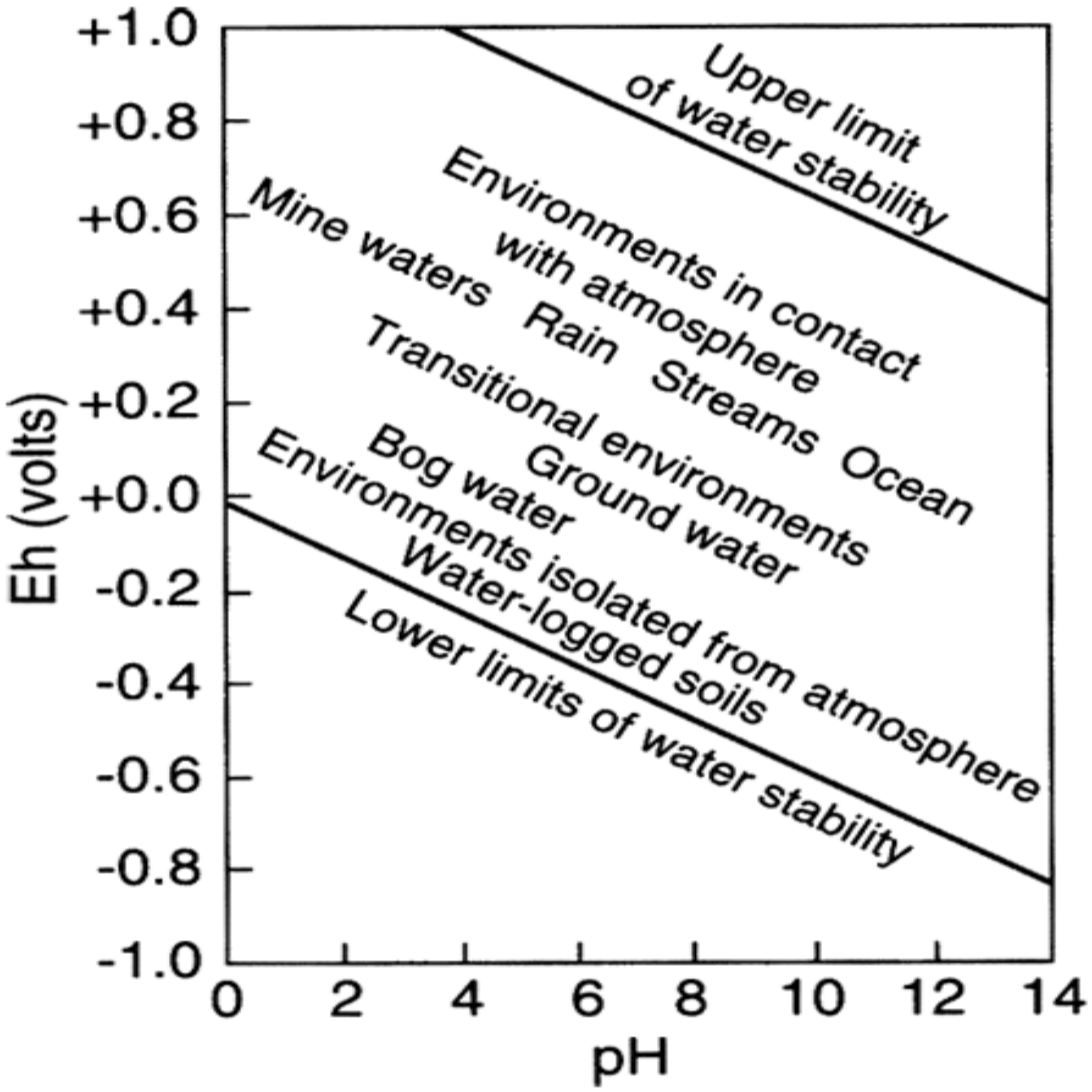

Figure 2.7. Eh-pH (Pourbaix) diagram exemplifying oxidising and reducing water environments (Macpherson and Towsend, 1998).

PHEs mobility within an environment depends on its speciation, weather a solute or particulate form is present within an environment (Bourg, 1988). Adsorption and precipitation processes can slow the rate at which PHEs travel through a fluvial system by slowing PHE exchanges. PHEs with organic and inorganic particulates in the solute phase can increase the transmission of PHEs downstream. PHEs can either be transported by convection dispersion and diffusion processes while in complexed and free forms and by solid-particle and solid diffusion processes while in adsorbed or precipitated forms (Figure 2.8) (Bourg, 1988). Redox potential strongly influences speciation of PHEs in the fluvial environment during initial pollution whilst a mine is working and later after a mine has closed during remobilisation of PHEs in during periods of increased rainfall.

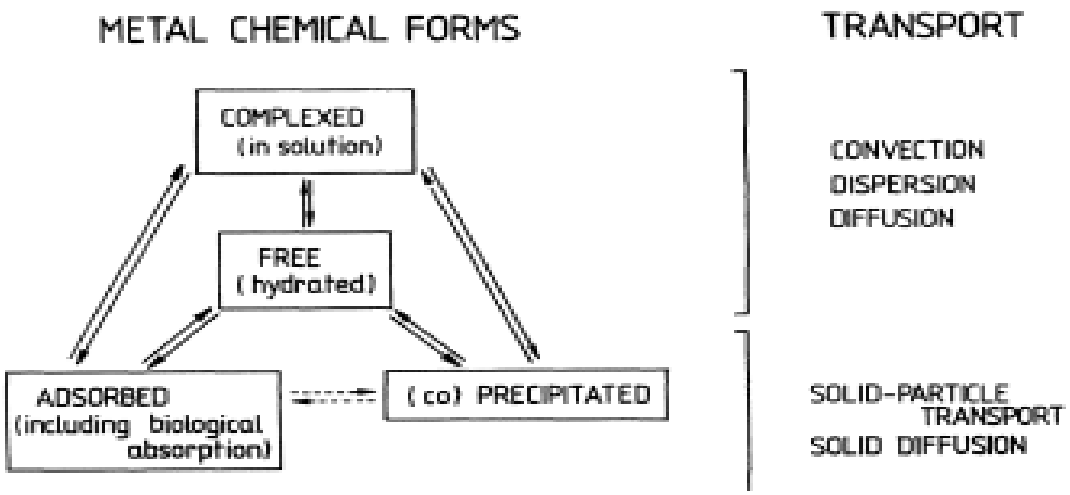

Figure 2.8. Speciation of PHEs in the fluvial environment (Bourg, 1988).

Oxidation of PHEs can lead to PHEs being present in the environment in particularly harmful toxic forms, such as chromium Cr^{3+} that can be oxidised by manganese oxides to Cr^{6+}(Whalley *et al.,* 1999). Cr^{3+} is a required trace element and Cr^{6+} is a carcinogen, this exemplifies that redox potential has the potential to influence the not only the speciation of PHEs between solute and particulate forms but also the form of PHEs present within a fluvial environment (Whalley *et al.,* 1999). pH and redox has the potential to affect speciation of PHEs, Fe from AMD has the potential to oxidise at the surface when mine waters exit an adit, the oxidation reduces the pH by releasing H^+ ions from release from H_2O during oxidation and this keeps Fe in solution as Fe^{2+} due to increased acidity (Figure 2.9). At mine sites of circum neutral drainage it is possible for PHEs to be present in oxidised potentially more hazardous forms (Bednar *et al.,* 2005).

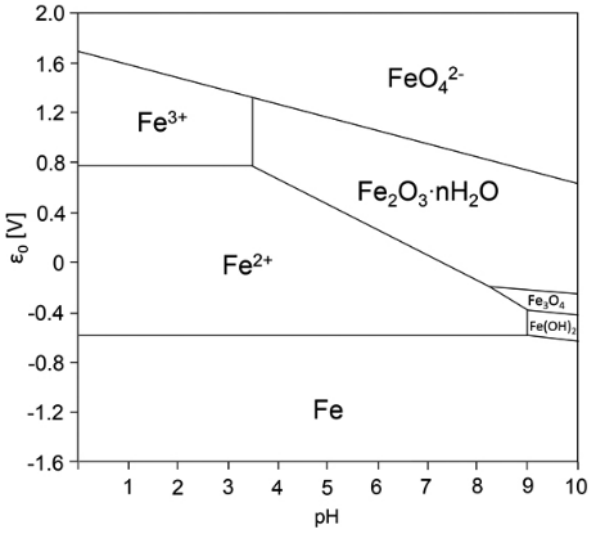

Figure 2.9. Eh-pH (Pourbaix) diagram exemplifying the relation of Fe speciation (Salgado *et al.,* 2013).

2.6.5 Dissolved oxygen

Dissolved oxygen can define the amount of gaseous oxygen (O_2) in mine water. It can be affected by flow rate and mine water temperatures. It is an important factor for aerobic treatment schemes. Dissolved oxygen is a required factor for water quality and there are minimum levels for maintain aquatic life defined by the WFD (The Water Framework Directive, 2015).

2.6.6 Temperature

Temperature of mine waters is controlled by air temperature. Changes in water temperature define physio-chemical equilibriums in rivers and thus control contaminant concentrations. Increased water temperature can increase PHE concentrations and reduce dissolve oxygen (The Water Framework Directive, 2015).

2.6.7 Flow rate

Flow rate can be affected by the rate precipitation on a catchment and is variable on an annual and daily scale, flow rate can affect turbidity, pH and PHE loading of a point source (Gzyl and Banks, 2007).

2.7 Temporal and spatial variability of PHE loads

PHE loads or fluxes refers to the amount of metal entering a fluvial system at a given point over a given period. Loads or fluxes can be calculated for varying temporal periods such as a year, day or hour. PHE load or flux calculations are based upon PHE concentrations per litre (i.e. mg/L) calculated against discharge (Cumecs m^3s^{-1}).

Hydroclimatic factors pertaining PHE load releases at a variety of spatial and temporal scales of the riverine environment can exemplify cyclic patterns dependent upon scale. Hydroclimatic factors can vary due to natural weather phenomena such as rainfall and storm events increasing flow and altering PHE loads entering a river (Guan *et al.,* 2016). Drought and rewetting can alter sediment associated loads affecting hydroclimatic variables such as turbidity, increasing particulate PHE loads in fluvial systems (Lin, *et al.,* 2018).

2.7.1 Temporal cycles of water chemistry and PHE loads

2.7.1.1 Vestigial acidity

First flush events have been identified by Younger (1997) as potentially occurring after the closure of a mine site. Post-closure waterlogging of mine workings and there subsequent mine water discharge are known as first flush events (Younger, 1997). A first flush of a mine site usually produces highly toxic water, due to acidity that has built up within the mine since closure and is classed as long-standing Vestigial acidity and can last ~10-40 years (Younger, 1997).

2.7.1.2 Juvenile acidity

Juvenile acidity forms from seasonal water table fluctuations which will in turn seasonally affect water quality (Younger, 1997). Increases in the water table over a seasonal temporal scale will be reflected in the hydroclimatic properties of a mine point source, as the water table increases pyrite oxidation will

increase which will reduce pH and increase factors that include EC, EH, turbidity and dissolved O_2 (Younger, 1997). Substantial acidity can be produced seasonally by periods of renewed pyrite oxidation with an increased water table (Younger, 1997). Reaction rates of a mine are limited to the rate of renewal of the mine water (Gzyl and Banks, 2007).

2.7.1.3 Annual cycles

Unpolluted upland streams exemplify increased dissolved PHE loading in later months of the year (July – December) during times of increased flow (Neal *et al.,* 2011). Changes from winter to summer months can exemplify a cycle of increased PHE loading during winter and later summer months and decreases in PHE load during months of low flow during spring and early summer. PHE concentrations of a fluvial system are higher in the summer months due to increased concentration of PHEs from a reduced flow but the total flux of PHEs to a fluvial system is commonly lower. In winter months the reverse takes place, PHE concentrations are lower due to dilution effects, the yet PHE flux is higher than in summer months (Lane *et al.,* 2003; Neal *et al.,* 2011; Ptacek *et al.,* 2014). Annual rainfall cycles affecting discharge vary due areas that experience monsoonal rains, decadal scale variability due to El Nino events that cause long term variation of wetter and drier years (Lane *et al.,* 2003).

2.7.1.4 Diel cycles

Studies have demonstrated diel cycles of PHE concentrations and hydroclimatic variables (Figure 2.10) (Moore *et al.,* 1996; Nimick *et al.,* 2007). It has been reported that PHE concentrations can alter by 500% in a diel cycle with hydroclimatic variables exemplifying neutral pH (Nimick *et al.,* 2007). There are several reported causes for diel cycle variation in and hydroclimatic variables and PHE concentrations, they include variation in PHE concentration input, diel flow variation, redox fluctuations, precipitation and dissolution processes, diel temperature fluctuations and biological photosynthetic processes (Nimick *et al.,* 2007). Photosynthetic reactions can alter the pH during the daytime, algal photosynthetic processes allow for cations to sorb onto them, this process can exemplify significant apparent lowering of PHE loads during the daytime (Rudall and Jarvis, 2012). During diel cycles of PHE concentrations can increase during night periods while pH and dissolved oxygen values fall (Figure 2.10). PHE concentration samples taken during the day can underestimate river fluxes of PHEs, this can lead to false annual fluxes of PHEs which may appear lower due to a regime of daytime sampling (Moore *et al.,* 1996; Rudall and Jarvis, 2012). Long term studies of diel cycle will enable hydroclimatic events such as rainstorms and snowmelt pluses and their relationship to PHE loading (Nimick *et al.,* 2007).

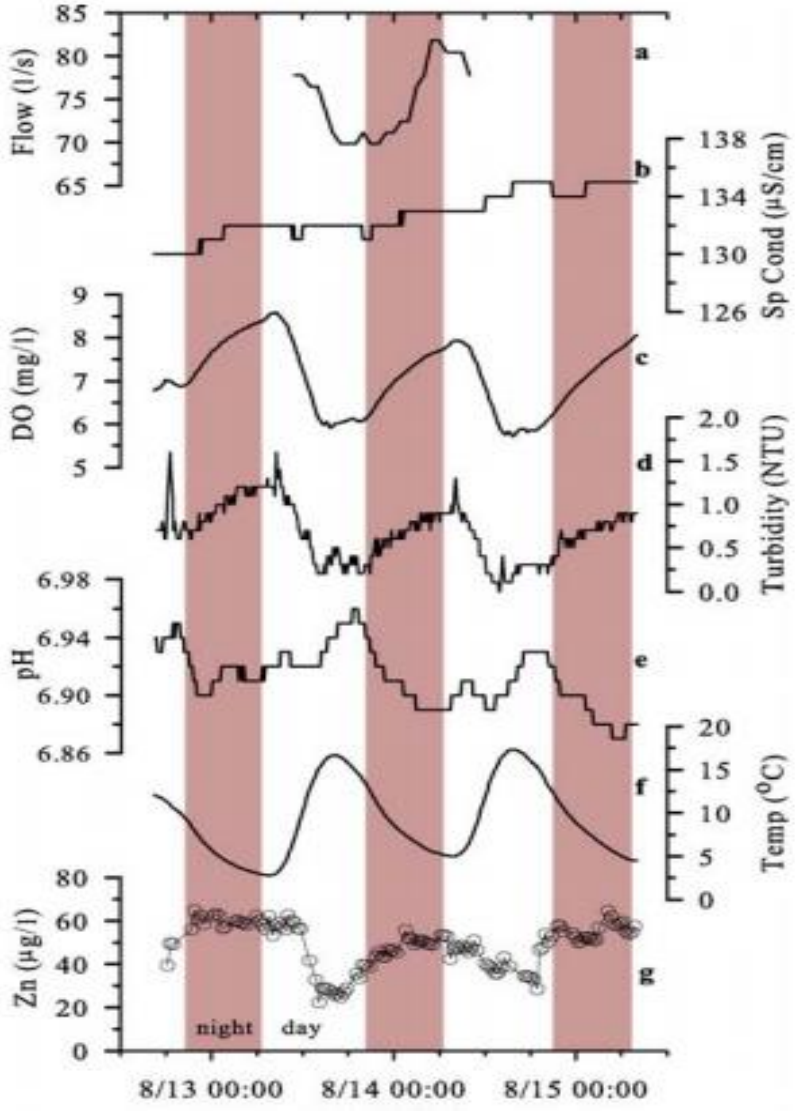

Figure 2.10. Example of a diel cycle at Zn mine at period of 24hrs (Nimick *et al.,* 2007).

2.7.2 Spatial distribution of PHE loads

2.7.2.1 Downstream distribution of PHE loads in solution

Solute PHE loads have the tendency to reduce in concentration downstream, processes of adsorption and precipitation remove PHEs from the solute load to the particulate load of a river (Brown and Hosseinipour, 1991; Pettersson *et al.,* 1993; Vega and Weng, 2013; Guan *et al.,* 2016). Solute loads can increase downstream with additional inputs of contaminated waters (Figure 2.11). Some instances have shown that solute loads do reach downstream at distances >10km from there sources such as the River Rheidol Zn contamination that extends >16k m of its river length (Fuge *et al.,* 1991).

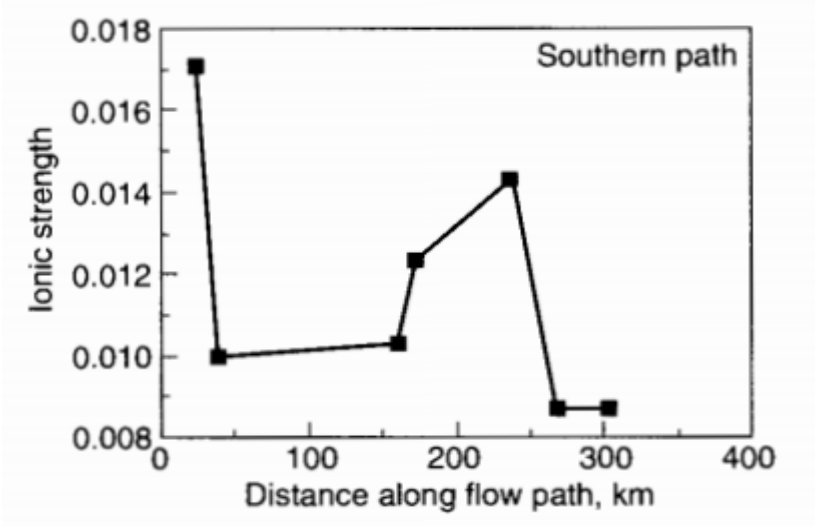

Figure 2.11. Ionic Strength indicating dissolved load of a river with an additional input of elements (Macpherson and Towsend, 1998).

2.7.2.2 Downstream distribution of particulate PHE loads

The majority of particulate matter within a river channel will deposit in channel as bottom sediments (Lin, *et al.,* 2003). Processes of adsorption and precipitation can incorporate PHEs with organic and particulate matter (Hartland *et al.,* 2012), which decreases the solute load and increases the particulate load, as stream or river energy decreases downstream particulates will be deposited as in channel and floodplain sediments (Lin, *et al.,* 2003).

2.7.2.3 PHE load storage and remobilization within the fluvial system

PHEs will eventually be stored in the floodplain environment due to adsorption and precipitation process forming particulate matter in alluvial deposits. These sediments can be remobilised during storm events and flooding which can transport PHEs and sediments further downstream in alluvial channels until it reaches a confluence or estuarine environment (Lin, *et al.,* 2003; Hartland *et al.,* 2012). Previously stored deposits of PHEs and identification of pre and post anthropogenic inputs to a fluvial system can be identified by loading at sediment profiles of areas such as overbank deposits (Macklin *et al.,* 1994).

2.8 Environmental quality guidelines

2.8.1 Global

Environmental quality guidelines act as mean to quantify PHE concentrations in the environment, this gives a means of identifying water bodies at risk from excessive concentrations of PHEs. The World Health Organisation (WHO) have identified safe limits for drinking waters on a global scale, to reduce the risk of health relating problems from PHEs (Table 2.1).

Table 2.1. WHO limits for PHEs adapted from WHO drinking water quality guidelines (World Health Organization, 2011).

Chemical	mg/l	µg/l
Arsenic	0.01	10
Barium	0.7	700
Cadmium	0.003	3
copper	2	2000
Lead	0.01	10
Nickel	3	3000

2.8.2 UK

Environmental quality guidelines for the UK have been defined by the WFD, which have been enforced since December 2000 (Table 2.2). The aim of the WFD is to achieve good ecological status in all water bodies by means of a collaborative approach between local authorities and landowners (Environment Agency Wales, 2002). The WFD also identifies parameters of hydroclimatic variables stating values for pH, DO_2 and river temperature.

Table 2.2. Limits for PHEs in freshwater adapted from standards and classifications of the WFD (The Water Framework Directive, 2015).

Chemical	mg/l	µg/l
Arsenic	0.05	50
Copper	0.001	1
Iron	1	1000
Zinc	0.0109*	10.9*

*With addition of background concentration

2.9 Remediation techniques

Remediation techniques are methods that have been developed to clean up a river or fluvial environment. Remediation techniques look at various methods to remove PHEs from mine waters before entering the environment, systems can be either passive or active. Passive systems are low cost and maintenance whereas in comparison it found the active systems are expensive and are considered only for small-scale short-term remediation schemes with passive systems looked at as longer-term solutions.

2.9.1 AMD

2.9.1.1 Passive treatment systems

There has been a significant amount of research pertaining to passive remediation of AMD (Sierra *et al.,* 2013; Nancucheo *et al.,* 2017; Marsay, 2018). Recent research regarding AMD has looked at passive remediation using biotreatments. Biotreatments have looked at the use of chemical lime treatments and biological methods using aerobic wetlands and bioreactors (Nancucheo *et al.,* 2017). There has been a recent

treatment study has looked at using sulphate reducing bacteria in the presence of zero-valent Fe and Cu, the study demonstrated that this could by an encouraging technology in the future treatment of high concentrations of sulphate and PHEs (Hu *et al.,* 2018). A recent study by Muhammad *et al.* (2018) also looked at bioremediation using organic and inorganic reactive media that used a combination of limestone, mushroom compost, woodchips and activated sludge in conjunction with sulphate reducing bacteria. Treatment proved successful for sulphide PHEs such as Fe, Pb Cu Zn and Al removing ~87-100% but the system did not successfully remove Mn, suggesting that this system would not be suitable for point source enriched in Mn (Muhammad *et al.,* 2018). Mn exhibits differing redox chemistry to other PHEs which explains the need for differing remediation techniques Mn compared to other PHEs (Cao *et al.,* 2001; Lee *et al.,* 2002). There are advantages to biomineralization and sulfidogenic bacteria, systems are relatively inexpensive in comparisons to active treatments that use reagents and energy, research pertaining the microbiology of acid tolerant sulfidogenic bacteria is increasing our understanding and improving technology which is leading to new approaches of AMD remediation (Nancucheo *et al.,* 2017).

2.9.1.2 Active treatment systems

Active treatments of AMD have been the scope of recent research in Wales with trial of systems at Cwm Rheidol mine during 2018 (Rose *et al.,* 2019) and laboratory trails of the Dyffryn Adda at Parys mountain during 2017 (Morgan *et al.,* 2017). The innovative technology used at these sites has used a combined treatment using ultrasound and electrolysis to produce magnesium hydroxide to raise pH and precipitate Fe as Fe hydroxide and potentially coprecipitate other PHE contaminants in stable hydroxide form (Rose *et al.,* 2019). Although the system is expensive to maintain, due to energy costs in comparison to passive systems that do not used energy, it is outweighed by the potential recovery of economic PHE pollutants (Morgan *et al.,* 2017).

2.9.2 Circum Neutral mine water

2.9.2.1 Passive and active treatment systems

Research pertaining circum neutral mines and their remediation is moderate when compared to AMD and its remediation. There has been some research looking at novel approaches to remediation using pelletised recovered hydrous ferric oxide (Mayes *et al.,* 2009), freshwater biofilms (Jones *et al.,* 2013; Jones *et al.,* 2015) and limestone closed bed reactors (Nuttall and Younger, 2000a). Further high-resolution hydrochemistry research pertaining to circum-mine drainage would be beneficial to enable identification of suitable wide scale remediation to take place at circum-neutral mine sites.

Chapter 3 - Study Area

The study location of Parc mine is situated in North Wales and Cwm Rheidol mine is situated in Mid Wales (Figure 3.1). The sites of differing geochemical and geological environments, Cwm Rheidol (pyrite-rich, low pH) and Parc mine (carbonate-rich, circum-neutral pH) are representative of range of mine sites within Wales and the rest of the UK including areas of Cumbria (Jarvis *et al.,* 2015), Cornwall (Whitehead *et al.,* 2005) and Western Wales (Natural Resources Wales, 2016). The study of these differing geochemical and geological study sites will provide findings relevant to UK mine sites and globally for legacy sites of a similar nature and unregulated mine sites (Environment Agency Wales, 2002; Carvalho, 2017).

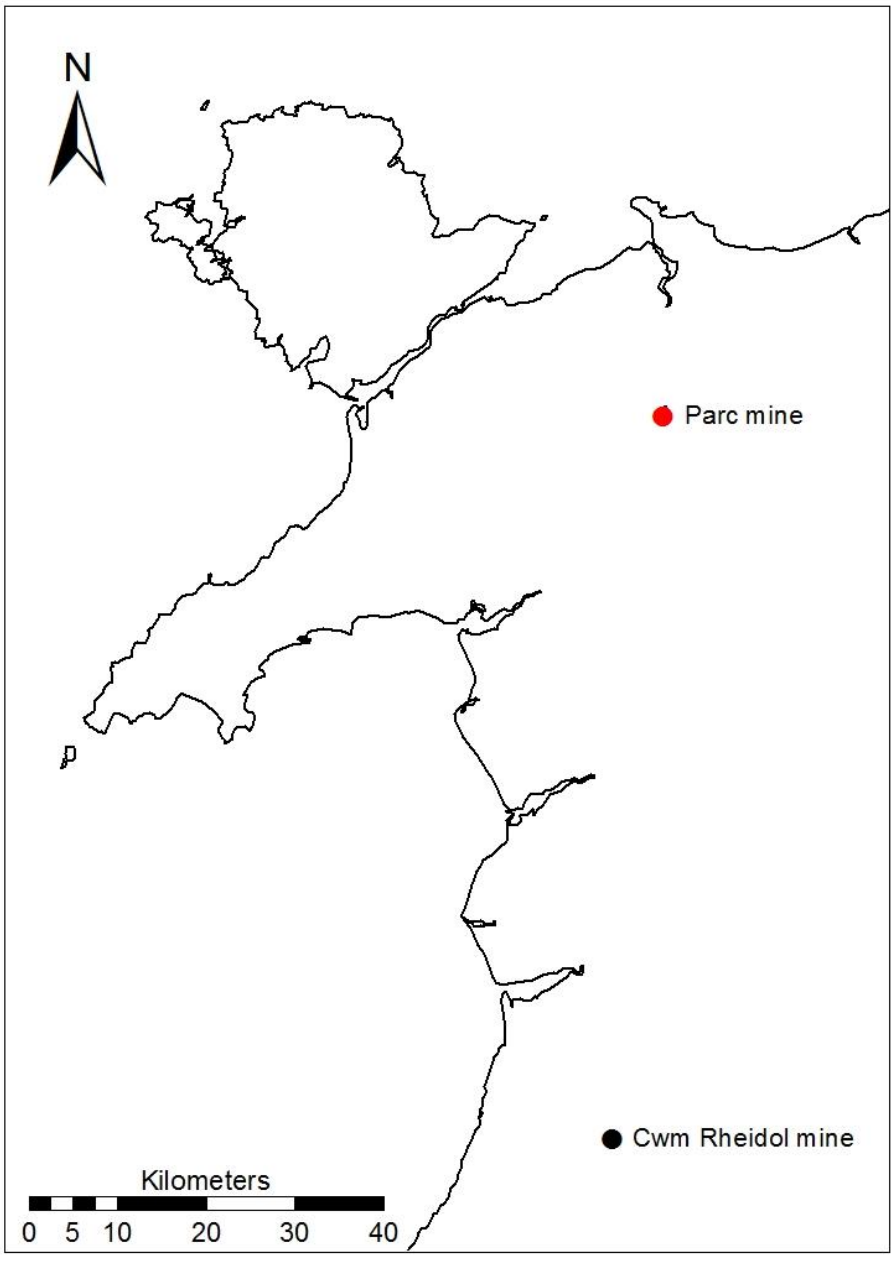

Figure 3.1. Parc and Cwm Rheidol mine locations Wales.

3.1 Parc mine

3.1.1 Location

Parc mine is a former Pb and Zn mine situated in the Gwydir forest, 2km west of Llanrwst in North Wales, and situated in the Llanrwst Mining District (Figure 3.2). Study sample locations are pre mine adit (A), Parc mine adit (B), post mine adit (C) and post mine tailings (D) (Figure 3.2).

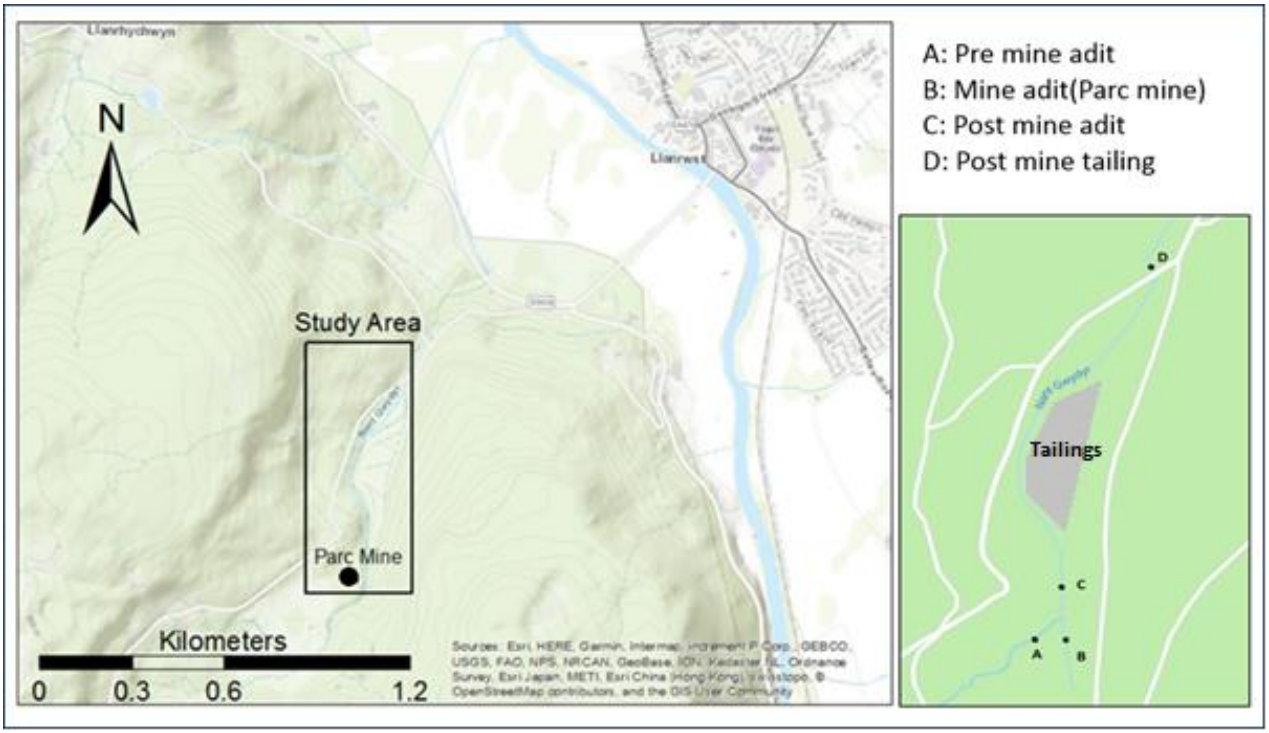

Figure 3.2. Location of Parc mine study area.

3.1.2 Geology

Parc mine exemplifies volcanogenic base-metal vein mineralisation in Ordovician volcanic and sedimentary rocks. The Llanrwst Orefield occurs in Ordovician strata proximal to large crustal fractures that have been active since the Silurian. Mineral deposits are Pb-Zn-Cu and occur sporadically in Silurian sediments, mineral deposits were produced over three mineralisation events (Haggerty and Bottrell, 1997). The mineralisation events took place during the middle Devonian and Tounasian (386-359 MA BP) with a later remobilisation of hydrothermal fluids during the Visean to Wesphalian (336-307 MA BP) (Haggerty and Bottrell, 1997). Dominant minerals present include sphalerite, galena and sulphide minerals. Sulphide minerals are present as fine-grained deposits in shales, tuffites and siltstones (Davies, *et al.,* 2016).

3.1.3 Mining history

Over 20 Pb and Zn mines operated within the Llanrwst Mining District in the early 20th century, with Parc (Figures 3.1 and 3.2) and Trecastell being the largest; producing over 6552 tonnes of Pb ore from 1892-1913 (Cooper *et al.,* 2000). Parc mine was operated until 1930s and reopened between 1952 and 1954 producing a total of 8 million tons of Pb and Zn (Shu and Bradshaw, 1995).

3.1.4 Post closure activity

The mining activity during the 1950s produced a substantial volume of tailings from ore floatation. A significant proportion of this material (totalling an estimated 250,000 tonnes) is stored in a tailings pile measuring c. 150x500x31 m situated on the banks of the Nant Gwydyr, situated in the centre of the study area (Figure 3.2). These tailings have been found to contain high concentrations of Zn and Pb (Shu and Bradshaw, 1995). Estimates from engineering topographical surveys suggests 13,000 tons of tailings material was eroded form the site between 1954 and 1978 (Gao and Bradshaw, 1995). A catastrophic erosion event in 1964 followed by continuous further erosion was the catalyst for remediation work in 1977-1978. To resolve this issue the tailings were remodelled and covered (Shu and Bradshaw, 1995). In 1992 a study by Gao & Bradshaw (1995) discovered that the tailings remediation had been successful, the land had recovered, and vegetation growth had taken place on the tailings. The PHE contamination entering the Nant Gwydir had also been reduced, but due to the nature of the cover used, gravel without a watertight cap in order to reduce costs, not eliminated. The Gravel cover still allows for leachate to enter the Nant Gwydir, at a lower concentration than pre-reclamation but at a level that exceeds the Water Framework Directive's (WFD) guidelines (The Water Framework Directive, 2015). It is estimated that capping would have reduced the PHE concentrations by a further 20% but the water contamination would still be greater than current guidelines by the WFD (The Water Framework Directive, 2015), further reduction would require engineering works (Gao and Bradshaw, 1995). Gao and Bradshaw (1995) also stated that the emissions from the mine audit are still unaddressed. In 2002 the Metal Mines strategy for Wales (MMSW) identified Parc mine as mine requiring further attention with regards to remediation (Environment Agency Wales, 2002).

3.1.5 Geomorphology

Parc mine is within the Gwydir forest located on western edge of the valley of Conwy (Figure 3.2), the geomorphology of the Conwy valley consists of a syncline that trends northeast to southwest, the valley has been subject to glaciation processes and post glacial alluvium deposition (Davies, *et al.,* 2016). More recently the area of the Gwydir forest has been subject to mining processes that have left a landscape scared by audits and tailings piles. The area of Parc mine is dominated by the large tailings pile produced in the 1950's which is now covered with grasses and acts as grazing pastures for farming.

3.1.6 Hydrology

Parc mine is situated on the Nant Gwydir a tributary of river Conwy. The Nant Gwydir drains from the South-West until it reaches Parc mine and the tailings pile where it is redirected around the outer limits of 1950s tailings pile and then flows on to the river Conwy in the lower Conwy catchment area (Figure 3.2).

3.1.7 Geochemistry

Parc mine water chemistry exhibits concentrations of Pb, Zn and Cd above at levels hazardous to life (Gao and Bradshaw, 1995; Davies, *et al.,* 2016). The Nant Gwydir exemplifies high levels of Zn (~3mg/l) and lower levels of Pb (~0.04mg/l), this is due to differences in the solubility of Zn and Pb and does not necessarily reflect concentration in sediment and bedrock within the mine. Low levels of Cd detected by Gao and

Bradshaw (1995) are an indication to a low level of Cd stored in the sediments and bedrock and are not due to low solubility unlike Pb (Gao and Bradshaw, 1995).

3.1.8 Biodiversity

The area of Parc mine encompasses vegetation that consist of non-metal tolerant and metal tolerant species, tree species in the area include *Alnus incana*, *Fagus sylvatica*, *Pinus sylvestris* and *Sorbus aucuparia* (Davies, *et al.,* 2016). Mosses including *Pinus sylvestris* and Rhytidiadelphus mosses and grasses are also in the area of Parc mine (Davies, *et al.,* 2016). Floodplain areas that surround the mine exemplify vegetation of meadow grasses that are not meatal tolerant and Parc mine tailings areas contain more PHE tolerant species of grasses and vegetation. To the North of the mine there is a reduced diversity in vegetation in comparison to the South of the study area (Figure 3.2). The area to the south near the Parc mine audit which has received no capping reclamation has proceeded to produce an environment with the potential of maintaining a Horseshoe Bat and rare metallophytes due to the presence of PHE tolerant vegetation that has inhabited the area that requires no maintenance.

3.2 Cwm Rheidol

3.2.1 Location

Cwm Rheidol is a Pb and Zn mine situated proximal to the river Rheidol near Aberystwyth in Mid-Wales, Cwm Rheidol mine adit discharge encompasses the mines of Ystumtuen, Penrhiw, Bwlchgwyn and Llwynteifi (Figure 3.3). Study sample locations are mine adits number 6 and 9 outlet (A), post mine outlet filtering (B), pre mine adit on the Afon Rheidol (C) and post mine adit on the Afon Rheidol (D) (Figure 3.3).

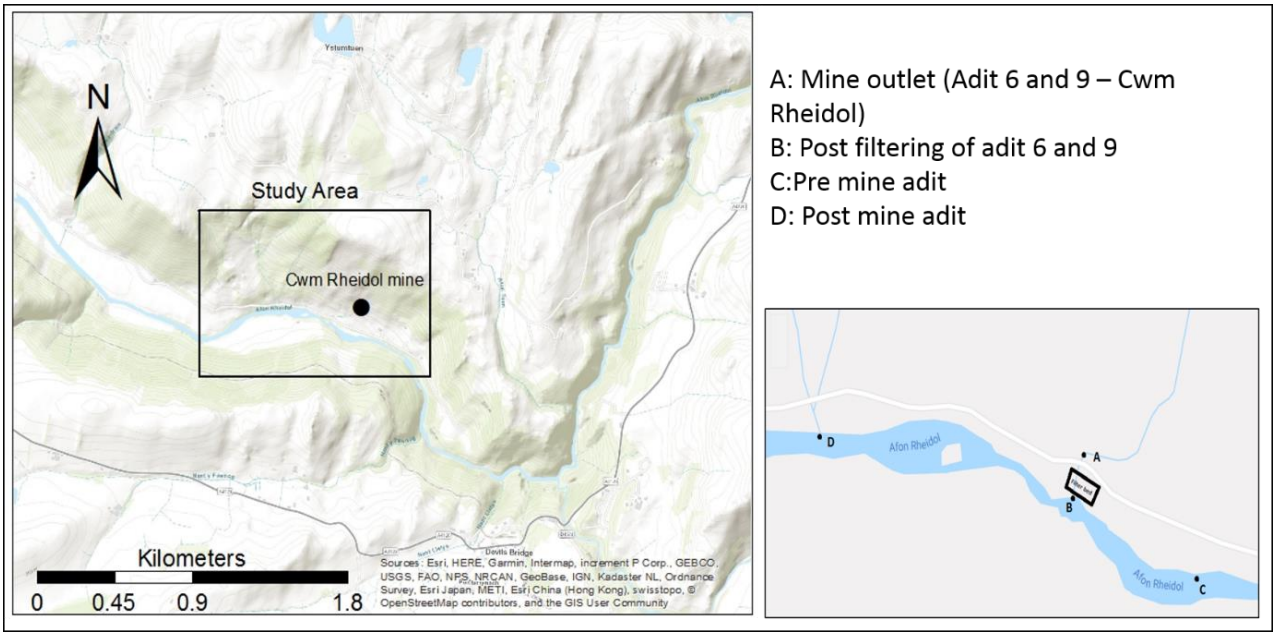

Figure 3.3. Cwm Rheidol mine site and the Afon Rheidol

3.2.2 Geology

Cwm Rheidol exemplifies base-metal and baryte veins in Lower Palaeozoic sedimentary rock. The mineral veins present in the area of Cwm Rheidol are situated in an area defined as the Central Wales Orefield, they occur in Ordovician and Silurian strata dominated by turbiditic mudstones (Cooper *et al.,* 2000; Palumbo-Roe and Colman, 2010). The area has been subject to two periods of mineralisation consisting of an early and a late stage, the early stage produced fine grain minerals with traces of cobalt and nickel and the later stage produced coarse grained galena. In the later stage mineralisation took place in the same fault zones to the early mineralization stage producing brecciated deposits (Cooper *et al.,* 2000). The mineral vein at Cwm Rheidol is known as the Castell lode, which extends across 10km it has been worked for Pb and Zn and Cu, primarily Pb and Zn at Cwm Rheidol (Fuge *et al.,* 1991). Minerals are present as galena (PbS), sphalerite (ZnS) and chalcopyrite ($CuFeS_2$) (Fuge *et al.,* 1991).

3.2.3 Mining history

According to records, the area of Cwm Rheidol was first mined in the 18th century, but there is a history of mining in the area since the Bronze Age. The earlier mine workings above the area of Cwm Rheidol on the plateau in the Ystumtuen area in 1824 were diverted to audit No.6, which was added at Cwm Rheidol to drain the valley. The mine waters drained into the River Rheidol and later a second adit known as adit No.9 was added. The adits act as point sources of contamination draining mine waters enriched with PHEs from the Cwm Rheidol mining area and surrounding mines (Edwards and Potter, 2007). Peak production was in 1905, that year 1537 tons of Zn ore and 46 tons of Pb ore were mined, mining continued until 1914 when it closed, but some mining continued occasionally until the mid-20th century (Edwards and Potter, 2007).

3.2.4 Post closure activity

The construction of the Cwm Rheidol hydroelectric power during the 1960s altered the flow of the River Rheidol, reducing it past the Cwm Rheidol mine site, this led to a decreased dilution effect of the mine waters entering the River Rheidol. To address the problem of mining contamination entering the River Rheidol, a limestone filter bed was installed shortly after the hydroelectric construction in the 1960s. After initial effectiveness of the limestone bed removing PHEs from the River Rheidol in 1969 it became blocked and ineffective in removing PHEs due to an adit rupture from adit No.9, causing it to clog with ochre. Later remedial works to the filter bed were carried out to improve the effectiveness of the filter but were unsuccessful (Edwards and Potter, 2007). In 2002 the MMSW, created by the Environment agency identified Cwm Rheidol as mine requiring remediation of mine water to meet water quality standards defined by the WFD (Environment Agency Wales, 2002). Proceeding the MMSW in 2007 pilot trials were carried out, initial works to manage mine water flow were emplaced on the site (Edwards and Potter, 2007). By 2010 a trail Vertical Flow Pond (VFP) and pumping of mine waters was introduced and initial findings have found the system effective in removing heavy PHEs from the mine waters (Williams, 2014). In 2014 a full scale VFP scheme has been commissioned requiring an area of 5000 m^2, it has not yet been introduced and the site of Cwm Rheidol is currently still being filtered by the pilot scale VFP (Williams, 2014).

3.2.5 Geomorphology

The site of Cwm Rheidol is accommodated in an area of a glacial trough (Adams, 1963). The site has been subject various anthropogenic mining activities and the site of Cwm Rheidol today is an area containing structures and earthworks remaining from mining along with buildings dating from times of active mining (Environment Agency Wales, 2002). Today the site of Cwm Rheidol is dominated by two large pipes on the landscape that pump water to the pilot VFP. The area of cwm Rheidol is situated in the valley wall of Cwm Rheidol the adits No. 6 and No. 9 are highlighted by areas of ochre stained mine tailings where the mine water previously flowed before the installation of pumps. There are tailings piles situated on the valley wall and at the bottom of the valley wall that remain barren.

3.2.6 Hydrology

Cwm Rheidol mined is hydrologically connected to several other mines of the area all of which drain from the No.6 and No.9 mine audits of Cwm Rheidol, prior to remediation theses audits drained directly into the River Rheidol (Figure 3.4). Remediation work in 2010 pumped the mine audits No.6 and No.9 directly into a passive treatment scheme before entering the River Rheidol, which is still the pathway of the of the mine water to this day (Williams, 2014).

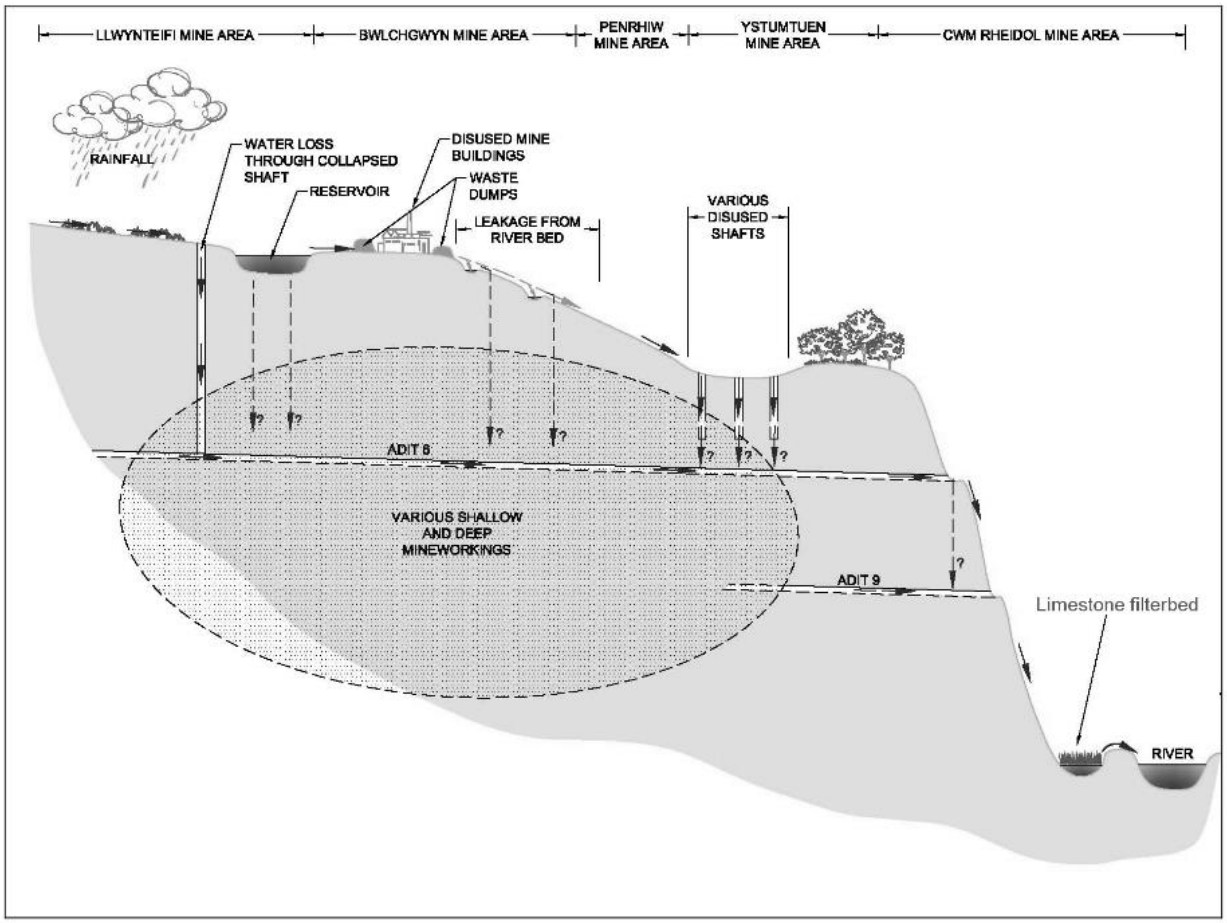

Figure 3.4. Hydrology of Cwm Rheidol and other proximal mine sites in the Rheidol valley (Edwards and Potter, 2007).

3.2.7 Geochemistry

Cwm Rheidol mine contains veins with significant deposits of pyrite and marcasite, the chemical weathering of these sulphide minerals through oxidation produces sulphuric acid which increases mine water acidity the resulting waters draining audits of Cwm Rheidol are very acidic, drainage waters have been reported with pH As low as 2.6 (Fuge *et al.,* 1991). PHEs in mine waters of Cwm Rheidol include Fe, Al, Zn, Cd and Ni. Levels of Zn, Cd and Pb are currently failing water quality standards defined by the WFD (Edwards and Potter, 2007; Williams, 2014; The Water Framework Directive, 2015).

3.2.8 Biodiversity

It has been reported that the River Rheidol fails standards set by the WFD for 16 km downstream from mine water inputs. Edwards and Potter (2007) reported that the mine water may be causing a negative effect on aquatic life (Edwards and Potter, 2007). The area of Cwm Rheidol is reported to have several lichens, some of which are rare in the context of the UK. There is reports of revegetation of silver birch on spoil areas also, although a vast area of spoil still remains barren of vegetation (Environment Agency Wales, 2002).

Chapter 4 - Methods

4.1 Field Methods

The Study will look to answer the research questions outlined in section 1.5 by completing the following objectives:

- Undertake synoptic sampling of waters to establish temporal variation of water chemistry over a range of timescales.
- Monitor hydrological conditions at the time of sampling.
- Quantify PHE fluxes (loads) and geochemical enrichment factors for PHE content in mine waters and recipient streams.
- Establish the variability in the percentage PHE removal by mine water treatment over a range of discharge conditions.
- Establish what metalliferous pollutants need to be remediated at each site.
- Identify differences in water quality variation between the two mine sites.
- To use the data to highlight future potential hazards.
- Gain an understanding of the required actions for remediation from the data.

4.1.1 Low resolution water quality monitoring and sampling

Measurements of pH, EC, Eh, and turbidity were measured in a laboratory within 24hrs of sampling. Dissolved O_2, stage, flow and temperature in the field at sample points A, B, C and D at Cwm Rheidol and at A1, B1, C1 and D1 for Parc mine (Figure 3.2, 3.3). Water sampling at Parc mine was carried out at the head of the Nant Gywdr (A1) proximal to the mine outlet (B1), post mixing of sample points A and B (C1) and downstream post the tailing area on the Nant Gywdr (D1) (Figure 3.2). Water sampling at Cwm Rheidol was upstream of the mine area on the Afon Rheidol (A), the mine adit No. 6 and No. 9 joint outlet (B), post filtration of the mine water from adits No.6 and No.9 (C) and post the mine mining area on the Afon Rheidol (Figure 3.3). Sampling carried out weekly at Parc mine and fortnightly at Cwm Rheidol mine between 27.11.8 to 28.03.19.

4.1.1.1 Water sampling

~30ml of 0.45 µm filtered water and ~30ml raw water was collected for inductively coupled plasma – optical emission spectroscopy (ICP-OES). Filtering was carried out to isolate the dissolved PHE load, with the 0.45 µm pore size traditionally used for this purpose (Pearce, 1991; Lee *et al.,* 2002; Kim *et al.,* 2007). Filter membranes were cellulose nitrate and samples were acidified in the field using 5 drops of 10% HNO_3. Raw water samples were collected to determine 'total' PHE concentrations in waters. An additional ~30ml of raw water was collected for anion analysis at each sample site A, B, C, D, A1, B1, C1 AND D1. Samples were collected in the centre of the river where flow was greatest, to ensure concentrations reflect the current values rather than sampling in stagnant areas with low or no flow, sampling in these areas may not give a

true reflection of the rivers PHE concentrations (Andersen, 2001; Kim *et al.,* 2007). Collected samples were collected as grab samples, the samples were collected water collection using a syringe. Anion samples were filtered directly into a sample bottle on site, samples were filtered to 0.2 micron to ensure no biological contamination and to remove any particulates (Michalski, 2018). During sample collection, syringes and sample bottles were pre-contaminated with the relevant sample (Andersen, 2001). 500 ml composite samples were collected at each site for laboratory analysis of pH, EC, Eh, and turbidity. Composite samples are a collection of several grab samples to ensure a homogenous is ascertained for each site (Andersen, 2001). All samples collected for PHE and anion determinations were stored at <5 °C prior to analysis (Kim *et al.,* 2007).

4.1.1.2 Dissolved oxygen (DO_2)

Dissolved oxygen was measured during water sample collection at sample points A, B, C and D at Cwm Rheidol mine (Figure 3.3) and at A1, B1, C1 and D1 at Parc mine, using a Lutron Dissolved Oxygen Meter PDO-519. The DO_2 meter was calibrated prior to each site visit to ensure accurate reading for each visit. The probe of the DO_2 meter was placed 5cm into the water in the centre of the flow at each site and left to stabilise for a period of 5 minutes before recording the recording the value, DO_2 measurements were recorded in mg/l.

4.1.1.3 Temperature (°C)

Temperature measurements were gained from the DO_2 meter and recorded at each sample site for all sample locations during DO_2 analysis. The probe of the DO_2 meter was placed in the water to a depth of 8cm to ensure its temperature probe was submerged and allowed to stabilize for 1 minute before recording the temperature in °C.

4.1.1.4 Discharge

River sections were surveyed at sample points A, B, C, and D at Cwm Rheidol and Parc mines (Figure 3.2 and 3.3). River sections were surveyed using a field tape to measure the width and a meter rule was used to measure each change in depth in relation to its bank full. From the cross-sectional data generalized cross sections were produced for sites that were not uniform channels (Cwm Rheidol sites C and D) so subsequent flow and stage measurements that were then taken during each sample trip could be applied to the cross sections to calculate discharge. Appendix A.1.1 and A.1.2 shows generalized cross section examples for sites C and D at Cwm Rheidol. Velocity was measure using a field-based water velocity meter and stage was measured using a meter rule at specific point identified during river cross section surveying which allowed accurate area calculations using the initial cross section data for each visit.

4.1.2 High-resolution water quality monitoring and sampling

In order to study shorter-term variability in water chemistry and discharge, water pH, EC, temperature, Eh, dissolved O_2 and turbidity was monitored at 15-minute intervals over periods of ~4-7 days at sample sites A ad D for Parc mine (Figure 3.2) and at sites C and D at Cwm Rheidol mine (Figure 3.3). Field

analysis of chemical properties was recorded using WTW Sentix 940 (pH), FDO p25 (DO_2) and TC 925 (EC) probes and associated WTW multi 3430 data logger and using the Aquaread Aquaprobe AP-700 and associated Aquaread Aquameter. Sampling locations reflect pre-mine water and post recipient stream water. At the same sites and at the same monitoring resolution, flow depth (stage) was measured using in-Situ Troll pressure sensors. The stage data was corrected for barometric pressure based on data collected concurrently using an in-Situ Baro-Troll logger. High resolution field probes were calibrated regularly throughout the study and prior each deployment to maintain the accuracy of data throughout the study and avoid any drift away from calibration that could potentially lead to data inaccuracies.

4.1.3 24-hour hourly water sampling

To provide data on short-term fluctuations in PHE and anion concentrations, hourly water sampling, using the procedure described above (4.1.2) and in conjunction with the water sampling method described in 4.1.1.1 and was conducted over a 24-hour period at Parc mine on 01.02.19-02.02.19.

4.2 Laboratory methods

Low resolution composite 500ml samples collected at both sites (Figure3.2 and 3.3) using the procedure outlined in 4.1.1.1. Low resolution composite water samples were analysed for pH, Eh, EC and turbidity within 24hrs of collection to ensure an accurate reading that reflects the pH of the water sample at time collection, due to the samples being raw unacidified samples if they are not analysed urgently PHE speciation can occur, which could potentially alter the values of chemical variables from time of collection (Kim *et al.,* 2007).

4.2.1pH

To analyse samples for pH within the laboratory environment composite water samples were analysed using a Hanna pH 209 meter and VWR pH electrode SJ 113. The pH electrode was calibrated using a 2-point calibration using Reagecon pH 4 and 7 buffer solutions. The composite water samples were placed into a 500ml glass beaker and the VWR pH electrode SJ 133 which was rinsed using deionised water before placing into the sample ensuring the electrode was submerged at least 10mm above the bulb of the probe. The reading on the Hanna pH 209 meter was then allowed to stabilise for 60 seconds before recording the reading.

4.2.2 Redox potential (Eh)

To analyse samples for Eh within the laboratory environment composite water samples were analysed for oxidation reduction potential (ORP) using a Hanna HI 991003 ORP meter and H1297 electrode. The ORP electrode was calibrated using Reagecon redox standard solution (250mv at 25°C). The composite water samples were placed into a 500ml glass beaker and the ORP electrode was rinse using deionised water before placing into the sample ensuring the probe was submerged at least 10mm above the bulb of the probe. The reading on the Hanna HI 991003 ORP meter was then allowed to stabilise for 180 seconds before recording the reading in mv.

The H1297 electrode is Ag/AgCl electrode to obtain Eh values from the ORP reading given a correction factor must be applied which correct values to what would be calculated using a standard hydrogen electrode, the correction factor for the H1297 electrode is +200mv (Vepraskas, 2002).

4.2.3 Electrical conductivity (EC)

To analyse samples for EC within the laboratory environment composite water samples were analysed using a Hanna EC 215 conductivity meter and Hanna EC electrode. The EC electrode was calibrated using Mettler Toledo 1413 µS/cm conductivity standard solution. The composite water samples were placed into a 500ml glass beaker and the EC electrode was rinsed using deionised water before placing into the sample ensuring the electrode was submerged at least 10mm above the bulb of the probe. The reading on the Hanna EC 215 conductivity meter was then allowed to stabilise for 60 seconds before recording the reading in µS/cm.

4.2.4 Turbidity

To analyse samples for turbidity within the laboratory environment composite water samples were analysed using a Hanna HI 93703 microprocessor turbidity meter. The meter was calibrated using HI93703-0 0 FTU and HI93703-10 10FTU solutions. The composite water samples were placed into a 10ml glass vial which was rinsed using deionised water and dried before placing each sample into the vial. The vial was then placed in the meter to take a reading and the lid of the meter placed over the vial. The reading on the Hanna HI 93703 microprocessor turbidity meter stabilised for 60 seconds before displaying the reading in FTU.

4.2.5 Anion analysis

To analyse samples for anion concentration, samples were collected at each sample site (Figures 3.2 and 3.3), collected samples were then diluted in the laboratory to a 5 in 1 ratio using deionised water to ensure good chromatograph resolution, running the samples neat on the ion chromatography instrument may results in overlapping of peaks which can yield inaccurate results (Figure 4.1).

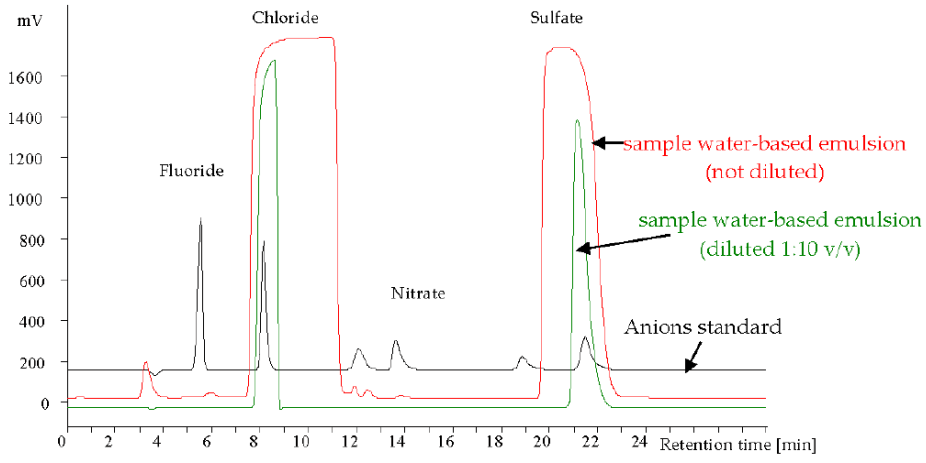

Figure 4.1. Example of a chromatograph of a sample that has been analysed undiluted and diluted (Michalski, 2018).

Dilution brings the samples concentrations into the correct range for analysis (within the range of the calibration concentrations). Filtering to 0.02µm and dilution preparation methods are required to allow samples to provide reliable results but also to reduce problems that could arise from unfiltered samples such as build-up of back pressures due to blockages within the ion chromatography instrument (Michalski, 2018).

The ion chromatography instrument used was a Metrohm 850 Professional IC. The instrument was set up with a Metrohm Metrosep anion exchange column and suppressed, samples were analysed at 35 ^{o}C and at a pressure of 10 MPa using a Na2Co3 and NaHCo3 eluent. The instrument detection method used was conductivity and the software used to run the Metrohm 850 Professional IC was MagIC Net. The method used follows the ASTM D4327-97 method (Appendix A.2).

To quantify the concentrations of anions within each sample a set of calibration standards was run to produce a regression equation that was applied to the samples that were subsequently run. A multi anion solution was used for calibration, figure 4.2 exemplifies the regression produced for sulphate.

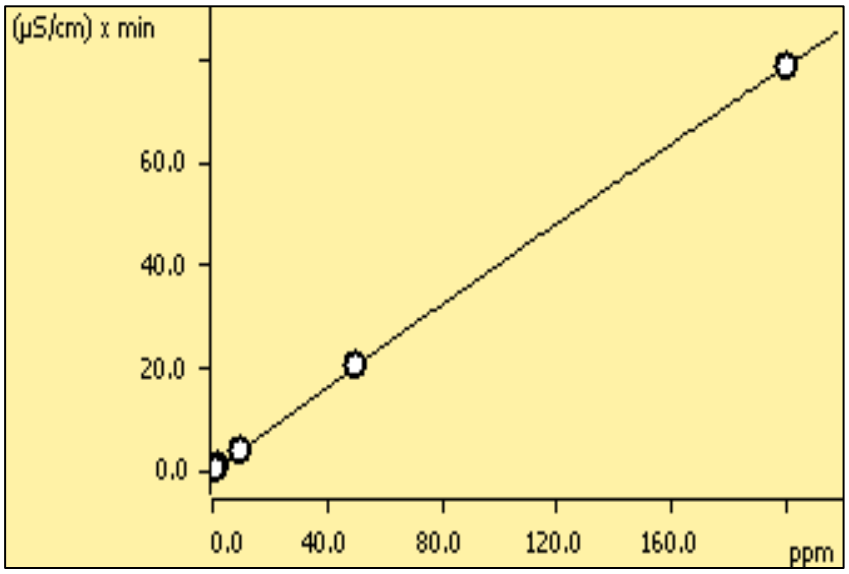

Figure 4.2. Regression of Sulphate standards for anion analysis.

Once samples were run, standards were reprocessed to ensure all anion peaks within the chromatograph were correctly analysed. Samples were reprocessed ensuring anion retention times were correct for the peaks present within the samples along with a 5% window for fluoride, chloride, nitrite, bromide, nitrate and phosphate. Sulphate required a 10% window due to high concentrations present within the samples producing a large peak (figure 4.3). Once reprocessing was complete sample concentration could then be exported for analysis.

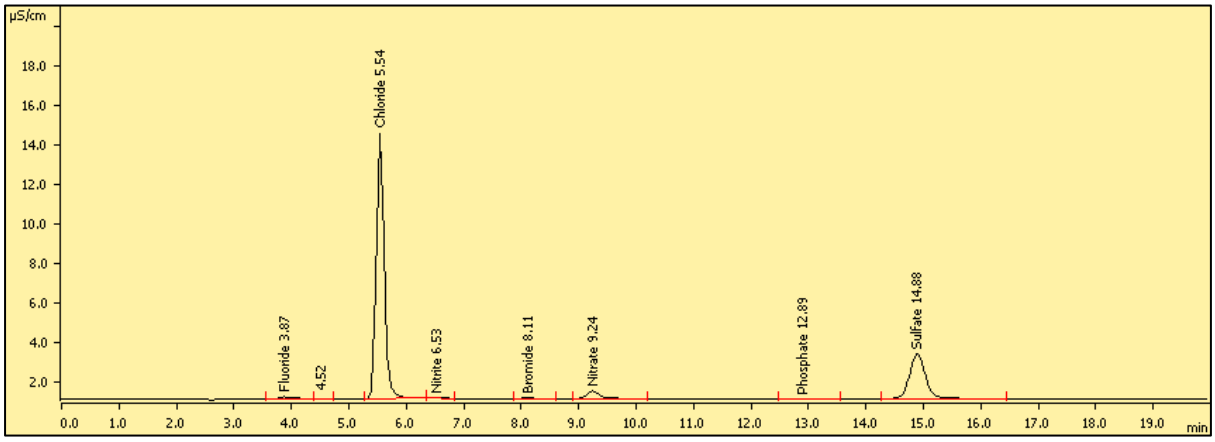

Figure 4.3. Chromatograph of a multi elemental anion standard.

4.2.6 Trace PHE and major cation analysis

Water samples were analysed for Ca, Mg, Cd, Cu, Fe, Pb and Zn by Inductively Coupled Plasma – Optical Emission Spectroscopy (ICP-OES). Samples were analysed using a Spectro Arcos optical emission spectrometer using radial plasma observation. Operating conditions followed the method from Spectro Arcos FHS22 (Table 4.1).

Table 4.1. Operating conditions of the Spectro Archos (ICP-OES)

Power	1280 W
Coolant flow	13 L/min
Auxiliary flow	0.8 L/min
Nebulizer flow	0.75 L/min
Plasma torch	quartz, 1.8 mm injector tube
Spray chamber	Cyclonic
Nebulizer	Seaspray
Sample aspiration rate	2.0 L/min
Replication read time	48 seconds

Calibrations were carried out using ESSLAB-808 multi elemental standard, diluted to produce a series of calibration standards at 0.05, 0.1, 0.5, 1, 2, 5 and 100 mg/L which were then run to produce regression equations for each element ensuring a correlation coefficient of >0.999 achieved for each element before analysis of samples (Figure 4.4). All water samples collected at both sites during low resolution sampling (Figures 3.2 and 3.3) and from the 24-hour sampling at Parc mine which was carried out at site D (Figure 3.2) were analysed.

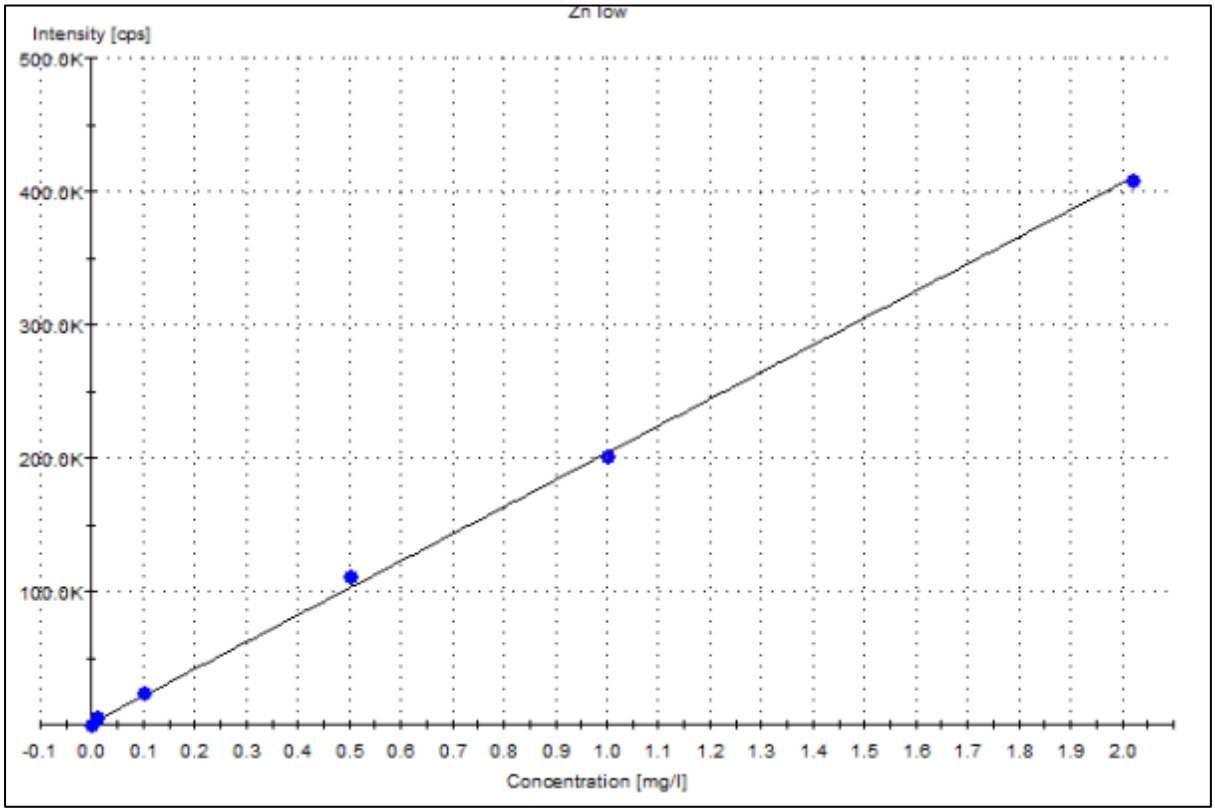

Figure 4.4. Regression of Low Zn standards for PHE and major cation analysis.

The limits of detection (LOD) and limits of quantification (LOQ) were calculated (Appendix A.3). The LOQ for Zn, Cd, Pb and Fe were 0.02, 0.01, 0.05 and 0.03 mg/L respectively. The equation for LOD and LOQ are also outlined below (Equation 4.1 and 4.2). The LOD and LOQ achieved is calculated from the Spectro Archos instrument, any reported concentrations of samples during analysis below the LOQ are not reliable and accuracy of data is in question, Figure 4.5 shows the wavelength for Zn and highlights the area of the peak that is quantifiable.

$$LOD = 3\ RSD_b\ c/SBR \quad \text{(Equation 4.1.) (Spectro, 2014).}$$

Where LOD is the limits of detection achieved, RSD_b is the standard deviation of 10 blank replicates, c is the concentration of the standard and SBR is the signal to background ratio (Spectro, 2014).

$$LOQ = 10\ RSD_b\ c/SBR \quad \text{(Equation 4.2.) (Spectro, 2014).}$$

Where LOQ is the limits of quantification achieved, RSD_b is the standard deviation of 10 blank replicates, c is the concentration of the standard and SBR is the signal to background ratio (Spectro, 2014). Results software allowed results to be reportable to three significant figures in mg/L, therefor any results below 0.01mg/L were and classified as 0.00 mg/L.

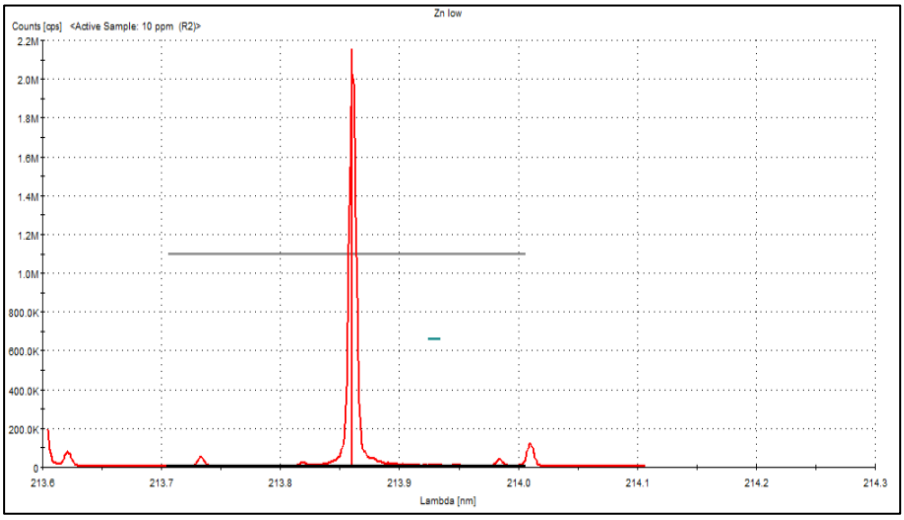

Figure 4.5. ICP-OES peak for Zn, it shows the wavelength (Lambda nm) on the x axis and fluorescence intensity (CPS) on the y axis, the horizontal line across the peak in the centre denotes the area that is quantifiable (above LOQ).

4.3 PHE flux calculation

To enable PHE flux calculations to be carried out synoptic sampling of up and down stream sites and flow inputs from mine adits were sampled at Parc mine and Cwm Rheidol study sites (Figure 3.2 and 3.3) following sampling methods adapted from Kimball et al. (2007a) (Figure 4.6) (Kimball *et al.,* 2007a). PHE flux (load) calculations provides a complete picture of PHE loading on a steam or river, PHE loads provide an overview of chronic toxicity and PHE concentrations provide an overview of acute toxicity. Synoptic samples were able to provide snapshot of PHE loads (Equation 4.3) and identify inflows from adits and additional unidentified ground water inputs from areas such as tailings. Tracer injection may also be used as a method to identify increases and losses in load (Kimball *et al.,* 2007b).

$$\mathrm{M} = \mathrm{CQ}(0.0864) \text{ (Equation 4.3.)}$$

Where M is the flux of PHE in kg d^{-1}, C is the dissolved PHE concentration in µg l^{-1}, Q is the discharge in m3 s^{-1} and 0.0864 is the conversion factor to obtain flux in kg $d^{-}1$ (Kimball *et al.,* 2007a). The conversion factor was adjusted to provide loads for a week, month and year.

The velocity-area was used for discharge and load calculations, tracer injection methods were impractical. Tracer injection methods require injections of large volumes of tracer, ~hundreds of litres, which was not practical for this study due to remote localities (Kimball *et al.,* 2007a, Kimball *et al.,* 2007b). The tracer method is more accurate with regards to load calculations and accounts for hyporheic flow to a greater extent than velocity area calculations (Kimball *et al.,* 2007a). In light on this tracer solutions do not always mix with the hyporheic zone and still present errors in load calculations (Kimball *et al.,* 2007a). Due to practicality velocity-area measurements were used, requiring only minimal transportable equipment. To reduce errors precautions were made, where possible, channelized river sections were used. Areas for channelized measurements (velocity and depth) were marked so precise locations could be used for each

returning measurement and applied to initially measured cross sections. Considering measures to reduce errors the velocity-area approach will still have inaccuracy due unaccounted losses in the hyporheic zone which cannot be eliminated but despite this the tracer method still produces inaccuracy due to unaccounted hyporheic losses but to a lesser extent (Kimball *et al.,* 2007a, Kimball *et al.,* 2007b).

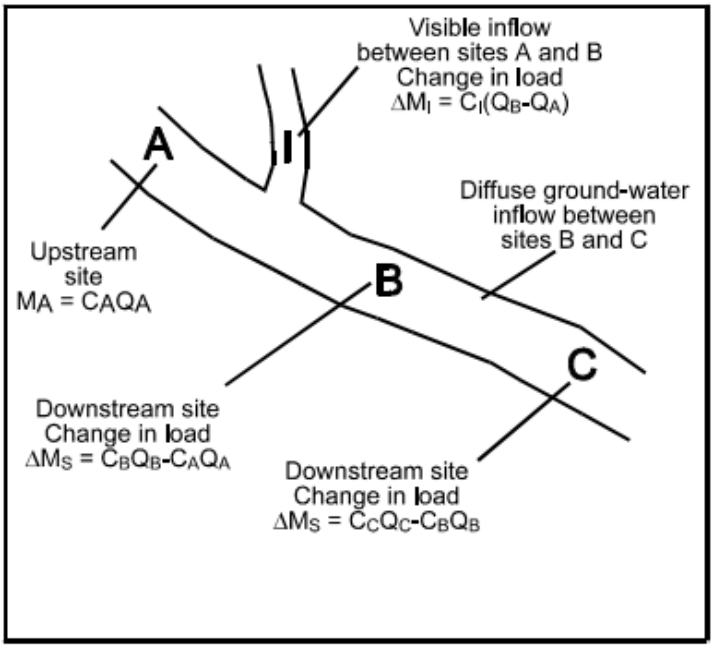

Figure 4.6. Schematic to exemplify Flux calculation and localities (Kimball *et al.,* 2007a).

To identify sources of PHEs from an inflow at sites such as site B at Cwm Rheidol and site B at Parc mine (Figure 3.2 and 3.3) i.e. between site A and B on figure 4.6 the following equation was used (Equation 4.4) (Kimball *et al.,* 2007a).

$$\Delta M_I = C_I(Q_B\text{-}Q_A)(0.0864) \text{ (Equation 4.4.)}$$

Where ΔM_I gives the load that can be accounted for from the inflow of the mine adit(s), C_I is the concentration of the input flow (i.e. sites B at Parc and Cwm Rheidol mine sites), Q_A is the discharge in L/s at site A and Q_B is the Discharge at site B also in L/s and 0.0864 is the conversion factor to kg/d^{-1} from mg/s^{-1} (Kimball *et al.,* 2007a).

To identify changes in net flux between site segments and to identify any additional groundwater inputs equation 4.5 was used.

$$\Delta M_{B\text{-}A} = M_B\text{-}M_A \text{ (Equation 4.5.)}$$

Where $\Delta M_{B\text{-}A}$ gives the change in sample load between the two sample sites, increases in the load (positive $\Delta M_{B\text{-}A}$ values) suggest additional sources of PHE contamination, for example from groundwater, and negative values indicate a loss of load between the sampling locations M_A and M_B are the loads at sample points A and B (or up and downstream). The total changes in load between sample sites provided a cumulative total of PHE load for each stretch of river in question at both sample sites (Kimball *et al.,* 2007a).

Contributions to the PHE load that were not sampled can be calculated using equation 4.6, this approached accounts for all additional sources of PHE input and it is not possible to distinguish quantities from specific sources (Kimball *et al.,* 2007a).

$$\Delta M_U = \Delta M_{B\text{-}A} - \Delta M_I \text{ (Equation 4.6.)}$$

ΔM_U is the load of the unsampled input in Kg/d^{-1}, $\Delta M_{B\text{-}A}$ and ΔM_I are identified in equations 4.4 and 4.5. Samples for low and high-resolution along with 24-hour samples were analysed for PHE flux.

4.4 Enrichment factor Calculation

Enrichment factor calculations were carried out at sites A B and D at Cwm Rheidol and at B C and D at Parc mine for low resolution sampling and 24-hour sampling at Parc mine site D. Upstream sites (site C at Cwm Rheidol and site A at Parc mine) were used as reference samples due to them representing conditions upstream of the mine audits at both sites. The reference element was used, due to the suitability of the data, magnesium being present in all samples and previous studies have used Fe as a reference element to analyse contaminated fluvial environments (Likuku *et al.,* 2013; Ediagbonya, 2015). The elements Zn, Pb, Cd and Fe were analysed for enrichment with a method adapted from Reimann and de Caritat (2005). The equation from Reimann and de Caritat (2005) uses a sample representative of background concentrations i.e. bedrock. For this study the upstream reference water samples were used in the equation background concentrations as a means of identifying enrichment (equation 4.7) (Reimann and de Caritat, 2005).

$$EF = \frac{[El]sample/[X]sample}{[El]upstream/[x]upstream} \text{ (Equation 4.7.)}$$

Where EF refers to the enrichment factor of the element in question. El refers to the element in question (Zn, Pb, Cd and Fe) and X refers to the reference element. Sample refers to the sample in question and upstream refers to the background upstream sample.

4.5 WFD Comparisons

In order to asses PHE concentrations within the fluvial environment of Parc and Cwm Rheidol mine sites comparisons have been made to standards and classifications set out by the WFD in 2015 (The Water Framework Directive, 2015). The WFD guidelines are for dissolved loads at a filtration of <0.045 µm, to make results comparable WFD guidelines have been comparted with filtered water samples. For Fe the concentration of 1mg/L has been set for fresh water long term concentration (Appendix A.4.1). Zinc additional concentrations are defined in Appendix A.4.1 at 10.9 µg/L in addition to the ambient background concentration (Appendix A.4.2), this is an addition of 4.1 µg/L, totalling 15 µg/L Zn limit for Cwm Rheidol and 2 µg/L total 12.9 µg/L for Parc mine. Lead concentrations were compared with maximum allowance control (MAC) for inland surface waters the limit defined for Pb is 14 µg/L (Appendix A.4.3). Cadmium is catchment dependant due to $CaCO^3$ levels (Appendix A.4.3). Appendix A.4.4 identifies the site-specific guidelines for Cd based from cation and anion analysis. To analysis any temporal changes in PHE concentration scatter graphs

on PHE concentration with time were produced. To asses any spatial variation n in PHE concentrations at specific sites for both mines, box plots were produced that represent the order of sampling at each site.

4.6 Graphical analysis

4.6.1 Trilinear plots

To establish water origins and asses water quality trilinear plots were produced. The Geochemists workbench® software was utilised. To produce trilinear plots that assess water quality and origins Ca^{2+}, Mg^{2+}, Na^{+}, K^{+}, HCO_3-, SO4- and Cl- were required, the concentrations of these were produced from cation and anion analysis. The parameters were then input into the software and this allowed for production of trilinear plots for low resolution monitoring of Parc and Cwm Rheidol, and 24-hour monitoring at Parc mine. Values of HCO_3- were calculation from Ca and Mg values obtained during cation ICP-OES analysis. To convert Ca and Mg to CaCO3 the following formula was used (Eqaution4.6) the equation was adapted (Boyd, 2015).

$$\mathrm{Ca}\left(\frac{100.08}{40.08}\right) + \mathrm{Mg}\left(\frac{100.08}{24.31}\right) \qquad \text{Equation 4.6. (Boyd, 2015).}$$

$CaCO_3$ values were then converted to HCO_3 this was calculated by multiplying $CaCO_3$ values by 1.22, for 100g of $CaCO_3$ there is 122g of HCO_3 (Basu, 2008). The calculation assumes that all alkalinity in the solution is HCO_3. The value obtained along with all other parameters was then entered into the Geochemist Workbench® software where the trilinear plot can be produced from the input parameters.

4.6.2 Speciation

To produce solubility diagrams for speciation of PHEs, activities of PHEs were calculated using The Geochemist Workbench® software – Speciate that can calculate activities and produce output activities for elements based from concentrations see Appendix A.5 for an example of the output obtained, PHE activities were calculated with recorded pressures and temperatures recorded during monitoring. The activities for Fe were then used with The Geochemist Workbench software® - Act 2 to produce a solubility diagram for Fe, this was then exported to Excel where a scatter Diagram was emplaced with the pH and Eh. Data for each site and for Parc mine, this was also repeated for Fe. For Pb, Cd and Zn solubility diagrams were adapted from Solutions, minerals and equilibria (Garells and Christ,1965). These were then imported to excel where scatter data for both sites was emplaced. All speciation diagrams were produced with generalized solubilities accounting for 1 ATM pressure and 25°C.

4.7 Statistical analysis

Statistical analysis was carried out using Microsoft Excel data analysis add on package. To define if the data was parametric or non-para metric, box plot analysis of PHE and chemical variables was carried out to assess the distribution of the data and define if the data is parametric or non-parametric. To assess differences in upstream and downstream chemical and PHE variable's, T-tests assuming unequal variance were carried out for Parc and Cwm Rheidol mine low resolution monitoring due to most of the data showing non normal distribution. To assess differences in PHEs at each of the sample sites, single factor Anova testing

was carried out for all PHEs at both sites for low resolution monitoring. To enable the relationships between hydroclimatic, chemical and PHE variables a range of Pearson's r correlations were produced for low- and high-resolution sampling was carried for both mines. The single factor Anova was also performed to assess correlations of hydroclimatic, chemical and PHEs for Parc mine 24-hour sampling. Significance was assessed at a level of <0.05.

Chapter 5 -Results & Discussion 1

5.1 Parc Mine – low resolution – weekly sampling

5.1.1 PHEs and WFD guidelines

During low resolution monitoring between 27.11.2018-28.03.2019 concentrations of Zn, Pb Cd and Fe in filtered samples were determined (Table 5.1 and Figure 5.1) at sites A, B, C and D at Parc mine (Figure 3.2). PHE concentrations have been compared to Water Framework Directive Standards for Specific Pollutants (WFD SFSP) values for Zn and Fe (Appendix A.4.1 and Figure 5.1). Iron has a standardised guideline whereas Zn guidelines are catchment dependent (Appendix A.4.2). Water Framework directive Maximum Allowance Control (WFD MAC) values were used for Cd and Pb (Appendix A.4.3), Cd guidelines are $CaCo_3$ dependant (Appendix A.4.4). Comparison of PHE concentrations with WFD guidelines will identify any potential PHE concentrations that do not conform to the values identified for good ecological status by the WFD (The Water Framework Directive, 2015).

Generally, a temporal variation in filtered PHE concentrations was found. Zinc was found to be above WFD SFSP guideline of 0.0129 mg/L at sites A, B C and D for Parc mine for the duration of the study, with the maximum Zn concentration (3.63 mg/L) occurring at site B. (Figure 5.1). Lead concentrations fluctuated between below and above the WFD MAC at site A B and C, with a maximum concentration of (0.4 mg/L); site D did not exceed the WFD MAC (Figure 5.1). Cadmium was found to exceed WFD MAC concentrations of 0.00045 and 0.0006 mg/L in 60% of determined samples for 40% of determined samples Cd was not detected. Iron was below the 1mg/L WFD SFSP for the duration of the study, with a maximum concentration of 0.19 mg/L at site B. (Figure 5.1). Importantly, at Site D, the bottom of the study reach, where PHEs are potentially being dispersed to the River Conwy, it is Zn and Cd concentrations that exceed WFD guidelines.

Maximum Zn and Cd concentrations from determined samples were found to be at site B adit, this was found of be the highest concentration in (Gao and Bradshaw, 1995) study with the for comparable sites. (Gao and Bradshaw, 1995) also identified a leachate pipe with higher concentrations of Zn and Pb than the adit, between sample sites C and D, this however is not reflected in site D concentrations for this study where there is generally a reduction in concentrations. In light of this additional PHE input between sites C and D may be identifiable when considering PHE load and dilution factors. Maximum concentrations of Pb and Fe were found to be at site C post adit mixing with the incoming Nant Gwydir (Site A) (Figure 5.1), this may be due to oxidation processes occurring after the mine water exits the adit, resulting in deposits of oxidised PHEs proximal to the mine adit (Brown and Hosseinipour, 1991). Control site PHE concentrations exhibited 100% of Zn, 12.5% Pb and 56.25 Cd concentrations above the WFD guidelines. Pearson r correlation analysed PHE concentrations, hydroclimatic variables and chemical parameters (Table 5.1) between filtered PHEs

correlations, filtered Pb and Fe had strongest significant correlation (0.418) and Zn and Fe had the second strongest filtered correlation (0.299) (Table 5.1).

Spatial distribution over the study area (Figure 3.2) is shown using box plot analysis of PHE concentrations, filtered Zn, Pb, Cd and Fe concentrations sampled between 27.11.18-27.03.19 (Figure 5.2, 5.3, 5.4 and 5.5). Mean values of Zn were 1.40, 2.94, 2.34 and 1.88 mg/L respectively for sites A, B C and D. Mean values of Pb were 0.0056, 0.0063, 0.0050 and 0.0044 mg/L respectively for sites A, B C and D. Mean values of Cd were 0.00375, 0.00375, 0.0044 and 0.0025 mg/L respectively for sites A, B C and D. Mean values of Fe were 0.0269, 0.0563, 0.0469 and 0.07 mg/L respectively for sites A, B C and D.

Previous research at the Nant Gywdr also sampled Zn and Pb concentrations at site A and found Zn concentrations of 1.55 mg/L and 0.29 mg/L for Pb (Gao and Bradshaw, 1995), the Zn concentration is within the interquartile range of this study (Figure 5.2) and are comparable Pb concentrations of the Gao and Bradshaw (1995) study are not within the interquartile range of this study. The lower Pb concentrations exhibited in this study for downstream site D could be attributed to a number of factors including analysis technique (Erickson *et al.,* 2018) and sampling regime (Kimball *et al.,* 2010). The comparison of Zn and Pb concentrations with the (Gao and Bradshaw, 1995) study suggests there is no change in Zn concentrations exiting the Nant Gwydir and possible reduction in Pb concentrations exiting the Nant Gwydir since 1995. The reduction in Pb concentrations exiting the Nant Gwydir may be due exhaustion on Pb leachates with the Adit and adjacent tailings dump (Younger, 1997). Control site A exhibited the lowest mean filtered Zn and Fe concentrations and site D exhibited the lowest Pb and Cd concentrations. Research by Gao and Bradshaw (1995) also found concentrations of a similar nature at the control site and confirms the findings of this study. This suggest that the controls site A may be subject to a geogenic bedrock source of Pb and Cd (Simpson *et al.,* 1996). Generally, PHE concentrations decrease downstream of the adit site B, suggesting the adit to be the primary source of contamination. Anova analysis confirms that Zn, Pb, Cd and Fe concentrations at sites A, B C and D are statistically significantly different ($p < 0.05$).

At downstream site D the mine water from Parc mine for Zn and Cd fall above WFD guidelines, this is also the case at the control site which is upstream of the mine water input at site B, this suggests that the Zn and Cd contamination may be resultant of another point source possibly geogenic, a likely reflection of the mineralisation within the Rheidol catchment (Fuge *et al.,* 1991).

Table 5.1 Pearson's r correlation of filtered (f), unfiltered (uf) PHE concentrations, chemical and hydroclimatic variables during low resolution monitoring at Parc mine.

	Fe (mg/L) f	Cd (mg/L) f	Pb (mg/L) f	Zn (mg/L) f	Fe (mg/L) uf	Cd (mg/L) uf	Pb (mg/L) uf	Zn (mg/L) uf	discharge (m3/s)	Stage (m)	Temperature (°C)	Turbidity (ntu)	DO_2 (mg/L)	Eh (V)	EC (mv)	pH
pH	0.139	0.087	-0.182	0.027	0.060	-0.129	-0.301	0.044	-0.274	-0.276	-0.129	-0.105	0.394	0.181	0.371	1
EC (mv)	0.377	0.005	-0.115	0.763	0.528	0.180	-0.010	0.753	-0.296	0.217	0.325	0.340	-0.244	0.144	1	
Eh (V)	-0.018	-0.435	-0.165	0.104	0.126	-0.278	-0.138	0.115	-0.271	-0.021	-0.443	0.081	0.030	1		
DO_2 (mg/L)	-0.094	-0.137	0.267	-0.370	-0.240	-0.334	-0.153	-0.360	0.123	-0.241	-0.274	-0.152	1			
Turbidity (ntu)	0.169	0.037	0.194	0.517	0.885	0.216	0.659	0.658	0.093	0.687	0.239	1				
Temperature (°C)	0.262	0.445	0.098	0.382	0.290	0.564	0.267	0.386	0.068	0.244	1					
Stage (m)	0.165	-0.008	0.082	0.534	0.645	0.192	0.765	0.588	0.305	1						
discharge (m3/s)	0.111	0.052	0.176	-0.265	0.039	-0.035	0.386	-0.207	1							
Zn (mg/L) uf	0.284	0.080	0.036	0.972	0.823	0.416	0.477	1								
Pb (mg/L) uf	0.239	0.269	0.272	0.424	0.635	0.325	1									
Cd (mg/L) uf	0.054	0.715	0.059	0.408	0.324	1										
Fe (mg/L) uf	0.216	0.119	0.096	0.685	1											
Zn (mg/L) f	0.299	0.083	0.016	1												
Pb (mg/L) f	0.418	0.073	1													
Cd (mg/L) f	0.212	1														
Fe (mg/L) f	1															

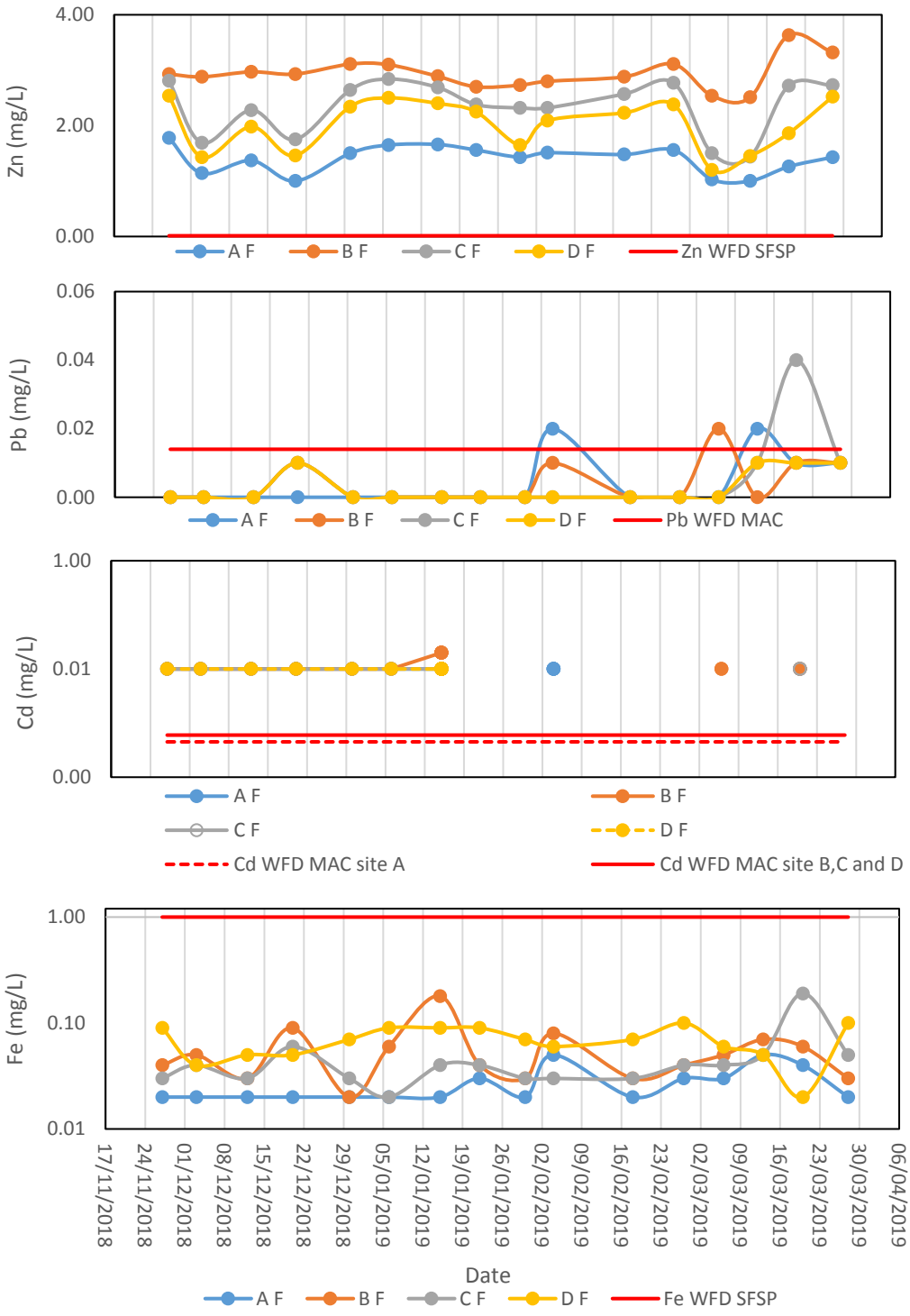

Figure 5.1. Filtered (0.45µ) PHE variability of weekly sampling carried out at Parc mine, Llanrwst – 27.11.2018-28.03.19. At sites A, B, C and D at Parc mine.

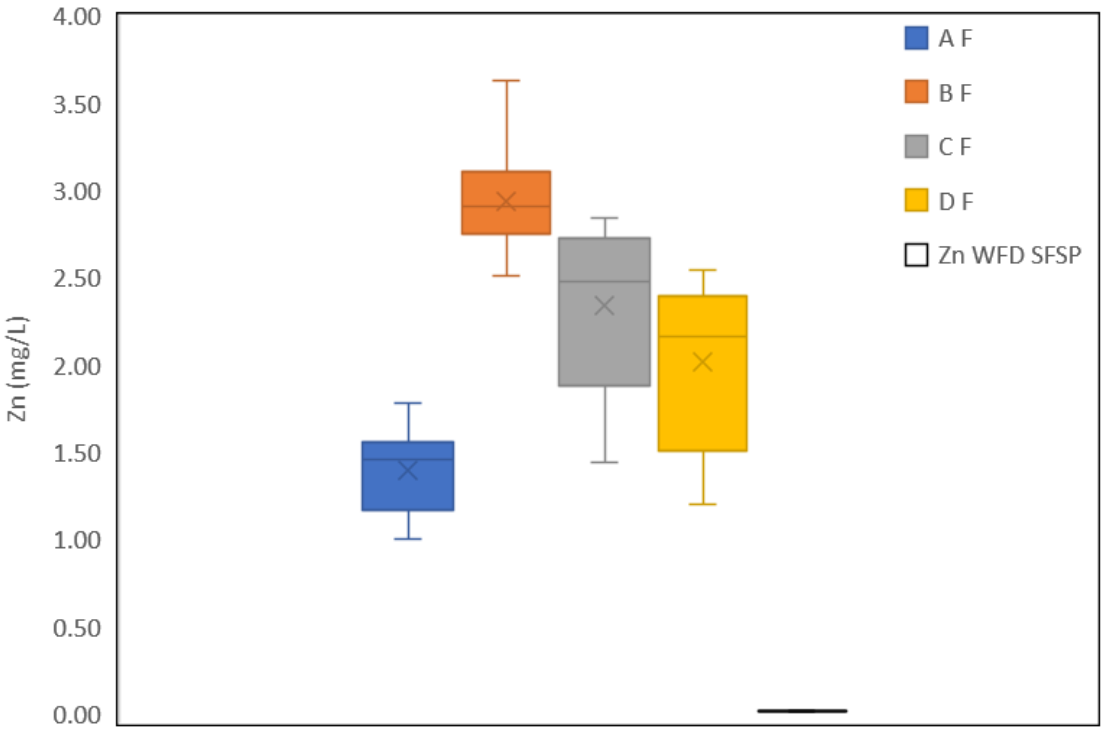

Figure 5.2 Filtered (0.45µ) Zn concentrations for sites A, B, C and D at Parc mine.

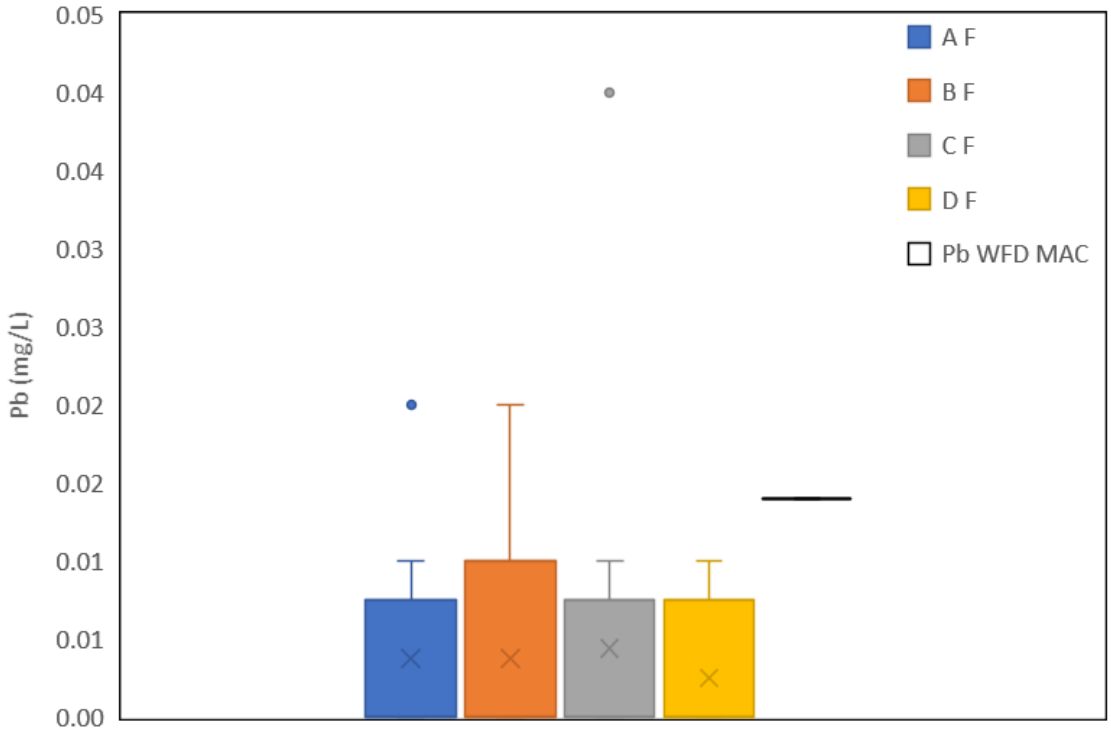

Figure 5.3 Filtered (0.45µ) Pb concentrations for sites A, B, C and D at park mine.

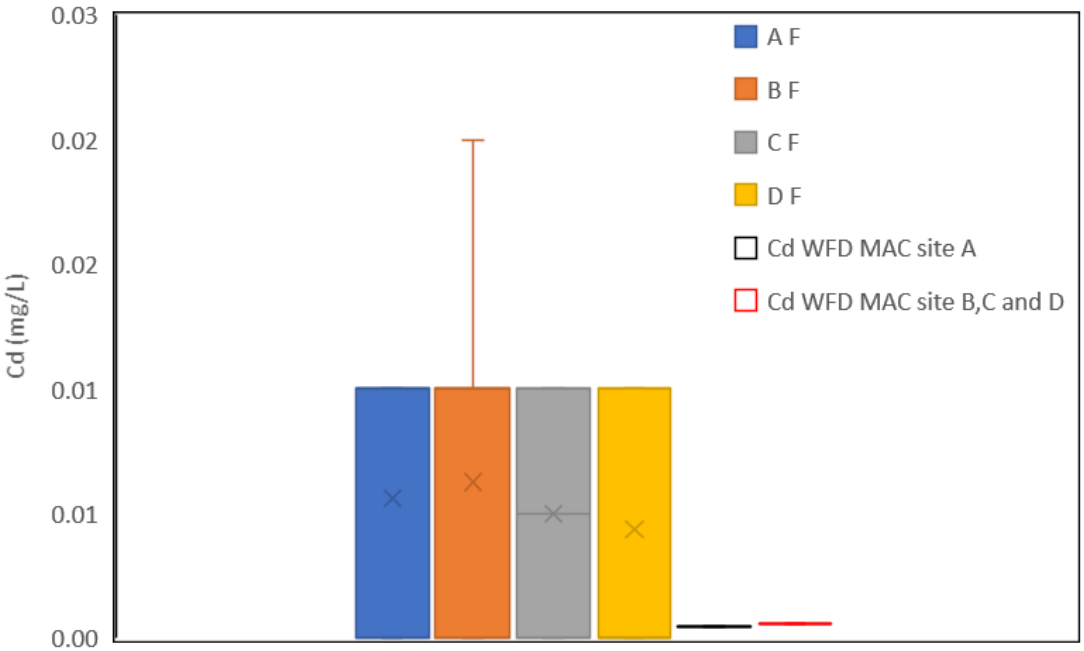

Figure 5.4 Filtered (0.45µ) Cd concentrations for sites A, B, C and D at Parc mine.

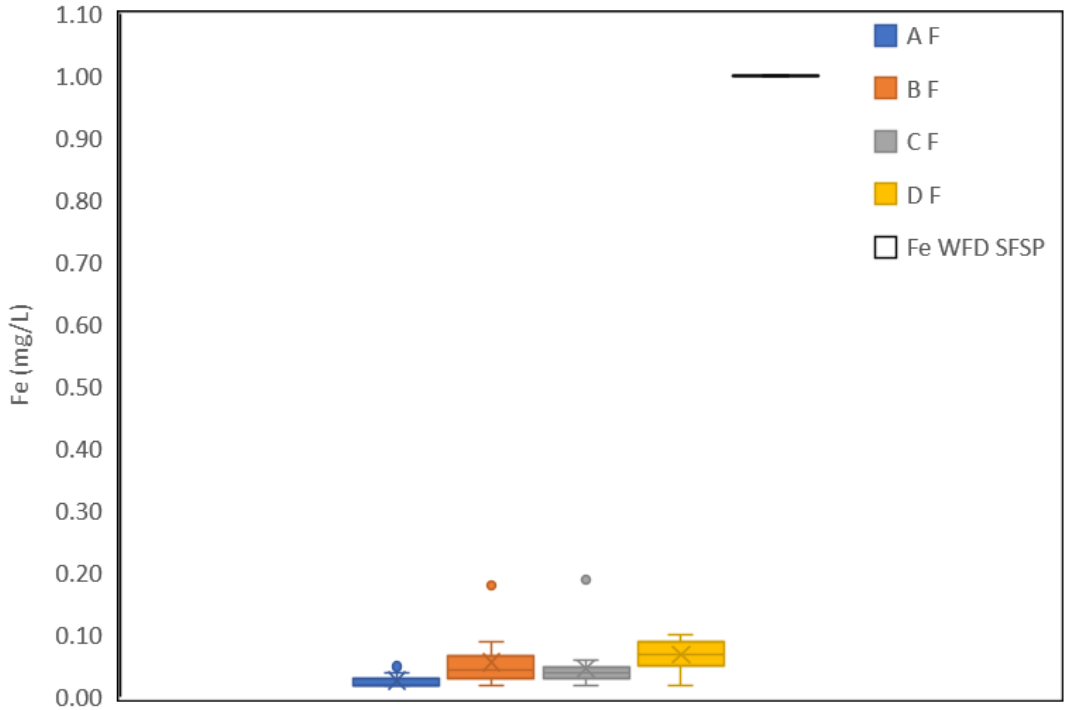

Figure 5.5 Filtered (0.45µ) Fe concentrations for sites A, B, C and D at Parc mine.

5.1.2 Total PHE concentrations and enrichment

During low resolution monitoring between 27.11.2018-28.03.2019 concentrations of Zn, Pb Cd and Fe in unfiltered samples were determined (Table 5.1 and Figure 5.1) at sites A, B, C and D at Parc mine (Figure 3.2). Unfiltered PHE concentrations were compared with filtered PHE concentrations to identify any temporal and spatial increases and decreases of particulate load. Unfiltered water PHEs also indicate the total PHE within the fluvial system. Unfiltered PHE concentrations at site D are of concern as they indicate the total of solute and particulate PHE in question entering the River Conwy. Comparison between unfiltered and filtered PHE concentration identify a temporally and spatial varied particulate-PHE load. Maximum concentrations of unfiltered PHEs were experienced at differing sampling times to maximum filtered concentrations. During periods of peak particulate PHE concentrations, increased PHE loads occur (Figure 5.1 and 5.6). Differences in particulate load at differing sites and times of the study may due to spatial and temporal changes in chemical properties that can alter speciation (Bourg, 1988; Gundersen and Steinnes, 2001; Zheng *et al.,* 2012).

Unfiltered PHE concentrations reached a maximum for site D of 3.31, 0.07, 0.01 and 2.15 mg/L for Zn, Pb, Cd and Fe, exceeding the WFD SPSS and WFD MAC values for filtered concentrations. This suggests the particulate concentrations contribute to Pb and Fe concentrations considerably at site D and are an important contributor to PHE total concentrations at site D. Maximum unfiltered Zn concentration during the study was at site B on 06.01.19 at 8.65 mg/L (Figure 5.6). The maximum Pb concentration during the study was found at site B on 06.01.19 at 0.30 mg/L (Figure 5.6). Maximum Cd concentration during the study was at site B on 06.01.19 and 20.03.19 at 0.02 mg/L (Figure 5.6). Maximum Fe concentration during the study was at site c on 06.01.19 at 9.27 mg/L (Figure 5.6). The increases and decreases in concentration throughout the period of the study may be identified by the significant correlation of unfiltered PHEs with temperature and stage (Figure 5.6 and Table 1). Pb and Fe exhibited particulate loads (>0.45µ) of 93.1% and 95.1% respectively.

Throughout the duration of the study maximum recorded unfiltered Zn, Cd, Pb and Fe concentrations were identified at site B adit for all PHEs. The data shows increased particulate load on 06.01.19 for all PHEs. Pearson r correlation testing showed Zn and Fe to have a strongest positive correlation and Pb and Fe had the second strongest positive correlation (Table 5.1).

During low resolution weekly monitoring between 27.11.18 -28.03.19 maximum unfiltered Zn, Pb Cd and Fe concentrations from the adit (sample site B) decrease generally downstream (Figures 5.7, 5.8, 5.9 and 5.10) site B is also where maximum enrichment occurs. Control site PHEs concentrations are lower for all Zn, Pb and Fe, Cd control site A concentration has a greater mean value for the for duration of the study than site D. Anova testing confirms that all sites A, B C and D for Zn, Pb Cd and Fe concentration value differences are significantly different with <0.05 p-value. The maximum enrichment is Fe at the adit site B enriched to a value of 37.85 and Pb enriched to a value of 7.31 mean enrichment of sites B, C and D also shows Pb and Fe

to be of the maximum enrichment with values of 5.96 and 26.75 respectively. Importantly the enrichment at site D where PHEs leave the area of Parc and go on to the Afon Conwy is 0.87, 0.99, 0.26 and 12.87 for Zn, Pb, Cd and Fe respectively.

In summary monitoring of unfiltered PHEs has identified significant concentrations of PHEs exiting the Nant Gwydir that exemplify a varied solute and particulate load with increased Pb and Fe at site D in comparison to upstream sites, this suggests that during transport Pb and Fe are subject to speciation from solute to particulate forms. Iron exhibits the greatest enrichment when exiting the area of Parc mine and adit site B exhibits the greatest enrichment within the Parc mine fluvial system.

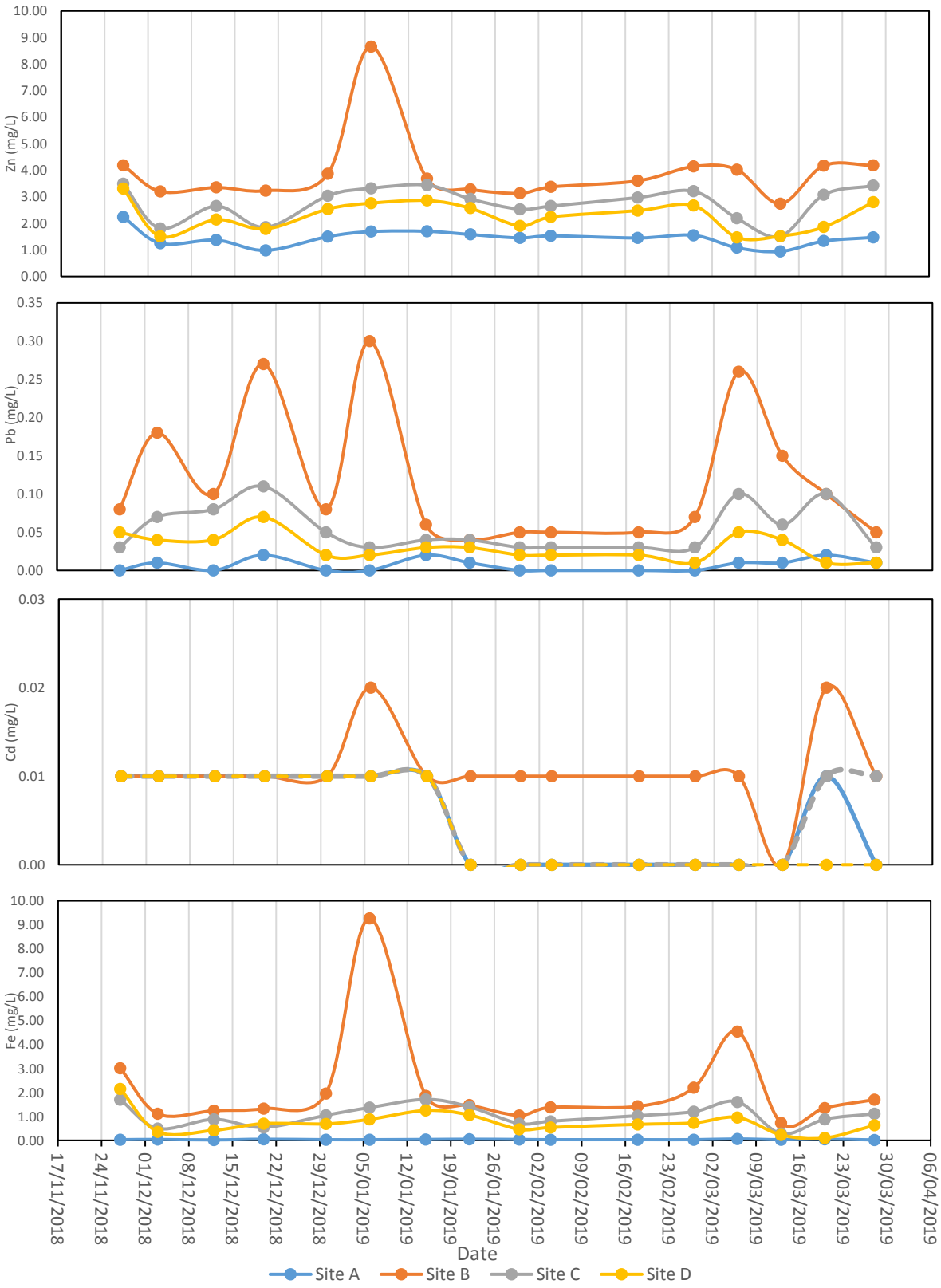

Figure 5.6. Unfiltered PHE variability of weekly sampling carried out at Parc mine, Llanrwst – 27.11.2018-28.03.19. At sites A, B, C and D at Parc mine.

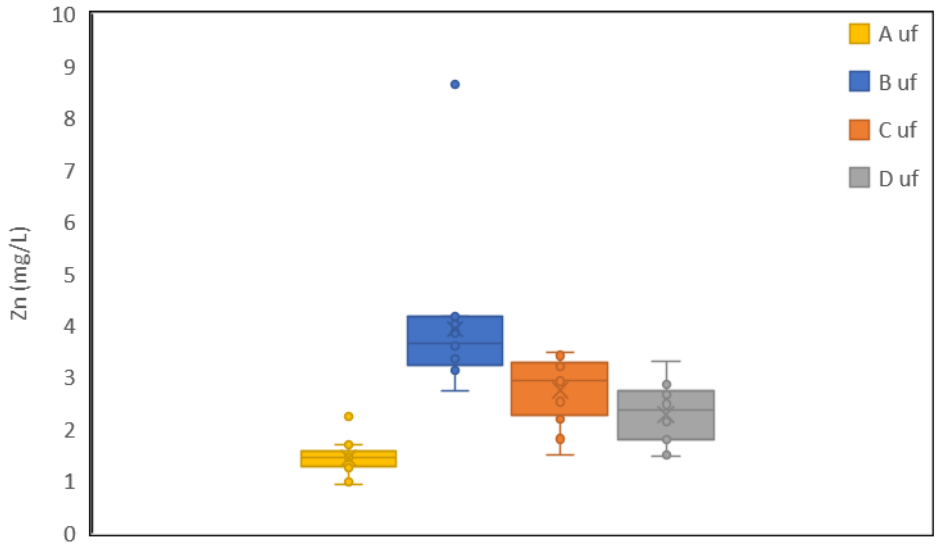

Figure 5.7. Unfiltered Zn concentrations of weekly sampling carried out at sites A, B, C and D Parc mine.

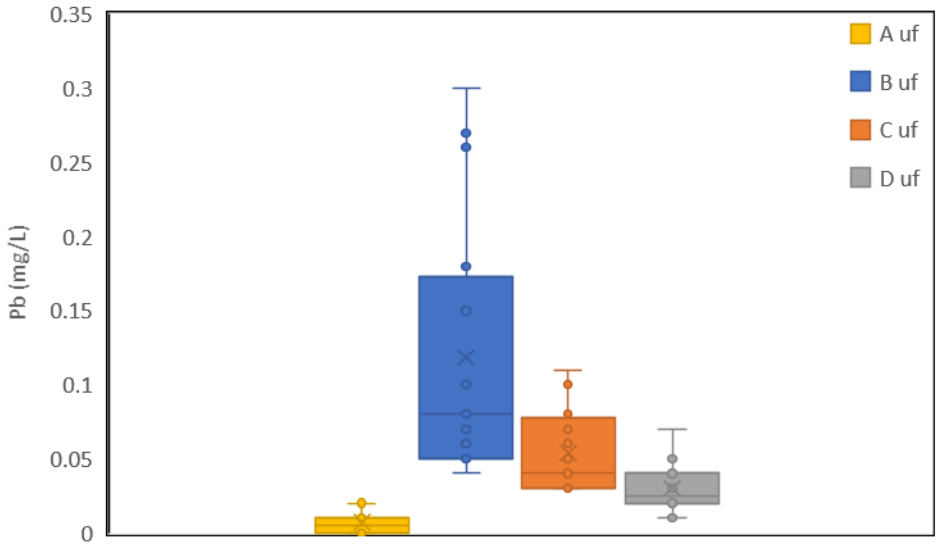

Figure 5.8. Unfiltered Pb concentrations of weekly sampling carried out at sites A, B, C and D Parc mine.

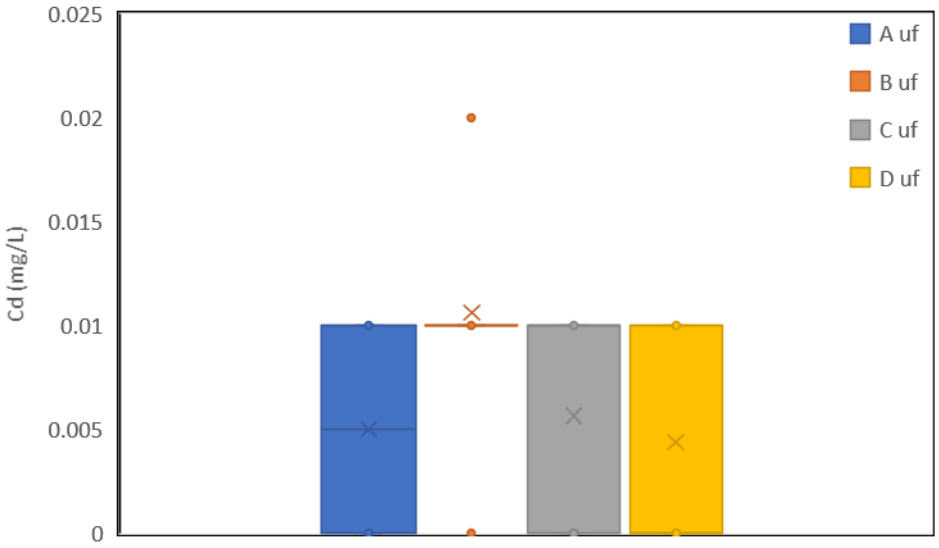

Figure 5.9. Unfiltered Cd concentrations of weekly sampling carried out at sites A, B, C and D Parc mine.

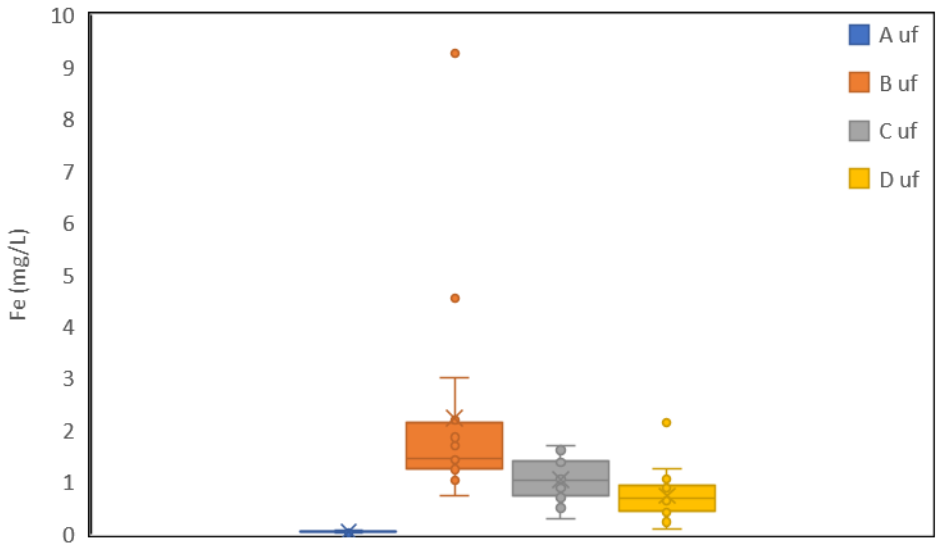

Figure 5.10. Unfiltered Fe concentrations of weekly sampling carried out at sites A, B, C and D Parc mine.

5.1.3 Hydroclimatic and chemical variables

During Low resolution monitoring between 27.11.2018-28.03.2019 chemical and hydroclimatic data was obtained on a weekly basis (Figure 5.11 and 5.21). Chemical and hydroclimatic variables were monitored as means of identifying any spatial and temporal correlations with PHE loading and concentrations. The obtained pH values varied on a weekly basis, mean pH values for the duration of the study ranged from 7.3 for control site A, 7.1 for adit site B, 7.2 for post adit mixing site C and 7.3 post tailings and adit site D. Pearson's r statistical analysis of pH shows significant $p < 0.05$ negative correlations with stage and discharge (Table 5.1) and is exemplified by Figures 5.11 and 5.12 on 13.03.19. pH shows a significant $p < 0.05$ negative correlation with unfiltered Pb concentrations (Table 5.1) and is exemplified by Figures 5.6 and 5.20. The correlation between pH and unfiltered Pb concentration can be explained by solubility; increasing pH will reduces solubility of Pb (Jickells, 1997). Unfiltered Pb concentrations have a significant ($p < 0.05$) positive correlation with discharge, where there is an increased discharge and there is an increase in Pb PHE concentration (Figures 5.11 and 5.1). Increased discharge can lead to decreased pH due to the influx of acidic rainwater, this influx of additional discharge has the capability of flushing oxidised PHEs contained within tailings, adits sites and flushing of juvenile acidity (Gundersen and Steinnes, 2001), this is likely to be what is happening at Parc mine during times of increased discharge.

Temperature has a significant positive correlation with EC (Table 5.1) and is exemplified by Figures 5.20 and 5.21 on 20.12.18. the relationship between EC and Temperature is further confirmed by unfiltered and filtered PHE concentration having significant positive correlation with temperature with the exception on filtered Cd (Table 5.1). EC also exhibits a significant negative relationship with discharge (Table 5.1) and is exemplified on 06.03.19-13.03.19 (Figures 5.11 and 5.12). During low resolution sampling at Parc mine control site A had a mean EC of 161mv, adit site B 281mv, post adit mixing site C: 231mv and after the tailings and adit: 271mv. The relationship found between EC, discharge and temperature is likely to be influenced by seasonal and diurnal changes in temperature and rainfall, which are confirmed to have an effect on electrical conductivity, an indication of PHEs within the fluvial system (Brooks *et al.,* 2010; Kimball *et al.,* 2010).

Redox potential during low resolution monitoring of Parc mine exhibited a negative correlation with filtered Pb and Cd (Table 5.1) but it is not possible to identify temporally on Figure 5.11 and 5.1. mean Eh Values showed little variation with values of 0.49, 0.50, 0.49 and 0.50 for sites A, B, C and D respectively. Redox showed a strong negative correlation with temperature and discharge (Table 5.1), this suggests with increases in temperature and discharge will reduce the redox potential, Figures 5.11 and 5.12 temporally exhibit the relationships between EH and temperature and discharge. This suggest at Parc mine increases in temperature and discharge decrease the oxidation of PHEs and inhibit PHE contamination (Cao *et al.,* 2001).

Dissolved oxygen shows significant ($p < 0.05$) negative correlation with temperature (Figure 5.11 and 5.12) and is confirmed by Pearson's correlation (Table 5.1). Dissolved oxygen also shows significant ($p < 0.05$) negative correlation with Zn, Cd and Fe and positive correlation with Pb. Filtered Pb also has negative

correlation with pH and EC with filtered Zn, Cd and Fe have a positive correlation with pH and EC. Dissolved oxygen mean concentrations were 11.24, 9.59, 10.41 and 10.22 for sites A, B, C and D. It is noted the adit exhibits the lowest DO_2 concentration followed by the post mixing site C. Dissolved oxygen exhibited a significant ($p < 0.05$) positive correlation with discharge. Dissolved oxygen levels at Parc mine are above minimum levels defined by the WFD standards and classifications of 2015 (The Water Framework Directive, 2015). The monitoring carried out at Parc mine suggests there is no impacts on biota from dissolved oxygen levels present at Parc mine.

Turbidity shows a significant correlation with stage and temperature (Table 5.1), with increases in temperature and stage there is an increase in turbidity as exemplified by Figures 5.11 and 5.12. Parc mine turbidity increases that coincide with changes in discharge and stage also show an increase in unfiltered PHE concentrations, suggesting that increased stage and temperature increase turbidity and thus PHE loading (Gzyl and Banks, 2007). Turbidity decreases at downstream sites C and D, may be due to dilution from additional discharge downstream or due to channel widening reducing flow rate and increasing deposition rates as the water travels downstream (Macklin and Lewin, 1989)**.** There is an increase PHE particulate load downstream, this does not correlate with turbidity, turbidity suggest a decrease downstream, this suggests that the increased turbidity upstream may be due to sediment or organic particulate matter upstream that is deposited as the channel widens (Macklin and Lewin, 1989; Madej, 2005). The hydroclimatic variables, stage and temperature have a correlation with turbidity and turbidity has significant correlation with unfiltered PHE concentrations, suggesting increases in discharge and temperature increase particulate loads identified by change in turbidity.

In summary temperature and discharge have significant correlations with chemical variables, the chemical variables have significant correlation with PHE concentrations, this confirms that spatially and temporally changes in hydroclimatic variables directly and indirectly control PHE concentrations and loads with the Nant Gywdr, temperature fluctuations account for short term changes in PHE concentration and loads, whereas discharge has a more varied effect on PHE concentration and loading over a period ~several days, this could be explained by varied rainfall regimes (Macdonald *et al.,* 2010).

Figure 5.11. Chemical variability of weekly sampling carried out at Parc mine, Llanrwst – 27.11.2018-28.03.19. At site A, B, C and D.

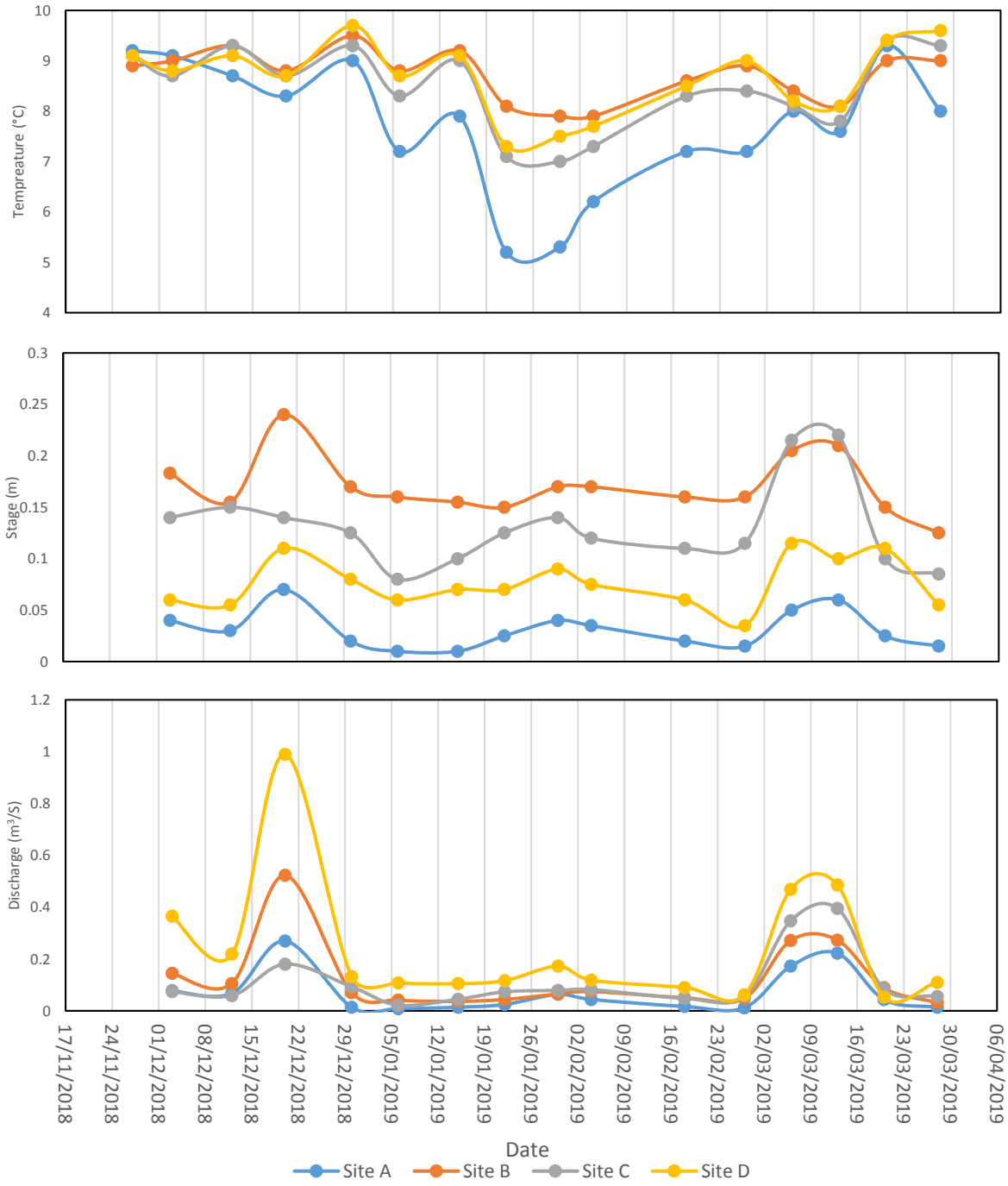

Figure 5.12. Hydroclimatic variability of weekly sampling carried out at Parc mine, Llanrwst – 27.11.2018-28.03.19. At site A, B, C and D.

5.1.4 PHE Load vs concentration

Mean PHE loads at Parc Mine were calculated based upon low-resolution monitoring (Table 5.2). Control site A exhibited the lowest PHE loads for all PHEs. During parts of the monitoring period, Pb and Cd were not detectable (<0.01 mg/l) resulting in a minimum load calculated as 0, therefore loads that have been identified as 0 have been classified as not applicable (N/A) (Table 5.2). Maximum mean Pb, Cd and Fe loads were found at site B and Zn from was at site D. Site B exhibited the maximum total f PHE load followed by site D. PHE loads at site C reduce from site B but there is a subsequent increase in PHE load downstream at site D.

Table 5.2. Total of Zn, Pb, Cd and Fe loads based on low resolution monitoring at Parc mine, Llanrwst 27.11.18-28.03.19. At sites A, B, C and D at Park mine.

Parc mine		**Zn kg/d**	**Pb kg/d**	**Cd kg/d**	**Fe kg/d**	**Zn t/y**	**Pb t/y**	**Cd t/y**	**Fe t/y**
A	min	1.24	N/A	N/A	0.02	0.45	N/A	N/A	0.01
	mean	**7.07**	**0.07**	**0.03**	**0.26**	**2.58**	**0.02**	**0.01**	**0.09**
	max	22.82	0.47	0.23	1.16	8.33	0.17	0.08	0.42
B	min	11.37	0.14	N/A	4.62	4.15	0.05	N/A	1.69
	mean	**37.99**	**1.93**	**0.10**	**20.74**	**13.87**	**0.70**	**0.04**	**7.57**
	max	145.84	12.19	0.45	106.73	53.23	4.45	0.16	38.96
C	min	6.20	0.06	N/A	2.56	2.26	0.02	N/A	0.93
	mean	**22.44**	**0.67**	**0.04**	**8.86**	**8.19**	**0.24**	**0.01**	**3.23**
	max	65.73	3.00	0.16	48.32	23.99	1.10	0.06	17.64
D	min	8.63	0.05	N/A	0.46	3.15	0.02	N/A	0.17
	mean	**39.41**	**0.90**	**0.11**	**12.92**	**14.39**	**0.33**	**0.04**	**4.71**
	max	153.14	5.99	0.86	59.89	55.90	2.19	0.31	21.86

Dilution factors based on mean discharge for the period of the study (Table 5.3) can help to explain spatial variation of PHE concentrations and loads exemplified at sites A, B, C and D (Figures 5.7, 5.8, 5.9 and 5.10). The dilution factor for sites C to site D of 2.12, suggests that loading from the adit is diluted from the upstream site A and then again between sites C and D. Site A demonstrated a dilution of 1.76 with the adit site B and may explain reduction in PHE concentrations from site B to Site C. The dilution factor shown at site C from sites A and B combined discharge indicates a loss of water, possibly due to river water seeping through underlying tailings due to a hydraulic gradient to groundwater caused by the pours nature of the tailings below (Schälchli, 1992; Brodie *et al.,* 2009). The reduction in discharge between sites A and B to C, results in a mean loss of load 22.62kg/d, 1.33kg/d, 0.09kg/d and 12.14kg/d for Zn, Pb, Cd and Fe respectively. The mean change in PHE load between sample sites A and B combined to sample site C indicates that there is a reduction in PHE load (Table 5.4), between sites C and D there is an increase in mean PHE loads of 16.97kg/d, 0.23kg/d, 0.07kg/d and 4.06kg/d for Zn, Pb, Cd and Fe respectively. This suggests that there is additional contamination entering the fluvial system from the tailings or the loss of water between sites A and B combined and C is possibly returning further downstream.

The subsequent increase in load at site D, indicating that there is an additional input of PHE contaminated water between sample sites C and D. The site C to D dilution factor of 2.12 confirms an additional input of water between sites C and D (Table 5.3). The increase in the PHE load from site C to D suggests that the water input is PHE-rich. A likely source is drainage from the tailings pile next to the river channel (Figure 3.2), with flushing of PHEs during periods of increased discharge. Previous studies have also identified significant contamination between sample sites C and D, from a legacy mine shaft and leachate drain and pipe (Gao and Bradshaw, 1995).

Figure 5.13 indicates that at all sites, periods of lower Zn concentration coincide with increased Zn load. The relationship between Zn load and concentration is a confirmed by a significant ($p < 0.05$) negative correlation (Table 5.5). Zinc can be co-precipitated with Fe, suggesting that increased Fe load from the mine adit site B, that subsequently oxidises on exposure to the atmosphere when leaving the mine and is visible at site B, may also reduce solute Zn concentration and overall the concentration of Zn within river water due to deposition of co-precipitated Zn with Fe upon Fe oxidation, this may explain the decreased Zn concentration during periods of increased load (Elderfield *et al.,* 1979; Nagorski *et al.,* 2003). Increased PHE loads occur with increased discharge (Figure 5.6 and 5.12), the increase in discharge suggests that reduction of Zn concentration, is due to dilution and the increased discharge would also increase the overall Zn load due to additional Zn from the increased volume of water entering the system. It is likely that increases in Zn load are due to increased discharge and that reduces PHE concentrations during periods of increased load due to a combination of co-precipitation and deposition of particulate PHEs and dilution. These processes can account for reduction of solute PHE concentrations during peak PHE loads.

In contrast to Zn, for Pb, Cd and Fe during the low-resolution study a positive significant relationship between load and concentration was found (Table 5.5) and (Figure 5.14, 5.15 and 5.16). Zinc variability demonstrating differences to Fe and Pb may be explained by pH of hydrolysis, Zn has a hydrolysis of pH 8.3 and therefor is relatively mobile below this, Fe and Pb have a lower pH of hydrolysis ~ pH 5-6. Cadmium however has a pH of hydrolysis ~ pH 8 and there should demonstrate similar temporal and spatial variability to Zn, this suggests that Cd may be in a less soluble and potentially bound to oxides or organic matter (Dvorak *et al.,* 1992). This suggests the mine is still experiencing juvenile or seasonal increases in contamination from periods of oxidation and washing from seasonal increases and decreases in flow and flooding, out washing mine waters (Elderfield *et al.,* 1979; Nagorski *et al.,* 2003).

Generally, Discharge demonstrated significant (<0.05) positive correlation with load for all sites and PHEs, this shows that increases in discharge are coincident with increases in load (Table 5.5). Concentration and discharge did not indicate a significant relationship with PHE concentrations with the exception of Zn at sites A, C and D, a significant (<0.05) negative relationship was demonstrated, indicating that increases in discharge decrease Zn concentrations. Effectively when discharge is increased PHE loads increase, and concentrations generally decrease for Zn, Fe and Cd show no significant relationship with discharge this

suggests that Fe and Cd concentration and load variation are attributed to a complex set of variables that are not identified. Pb however shows a positive correlation with discharge at all sites and is Signiant at the adit site B, this shows increases in discharge coincide with increases in Pb concentration. The differing nature of Zn and Pb concentrations in relation to discharge can be attributed to dilution and speciation Zn is primarily present in the solute form. Pb is primarily present in a particulate form that is subject to mobilisation during periods of increase discharge.

Data for site D, located towards the bottom of the Nant Gwydyr catchment, suggests that significant PHE loads being delivered into the River Conwy (Table 5.2). The total loads exemplified at site D are resultant from PHE inputs from the mine adit and the tailings area downstream of the adit. The load at Parc mine varies temporally over the period of the study, controlled by hydroclimatic factors that are driven by localised climate regimes of rainfall and temperature change due to seasonality.

Table 5.3. Dilution of load based on mead discharge at sites A, B, C and D.

Site	Dilution
a-b	**1.76**
a+b-c	**0.58**
b-c	**0.91**
c-d	**2.12**

Table 5.4. Change in load between sample sites (positive values indicate and increase, and negative values indicate a loss of PHE load).

Site(s)	Zn kg/d	Pb kg/d	Cd kg/d	Fe kg/d
Total load post A and B mixing	45.06	2.00	0.13	0.13
Total load from adit B	37.99	1.93	0.10	20.74
Total load loss at C-(A+B)	-22.62	-1.33	-0.09	-12.14
Total load increase at D-C	16.97	0.23	0.07	4.06

Table 5.5. PHE load, concentration and discharge Pearson r correlation, PHE loads and concentrations calculated at sample sites A, B, C and D.

Site A	Zn mg/L	Pb mg/L	Cd mg/L	Fe mg/L	Discharge m3/s	Zn kg/d	Pb kg/d	Cd kg/d	Fe kg/d
Zn mg/L	1.000								
Pb mg/L	-0.365	1.000							
Cd mg/L	0.047	0.323	1.000						
Fe mg/L	-0.343	0.583	0.039	1.000					
Discharge m3/s	-0.921	0.414	-0.002	0.408	1.000				
Zn kg/d	-0.917	0.391	-0.002	0.436	0.992	1.000			
Pb kg/d	-0.786	0.595	0.180	0.475	0.907	0.880	1.000		
Cd kg/d	-0.505	0.469	0.519	0.277	0.618	0.619	0.820	1.000	
Fe kg/d	-0.855	0.473	0.019	0.598	0.949	0.950	0.922	0.656	1.000
Site B	Zn mg/L	Pb mg/L	Cd mg/L	Fe mg/L	Discharge m3/s	Zn kg/d	Pb kg/d	Cd kg/d	Fe kg/d
Zn mg/L	1.000								
Pb mg/L	0.485	1.000							
Cd mg/L	0.697	0.224	1.000						
Fe mg/L	0.940	0.632	0.560	1.000					
Discharge m3/s	-0.271	0.643	-0.309	-0.114	1.000				
Zn kg/d	-0.121	0.749	-0.165	0.052	0.980	1.000			
Pb kg/d	-0.141	0.711	-0.172	0.018	0.976	0.989	1.000		
Cd kg/d	-0.066	0.643	0.173	0.038	0.834	0.885	0.903	1.000	
Fe kg/d	0.154	0.773	0.032	0.419	0.668	0.784	0.740	0.694	1.000
Site C	Zn mg/L	Pb mg/L	Cd mg/L	Fe mg/L	Discharge m3/s	Zn kg/d	Pb kg/d	Cd kg/d	Fe kg/d
Zn mg/L	1.000								
Pb mg/L	-0.540	1.000							
Cd mg/L	0.215	0.316	1.000						
Fe mg/L	0.692	-0.233	0.003	1.000					
Discharge m3/s	-0.720	0.494	-0.362	-0.257	1.000				
Zn kg/d	-0.571	0.526	-0.370	-0.054	0.954	1.000			
Pb kg/d	-0.678	0.709	-0.205	-0.126	0.932	0.946	1.000		
Cd kg/d	-0.168	0.609	0.762	-0.298	-0.079	-0.092	0.112	1.000	
Fe kg/d	-0.275	0.459	-0.315	0.379	0.672	0.835	0.802	-0.176	1.000
Site D	Zn mg/L	Pb mg/L	Cd mg/L	Fe mg/L	Discharge m3/s	Zn kg/d	Pb kg/d	Cd kg/d	Fe kg/d
Zn mg/L	1.000								
Pb mg/L	-0.584	1.000							
Cd mg/L	0.100	0.401	1.000						
Fe mg/L	0.557	0.117	0.194	1.000					
Discharge m3/s	-0.625	0.910	0.270	-0.072	1.000				
Zn kg/d	-0.492	0.893	0.343	0.003	0.984	1.000			
Pb kg/d	-0.518	0.883	0.300	-0.002	0.980	0.990	1.000		
Cd kg/d	-0.279	0.740	0.621	-0.004	0.809	0.870	0.871	1.000	
Fe kg/d	-0.418	0.864	0.263	0.269	0.899	0.911	0.932	0.762	1.000

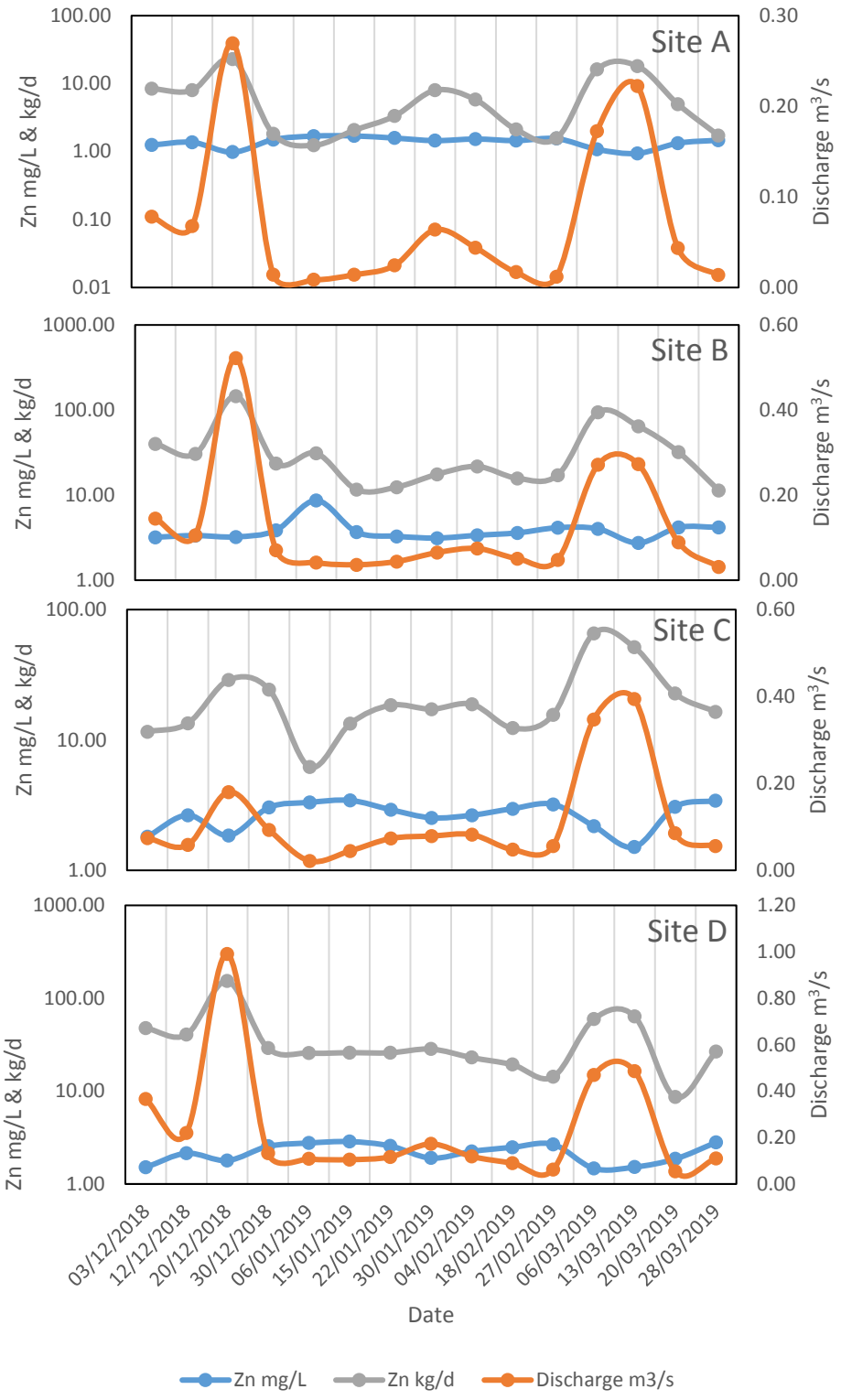

Figure 5.13. Unfiltered Zn concentration (mg/L), load (kg/d) and discharge (m^3/s) relationship at Parc mine sites A, B, C and D during low resolution monitoring between 03.12.18-28.03.19.

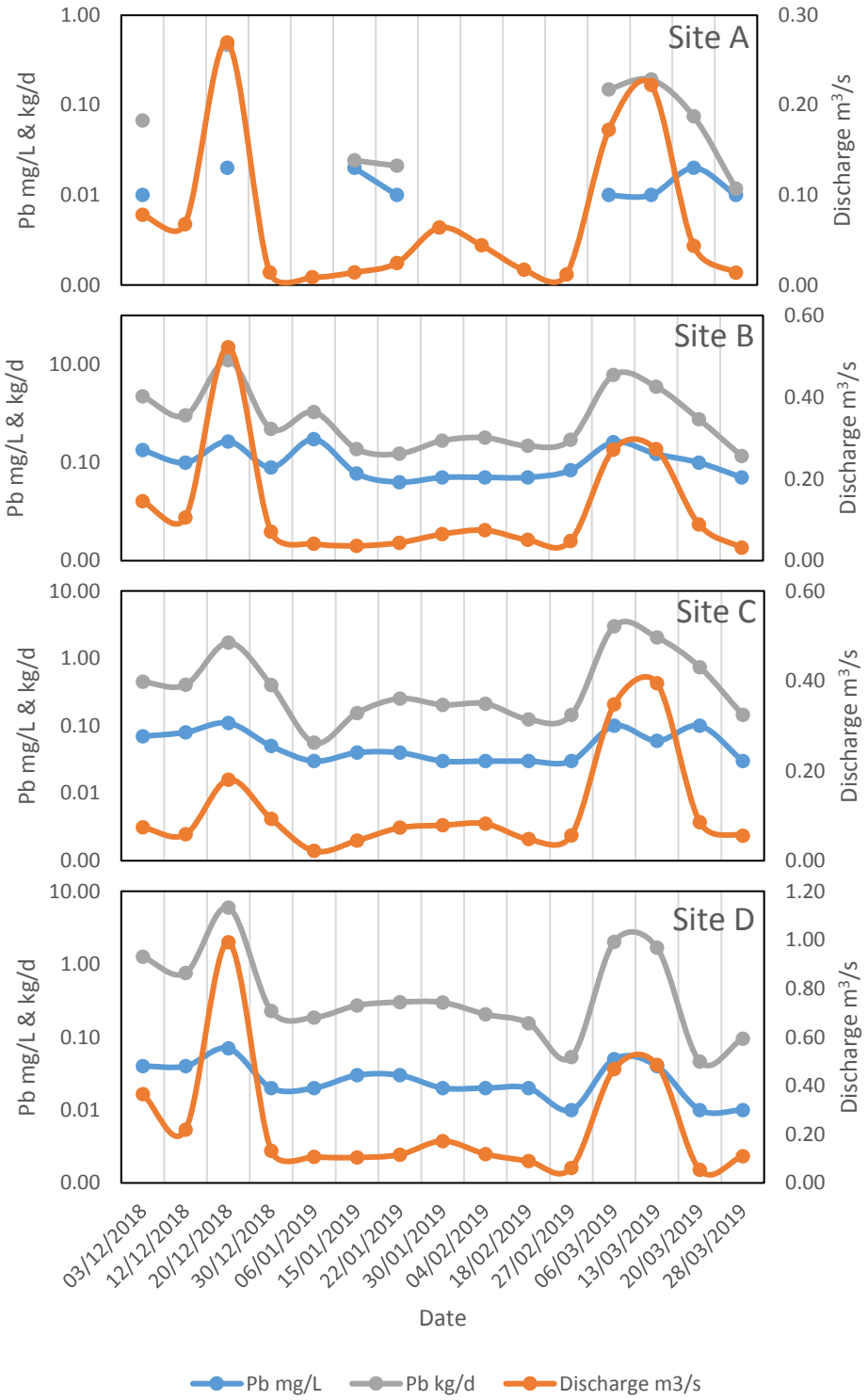

Figure 5.14. Unfiltered Pb concentration (mg/L), load (kg/d) and discharge (m^3/s) relationship at Parc mine based on sites A, B, C and D low resolution monitoring 03.12.18-28.03.19.

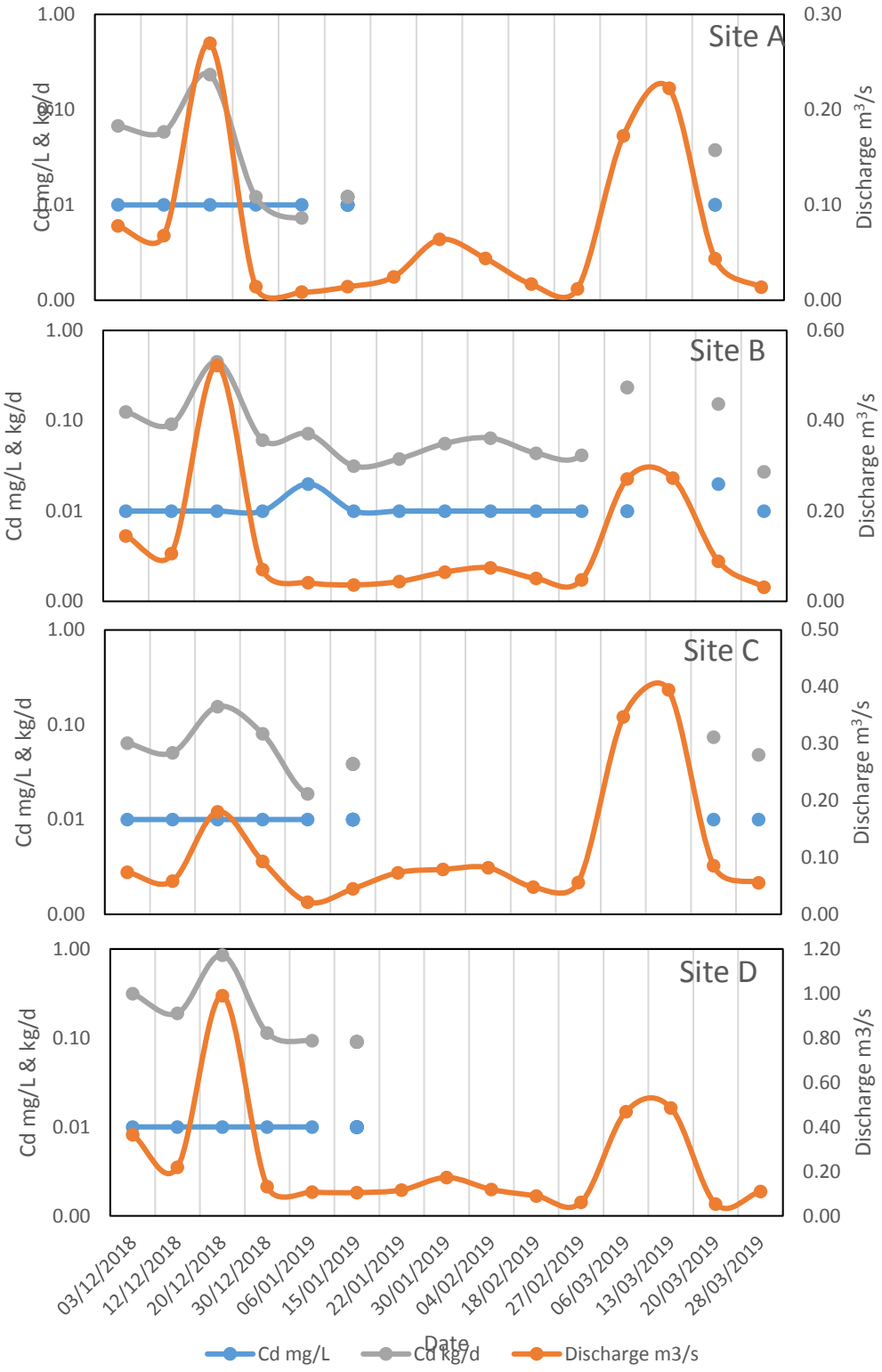

Figure 5.15. Unfiltered Cd concentration (mg/L), load (kg/d) and discharge (m^3/s) relationship at Parc mine based on sites A, B, C and D low resolution monitoring 03.12.18-28.03.19.

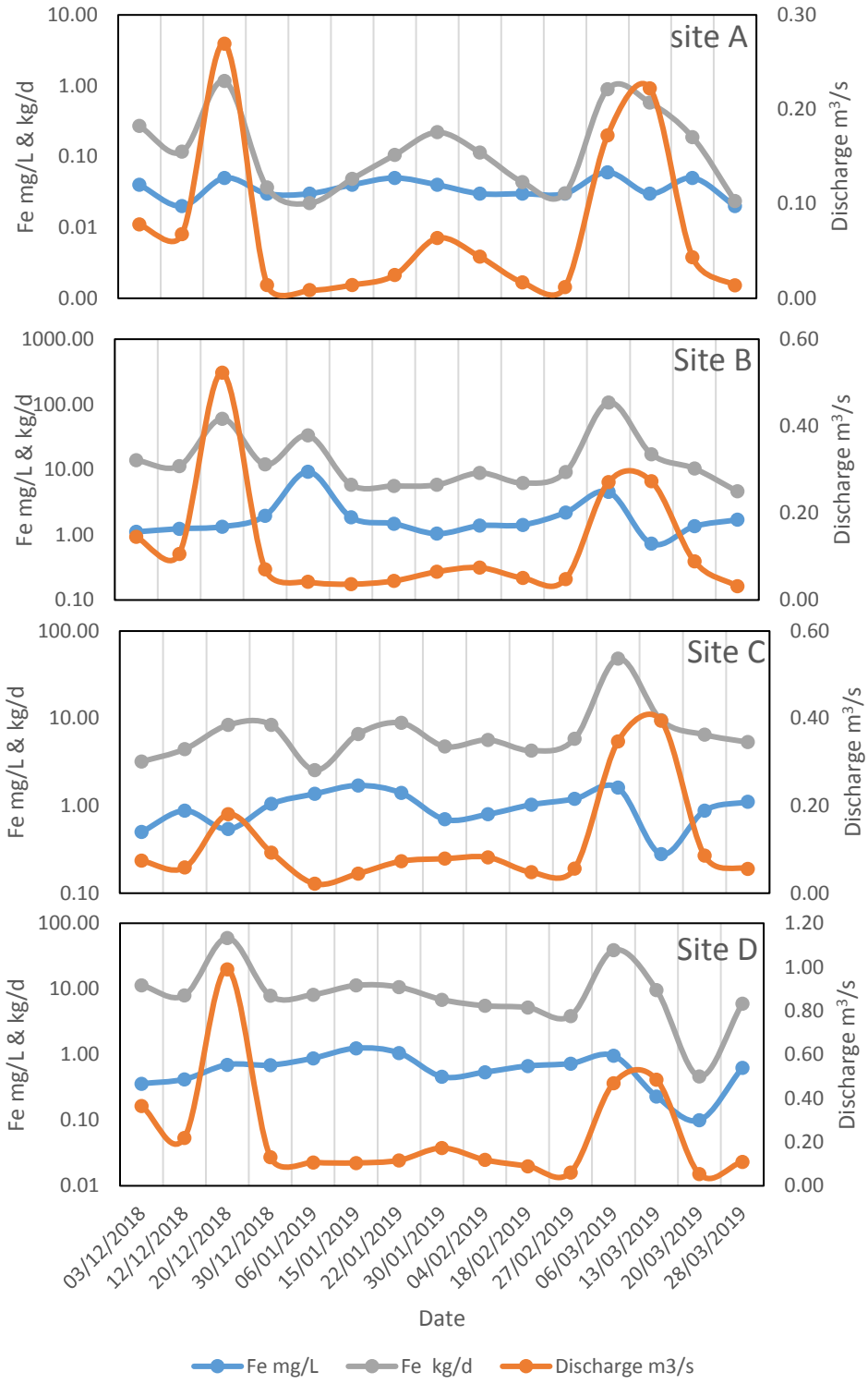

Figure 5.16. Unfiltered Fe concentration (mg/L), load (kg/d) and discharge (m^3/s) relationship at Parc mine based on sites A, B, C and D low resolution monitoring 03.12.18-28.03.19.

5.1.5 PHE Speciation

During low resolution monitoring the dominant geochemical PHE species was analysed for each sample site, calculated as a mean value for the period of the study, they were calculated using pH and redox potential data, it was found that there was little spatial variation in the species of PHEs at all sample sites for the study. The dominant species of Zn was Zn_{2+} (Figure 5.17), Pb was $PbSO_4$ (Figure 5.18), Fe was $Fe(OH)_3$ (Figure 5.19) and Cd was Cd_{2+} (Figure 5.20). Zinc and Cd are present in soluble dissolved forms and that Pb and Fe are in sulphide forms that are generally more insoluble, this conforms with increased particulate loads for Fe and Pb in section 5.1.2. Iron is likely to be present as $Fe(OH)_3$ due to oxidation processes occurring as mine waters interact with the atmosphere. Pb present as PbSO is can explain the low concentrations analysed during the study, PbSO is relatively insoluble and therefore immobile. The presence of Zn and Cd in soluble forms confirms the consistently high concentrations demonstrated temporally and spatially throughout the study (Shooter, 1976).

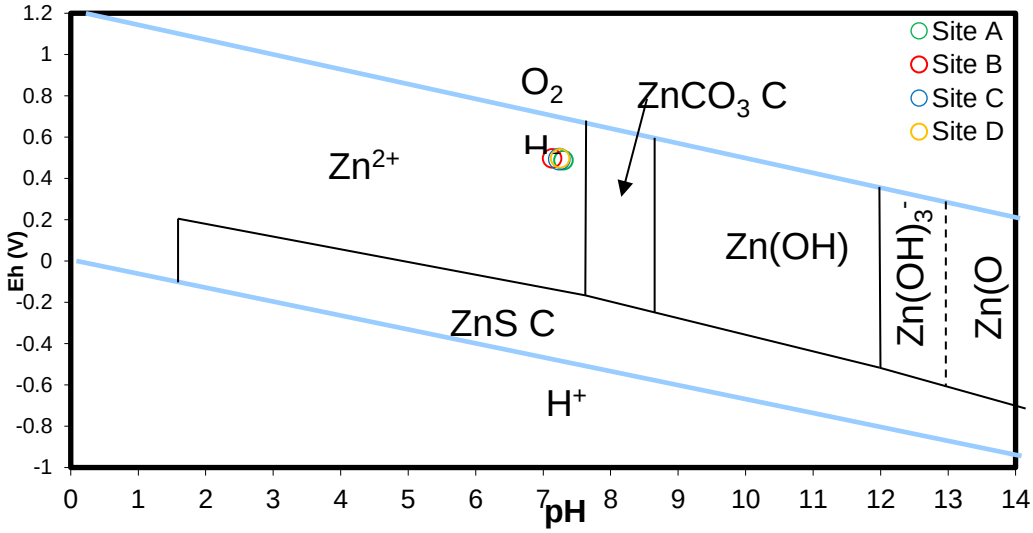

Diagram $FeCl^+$, T = 8.38 °C , P = 1.013 bars, a [main] = $10^{-.02808}$, a [H_2O] = 1, a [Ca^{++}] = $10^{-.1085}$, a [Mg^{++}] = $10^{-.1047}$, a [Na^+] = $10^{-.02808}$, a [K^+] = $10^{-.02858}$, a [HCO_3^-] = $10^{-.0278}$, a [SO_4^{--}] = $10^{-.1125}$, a [Cl^-] = $10^{-.02858}$, a [Pb^{++}] = $10^{-.02808}$, a [Zn^{++}] = $10^{-.02808}$

Figure 5.17. Speciation of Zn at Parc mine, sample sites A, B, C and D, based on mean pH and redox values from weekly low-resolution sampling. Adapted from (Garells and Christ,1965).

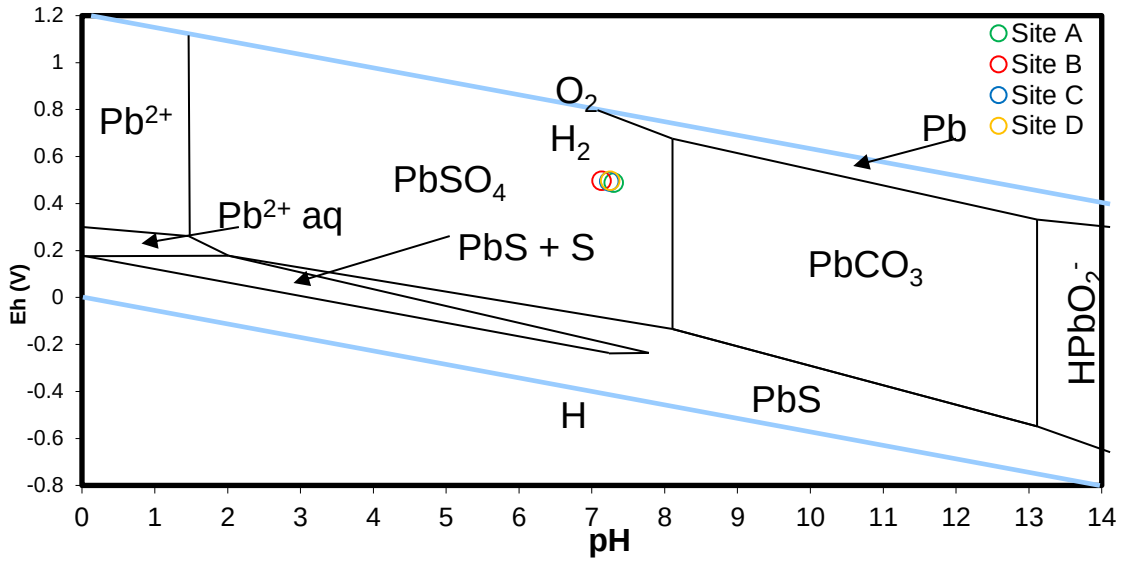

Diagram $FeCl^+$, T = 8.38 °C , P = 1.013 bars, a [main] = $10^{-.02808}$, a [H_2O] = 1, a [Ca^{++}] = $10^{-.1085}$, a [Mg^{++}] = $10^{-.1047}$, a [Na^+] = $10^{-.02808}$, a [K^+] = $10^{-.02858}$, a [HCO_3^-] = $10^{-.0278}$, a [SO_4^{--}] = $10^{-.1125}$, a [Cl^-] = $10^{-.02858}$, a [Pb^{++}] = $10^{-.02808}$, a [Zn^{++}] = $10^{-.02808}$

Figure 5.18. Speciation of Pb at Parc mine, sample sites A, B, C and D, based on mean pH and redox values from weekly low-resolution sampling (Garells and Christ,1965).

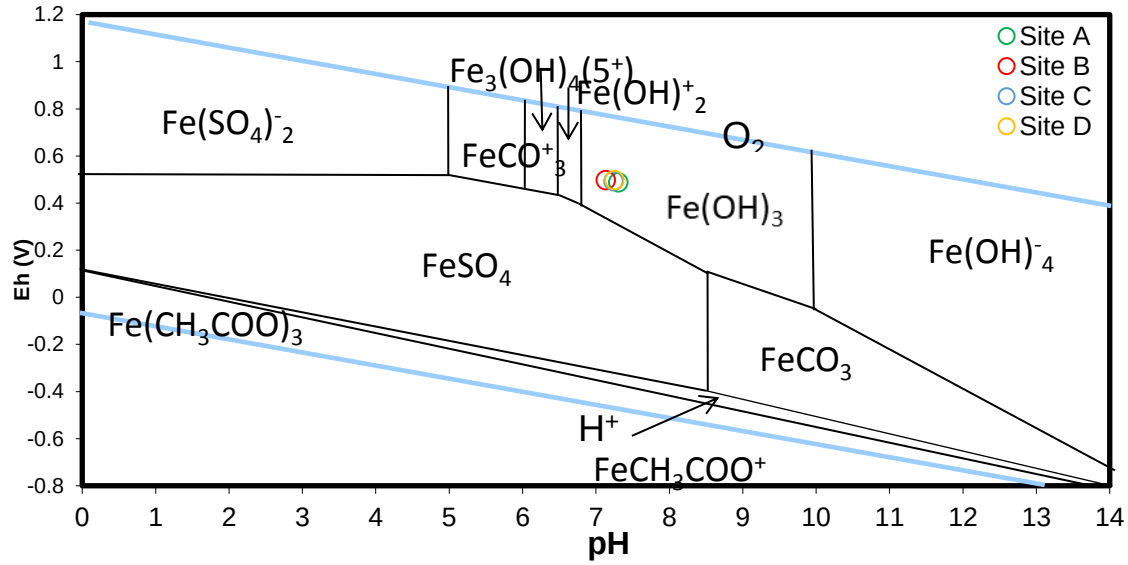

Diagram $FeCl^+$, T = 8.38 °C , P = 1.013 bars, a [main] = $10^{-.02808}$, a [H_2O] = 1, a [Ca^{++}] = $10^{-.1085}$, a [Mg^{++}] = $10^{-.1047}$, a [Na^+] = $10^{-.02808}$, a [K^+] = $10^{-.02858}$, a [HCO_3^-] = $10^{-.0278}$, a [SO_4^{--}] = $10^{-.1125}$, a [Cl^-] = $10^{-.02858}$, a [Pb^{++}] = $10^{-.02808}$, a [Zn^{++}] = $10^{-.02808}$

Figure 5.19. Speciation of Fe at Parc mine, sample sites A, B, C and D, based on mean pH and redox values from weekly low-resolution sampling (Garells and Christ,1965).

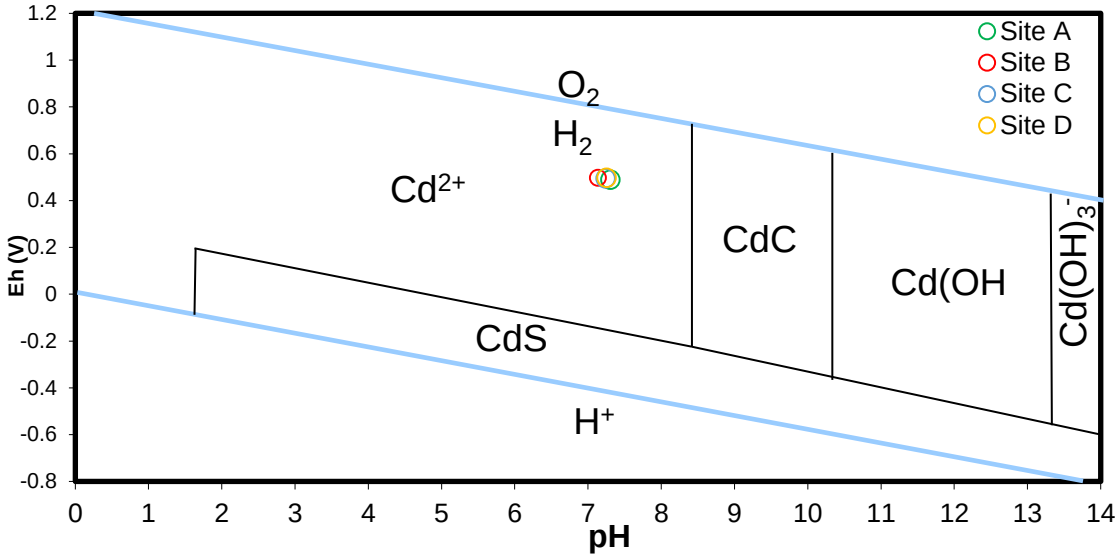

Diagram $FeCl^{+}$, T = 8.38 °C , P = 1.013 bars, a [main] = $10^{-.02808}$, a [H_2O] = 1, a [Ca^{++}] = $10^{-.1085}$, a [Mg^{++}] = $10^{-.1047}$, a [Na^{+}] = $10^{-.02808}$, a [K^{+}] = $10^{-.02858}$, a [HCO_3^{-}] = $10^{-.0278}$, a [SO_4^{--}] = $10^{-.1125}$, a [Cl^{-}] = $10^{-.02858}$, a [Pb^{++}] = $10^{-.02808}$, a [Zn^{++}] = $10^{-.02808}$

Figure 5.20. Speciation of Cd at Parc mine, sample sites A, B, C and D, based on mean pH and redox values from weekly low-resolution sampling (Garells and Christ,1965).

5.1.6 Water origins

Anion and cation analysis, interpreted using trilinear plots, was carried out to ascertain water origins at each sample site for Parc mine during the low-resolution weekly sampling (Figures 5.21, 5.22, 5.23 and 5.24). There was little temporal variation of water at all sites, with all samples being clustered for each site. All Sample sites showed minor temporal and spatial variation in water origin quality over the period of the study (Figure 5.25). The waters at all sample sites demonstrated values that fall into calcium carbonate rich water category (Figure 2.2). The waters are likely to be buffered from localised carbonate rich limestone bedrock geology which would account for the waters exemplifying a carbonate rich chemistry, the values obtained at each site are also being sulphide rich waters which may be explained from the mineralization from within the mine and surrounding areas in light of this carbonate waters are the dominant group at Parc mine. Limestone geology buffers pH which would reduce AMD and stop sulphide rich waters becoming the dominant water group (Bikundia and Mohan, 2014; Michalski, 2018).

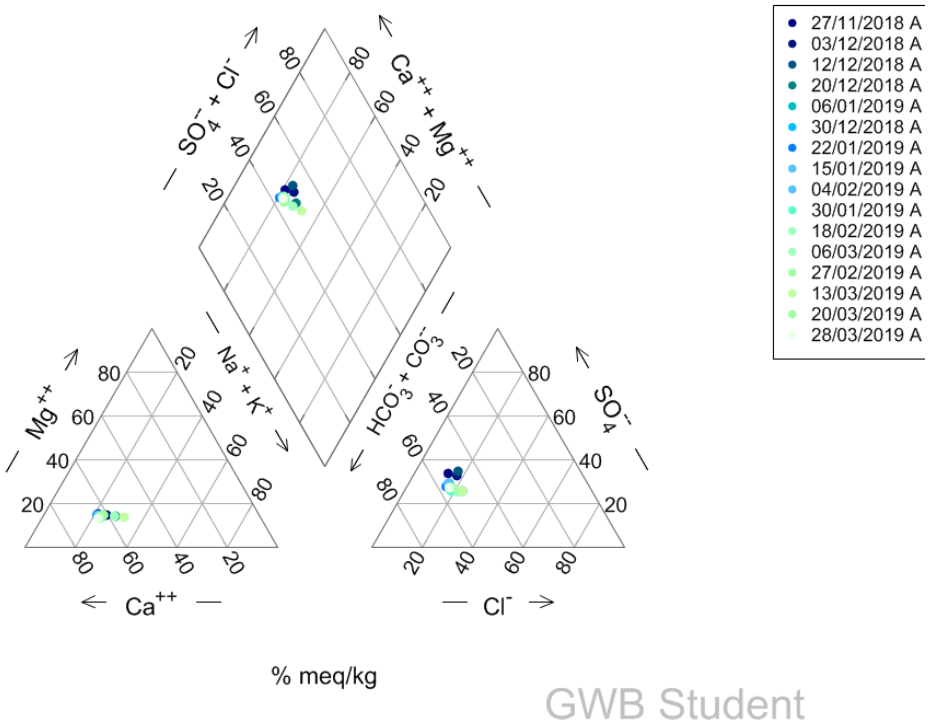

Figure 5.21. Water origins of low-resolution sampling carried out at Parc mine - 27.11.2018-28.03.2019. At site A control site.

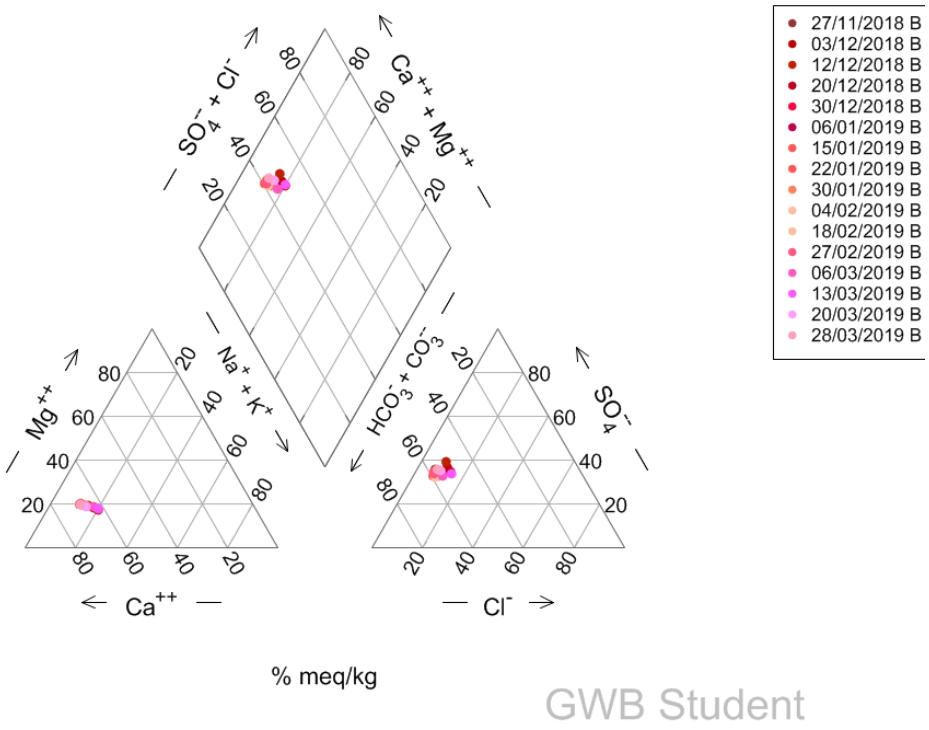

Figure 5.22. Water origins of low-resolution sampling carried out at Parc mine - 27.11.2018-28.03.2019. At site B adit.

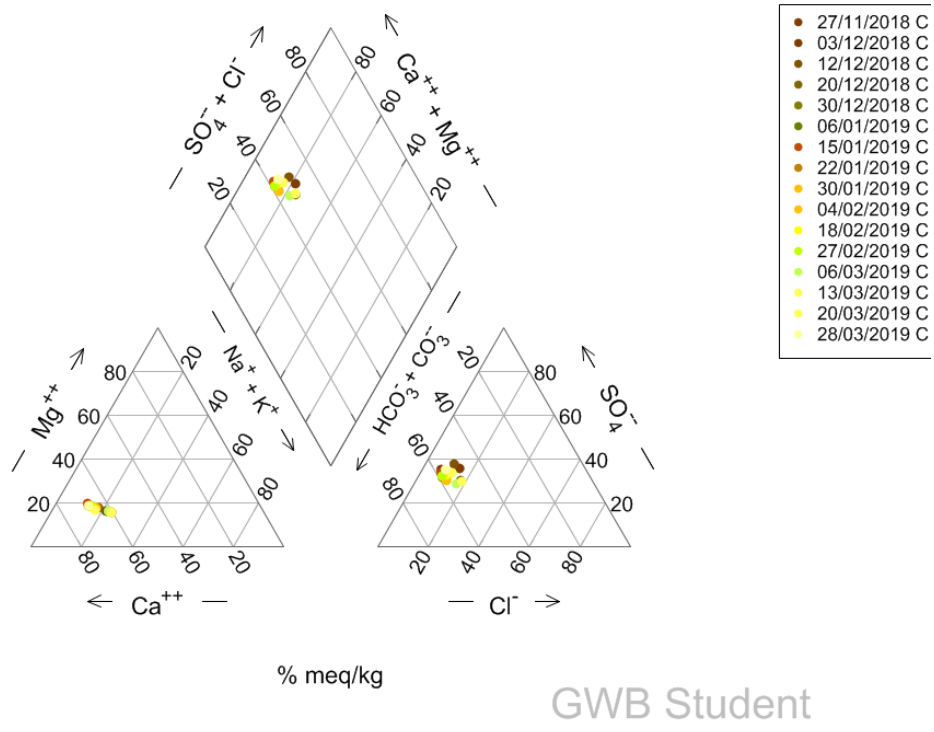

Figure 5.23. Water origins of low-resolution sampling carried out at Parc mine - 27.11.2018-28.03.2019. At site C post adit mixing.

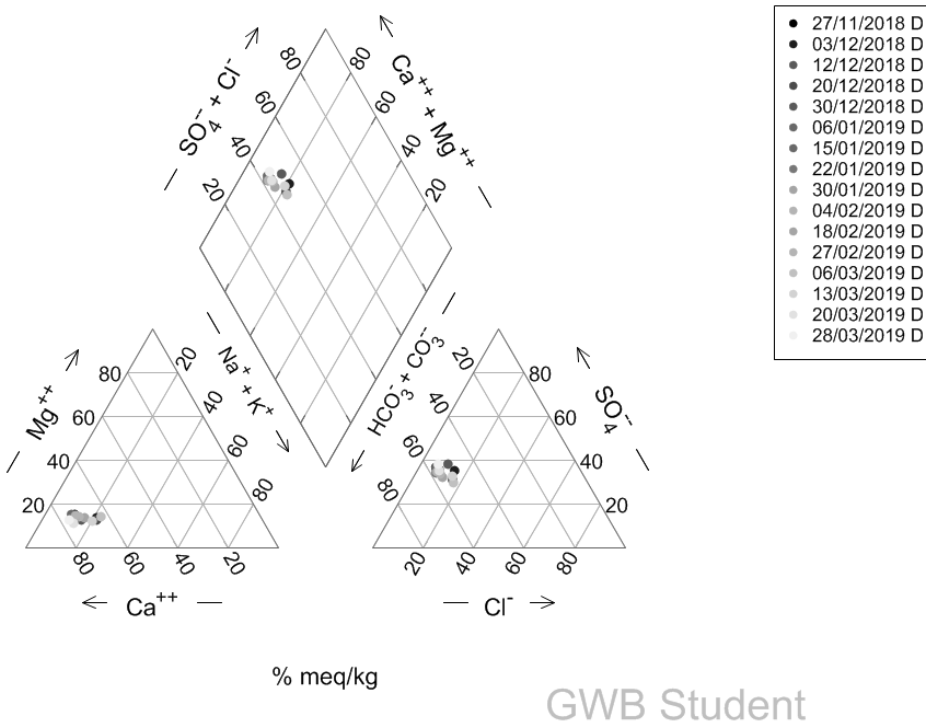

Figure 5.24. Water origins of low-resolution sampling carried out at Parc mine - 27.11.2018-28.03.2019. At site D post adit and mine tailings.

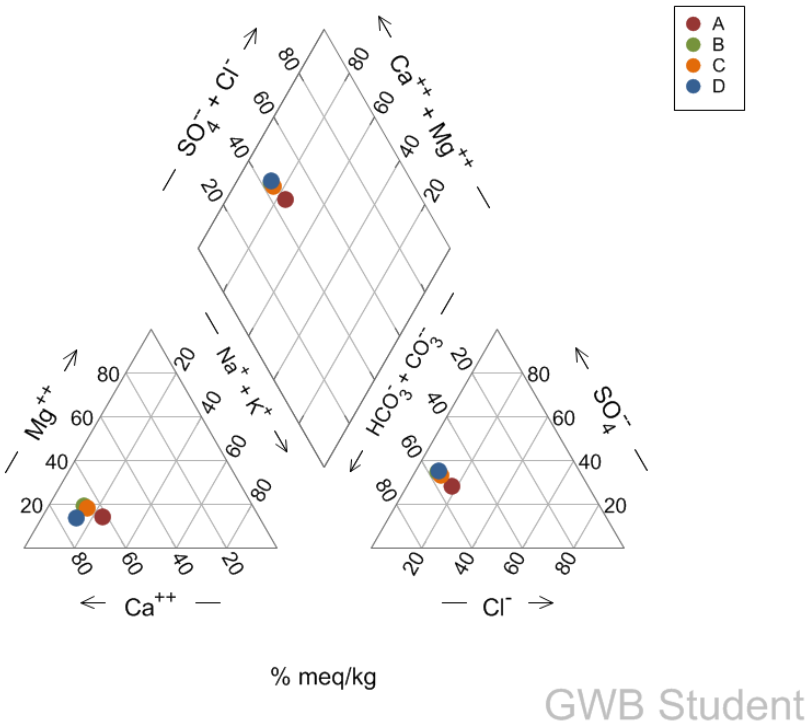

Figure 5.25. Mean water origins of low-resolution sampling carried out at Parc mine - 27.11.2018-28.03.2019. At sites A, B, C and D at park mine, site A 0m upstream control site, site B 13.9m adit outlet, site C 38.7m post adit input and site D 800.9m post tailings deposits.

5.2 Parc mine - high-resolution monitoring

5.2.1 High-resolution – 31.01.19-04.02.19

High-resolution monitoring of chemical and hydroclimatic variability was carried out at Parc mine, to assess and identify any relationships between hydroclimatic variability and changes in chemical parameters at sample sites A, B, C and D (Figure 5.26 and 5.27). pH EC, DO_2 demonstrated daily variability. The hydroclimatic variables temperature and stage also demonstrated variation, temperature showed variation daily on a daily scale, stage showed variation over a period ~several days (Figure 5.27). Temperature has significant ($p < 0.05$) correlation with pH, EC and DO_2 upstream and pH EC and DO_2 downstream (Table 5.6). Stage showed significant correlation with pH, EC and DO_2 at upstream and downstream sites (Table 5.6). Independent samples T-tests on pH, EC and DO_2 between upstream and downstream sample sites exhibited significant difference ($p < 0.05$).

Observed daily cycling can be explained by several factors, it is possible dissolution and precipitation of carbonate minerals driven by changes in temperature may be a cause of pH variation. Observed daily cycles of chemical variables and hydroclimatic variables are synchronous and are confirmed by significant correlations with chemical variable (Table 5.6)

The data suggests temperature and stage act as a control on chemical variables at upstream and downstream sites at a high-resolution. High-resolution data shows that there is daily variability identifiable with chemical parameters, due to the nature of low resolution monitoring these daily cycles are missed. High-resolution monitoring shows that more accurate and detailed water quality assessments are possible in comparison to a low-resolution monitoring regime. Downstream EC shows an increasing EC value for the period of monitoring and does not follow the trend of upstream EC variation, this may be due to an electrode error during deployment (Figure 5.26) or possible natural phenomena due a snowmelt pulse that was taking place over the period of high-resolution monitoring from the area of the tailings, suggesting that melt water from snow on the tailings area may have seeped into the tailing leaching PHEs to the Nant Gwydir prior to sample site D. Possible adsorption from biofilms that are active during the day may be another source of daily variation in chemical variables (Nimick *et al.,* 2007).

Table 5.6 Pearson's r correlations of high-resolution sampling 31.01.19-04.02.19

+	Temperature (°C) upstream	pH upstream	DO_2 (mg/L) upstream	Electrical conductivity (µS/cm) upstream	Stage (m) upstream	Temperature (°C) downstream	pH downstream	DO_2 (mg/L) downstream	Electrical conductivity (µS/cm) downstream	Stage (m) downstream
Temperature (°C) upstream	1									
pH upstream	0.202	1								
DO_2 (mg/L) upstream	-0.814	-0.383	1							
Electrical conductivity (µS/cm) upstream	-0.515	-0.402	0.647	1						
Stage (m) upstream	0.461	0.382	-0.855	-0.707	1					
Temperature (°C) downstream	0.912	0.033	-0.555	-0.401	0.191	1				
pH downstream	-0.111	-0.260	0.567	0.325	-0.755	0.142	1			
DO_2 (mg/L) downstream	-0.768	-0.351	0.979	0.641	-0.882	-0.540	0.629	1		
Electrical conductivity (µS/cm) downstream	-0.180	-0.419	0.694	0.614	-0.916	0.141	0.781	0.709	1	
Stage (m) downstream	0.297	0.210	-0.565	-0.514	0.673	0.114	-0.482	-0.570	-0.639	1

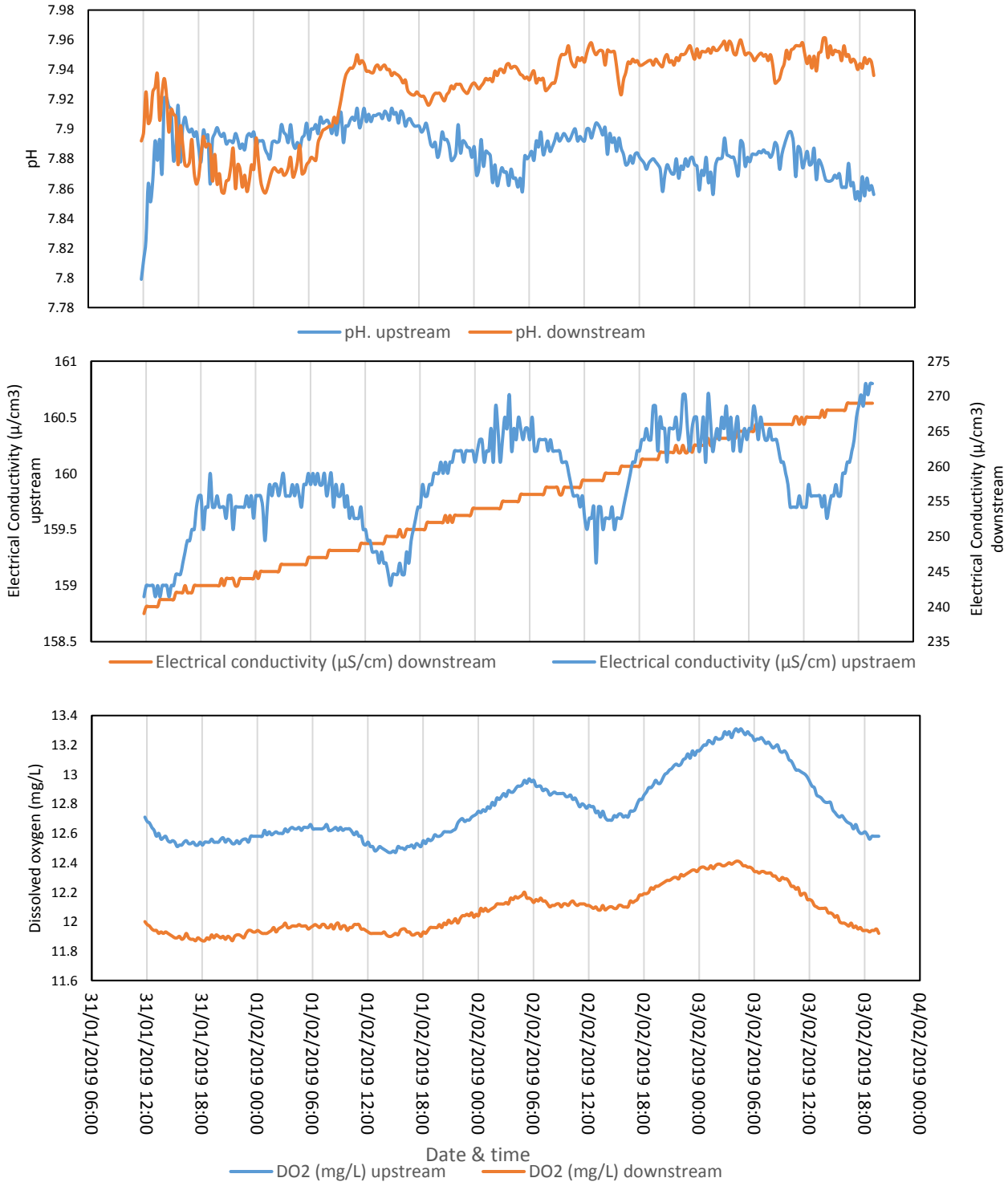

Figure 5.26. Chemical variability of high-resolution sampling carried out at Parc mine, Llanrwst – 31.01.2019-04.02.2019. At site A and D. Site A 0m upstream control site, site D 800.9m from site A post tailings deposits downstream. Downstream EC values are to be considered with cation, reliably of the data is in question due to it exemplifying poor variation and steadily increasing during the monitoring period.

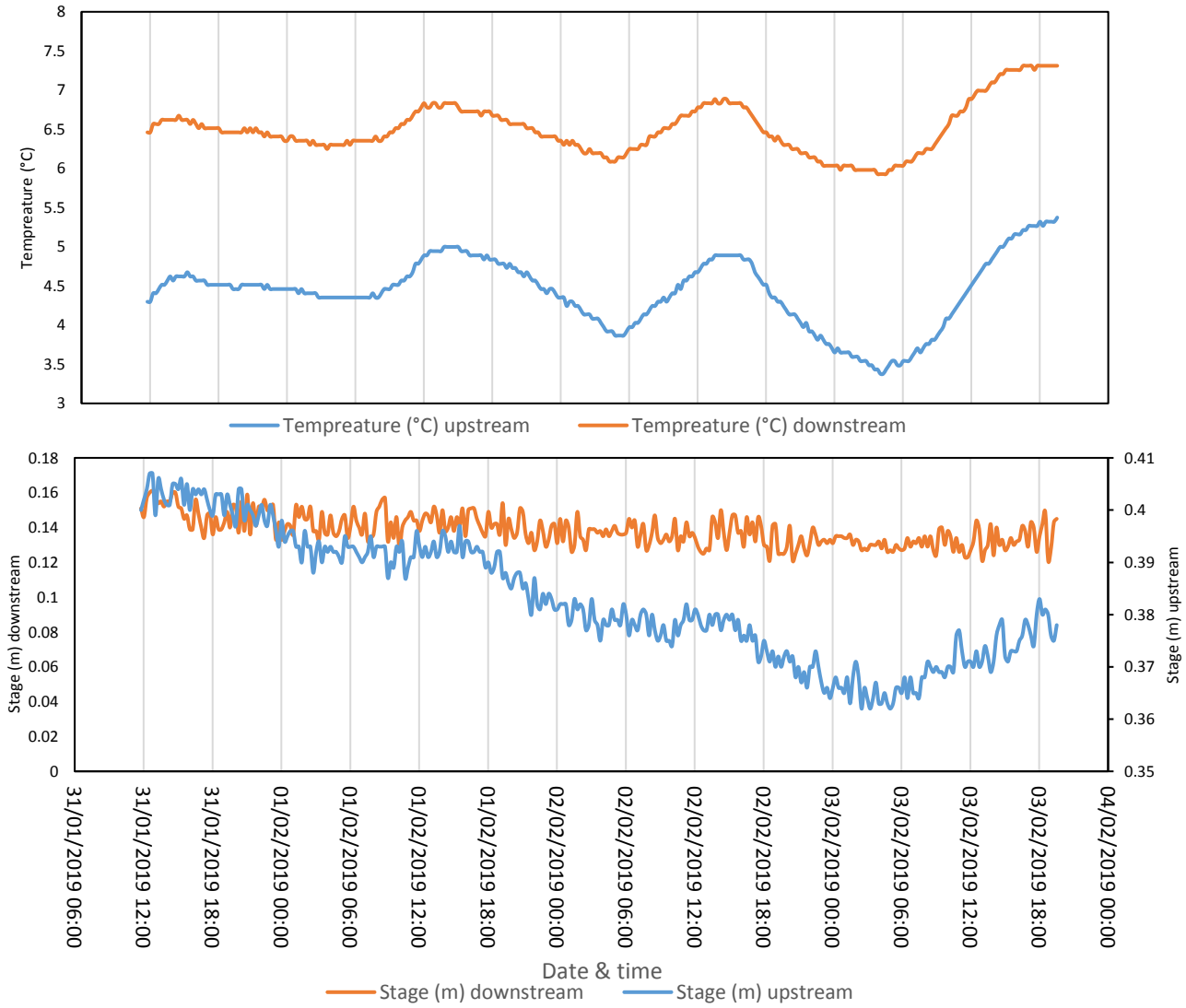

Figure 5.27. Hydroclimatic variability of high-resolution sampling carried out at Parc mine, Llanrwst – 31.01.2019-04.02.2019. At site A and D. Site A 0m upstream control site, site D 800.9m from site A post tailings deposits downstream.

5.2.2 High-resolution – 28.02.19-06.03.19

High-resolution monitoring of chemical and hydroclimatic variability was carried out on a second occasion at Parc mine, to assess and identify any relationships between hydroclimatic variability and changes in chemical parameters at sample upstream site A and downstream site D (Figure 5.28 and 5.29). pH and DO_2 demonstrated daily variability similar to first high-resolution monitoring at Parc mine. Temperature and stage also demonstrated variation, temperature showed variation daily, stage showed variation over a period several days (Figure 5.29). Temperature has significant correlation with pH and DO_2 upstream and pH and DO_2 downstream (Table 5.7). Stage showed significant correlation with EC at upstream and downstream sites (Table 5.7). The data suggests that EC is controlled primarily by changes in stage and pH and DO_2 are primarily controlled by temperature, there may be other explanations for daily variation that have not been accounted for in this study that were mentioned in the first high-resolution monitoring, such as precipitation and dissolution of carbonate bedrock and biological controls from biofilms (Nimick *et al.,* 2007). Based upon the data from this study, it can be said that it is a combination of hydroclimatic factors that affect short term chemical variability, previous studies have also suggested that there are other mechanisms that also contribute to chemical variability (Sullivan and Drever, 2001; Nimick *et al.,* 2007; Pizarro *et al.,* 2010).

Independent samples T-tests on pH, EC and DO_2 between upstream and downstream sample sites exhibited significant difference ($p < 0.05$). The significant difference in chemical parameters between upstream and downstream sites may be accounted for by spatial variability but it could also be due to the use in differing brands of monitoring system. The data from this high-resolution monitoring shows similar trends to the first high-resolution monitoring at Parc mine exemplifying diel cycling for pH and EC. The data also suggests that variation in temperature and stage act as a control on chemical variables at upstream and downstream sites. Downstream EC shows variation confirming that the EC recorded downstream in the first high-resolution monitoring to be incorrect (Figures 5.26 & 5.28).

Table 5.7 Pearson's r correlations of high-resolution sampling 280219-060319

	Temperature (°C) upstream	pH upstream	DO_2 (mg/L) upstream	Electrical conductivity (µS/cm) upstream	Stage (m) upstream	Temperature (°C) downstream	pH downstream	DO_2 (mg/L) downstream	Electrical conductivity (µS/cm) downstream	Stage (m) downstream	TDS (mg/L) Downstream	Turbidity (NTU) Downstream
Temperature (°C) upstream	1											
pH upstream	0.012	1										
DO_2 (mg/L) upstream	-0.874	0.149	1									
Electrical conductivity (µS/cm) upstream	0.252	0.826	0.010	1								
Stage (m) upstream	-0.549	-0.498	0.220	-0.794	1							
Temperature (°C) downstream	0.904	-0.299	-0.661	0.583	-0.794	1						
pH downstream	0.304	0.901	-0.087	0.864	-0.685	0.563	1					
DO_2 (mg/L) downstream	-0.246	0.140	0.581	0.338	-0.285	-0.020	0.075	1				
Electrical conductivity (µS/cm) downstream	0.509	-0.624	-0.205	0.900	-0.908	0.795	-0.767	0.318	1			
Stage (m) downstream	-0.341	0.816	0.046	-0.949	0.831	-0.654	0.876	-0.278	-0.932	1		
TDS (mg/L) Downstream	0.509	-0.624	-0.205	0.900	-0.908	0.795	-0.767	0.318	1.000	-0.932	1	
Turbidity (NTU) Downstream	-0.244	-0.410	0.419	-0.311	0.166	-0.251	-0.452	0.474	-0.311	0.352	-0.311	1

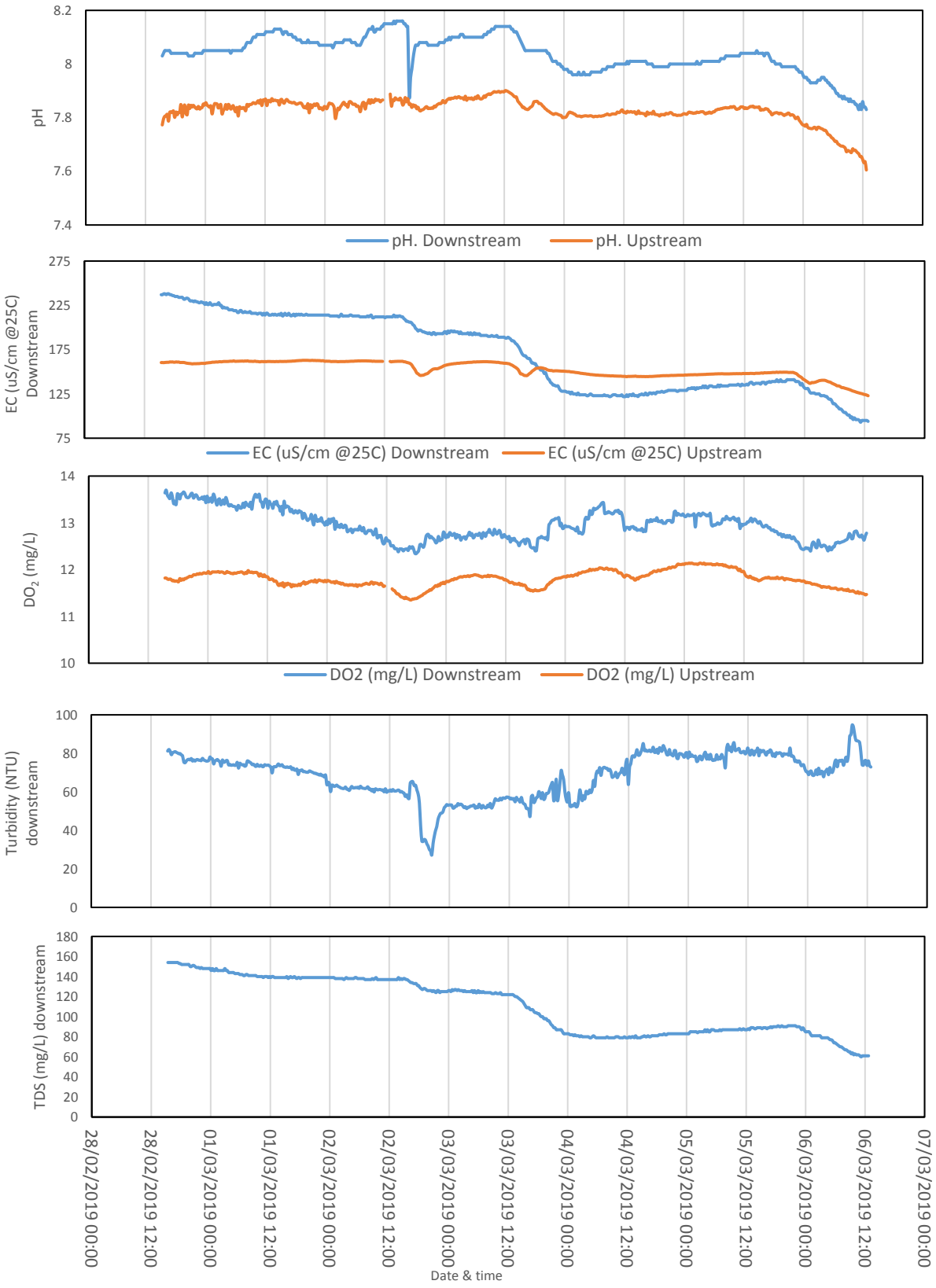

Figure 5.28. Chemical variability of high-resolution sampling carried out at Parc mine, Llanrwst – 28.02.2019-06.03.2019. At site A and D. Site A 0m upstream control site, site D 800.9m from site A post tailings deposits downstream.

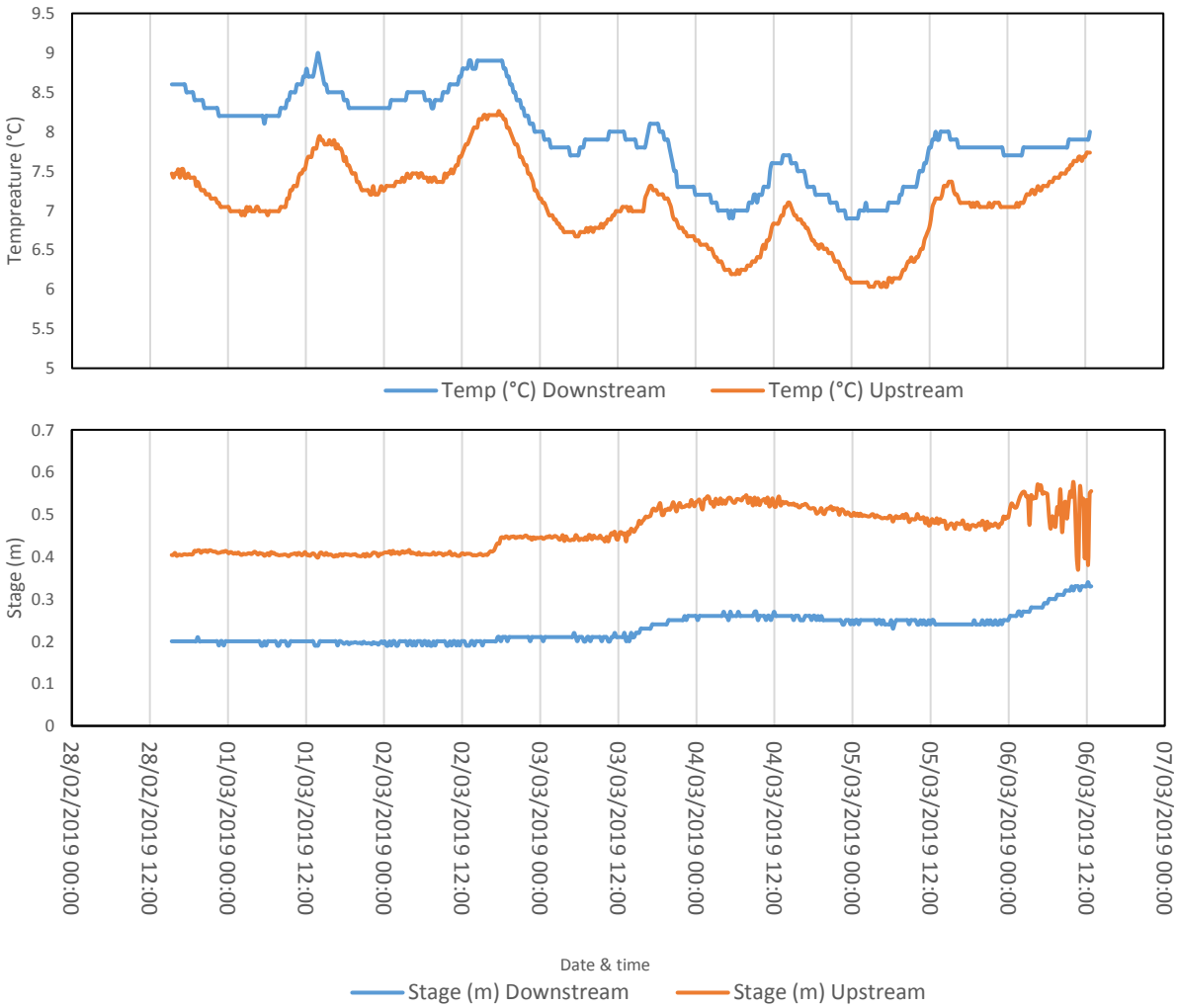

Figure 5.29. Hydroclimatic variability of high-resolution sampling carried out at Parc mine, Llanrwst – 28.02.2019-06.03.2019. At site A and D. Site A 0m upstream control site, site D 800.9m from site A post tailings deposits downstream.

Chapter 6 -Results & Discussion 2

6.1 Parc mine - High-resolution sampling

6.1.1 PHEs and WFD guidelines

High temporal resolution monitoring of chemical and hydroclimatic variables was carried out at Parc mine between 01.02.2019-02.03.19. During this sampling, hourly filtered and unfiltered water samples were collected for cation and anion analysis with the aim of quantifying PHE contamination, defining the speciation of any PHEs and assess water origins at site D of Parc mine. Data will be compared with low resolution monitoring to identify whether differing patterns in water geochemistry can be observed from a different, higher-resolution monitoring regime. PHE concentrations have been compared to Water Framework Directive Standards for Specific Pollutants (WFD SFSP) values for Zn and Fe (Appendix A.4.1 and Figure 6.1). Iron has a standardised guideline whereas Zn guidelines are catchment dependent (Appendix A.4.2). Water Framework directive Maximum Allowance Control (WFD MAC) values were used for Cd and Pb (Appendix A.4.3), Cd guidelines are $CaCo^3$ dependant (Appendix A.4.4). Comparison of PHE concentrations with WFD guidelines will identify any potential PHE concentrations that do not conform to the values identified for good ecological status.

In general correlations between chemical and hydroclimatic variables (Table 6.1) show stronger correlation for 24-hour monitoring than demonstrated by low resolution monitoring. This could potentially be due to the increased availability of data, specifically for PHEs, sampled at an hourly rate for 24-hour monitoring, the increased resolution has enabled strong correlation relationships of PHEs, hydroclimatic and climatic variable's to be identified more accurately (Diederichs and Karplus, 1997; Evans, P. R. and Murshudov, 2013). The primary cause could be potentially due to other unmonitored variables that have had less of an influence on monitored correlations over a short temporal period, than a long-term monitoring period that has potentially more influence from the unmonitored variables, such as ground water influences, soil moisture and atmospheric pressure.

Low resolution monitoring identified Zn and Cd as being of environmental concern, whereas Cd concentrations during high-resolution monitoring were not detectable. This suggest that if high-resolution monitoring is to be carried out on a site it will be required to be carried out over a period of several days to identify any trends that may be controlled by a variation that occurs over several days in synchrony with diurnal variation. Pb has been identified as exceeding the WFD guideline at site D during 24-hour monitoring reaching a maximum of 0.2 mg/L. For Zn a maximum concentration of 2.62 mg/L was demonstrated this was higher than the maximum concentration for Zn during low resolution monitoring (2.54 mg/L), this is also reflected in Zn mean concentration, 24-hour monitoring demonstrated a mean concentration of 2.42 mg/l and low resolution weekly monitoring demonstrated a mean concentration of 1.88 mg/L. 24-hour monitoring

has identified an increased concentration for Zn. 24-hour monitoring has identified Zn and Pb to be of concern for a good ecological status as defined by the WFD (The Water Framework Directive, 2015). Zinc exceeds the WFD guideline for the duration of monitoring, Fe remains below the guideline for the duration of the study and Pb exceeded guidelines on twice during monitoring (Figure 6.1 and 6.2).

Temperature is identified as having the strongest significant correlation between the hydroclimatic variables and chemical parameters (Table 6.1). This may be due to temperature exemplifying a diurnal variation enabling correlation to be identified over a short temporal scale. Low correlation values for stage and PHEs, may be due to stage demonstrating variation over longer temporal periods than 24-hour monitoring can detect.

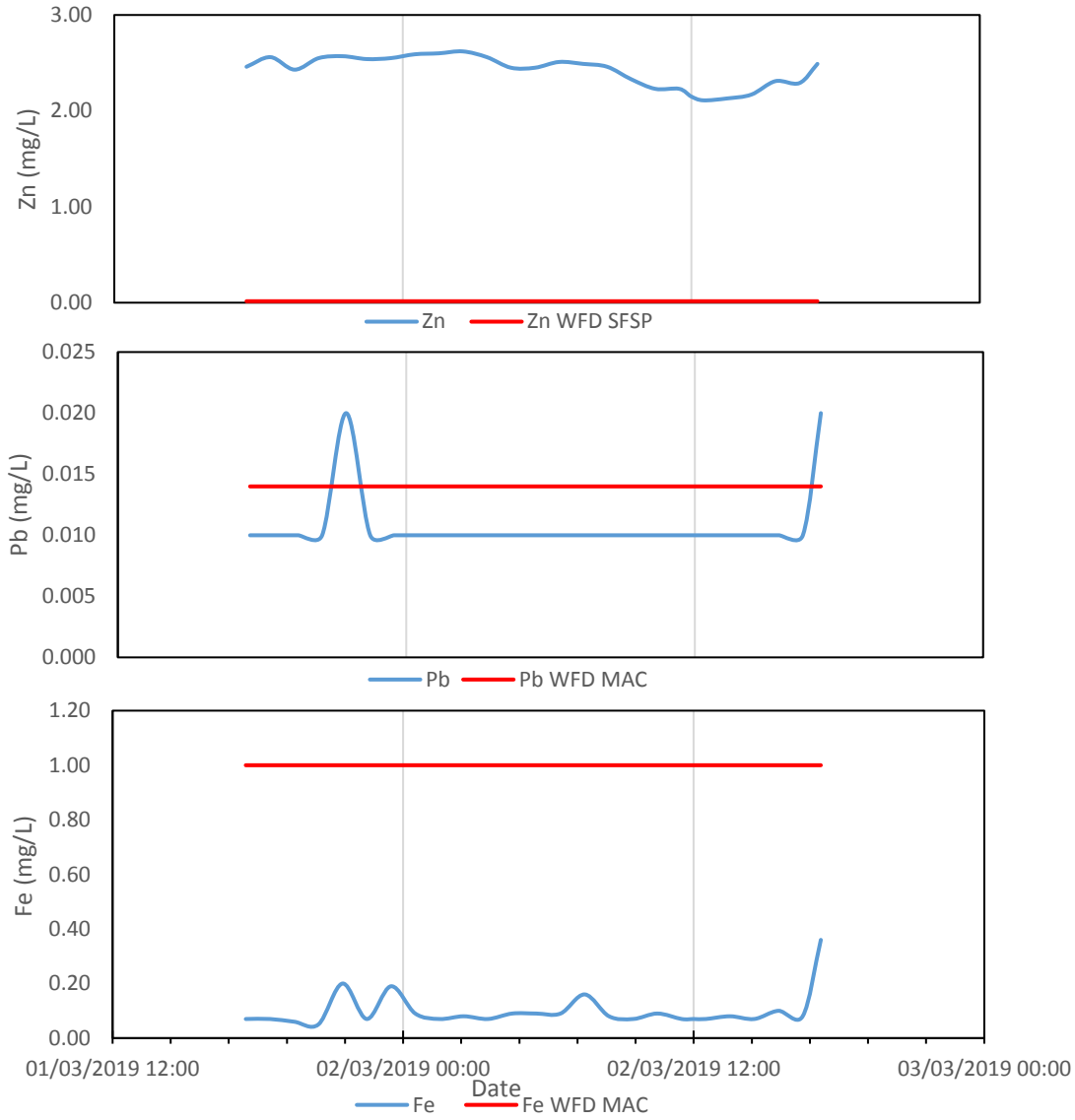

Figure 6.1. Filtered (0.45µ) PHE variability of hourly sampling carried out at site D Parc mine, Llanrwst – 01.02.2019-02.03.19.

Table 6.1. - Parc mine – Pearsons r correlation of 24-hour high-resolution sampling – 01.03.19-02.03.19.

	Temperature	pH upstre	DO_2 mg/L	EC (µS/cm	Stage (m)	Temperature	pH downst	DO_2 mg/L	EC (µS/cm	Stage (m)	TDS (mg/L)	Turbidity	Discharge	Zn (mg/L)	Pb (mg/L)	Cd (mg/L)	Fe (mg/L)
Temperature (°C)	1																
pH upstream	0.408	1															
DO_2 mg/L upstre	-0.966	-0.351	1														
EC (µS/cm)	-0.628	-0.020	0.685	1													
Stage (m) upstre	0.318	-0.285	-0.441	-0.844	1												
Temperature (°C)	0.918	0.486	-0.911	-0.669	0.275	1											
pH downstream	0.268	0.678	-0.139	0.416	-0.654	0.380	1										
DO_2 mg/L downst	-0.739	-0.428	0.758	0.595	-0.297	-0.875	-0.376	1									
EC (µS/cm)	-0.701	-0.281	0.776	0.883	-0.698	-0.728	0.094	0.705	1								
Stage (m) downst	0.535	-0.227	-0.602	-0.484	0.446	0.388	-0.271	-0.331	-0.422	1							
TDS (mg/L) downst	-0.738	-0.324	0.806	0.880	-0.670	-0.775	0.048	0.782	0.985	-0.419	1						
Turbidity (NTU)	-0.371	-0.207	0.381	0.338	-0.116	-0.579	-0.377	0.781	0.328	0.000	0.427	1					
Discharge m3/s	0.515	0.005	-0.518	-0.502	0.433	0.549	-0.022	-0.655	-0.461	0.546	-0.519	-0.441	1				
Zn (mg/L) downst	-0.496	-0.742	0.373	0.016	0.299	-0.676	-0.763	0.635	0.208	0.097	0.276	0.518	-0.257	1			
Pb (mg/L) downst	0.246	-0.256	-0.390	-0.801	0.836	0.226	-0.718	-0.171	-0.594	0.384	-0.576	-0.057	0.301	0.334	1		
Cd (mg/L) downst	N/A	N/A	N/A	N/A	N/A	N/A	N/A	N/A	N/A	N/A	N/A	N/A	N/A	N/A	N/A	1	
Fe (mg/L) downst	0.354	-0.252	-0.526	-0.835	0.869	0.242	-0.670	-0.200	-0.722	0.558	-0.669	0.101	0.345	0.447	0.821	N/A	1

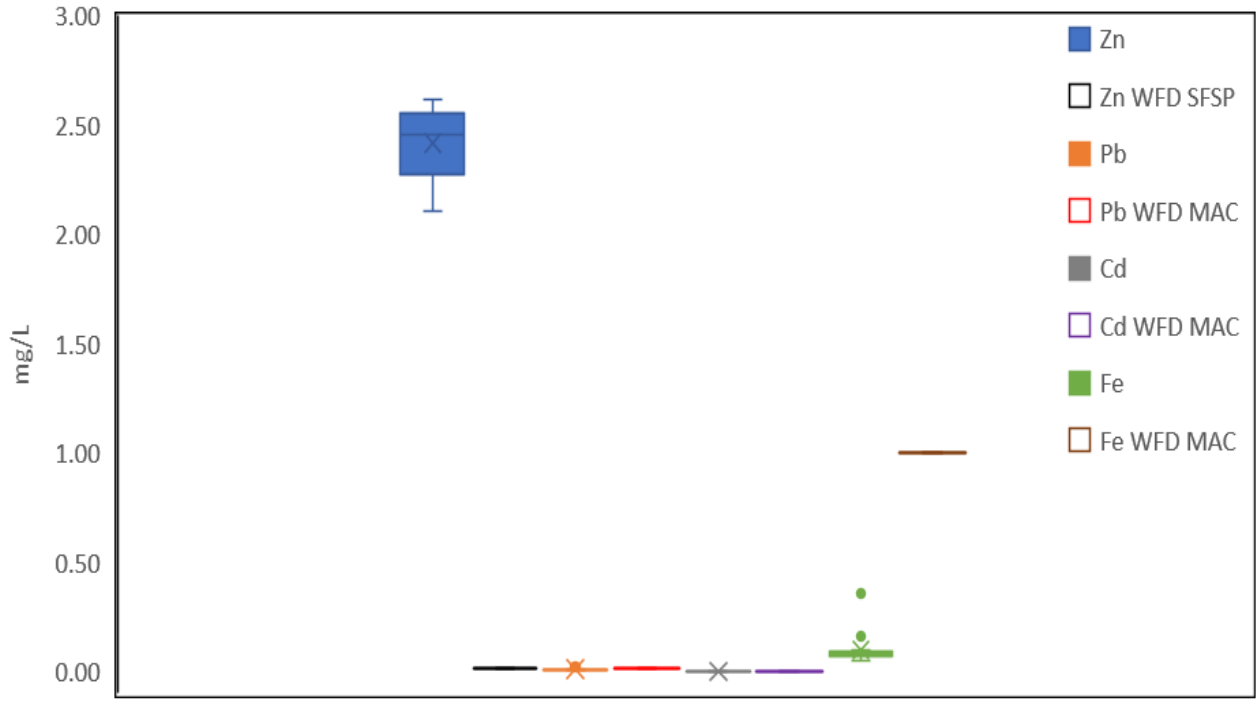

Figure 6.2. Filtered (0.45µ) PHE concentrations of hourly sampling carried out at site D Parc mine, Llanrwst – 01.02.2019-02.03.19.

6.1.2 Total PHE concentrations and enrichment

Unfiltered PHE concentrations were compared with filtered PHE concentrations to identify concentrations of particulate loads and the controls upon them. Unfiltered water PHEs also indicate the total PHE within the fluvial system. Unfiltered PHE concentrations at site D are of concern as they indicate the total of solute and particulate PHE in question entering the River Conwy. Unfiltered PHE concentration comparisons with filtered PHE concentrations identified a temporally and spatial varied particulate load. Particulate loads, based on mean filtered and unfiltered concentrations of PHEs exhibit a particulate load of 11.36%, 33.33% and 86.93% for Zn, Pb and Fe respectively. The particulate loads demonstrated can be explained by the relative solubility, Zn is relativity soluble at a wide range of pH, Pb is relatively insoluble, with circum neutral drainage, it is likely that Pb will be primarily be in a particulate form (Jickells, 1997; Bird *et al.,* 2009; Moncur *et al.,* 2014; Guan *et al.,* 2016).

PHEs show variation over the monitoring period (Figure 6.3), PHEs primarily in solution show stronger correlation with chemical variables, primarily Zn. Pb and Fe have greater particulate loads than Zn and demonstrate greater correlation with hydroclimatic variables (Table 6.1). Diurnal variation is demonstrated by Zn, which could be explained by the majority of the Zn being present in solute form (<0.45μm), making it more susceptible to chemical controls, chemical controls have been found to demonstrate diurnal variation (Nagorski *et al.,* 2003; Rudall and Jarvis, 2012). The increased particulate loads of Pb and Fe are more likely to be controlled by changes in stage, which will transport particulate loads (>0.45 μm) at varying rates dependent upon increases and decreases in flow. Pearsons r correlation data confirms that stage has stronger significant ($p < 0.05$) correlations with Pb and Fe than with Zn. Temperature shows a stronger significant correlation with Zn and temperature has stronger correlations with chemical variables of pH, EC and DO_2, this confirms temperature has a greater effect on chemical variable's and PHEs in solution.

At site D during 24-hour monitoring Zn demonstrated the greatest mean concentration of 2.73mg/L, with Pb (mean of 0.015 mg/L), Fe (mean of 0.765 mg/L) and Cd (not detectable) present in lower concentrations (Figure 6.4). Despite Zn demonstrating the maximum concentration of PHEs in question, it is Fe that demonstrates the maximum enrichment, followed by Pb and Zn had the minimum enrichment compared to the upstream control site (Figure 6.5). Enrichment data suggest that Zn enrichment at site D has returned to levels considered resultant of geogenic loading at site D, while the enrichments of Pb and Fe at site D still demonstrate enrichment that suggests anthropogenic activity from mining upstream is still having an effect at site D (Reimann and Garrett, 2005).

In summary of the PHEs investigated, Zn demonstrates the greater relative presence in filtered waters, whereas other PHEs show a greater association with >0.45 um particulates present within raw water samples. This suggests that Zn is primarily present in a dissolved form and therefore more susceptible to chemical controls than hydroclimatic controls. Pb and Fe have increased particulate loads and are therefore

more susceptible to physical hydroclimatic controls than chemical controls such as changes in stage. Filtered and unfiltered PHEs loads and concentrations have differing primary controls upon there temporal and spatial variability but are ultimately controlled by both chemical and hydroclimatic controls. Zn unfiltered concentration is of greatest concern to providing a good ecological status as defined by the WFD (The Water Framework Directive, 2015).

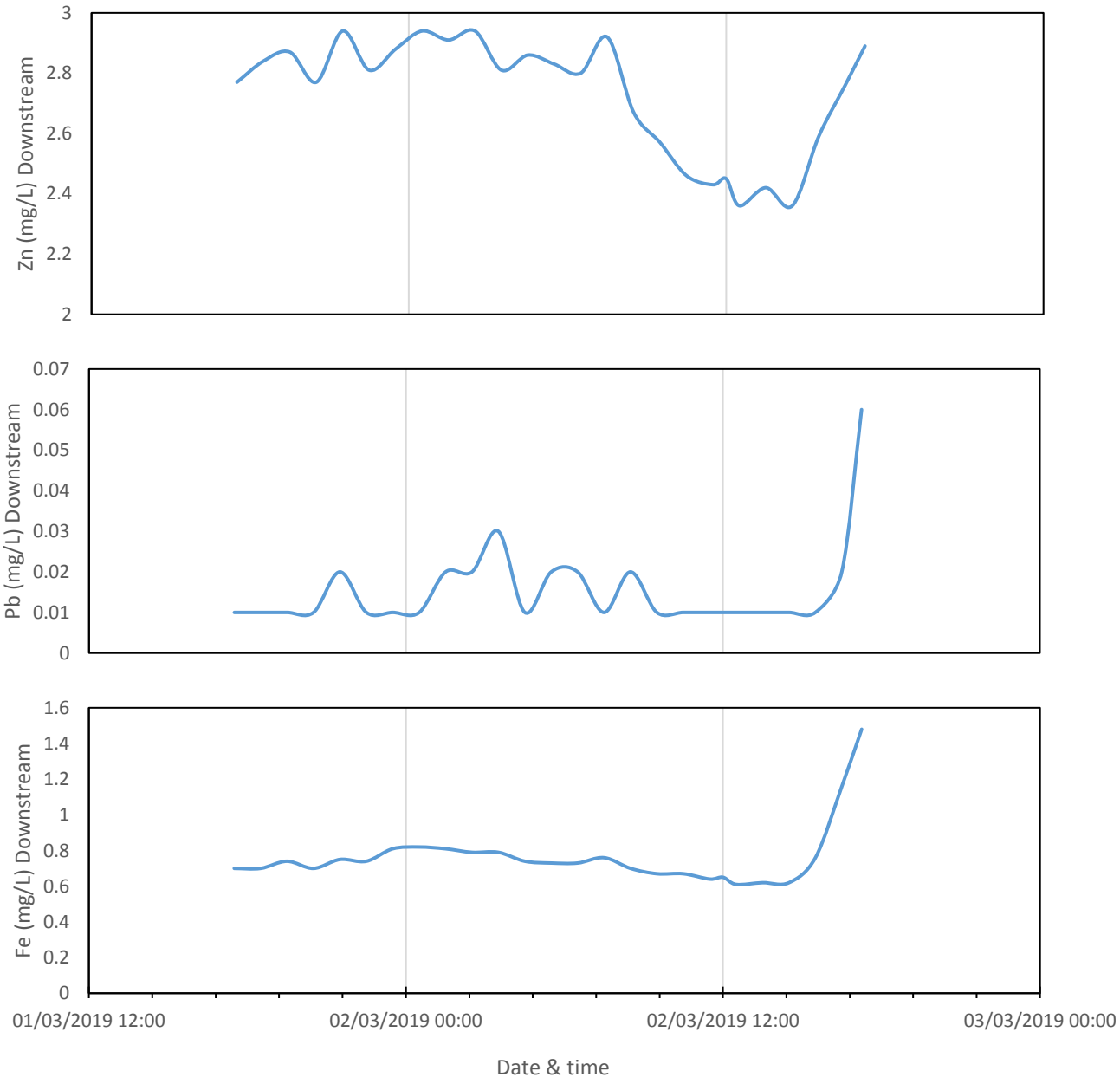

Figure 6.3. unfiltered PHE variability of 24-hour, high-resolution sampling carried out at site D Parc mine, Llanrwst – 01.03.2019-02.03.2019

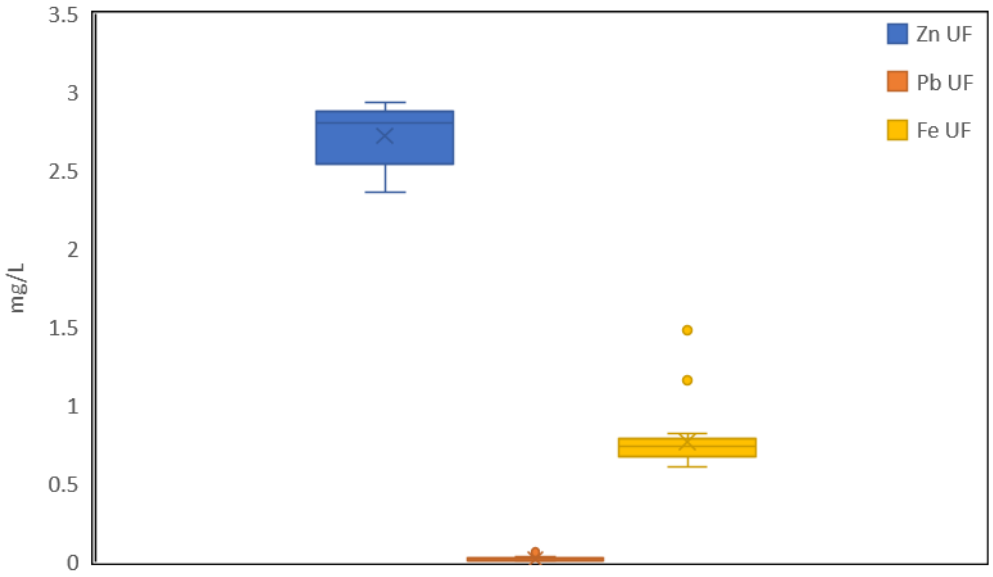

Figure 6.4. unfiltered PHE variability of 24-hour, high-resolution sampling carried out at site D 800.9m from control site post tailings deposit Parc mine, Llanrwst – 01.03.2019-02.03.2019.

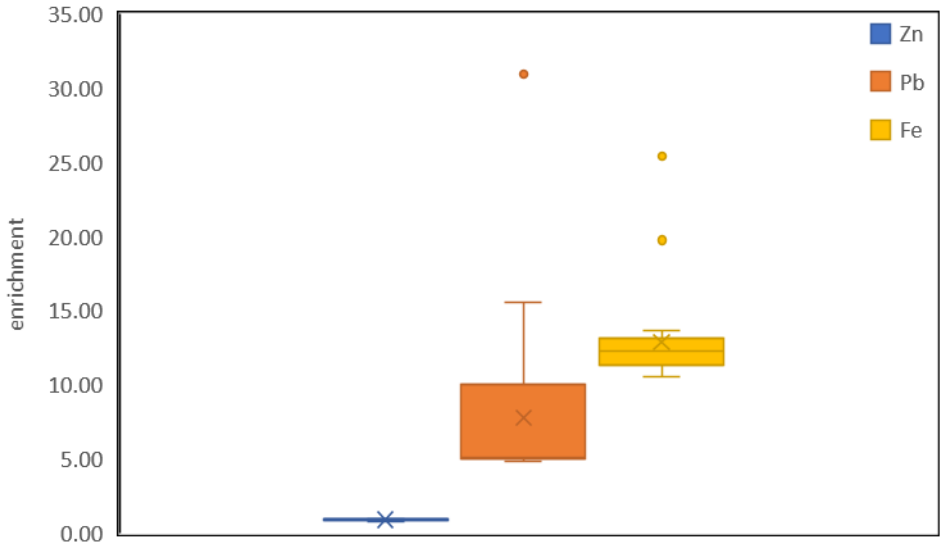

Figure 6.5. Total Zn, Pb, Cd and Fe concentration enrichment (unfiltered – UF) for Parc mine, Llanrwst – 01.02.2019-02.03.19.

6.1.3 Hydroclimatic and Chemical variables

During 24-hour monitoring of PHEs at downstream site D, pH, EC, DO_2 and turbidity were monitored at site D and upstream site C. Chemical and hydroclimatic variables were monitored as means of identifying any spatial and temporal correlations with PHE loading and concentrations. 24-hour monitoring was carried out to identify diurnal trends that were not identified during low resolution monitoring. Statistical difference analysis via an unequal variance T-test demonstrated upstream and downstream pH EC and DO_2 to be statistically significantly different ($p < 0.05$). 24-hour monitoring demonstrated a mean upstream pH 7.85 and a downstream pH 8.1, this may have been due to the mine water from adit site B increasing river water temperature. Low resolution monitoring between 27.11.18-28.03.19 of the adit site B demonstrated a mean temperature of 8.73 °C with a mean discharge dilution factor of 1.76 between sites A and B, this can account for the increase in temperature downstream at site D of the Nant Gwydyr. Temperature shows the strongest correlation for hydroclimatic variables with pH, EC, and DO_2, suggesting that temperature is the primary hydroclimatic control for diurnal variability.

Turbidity exhibits variation with discharge (Figures 6.6 and 6.7); Pearsons r correlation shows a significant ($p < 0.05$) negative correlation (Table 6.1), suggesting that variation in turbidity is not diurnal. Total dissolved solids (TDS) show variation during 24-hour monitoring (Figure 6.6) and shows a significant ($p < 0.05$) correlation with discharge (Table 6.1), suggesting that increases in discharge increase TDS. A significant positive correlation between TDS and total Zn suggests that the majority of Zn is in a dissolved form (Table 6.1).

In summary, diurnal cycling of pH, DO_2 and EC are apparent for site D, controlled primarily by temperature changes that are subject to daily fluctuation during night and day (Sullivan and Drever, 2001; Nagorski *et al.,* 2003; Rudall and Jarvis, 2012). Turbidity and TDS show variation primarily controlled by discharge and stage. Total dissolved solids demonstrate variation over longer temporal periods ~days, due to processes controlling discharge and stage, such as rainfall regimes.

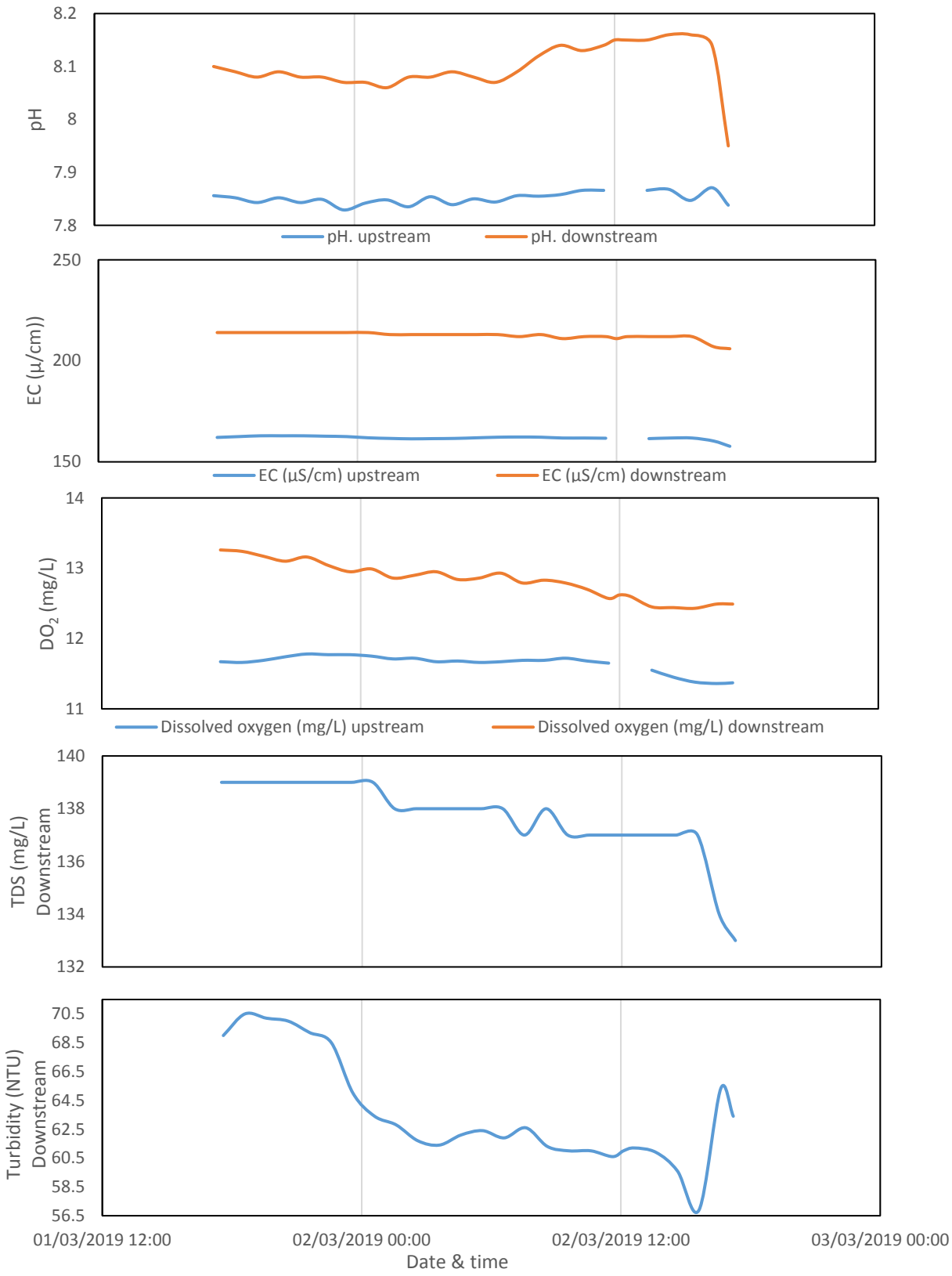

Figure 6.6. Chemical variability of 24-hour, high-resolution sampling carried out at Parc mine, Llanrwst – 01.03.2019-02.03.2019. At site A and D. Site A 0m upstream control site, site D 800.9m from site A post tailings deposits downstream.

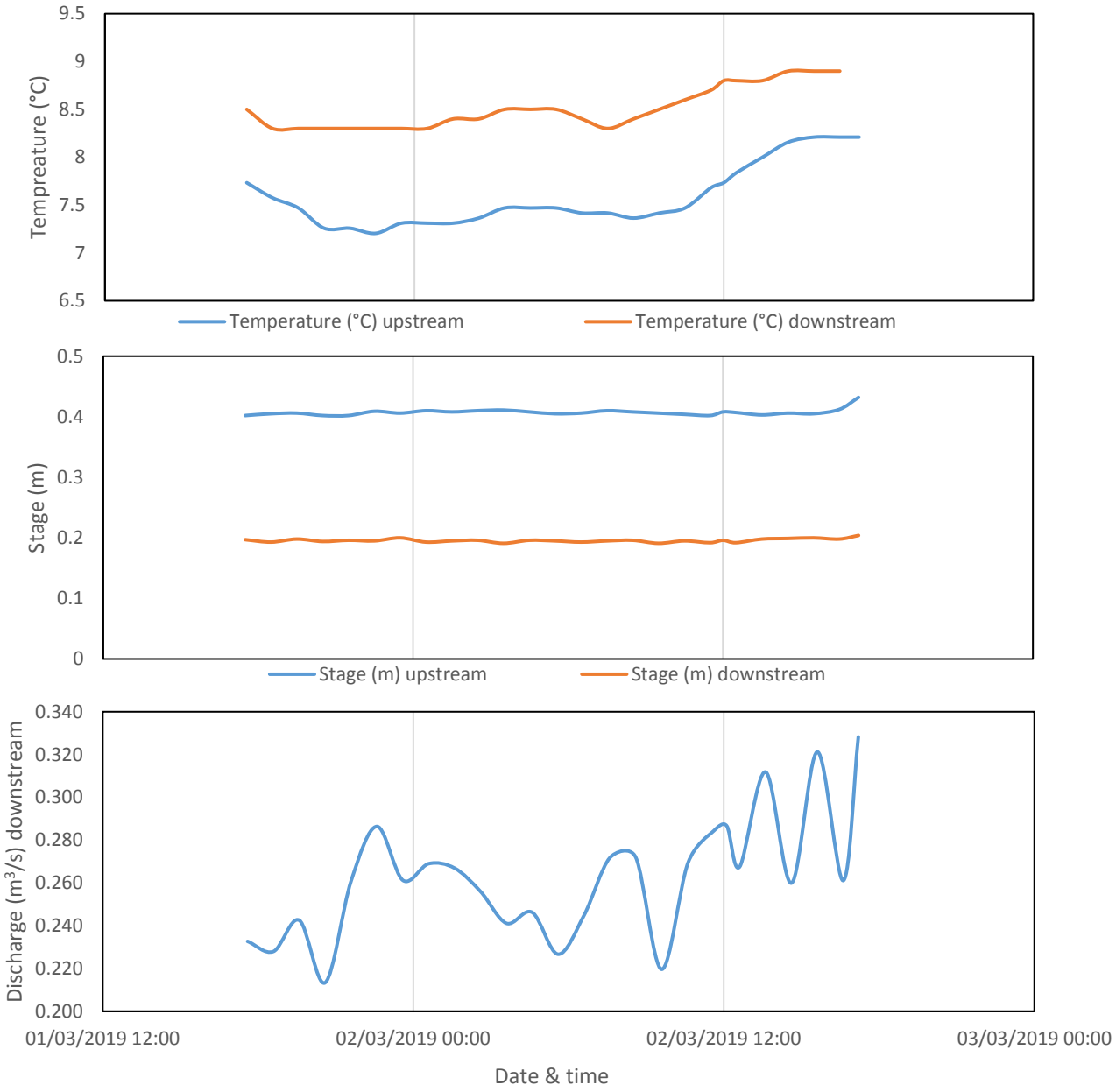

Figure 6.7. Hydroclimatic variability of 24-hour, high-resolution sampling carried out at Parc mine, Llanrwst – 01.03.2019-02.03.2019. At site A and D. Site A 0m upstream control site, site D 800m from site A post tailings deposits downstream.

6.1.4 Load vs concentration

24-hour, hourly synoptic water sampling enabled concentrations of PHEs to be determined. Hourly discharge rates were also calculated from velocity and stage monitoring at a measured cross section at site D. Discharge data was used to calculate minimum, mean and maximum PHE loads (Table 6.2). Zinc demonstrated an estimated annual load of 22.53 t/y, Pb annual load was 0.13 t/y and Fe had a mean load of 6.39 t/y base upon discharge during the study. The resultant loads are higher than the calculated loads for low resolution monitoring for Zn, which exhibited a 56.57% increase and Fe which demonstrated a 35.67% increase. Lead demonstrated a 60.61% decrease. Cadmium was not detected during 24-hour high-resolution monitoring and therefore load calculations are not applicable (N/A).

Pearsons r correlation of PHE load and concentration for Zn (0.402), Pb (0.985) and Fe (0.944) are significant ($p < 0.05$) (Table 6.3), this suggests increases in load are associated with increases in concentration. However, Zn shows a weaker relationship, indicating that Zn load may be influenced by additional factors. Given that load is a function of concentration and discharge, it is possible that Zn demonstrates a different load-concentration-discharge relation to Pb and Fe associated with the release of Zn under different discharge conditions (Figure 5.14, 5.15 and 5.16). This suggests the mine is still experiencing increases in contamination from periods of oxidation and washing from diurnal increases and decreases in flow and flooding out washing mine waters (Elderfield *et al.,* 1979; Nagorski *et al.,* 2003). During the 24-hour monitoring period discharge identified positive significant correlation with discharge, however concentration did not exhibit any significant correlation with discharge (Table 6.3). This suggest that discharge is a controlling factor of load but has no effect on concentrations during 24-hour monitoring suggesting the controls on concentration variation are different and primarily controlled by chemical variability.

All PHE loads show diurnal variation (Figures 6.8, 6.9 and 6.10), that is influenced by variation in discharge during the last 1.5 hours of the 24-hour monitoring period. The total loads exemplified at site D for 24-hour monitoring resulting from PHE inputs from the mine adit and the tailings area downstream of the adit. The load of PHEs at Parc mine varies temporally over the period of the study controlled by hydroclimatic factors that are driven by localised climate regimes of rainfall and temperature change due to seasonality.

Table 6.2. Total mean loads for Zn, Pb, Cd and Fe based on high-resolution 24-hour monitoring at Parc mine, Llanrwst 01.0319-02.0319.

		Kg/d	t/y
Zinc	**Min**	48.77	17.80
	Mean	61.72	22.53
	Max	81.96	29.92
Lead	**Min**	0.18	0.07
	Mean	0.36	0.13
	Max	1.70	0.62
Cadmium	**Min**	N/A	N/A
	Mean	N/A	N/A
	Max	N/A	N/A
Iron	**Min**	12.72	4.64
	Mean	17.51	6.39
	Max	41.97	15.32

Table 6.3. Pearson's r correlation PHE load, concentration and discharge at site D Parc mine (Figure 3.2) during 24-hour monitoring 01.0319-02.0319.

	Zn mg/l	*Pb mg/l*	*Fe mg/l*	*Discharge m3/s*	*Zn kg/d*	*Pb kg/d*	*Fe kg/d*
Zn mg/l	1.000						
Pb mg/l	0.334	1.000					
Fe mg/l	0.447	0.821	1.000				
Discharge m3/s	-0.257	0.301	0.345	1.000			
Zn kg/d	0.402	0.522	0.637	**0.780**	1.000		
Pb kg/d	0.274	0.985	0.845	**0.425**	0.601	1.000	
Fe kg/d	0.269	0.806	0.944	**0.624**	0.784	0.871	1.000

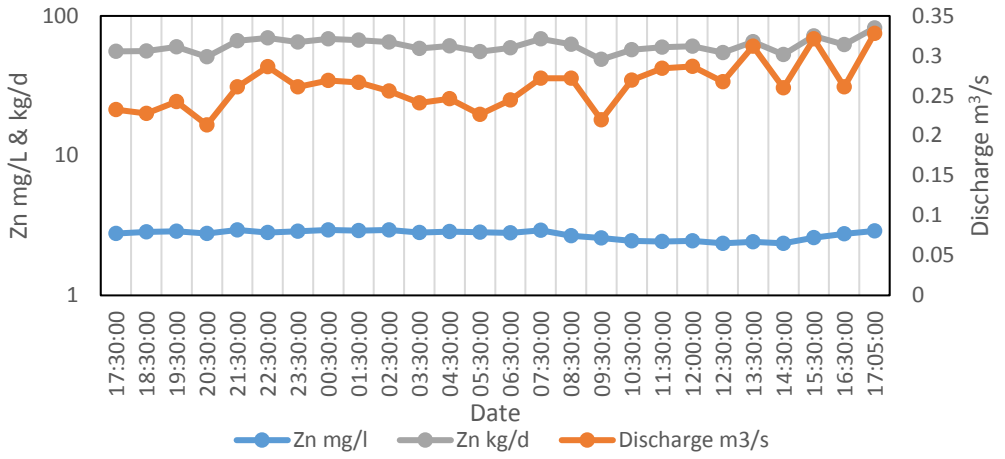

Figure 6.8. Mean total unfiltered Zn concentration, load and discharge relationship at Parc mine based on site D high-resolution monitoring 01.03.19-02.03.19.

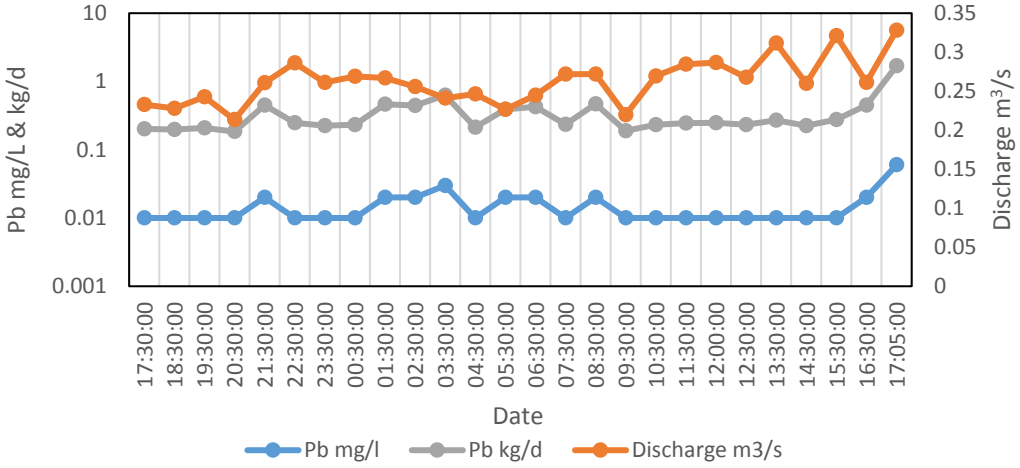

Figure 6.9. Mean total unfiltered Pb concentration, load and discharge relationship at Parc mine based on site D high-resolution monitoring 01.03.19-02.03.19.

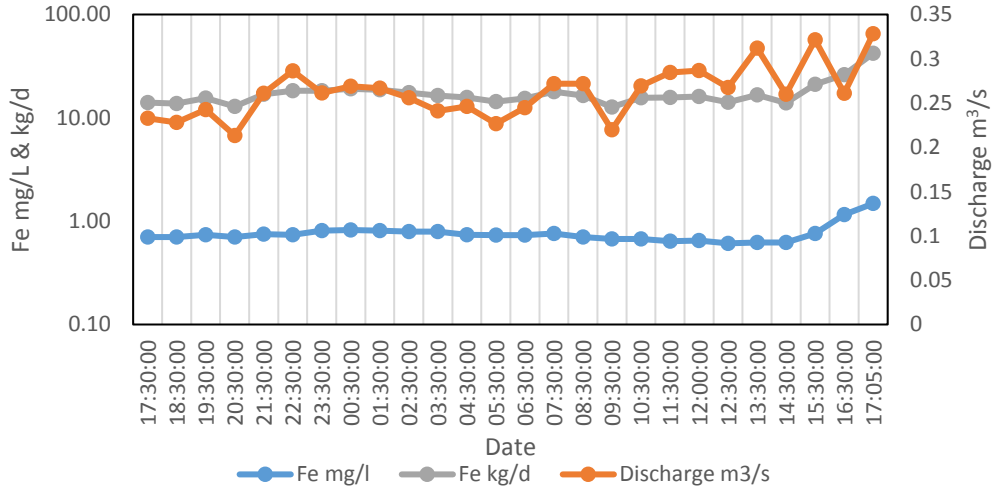

Figure 6.10. Mean total unfiltered Fe concentration, load and discharge relationship at Parc mine based on site D high-resolution monitoring 01.03.19-02.03.19.

6.1.5 PHE Speciation

Results of 24-hour resolution monitoring of the dominant geochemical PHE species was carried out for each sample site, calculated using pH and redox potential analysis, there was little temporal variation in the species of PHEs at all sample site D. The dominant species of Zn was $ZNCO_3$ (Figure 6.11), Pb was $PbSO_4$ (Figure 6.12), Cd was Cd^{2+} (Figure 6.13) and Fe was $Fe(OH)_3$ (Figure 6.14). Zinc is in a carbonate form, Pb and Fe are in sulphide forms that are generally more insoluble, this conforms with increased particulate loads for Fe and Pb in section 6.1.2. Iron is likely to be present as $Fe(OH)_3$ due to oxidation processes occurring as mine waters interact with the atmosphere promoting precipitation. Pb present as PbSO can explain the low concentrations analysed during the study, PbSO is relatively insoluble and therefore immobile in periods of low flow. The presence of Zn in a soluble carbonate form confirms the consistently high concentration demonstrated temporally and spatially throughout the study for Zn (Shooter, 1976). 24-hour monitoring in comparison to low-resolution monitoring analysis for speciation has identified Zn to be in different chemical facies.

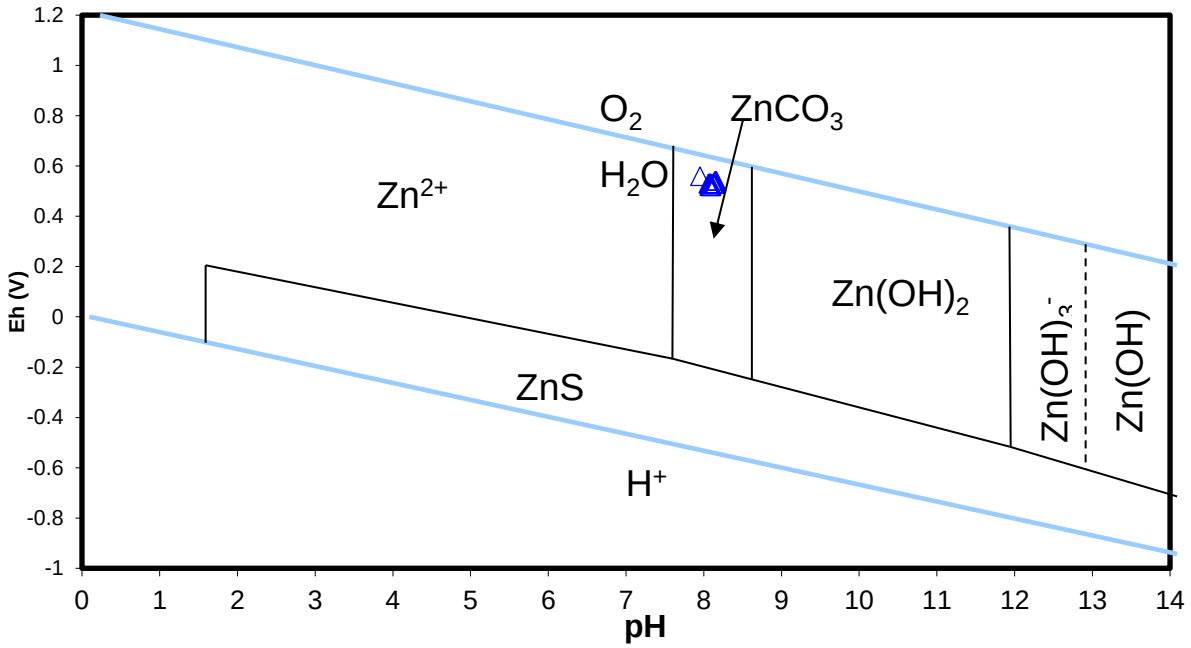

Figure 6.11. Speciation of Zn at Parc mine, sample site D, based on mean pH and redox values from 24-hour monitoring. Adapted from (Garells and Christ,1965).

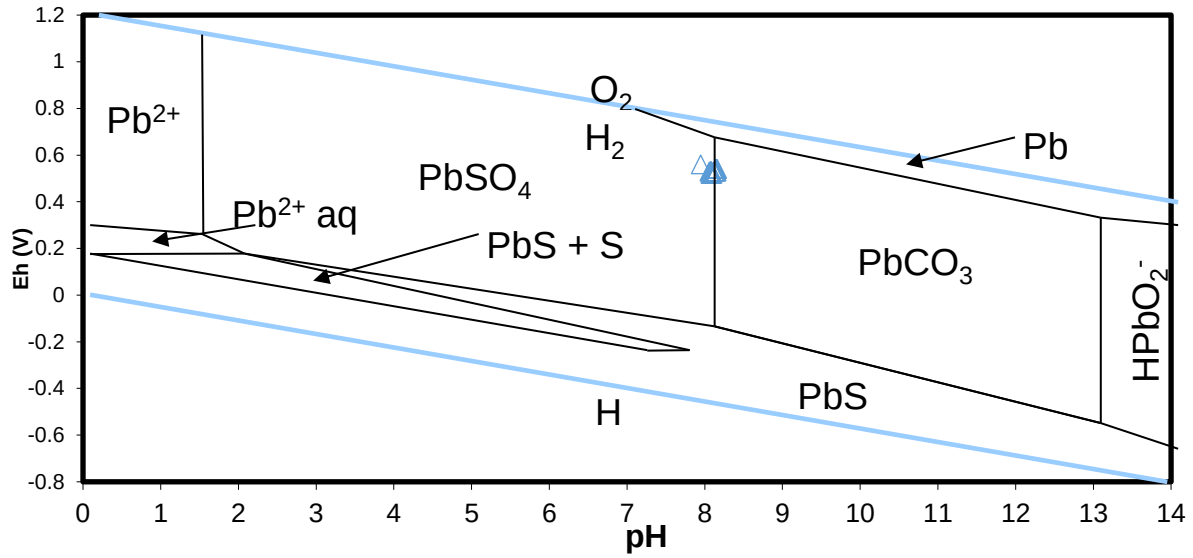

Figure 6.12. Speciation of Pb at Parc mine, sample site D, based on mean pH and redox values from 24-hour monitoring. Adapted from (Garells and Christ,1965).

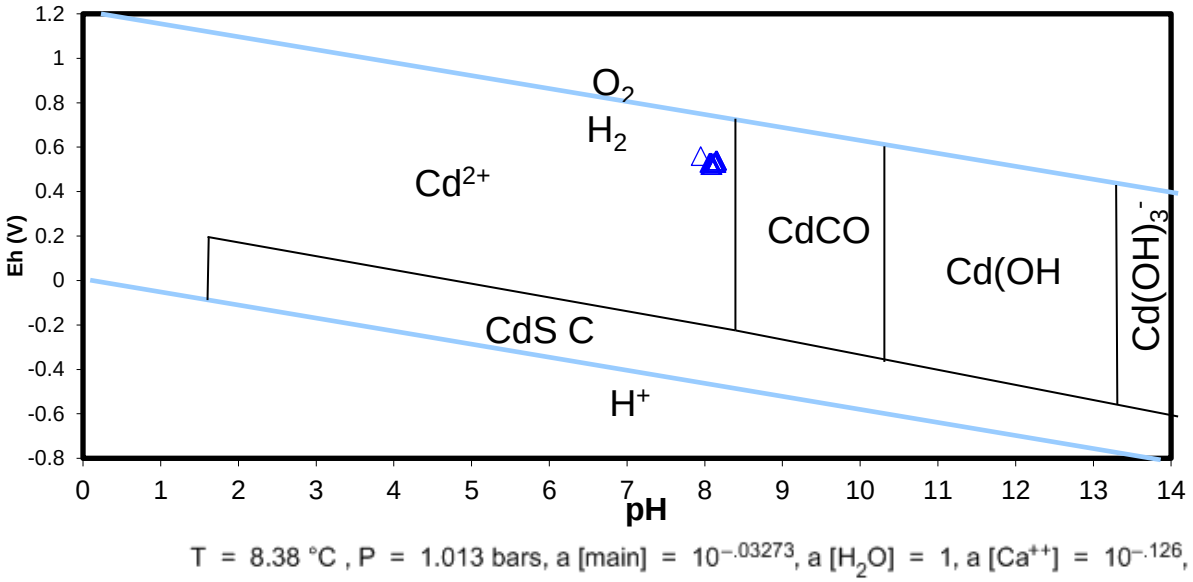

Figure 6.13. Speciation of Cd at Parc mine, sample site D, based on mean pH and redox values from 24-hour monitoring. Adapted from (Garells and Christ,1965).

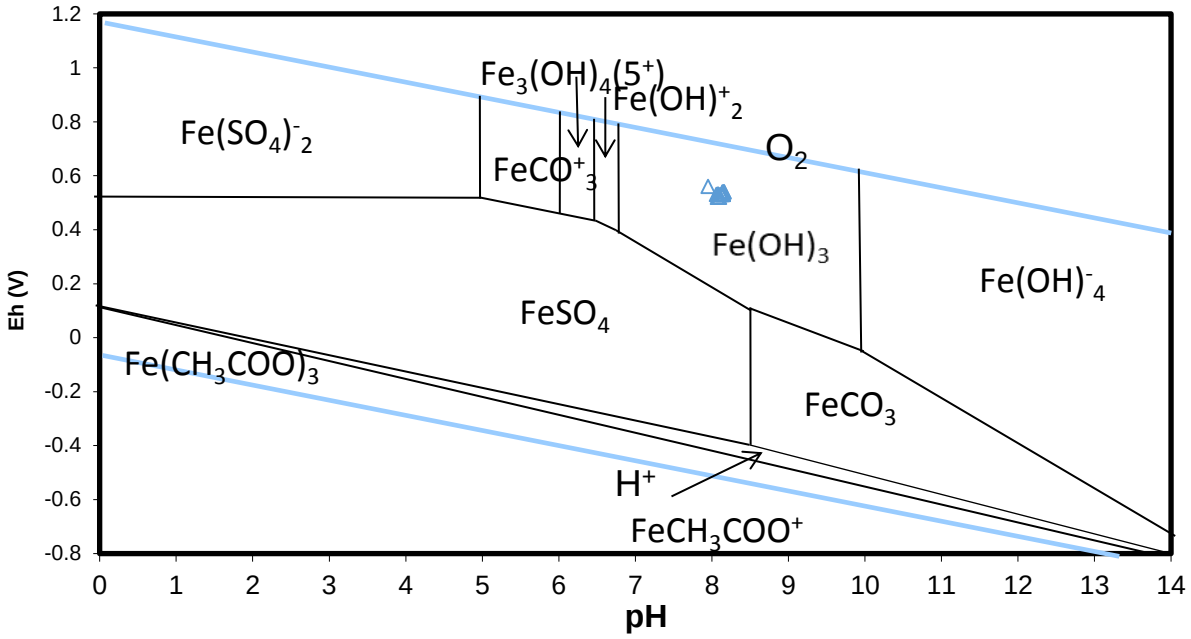

T = 8.38 °C , P = 1.013 bars, a [main] = $10^{-.03273}$, a [H_2O] = 1, a [Ca^{++}] = $10^{-.126}$, a [Mg^{++}] = $10^{-.121}$, a [Na^{+}] = $10^{-.03273}$, a [K^{+}] = $10^{-.03348}$, a [HCO_3^{-}] = $10^{-.03241}$, a [SO_4^{--}] = $10^{-.1314}$, a [Cl^{-}] = $10^{-.03348}$, a [Zn^{++}] = $10^{-.03273}$, a [Fe^{++}] = $10^{-.03273}$

Figure 6.14. Speciation of Fe at Parc mine, site D, based on mean pH and redox values from 24-hour monitoring. Adapted from (Garells and Christ,1965).

6.1.6 Water origins

Anion and cation analysis, interpreted using trilinear plots, was carried out to ascertain water origins at each sample site for Parc mine during the 24-hour monitoring (Figure 6.15). For the duration of the monitoring period sample site D showed little variation exhibiting the same chemical facies as low-resolution monitoring produced for site D (Figure 5.24). The water at site D is typical of calcium carbonate rich waters (Figure 2.2). The water at site D is likely to be buffered from localised carbonate rich limestone bedrock geology which would account for the waters exemplifying a carbonate rich chemistry, the water at site D is rich in sulphide, which may be explained from the mineralization from within the mine and surrounding areas by weathering of minerals including ZnS, in light of this carbonate waters are the dominant group at Parc mine. Limestone geology buffers pH which would reduce AMD and stop sulphide rich waters becoming the dominant water group (Bikundia and Mohan, 2014; Michalski, 2018). Data for high and low-resolution sampling provide similar results in terms of water chemistry as represented by trilinear plots. This suggests that, during the time of sampling at least, the water chemistry is temporally stable and that there are no shorter duration fluctuations in water chemistry that are not identified by low resolution sampling.

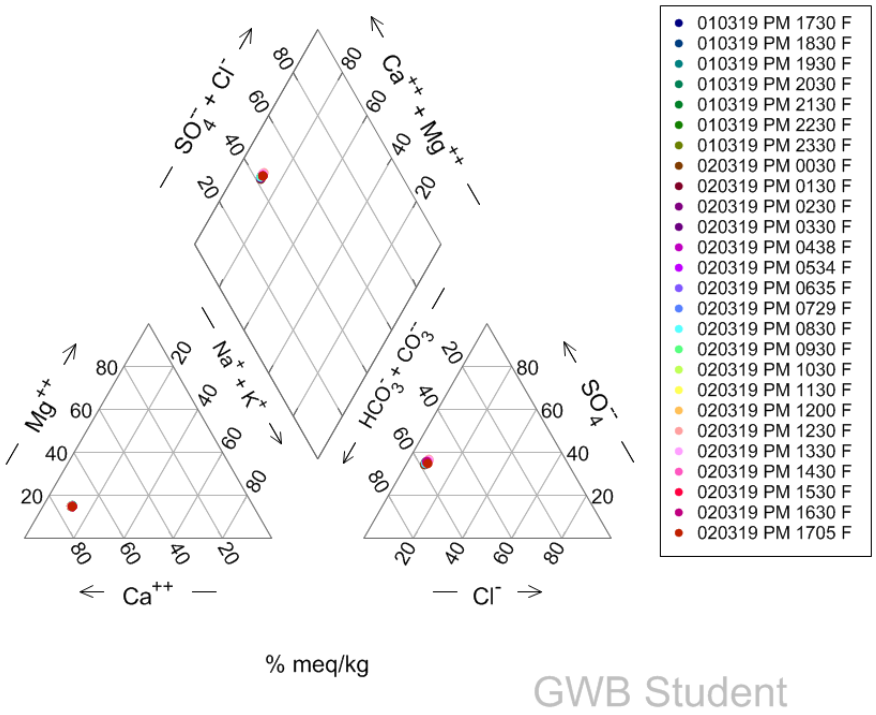

Figure 6.15. Mean water origins of high-resolution 24-hour sampling carried out at Parc mine - 27.11.2018-28.03.2019. At site D post tailings deposits, 800.9m from control and 787m from site B adit.

Chapter 7- Results & discussion 3

7.1 Cwm Rheidol Mine - Low resolution – fortnightly sampling

7.1.1 PHEs and WFD guidelines

During low resolution monitoring between 27.11.2018-28.03.2019 concentrations of Zn, Pb Cd and Fe in filtered samples were determined (Table 7.1 and Figure 7.1) at sites A, B, C and D at Cwm Rheidol mine (Figure 3.3). PHE concentrations have been compared to Water Framework Directive Standards for Specific Pollutants (WFD SFSP) values for Zn and Fe (Appendix A.4.1 and Figure 7.1). Iron has a standardised guideline whereas Zn guidelines are catchment dependent (Appendix A.4.2). Water Framework directive Maximum Allowance Control (WFD MAC) values were used for Cd and Pb (Appendix A.4.3), Cd guidelines are $CaCo_3$ dependant (Appendix A.4.4). Comparison of PHE concentrations with WFD guidelines will identify any potential PHE concentrations that do not conform to the values identified for good ecological status.

Generally, a temporal variation in filtered PHE concentrations was found. Zinc was found to be above WFD SFSP guideline of 0.015 mg/L at sites A, B C and D for Cwm Rheidol mine site for the duration of the study, the maximum concentration recorded during the study was at site A on 27.02.19 91.55 mg/L (Figure 7.1). Lead concentrations fluctuated between below and above the WFD MAC at site A, site B exceeded Pb concentrations for the duration of the study and importantly at control site C and downstream site D Pb did not exceed the WFD MAC (Figure 7.1). Cadmium was found to exceed WFD MAC concentrations of 0.0009 and 0.0015 mg/L for the duration of the study at sites A and B at sites C and D 40% of determined samples exceeded the WFD MAC of 0.00045 mg/L, in 60% of determined samples Cd was not detected. Iron was below the 1mg/L WFD SFSP for the duration of the study, at sites C and D. Sites A and B exceeded the WFD SFSP for the duration of the study with a maximum concentration of 122.66 mg/L at site A (Figure 7.1). Importantly, at Site D, the bottom of the study reach, where PHEs have been dispersed to the River Rheidol, it is Zn and Cd concentrations that exceed WFD guidelines.

It is notable that Zn and Cd are above WFD guidelines at control site C, this may be due to several factors, contamination from mining upstream (Fuge *et al.,* 1991), geogenic loading from bedrock proximal or upstream of the mine site (Bird *et al.,* 2014; Shea *et al.,* 2016). The site selected as a control site may have too close to the vicinity of the mine and any proximal geogenic inputs additional monitoring further upstream would be required to ascertain this.

Sites A and B exceed the WFD guidelines for PHEs, it is notable that there is a reduction in Zn, Cd and Fe concentrations between sites A and B, but it is not efficient to reduce PHE concentrations below the WFD guidelines, Pb experiences an increase in concentration from site A to site B, this further supports that Pb contamination is from a geogenic bedrock source proximal to sites B, C and D. the impact of Zn, Cd and Fe from site B on concentrations demonstrated at site D is minimal and may be explained by dilution factors.

Correlation analysis of filtered PHEs found that Zn and Cd to have the strongest significant $p < 0.05$ (0.992) positive filtered correlation and Zn and Fe (0.979) exhibited the second strongest significant $p < 0.05$ positive filtered correlation, followed by Cd and Fe (0.958) (Table 7.1). It was also exemplified that Pb and Fe exhibit a negative correlation, but this is a weaker correlation than the positive correlations exemplified with Zn and Cd. This identifies that there is similarity in the in the variation of Zn and Cd suggesting the controls on Zn and Cd concentrations may be o f a similar nature.

Mean Zn filtered concentrations during monitoring (27.11.2018-28.03.2019) were 66.08, 17.25, 0.11 and 0.14 mg/L for sites A, B, C and D (Figures 7.2 and 7.3). Pb demonstrated mean filtered concentrations of 0.12, 0.58, 0.001 and 0.001 mg/L for sites A, B, C and D (Figures 7.4 and 7.5). Cd demonstrated mean filtered concentrations of 0.1, 0.03, 0.004 and 0.004 mg/L for sites A, B, C and D (Figures 7.6 and 7.7). Fe demonstrated mean filtered concentrations of 65.4. 5.81, 0.1 and 0.096 mg/L for sites A, B, C and D (Figures 7.8 and 7.9).

The filter bed exhibited an efficiency of 73.9%, 70.0% and 91.1% removal of Zn, Cd and Fe respectively. The efficiency has improved for Zn removal since 2014, where the efficiency was reported to be 60% for the period of January to March 2014 (Williams, 2014). The data suggests decrease in efficiency of Cd and Fe removal since previous research Cd was reported to have a removal rate of 87% in May 2012 and the average removal rate of Fe was 98% for the period of 2010-14(Williams, 2014). Lead exhibited a 79.3% increase in concentrations during the filtration process. This does not follow the research of (Williams, 2014) where an average 99% decrease in Pb concentration was found for the period 0f 2010-14. The data suggests the overall efficiency of the filter bed has decreased since previous research in 2014, this may be due factors that include changes in concentrations from the adit sites, build-up of ocherous sludge in the filter bed reducing its efficiency (Williams, 2014).

At site D post mixing of the filtered mine water with the River Rheidol, Zn and Cd fall above WFD guidelines, this is also the case at the control site which is upstream of the mine water input, this suggests that the Zn and Cd contamination may be resultant of another point source possibly geogenic or anthropogenic in the form of another mining site upstream (Fuge *et al.,* 1991).

Table 7.1 Pearson's r correlation of filtered (f), unfiltered (uf) PHE concentrations, chemical and hydroclimatic variables.

	Fe (mg/L) f	Cd (mg/L) f	Pb (mg/L) f	Zn (mg/L) f	Fe (mg/L) uf	Cd (mg/L) uf	Pb (mg/L) uf	Zn (mg/L) uf	Discharge (m3/s)	Stage (m)	Temperature (°C)	Turbidity (ntu)	DO_2 (mg/L)	Eh (V)	EC (mv)	pH
pH	-0.688	-0.803	-0.547	-0.804	-0.745	-0.813	-0.547	-0.805	0.661	0.749	-0.788	-0.717	0.789	-0.916	-0.882	1.000
EC (mv)	0.937	0.968	0.132	0.978	0.955	0.967	0.131	0.978	-0.572	-0.573	0.737	0.894	-0.889	0.790	1.000	
Eh (V)	0.587	0.707	0.541	0.712	0.638	0.725	0.542	0.714	-0.587	-0.708	0.671	0.705	-0.724	1.000		
DO_2 (mg/L)	-0.818	-0.875	-0.174	-0.863	-0.835	-0.887	-0.178	-0.864	0.574	0.573	-0.758	-0.807	1.000			
Turbidity (ntu)	0.879	0.885	0.020	0.901	0.883	0.885	0.019	0.900	-0.448	-0.457	0.645	1.000				
Temperature (°C)	0.587	0.737	0.477	0.688	0.625	0.743	0.475	0.688	-0.693	-0.711	1.000					
Stage (m)	-0.369	-0.516	-0.600	-0.493	-0.430	-0.531	-0.605	-0.496	0.904	1.000						
Discharge	-0.420	-0.540	-0.463	-0.512	-0.468	-0.548	-0.465	-0.513	1.000							
Zn (mg/L) uf	0.978	0.992	-0.005	1.000	0.987	0.989	-0.004	1.000								
Pb (mg/L) uf	-0.172	0.024	0.999	-0.006	-0.087	0.044	1.000									
Cd (mg/L) uf	0.949	0.998	0.041	0.988	0.962	1.000										
Fe (mg/L) uf	0.993	0.968	-0.089	0.987	1.000											
Zn (mg/L) f	0.979	0.991	-0.007	1.000												
Pb (mg/L) f	-0.172	0.022	1.000													
Cd (mg/L) f	0.958	1.000														
Fe (mg/L) f	1.000															

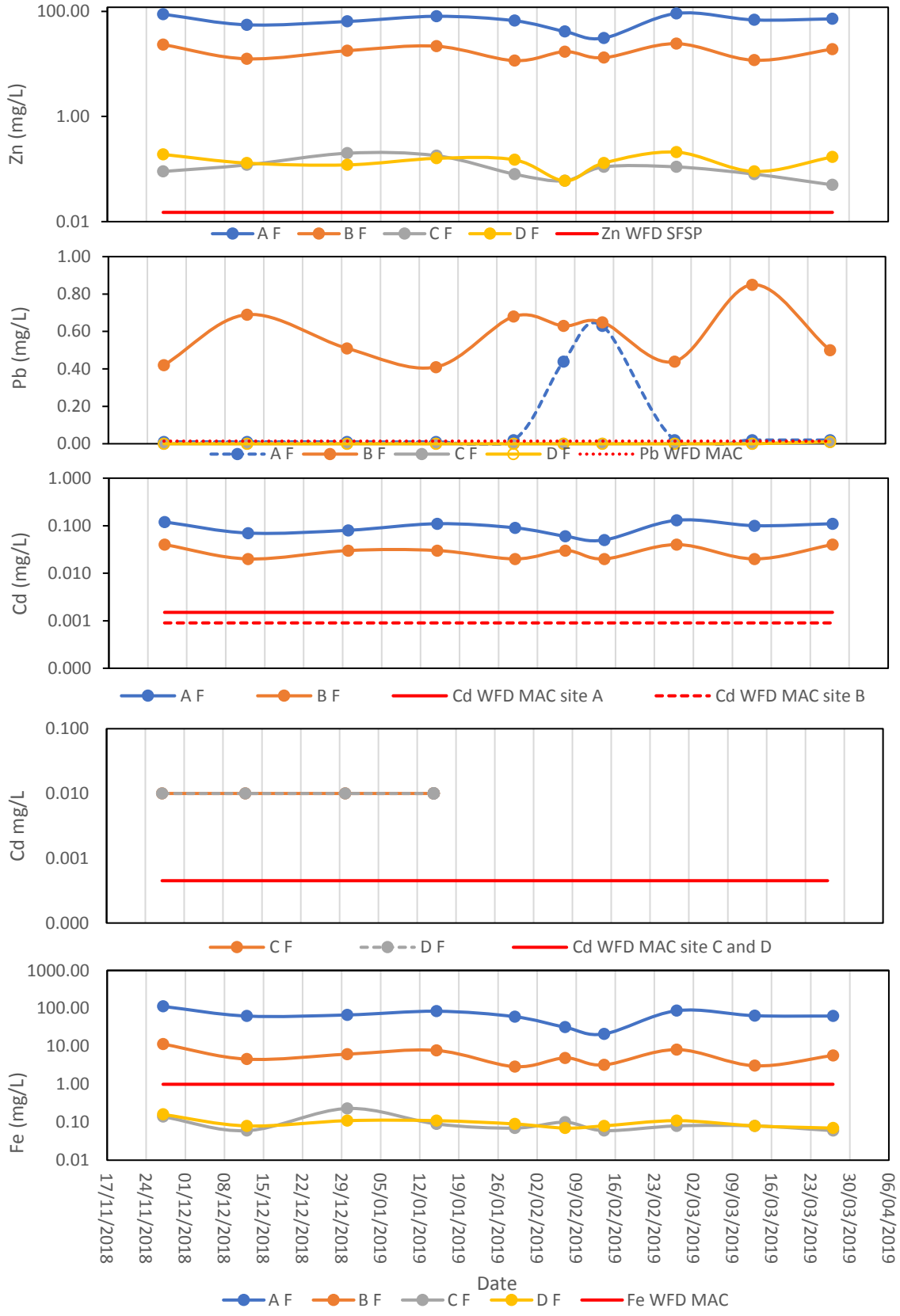

Figure 7.1. Filtered (0.45µ) PHE variability of weekly sampling carried out at Cwm Rheidol mine 27.11.2018-28.03.19.

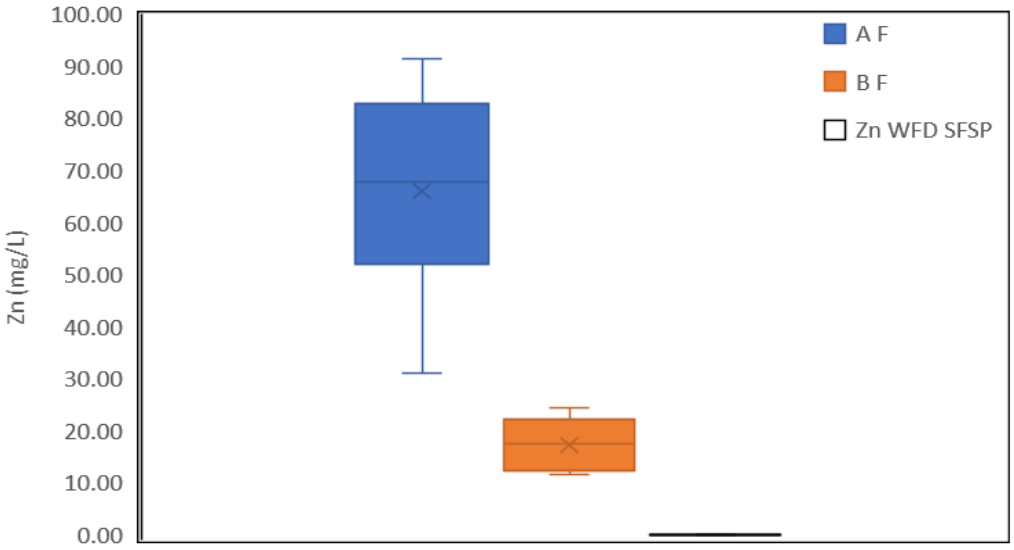

Figure 7.2. Filtered (0.45µ) Zn concentrations for sites A and B at Cwm Rheidol.

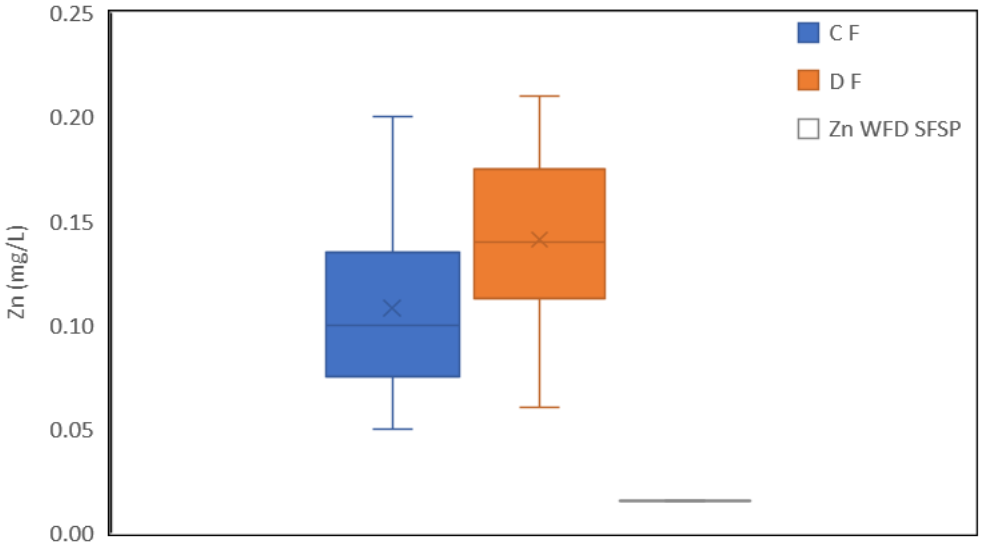

Figure 7.3. Filtered (0.45µ) Zn concentrations for sites C and D at Cwm Rheidol.

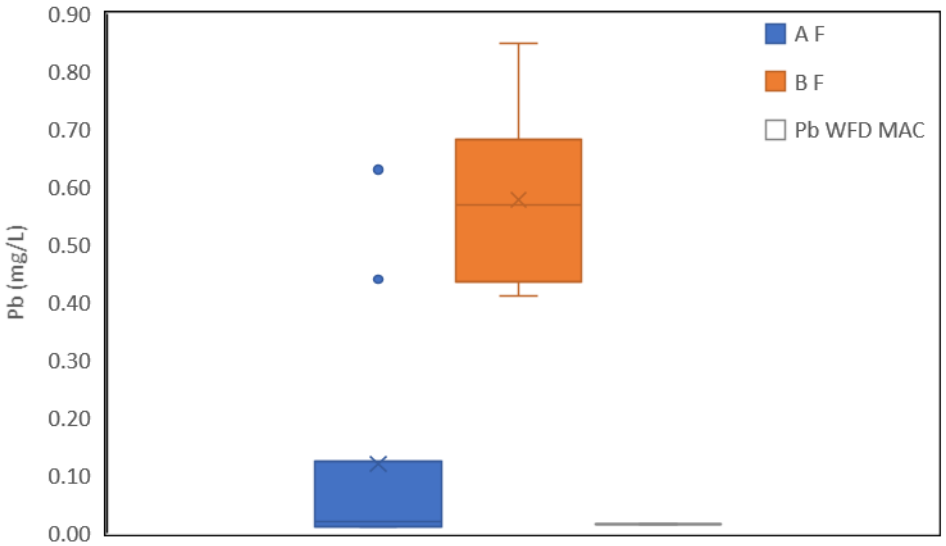

Figure 7.4. Filtered (0.45µ) Pb concentrations for sites A and B at Cwm Rheidol.

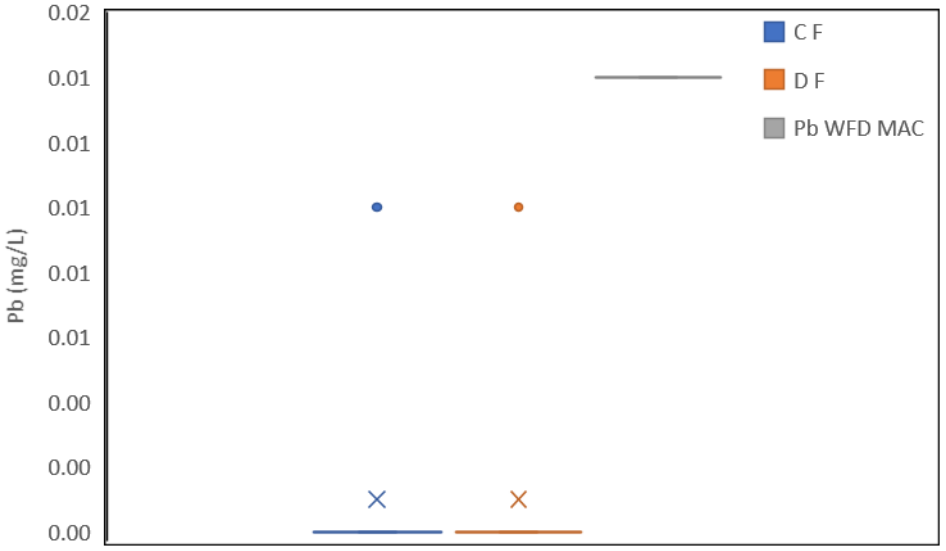

Figure 7.5. Filtered (0.45µ) Pb concentrations for sites C and D at Cwm Rheidol.

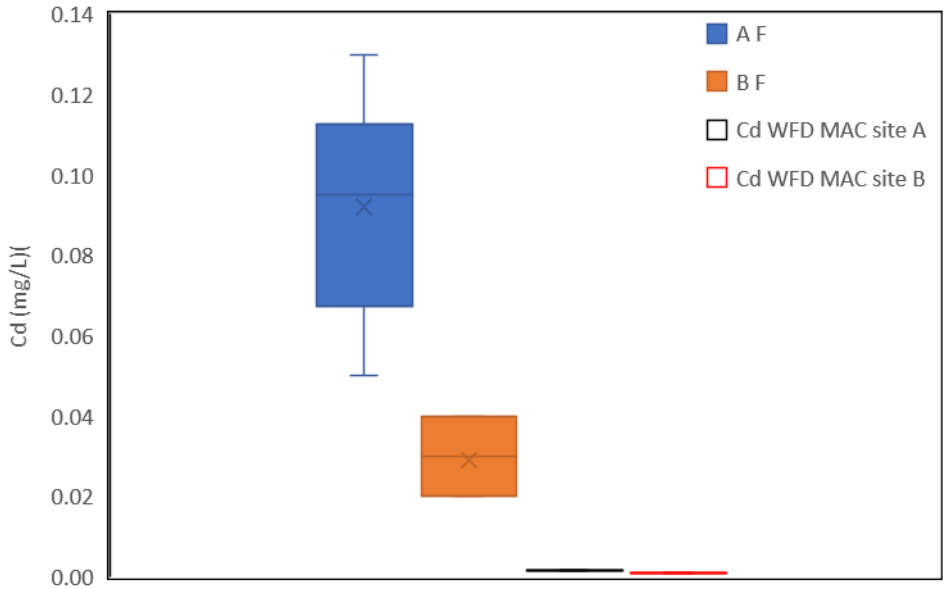

Figure 7.6. Filtered (0.45µ) Cd concentrations for sites A and B at Cwm Rheidol.

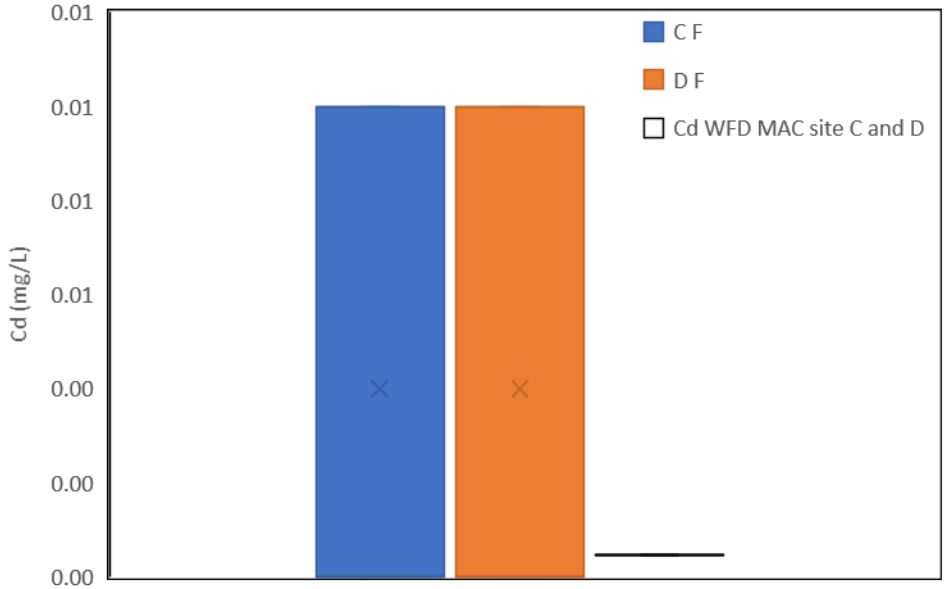

Figure 7.7. Filtered (0.45µ) Cd concentrations for sites C and D at Cwm Rheidol.

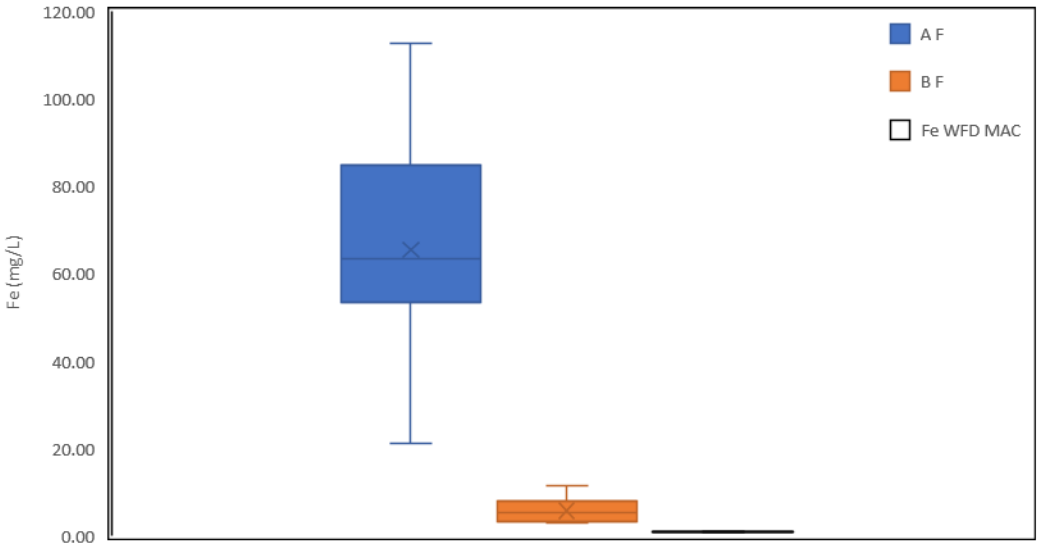

Figure 7.8. Filtered (0.45µ) Fe concentrations for sites A and B at Cwm Rheidol.

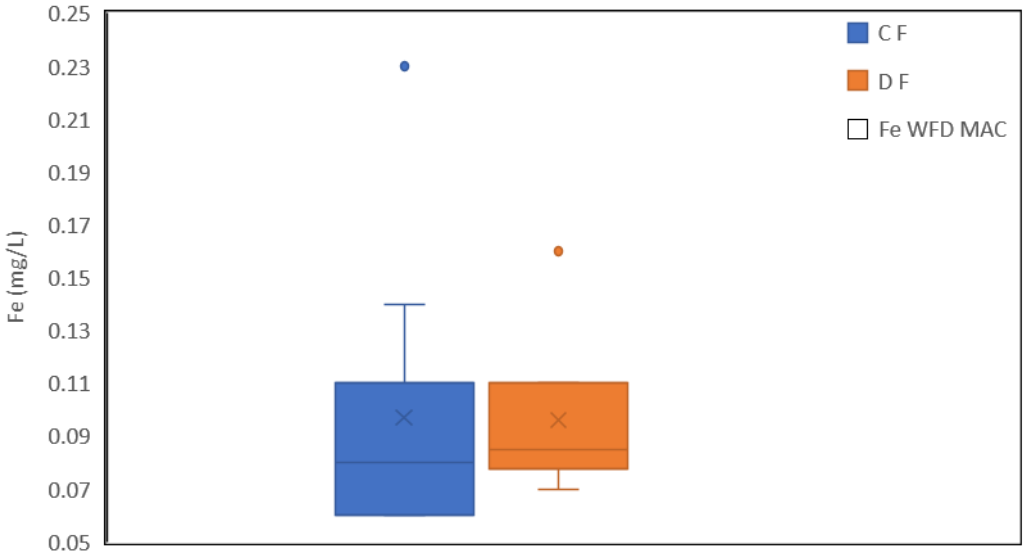

Figure 7.9. Filtered (0.45µ) Fe concentrations for sites C and D at Cwm Rheidol.

7.1.2 Total PHE concentrations and enrichment

During Low resolution monitoring between 27.11.2018-27.03.2019 unfiltered water PHEs Zn, Pb Cd and Fe have been analysed at sites A, B, C and D at Cwm Rheidol mine (Figure 3.3 & Figure 7.10). Unfiltered PHE concentrations were compared with filtered PHE concentrations to identify any temporal and spatial increases and decreases of particulate load. Unfiltered PHE concentrations at site D are of concern as they indicate the total of solute and particulate PHE in question entering the River Conwy. Comparisons between unfiltered PHE concentrations with filtered PHE concentrations identified a temporally and spatial varied particulate load. Maximum concentrations of unfiltered PHES were experienced at differing sampling times to maximum filtered concentrations. Differences in particulate load at differing sites and times of the study may due to spatial and temporal changes in chemical properties that can alter speciation (Bourg, 1988; Gundersen and Steinnes, 2001; Zheng *et al.,* 2012).

Unfiltered PHE concentrations reached a maximum for site D of 0.36, 0.01, 0.01 and 0.51 for Zn, Pb, Cd and Fe, this follows the trend of filtered concentrations, and confirms Zn and Cd are failing WFD guidelines. Zn maximum during the period of monitoring was at site A (91.39 mg/L). Comparisons between filtered and unfiltered Zn concentrations suggests that Zn is primarily present as a solute form (Figure 7.1 and 7.10). Mean PHE unfiltered concentrations exhibited a 17.7% increase for Fe and a 7.74% increase for Cd, Zn and Pb showed no mean increase of particulate (>0.45µ) concentration for all sites A, B, C and D.

The maximum Pb unfiltered concentration during the study was at site B (0.9 mg/L) (Figure 7.10). There is mean Pb particulate load of 30.6 % at Site A and 6.2 % particulate load at site B, this suggests that the filter is reducing the particulate of Pb load but the overall concentration of Pb is increasing by 96.5% from site A to sample site B suggesting an additional input of Pb during filtration. Filtered Pb concentrations of 0.44 and 0.63 on the 07.02.19 and 14.02.19 (Figure 7.1), identified as outliers during boxplot analysis (Figure 7.4) are confirmed to be incorrect due lower concentrations exhibited from unfiltered Pb concentrations for site A on 07.02.19 and 14.02.19 (7.10). Pearson's r correlation for unfiltered Pb showed poor, statistically insignificant correlation for unfiltered Zn Cd and Fe, whereas unfiltered Zn, Cd and Fe show significant ($p < 0.05$) positive correlations, suggesting the controls on Pb concentrations are different from the controls on Zn, Cd and Fe concentrations (Table 7.1). This may be due to Pb relative insolubility (Shooter, 1976). Maximum Cd concentration during the study was at site A (0.13 mg/L) (Figure 7.10), this does follow the trend of filtered Cd concentrations on 27.02.19, where the maximum concentration of Cd was experienced (Figure 7.1) of Cd was 0.13 mg/L also suggesting the total load is in solution or at <0.045 µm.

The maximum total Fe concentration during the study was at site A (114.99 mg/L) (Figure 7.10), there is an increase in particulate concentrations of Fe at site A there in a 10.3% particulate load and at site B there is a 57.0% particulate load, the increase is due to a number of factors that include; the increase of pH at the filter bed cause precipitation of Fe and oxidation of the mine water as it is exposed to the atmosphere during filtration (Shooter, 1976; Brown and Hosseinipour, 1991).

During low resolution weekly monitoring between 27.11.18-27.03.19 at Cwm Rheidol mine maximum unfiltered Zn, Cd and Fe concentrations were found to be from the adit (sample site A) and maximum Pb concentrations were at post filtration (sample site B). PHE concentrations decrease post filtration for Zn, Cd and Fe (Figures 7.11, 7.15 and 7.17), Pb increases post filtration (Figure 7.13). Statistical analysis using an unequal variance t-test confirms that all sites A, B C and D for Zn, Pb Cd and Fe concentration value differences are significantly different with <0.05 p-value, with the exception of Cd at sites C and D. Between adit sample site A and post filter site B there is a 75.9% mean decrease in Zn concentration, 96.5 % increase in Pb concentrations, 69.3 % reduction of Cd concentrations and a 81.5 % reduction in Fe concentrations (Figures 7.11, 7.13, 7.15 and 7.17). Results of filter effectiveness were 60, 99, 83 and 99 % removal between 2010-14 for unfiltered Zn Pb, Cd and Fe, this follows the trend exhibited for filter concentrations and further suggests that the effectiveness of the filter has reduced since previous monitoring (Williams, 2014).

The downstream sample site D shows a 30.8 % increase in Zn and 23.4 % in Fe concentrations from the upstream control site C. Cd showed a 0 % increase and Pb showed a 60 % reduction from control site C (Figures 7.12, 7.14, 7.16 and 7.18). this suggest that the Cwm Rheidol filter bed is contributing to Zn and Fe concentrations and that it has no effect on Cd concentrations, the reduction in Pb from the Control site C suggests that the controls site is subject to another point source of contamination, this confirms the findings for filtered PHE concentrations.

Maximum enrichment of Zn during low resolution monitoring was at adit site A, enriched 39.62 and Fe enriched 28.15 against background concentrations at control site C. Cd maximum enrichment was found to be at downstream site D 0.97. Pb maximum enrichment was found to at post filtration site B were an enrichment of 5.65 was found. Downstream site D exhibited a maximum enrichment of 1.87 for Zn, followed by Pb enriched to a maximum of 0.09, Cd 0.97 and Fe 1.43 against background concentrations from control site C. The enrichment factors suggest that Zn and Fe are enriched from the control site but Pb and Cd are not subject to enrichment, the source of the Zn and Fe enrichment is the filter outlet.

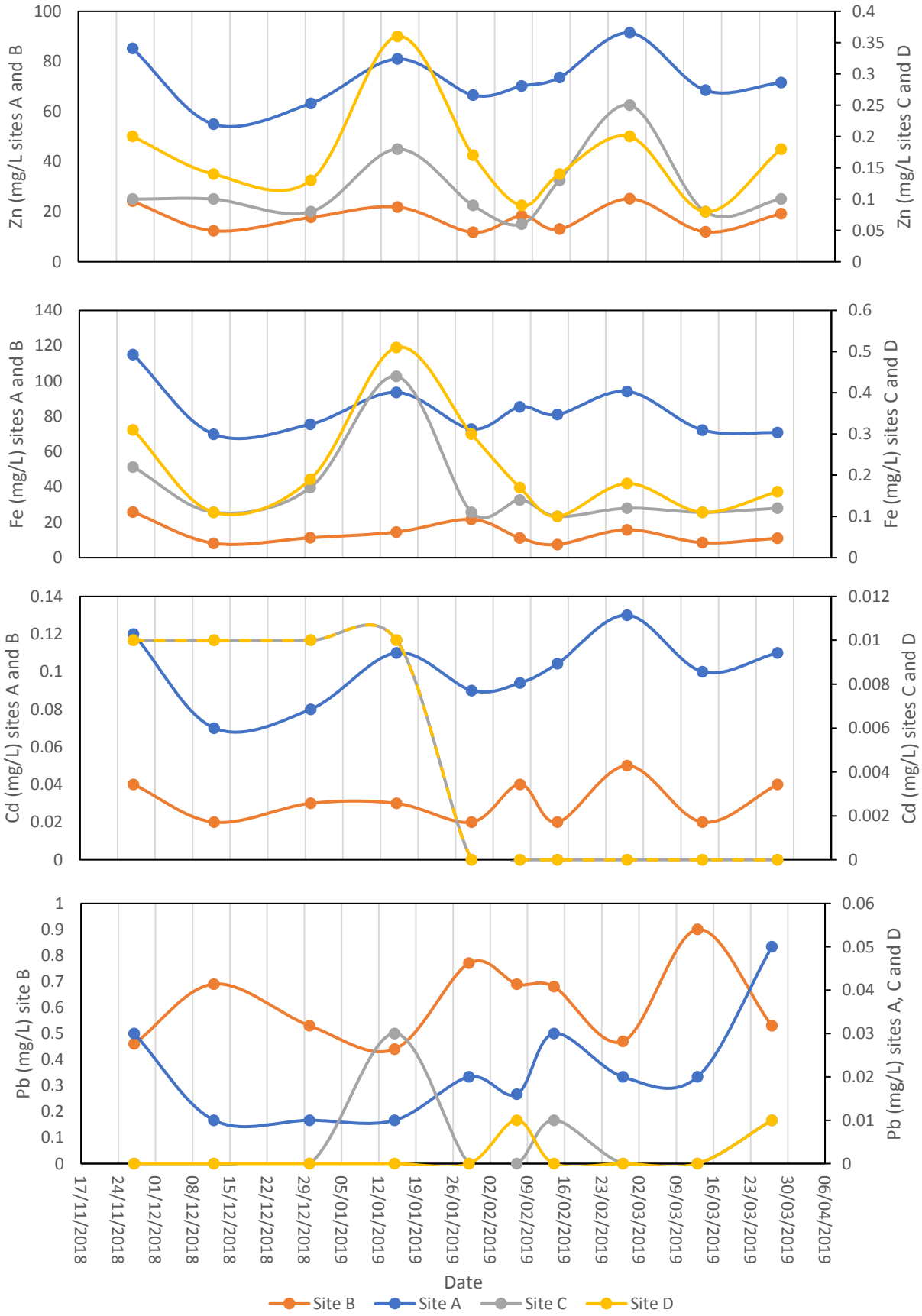

Figure 7.10. Unfiltered total load PHE variability of low-resolution sampling carried out at Cwm Rheidol mine – 27.11.2018-28.03.19.

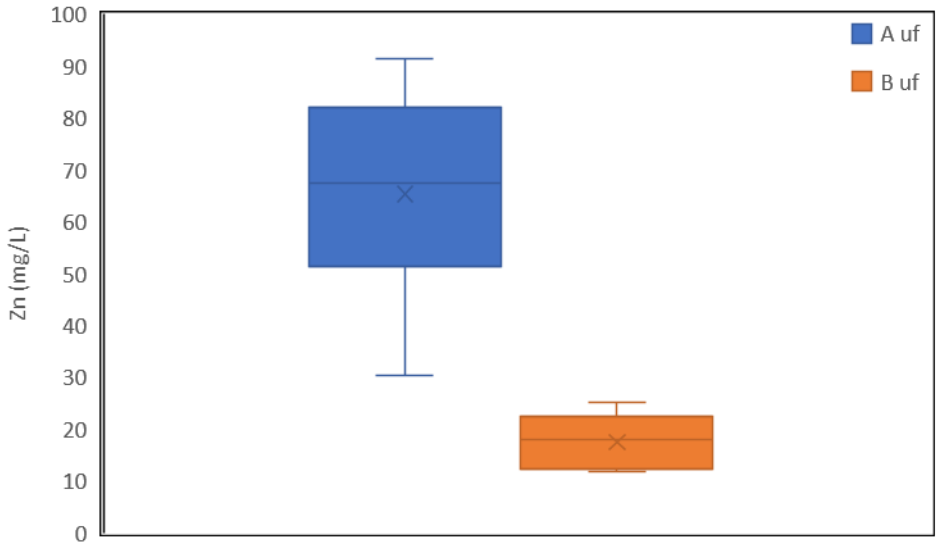

Figure 7.11. Unfiltered Zn concentrations for sites A and B at Cwm Rheidol.

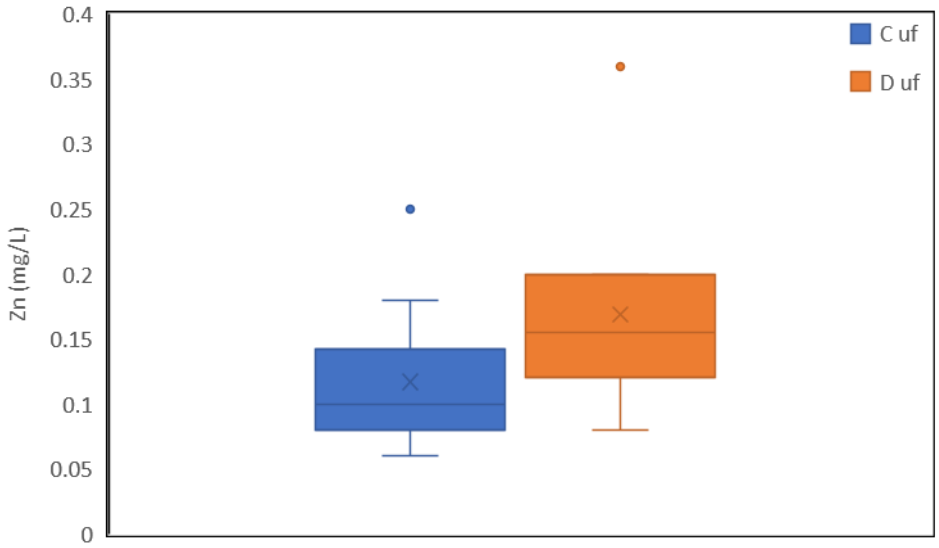

Figure 7.12. Unfiltered Zn concentrations for sites C and D at Cwm Rheidol.

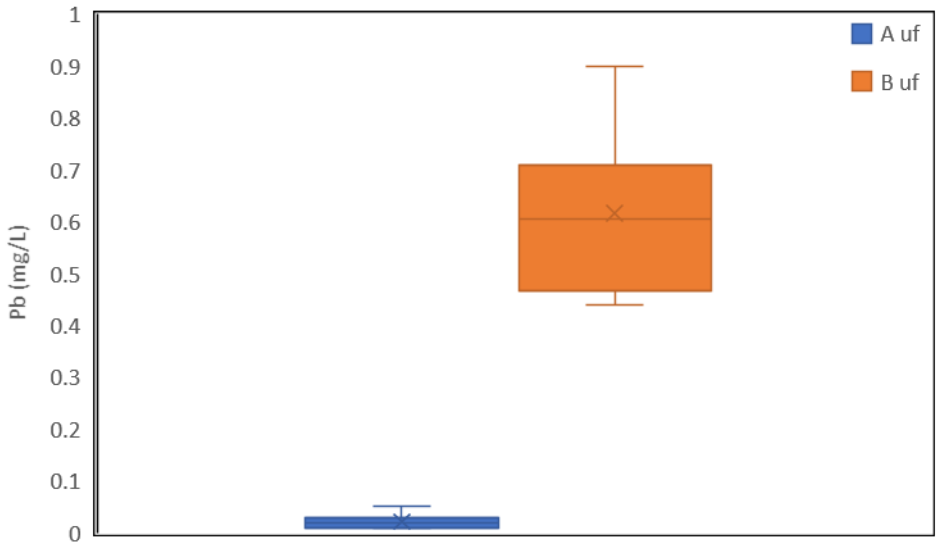

Figure 7.13. Unfiltered Pb concentrations for sites A and B at Cwm Rheidol.

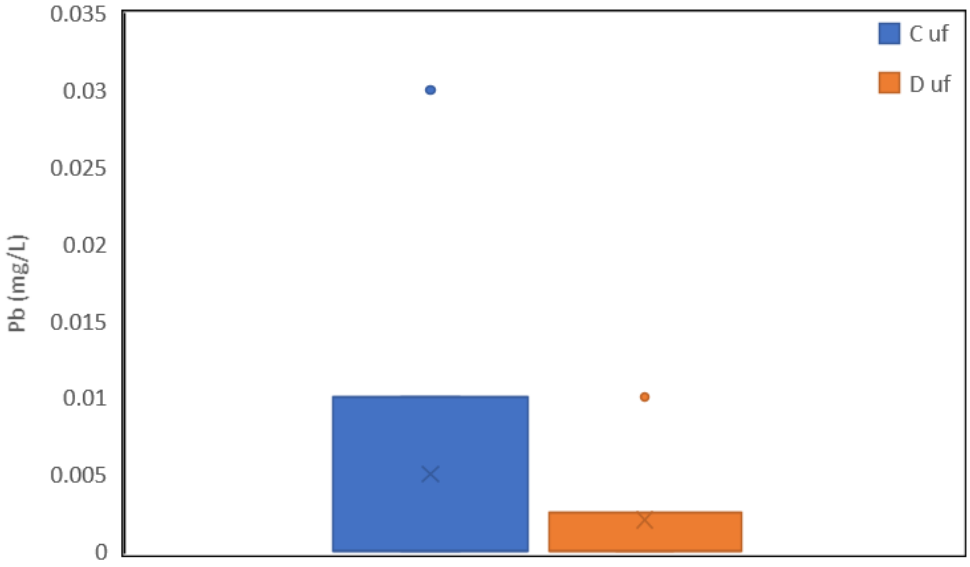

Figure 7.14. Unfiltered Pb concentrations for sites C and D at Cwm Rheidol.

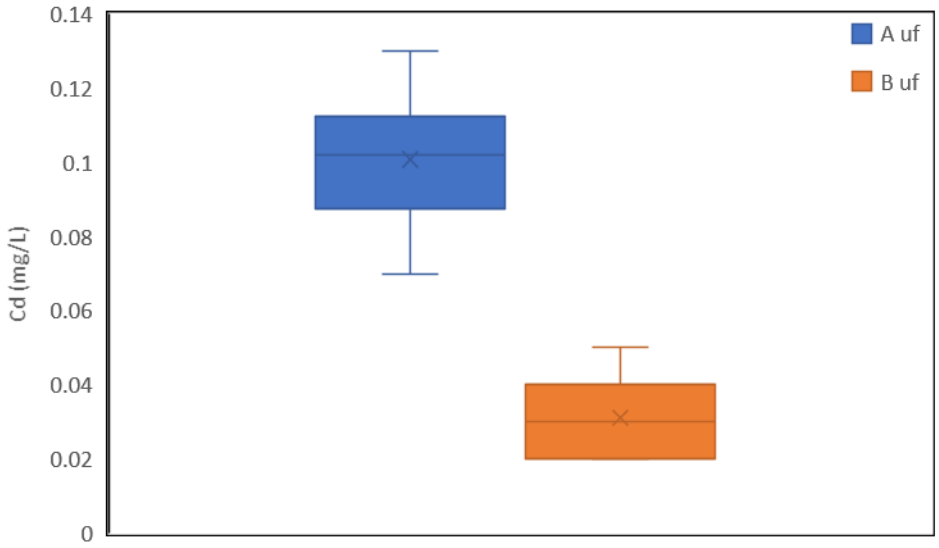

Figure 7.15. Unfiltered Cd concentrations for sites A and B at Cwm Rheidol.

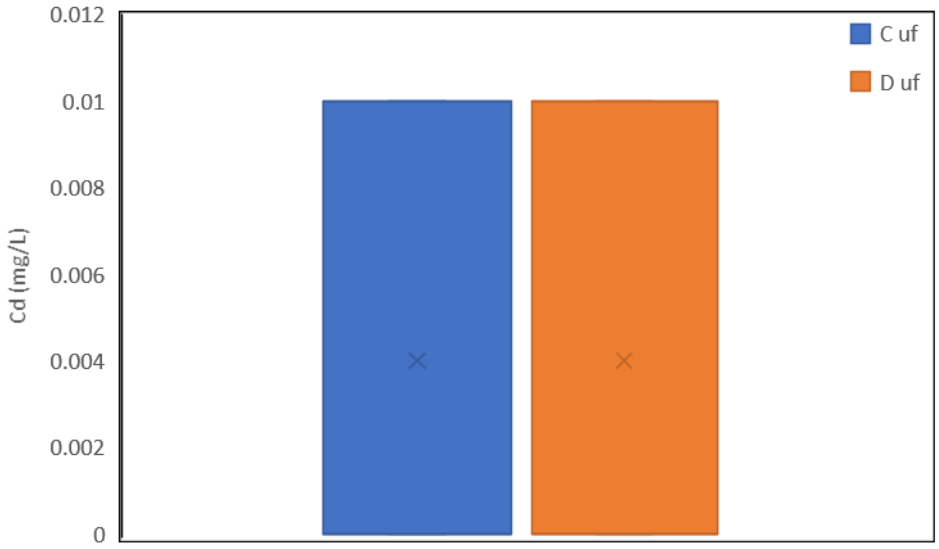

Figure 7.16. Unfiltered Cd concentrations for sites C and D at Cwm Rheidol.

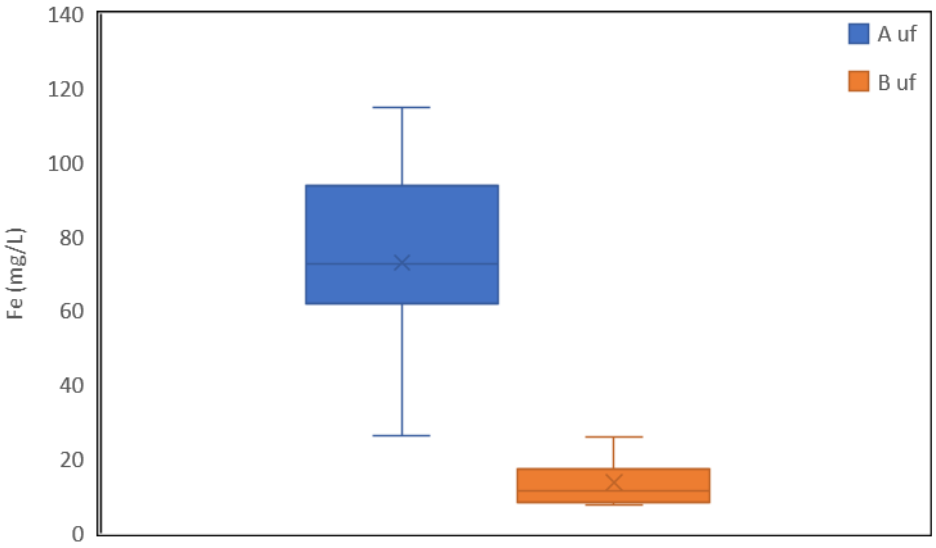

Figure 7.17. Unfiltered Fe concentrations for sites A and B at Cwm Rheidol.

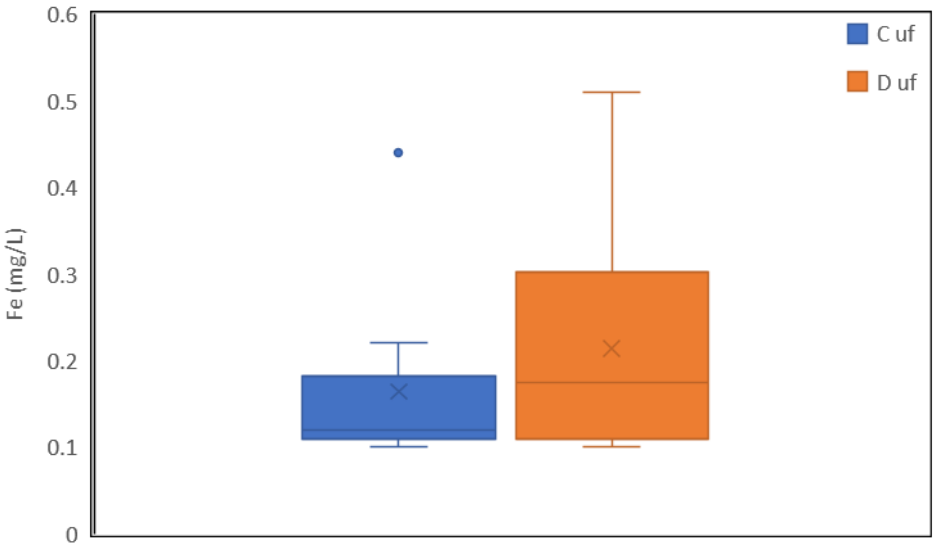

Figure 7.18. Unfiltered Fe concentrations for sites C and D at Cwm Rheidol.

7.1.3 Hydroclimatic and chemical variables

During Low resolution monitoring between 27.11.2018-27.03.2019 chemical and hydroclimatic data was obtained on a weekly basis (Figure 7.19 and 7.20). Chemical and hydroclimatic variables were monitored as means of identifying any spatial and temporal correlations with PHE loading and concentrations. The obtained pH values varied on a weekly basis, mean pH values for the duration of the study ranged from 3.0 for adit site A, 3.6 for post filter site B, 6.09 for control site C and 5.99 post filter site D. Pearson's r statistical analysis of pH shows negative correlations with EC, Eh, turbidity, temperature and all PHEs analysed (Zn, Pb, Cd and Fe), pH also showed positive with DO_2, stage and discharge (Table 7.1) and is exemplified by Figures 7.19 and 7.20. PHE concentration negative correlation with pH and positive correlation with discharge (Table 7.1) suggests as discharge increases PHE concentrations reduce and pH increases is exemplified by Figures 7.1, 7.10, 7.19 and 7.20. pH negative correlation with temperature is exemplified at site B on 29.01.19 at site B (Figures 7.19 and 7.20) this suggests temperature as well as discharge has a direct control on pH the filter bed raises the mean pH this is due to the addition of calcareous media within the filter bed (Williams, 2014). The reduction in pH at D is likely to be due to the input of acidic water from filter sample site B. The negative correlation of pH with temperature can be accounted for by increasing temperature that increases PHE concentrations by concentration, that are then subject to oxidation releasing acid as part of the oxidation process (Marsay, 2018).

EC has negative correlation relationships with DO_2, stage and discharge, and has positive correlations with Eh, turbidity, temperature and all PHEs except for filtered Pb. Positive and negative relationships with temperature and discharge suggest they have a direct control on EC (Figures 7.19 and 7.20). During low resolution sampling at Cwm Rheidol adit site A had a mean EC of 1362mv, post filter site B 550 mv, control site C 70.9 mv and after filter site D 73.4 mv. This suggest the filter mine water has a minimal effect on the downstream EC. EC has significant positive correlation with temperature (Table 7.1), this confirms temperature influences EC with increasing temperature, increased evaporation occurs and PHE concentrations increase. In turn increases in flow and discharge demonstrate a reduction in EC confirmed by a significant ($p < 0.05$) negative correlation (Table 7.1). Values of EC show variation that reflect seasonal and diurnal changes in temperature and stage (Brooks *et al.,* 2010; Kimball *et al.,* 2010)

Redox potential during low resolution monitoring of Cwm Rheidol mine site exhibited a similar trend to EC and the positive relationship between EC and Eh confirms their correlation with PHEs and other chemical variables (Table 7.1). Increases in temperature, increases redox potential and increases in discharge reduces redox potential (Table 7.1 and Figures 7.19 and 7.20). Mean Eh Values showed little variation between adit and filter sites and upstream and downstream sites with values of 0.7, 0.7, 0.46 and 0.45 for sites A, B, C and D respectively. The elevated redox potential demonstrated at sites A and B is likely be to increased oxidation processes occurring due to PHE rich mine water exposure to atmosphere during filtration after exiting the mine water drainage system which will result in oxidation and increased acidity. Table 7.1 exhibits a significant ($p < 0.05$) positive correlation with redox, the mine water exhibited temperatures that

were in excess of monitored temperatures in the River Rheidol, this may also explain the elevate redox potential experienced from the adit and filter bed (Macpherson and Towsend, 1998; Cao *et al.,* 2001).

Dissolved oxygen correlation with chemical and hydroclimatic variables followed a similar trend to pH demonstrating negative correlation for EC, Eh, turbidity, temperature and PHEs except for Pb. DO_2 demonstrated positive correlation with stage, discharge and pH (Table 7.1). The correlation identified with temperature and discharge suggests that temperature and discharge control DO_2 levels at cwm Rheidol mine. Dissolved oxygen mean concentrations were 8.1, 9.8, 10.9 and 10.59 mg/L for sites A, B, C and D. It is noted the adit exhibits the lowest DO_2 concentration followed by the post filtration site B. Dissolved oxygen levels at Cwm Rheidol mine are above minimum levels defined by the WFD standards and classifications of 2015 (The Water Framework Directive, 2015). Monitoring carried out at Cwm Rheidol mine suggests there is no impacts on biota from dissolved oxygen.

Turbidity shows a positive correlation with temperature (Table 7.1) and negative correlation with discharge. This relationship suggest increases in temperature will increase turbidity and increases in discharge will reduce turbidity this is exemplified by Figures 7.19 and 7.20. This suggests that temperature increases will increase turbidity while increases in discharge reduce the turbidity. Turbidity is notably higher in mine water sample than river water samples (7.19), due to oxidation and precipitation process taking place as the mine water is exposed to the atmosphere introducing oxygen (Marsay, 2018), media to raise the pH will inevitably reduce the solubility increasing precipitation (Jickells, 1997).

In summary temperature and discharge have significant correlations with chemical variables, the chemical variables have significant correlation with PHE concentrations, this confirms that spatially and temporally changes in hydroclimatic variables directly and indirectly control PHE concentrations and loads of the River Rheidol, temperature fluctuations account for short term changes in PHE concentration and loads, increases in temperature exemplify increase in PHE concentration. whereas discharge has a more varied effect on PHE concentration and loading over a period of several days, explained by varied rainfall regimes (Macdonald *et al.,* 2010). Temperature increases coincide with reduced flow and increase the effectiveness of the filtration (Figures 7.1 and 7.19)

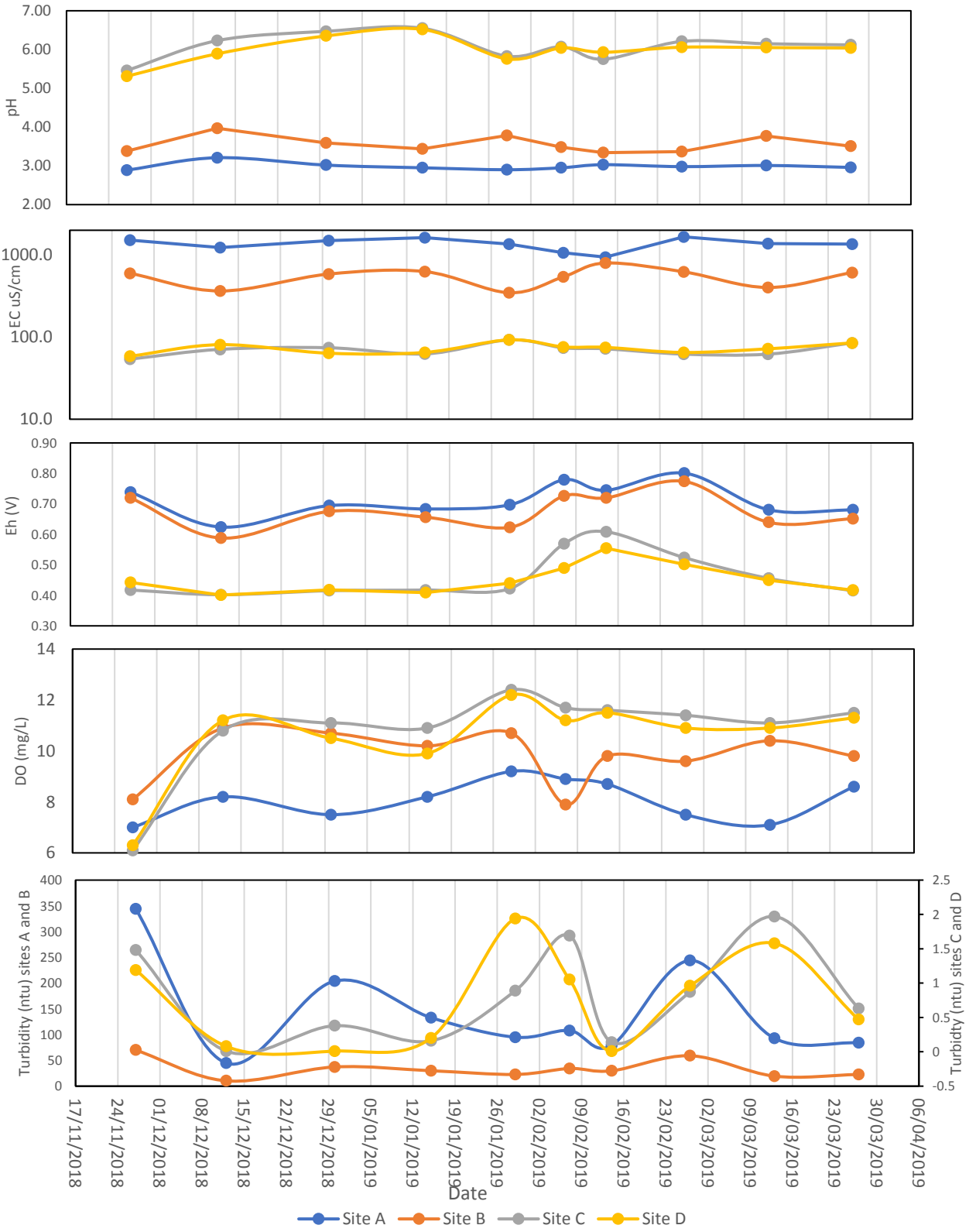

Figure 7.19. Chemical variability of low-resolution sampling carried out at Cwm Rheidol mine – 27.11.2018-28.03.19.

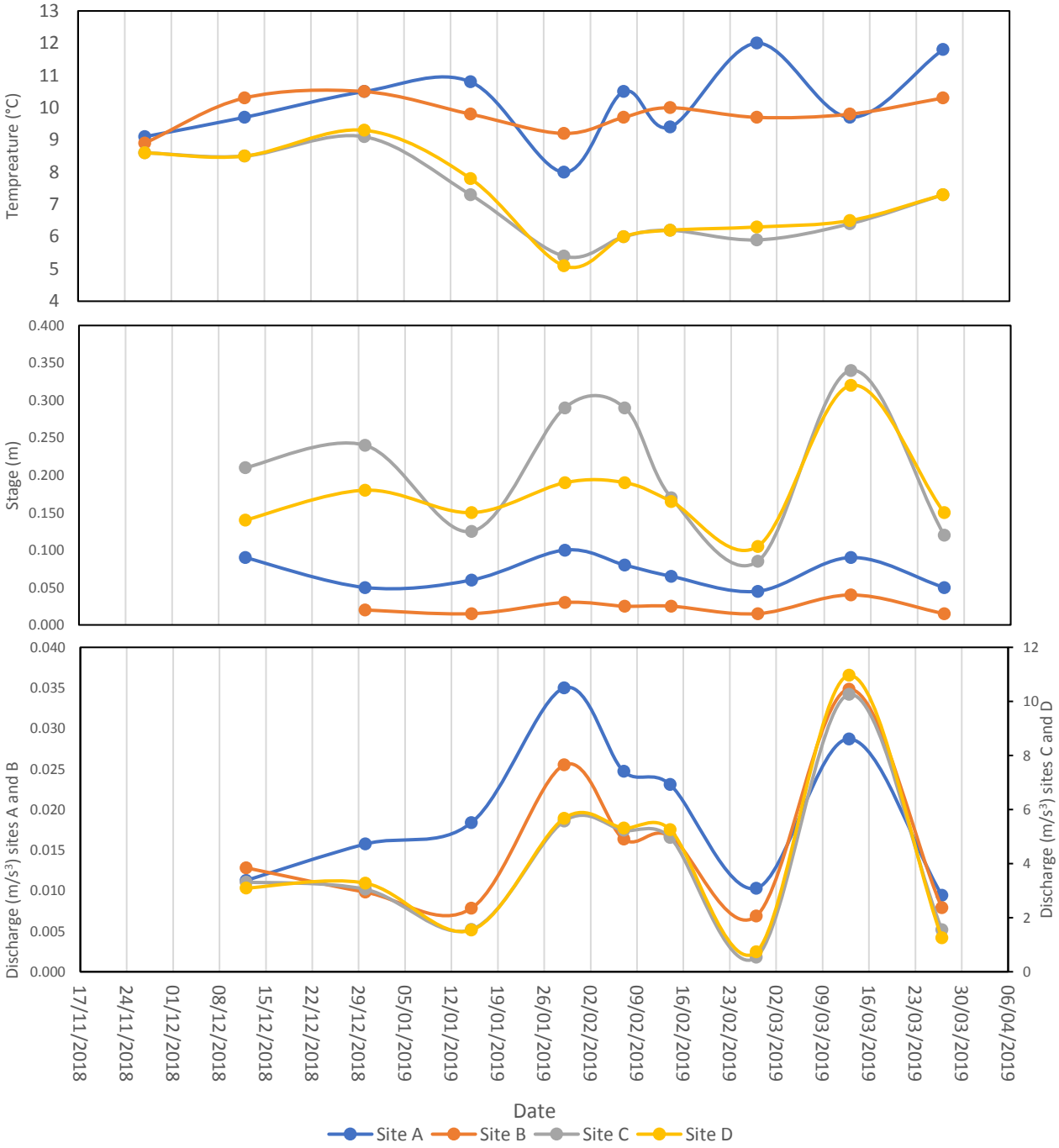

Figure 7.20. Hydroclimatic variability of low-resolution sampling carried out at Cwm Rheidol mine – 27.11.2018-28.03.19.

7.1.4 PHE Load vs concentration

During low-resolution monitoring at Cwm Rheidol mean PHE loads were calculated (Table 7.2). Downstream site D at the lowest reach of the study on the River Rheidol demonstrated an increase of Zn and Fe from upstream control site C and suggests the increases of Zn and Fe sampled at site D can be attributed to the input of from the Cwm Rheidol mine drainage and localised geogenic sources. During periods of the study, Pb and Cd were not detected, resulting in a not detected concentrations being classified as N/A (Table 7.2). Maximum mean Zn, Cd and Fe loads were found to be from site A and Pb from was at site B. Site A exhibited the maximum total of PHEs followed by site B where there input to the Afon Rheidol occurs.

Table 7.2. Total loads for Zn, Pb, Cd and Fe based on low resolution monitoring, Cwm Rheidol mine 27.11.18-28.03.19 at sites A, B, C and D.

Cwm Rheidol		**Zn kg/d**	**Pb kg/d**	**Cd kg/d**	**Fe kg/d**	**Zn t/y**	**Pb t/y**	**Cd t/y**	**Fe t/y**
A	min	53.38	0.01	0.07	52.47	19.48	N/A	0.02	19.15
	mean	**102.93**	**0.03**	**1.58**	**110.54**	**37.57**	**0.01**	**0.58**	**40.35**
	max	201.22	0.06	2.72	220.24	73.44	0.02	0.99	80.39
B	min	13.70	0.06	0.02	9.03	5.00	0.02	0.01	3.29
	mean	**40.66**	**0.91**	**0.33**	**39.74**	**14.84**	**0.33**	**0.12**	**14.50**
	max	201.22	2.71	2.72	220.24	73.44	0.99	0.99	80.39
C	min	11.65	N/A	N/A	5.59	4.25	N/A	N/A	2.04
	mean	**35.35**	**1.04**	**0.86**	**49.73**	**12.90**	**0.38**	**0.31**	**18.15**
	max	70.90	4.29	2.87	97.48	25.88	1.57	1.05	35.58
D	min	12.70	N/A	N/A	11.43	4.64	N/A	N/A	4.17
	mean	**49.86**	**0.57**	**0.85**	**67.16**	**18.20**	**0.21**	**0.31**	**24.51**
	max	83.37	4.59	2.83	147.12	30.43	1.68	1.03	53.70

Mean discharge dilution factors (Table 7.3) confirm spatial variation of PHE concentrations exemplified at sites A, B, C and D (Figures 7.1-7.18) and loads (Table 7.2). Site A demonstrated a dilution of 1.07 with the filtration site B suggesting no change in the discharge between sites. The dilution factor shown at site D from site B filtration discharge indicates a dilution 250 times from filtration site B, suggesting concentrations of PHEs are reduced 250 times when entering the River Rheidol. The dilution between upstream site c and downstream site D of 0.96 suggests there is minimal change in discharge. Dilution factors values are exemplified by discharge values in Figure 7.20. The dilution factor of the adit site A and filter bed site B (Table 7.7) suggests there is gain of discharge from the adit during filtration, this confirms that the filter bed is influencing reduction of PHE concentrations.

The mean change in PHE load between sample sites A and B shows a reduction in Zn, Cd and Fe loads and an increase in Pb load. The total load from sites B and C combined shows the greatest load is from Fe followed by Zn Pb and Cd respectively. There is a loss of load for all PHEs at site D from the total combined loads of upstream control site C and post filtration site B. Between the upstream site C and downstream site D there is an increase in Zn and Fe loads and a decrease in Pb and Cd loads (Table 7.4). The loss of load at

site D from the combined load of sites C and B can be explained by the dilution of input of PHEs from the filter site B into the River Rheidol, the mean dilution factor of 0.004 for the duration of the study suggests the mine water is subject to rapid change of chemical parameters such as pH and redox (Figure 7.19) reducing solubility causing the mine water PHEs to rapidly precipitate (Jickells, 1997). PHEs with increased particulate loads (Fe and Pb) are likely to deposit where the River Rheidol channel widens allowing for deposition prior to reaching site D (Macklin and Lewin, 1989). Zn primarily being in solution whilst entering the Rheidol and having a pH of hydrolysis of 8.3 remains in solution in the Rheidol and has not precipitated by time it reaches site D, this can explain the increase from site C to D evident in the study. Pb and Cd being present at relatively low concentrations at site B suggests that the dilution of Pb and Cd outweighs the additional input from site B, accounting for an effective reduction in Pb and Cd loads at downstream site B.

Pearson's r correlation analysis of PHE load and concentration (Table 7.5) showed a positive correlation of all analysed PHEs load and concentration at site A, this suggests when increases in load occur the concentration also increase (Table 7.5) (Figures 7.21, 7.22, 7.23 and 7.24). This suggests the mine is still experiencing juvenile or seasonal increases in contamination from periods of oxidation and washing from seasonal increases and decreases in flow and flooding out washing mine waters (Elderfield *et al.,* 1979; Nagorski *et al.,* 2003). Previous research has identified that there is a seasonal trend n PHE loads and concentrations (Williams, 2014)At site B there is negative correlation between Zn and Cd loads and concentrations and there is a positive correlation for Pb and Fe loads and concentrations, this suggest increasing loads of PHEs correlates with decreasing concentrations of Zn and Cd and increasing concentrations Pb and Fe (Table 7.5) (Figures 7.21, 7.22, 7.23 and 7.24. At site C there is negative correlation between Zn concentrations and loads and positive correlation between Pb, Cd and Fe loads and concentrations, this suggests that at control site increasing loads of Pb, Cd and Fe correlate with increases in concentrations whereas increasing Zn loads coincide with decreasing Zn concentrations (Table 7.5) (Figures 7.21, 7.22, 7.23 and 7.24). The data presented suggests that increased discharge increases particulates in the system (Figures Pb and Fe that are present in insoluble forms on Pb and Fe concentration (Shooter, 1976).

Generally, discharge demonstrates a positive significant correlation (<0.05) with PHEs at sites A and B, the increased load during increased discharge at sites A and B is likely to be resultant of flushing of PHEs from the mine water due to juvenile acidity. At sites C and D Zn and Fe demonstrate a significant positive correlation (<0.05) but Pb and Cd do not show any significant correlation, this is possibly due to low concentrations present in the River Rheidol in comparison to the adit and filter sites that have not enabled accurate correlation to be carried out for these sites. Filtration site B demonstrates a significant negative correlation (<0.05) for Zn suggesting increases in discharge are increasing dilution and effectively reducing concentrations during periods of increased discharge, in spite of this Pb demonstrates a positive significant relationship at site B suggesting increases in discharge are increasing the Pb concertation, this is likely due to Pb being present as a insoluble particulate form from the adit, that is being flushed and mobilised during increased discharge. This process for Pb would make the filter less effective and the processes involved with

Zn appear more effective during periods of increased discharge considering this it is likely that dilution is the cause of decreased Zn concentration during increased discharge rather than increased effectiveness of the filter. The correlation with discharge highlights the complex nature of PHE load and concentration spatial and temporal variation.

At site D the same trend is experienced as site C, correlations for PHEs follow the same trend. The loads of PHEs demonstrated at site D show an increase from the control site for Zn, Cd and Fe, the concentrations however show negligible increase that can be explained dilution.

Table 7.3. Dilution of load based on mead discharge at sites A, B, C and D.

Site	Dilution
a-b	1.07
b-d	0.004
c-d	0.96

Table 7.4 mean changes in PHE load for low resolution monitoring between 27.11.18-28.03.19.

Load	Zn kg/d	Pb kg/d	Cd kg/d	Fe kg/d
Total loss/Gain at B - post filtration of site A	-622.70	8.79	-1.03	-707.97
Total post B and C mixing	760.12	19.54	9.18	894.70
Total loss/gain at site D - post B and C mixing	-261.53	-13.80	-0.64	-223.14
Total loss/gain at site D from C	145.11	-4.68	-0.02	174.25

Table 7.5 PHE load, concentration and discharge Pearson r correlation, PHE loads and concentrations calculated at sample sites A, B, C and D.

Site A	Zn mg/L	Pb mg/L	Cd mg/L	Fe mg/L	Discharge m3/s	Zn kg/d	Pb kg/d	Cd kg/d	Fe kg/d
Zn mg/L	1.000								
Pb mg/L	-0.044	1.000							
Cd mg/L	0.487	0.424	1.000						
Fe mg/L	0.958	-0.246	0.253	1.000					
Discharge m3/s	-0.318	-0.171	-0.185	-0.330	1.000				
Zn kg/d	0.290	-0.241	-0.012	0.290	0.802	1.000			
Pb kg/d	-0.395	0.528	0.131	-0.538	0.715	0.435	1.000		
Cd kg/d	-0.223	-0.072	0.077	-0.292	0.961	0.791	0.756	1.000	
Fe kg/d	0.348	-0.320	-0.083	0.384	0.737	0.988	0.321	0.706	1.000
Site B	Zn mg/L	Pb mg/L	Cd mg/L	Fe mg/L	Discharge m3/s	Zn kg/d	Pb kg/d	Cd kg/d	Fe kg/d
Zn mg/L	1.000								
Pb mg/L	-0.855	1.000							
Cd mg/L	0.894	-0.649	1.000						
Fe mg/L	0.243	-0.186	0.197	1.000					
Discharge m3/s	-0.744	0.943	-0.617	-0.022	1.000				
Zn kg/d	-0.516	0.848	-0.365	0.014	0.939	1.000			
Pb kg/d	-0.720	0.936	-0.593	-0.058	0.996	0.937	1.000		
Cd kg/d	-0.351	0.756	-0.091	0.029	0.798	0.937	0.797	1.000	
Fe kg/d	-0.532	0.633	-0.436	0.626	0.731	0.664	0.692	0.574	1.000
Site C	Zn mg/L	Pb mg/L	Cd mg/L	Fe mg/L	Discharge m3/s	Zn kg/d	Pb kg/d	Cd kg/d	Fe kg/d
Zn mg/L	1.000								
Pb mg/L	0.359	1.000							
Cd mg/L	0.014	0.329	1.000						
Fe mg/L	0.328	0.858	0.571	1.000					
Discharge m3/s	-0.604	-0.370	-0.347	-0.353	1.000				
Zn kg/d	-0.374	-0.140	-0.310	-0.255	0.907	1.000			
Pb kg/d	0.309	0.845	0.113	0.540	-0.213	0.128	1.000		
Cd kg/d	-0.127	0.024	0.941	0.263	-0.272	-0.285	-0.109	1.000	
Fe kg/d	-0.522	0.032	-0.022	0.177	0.847	0.752	0.001	-0.101	1.000
Site D	Zn mg/L	Pb mg/L	Cd mg/L	Fe mg/L	Discharge m3/s	Zn kg/d	Pb kg/d	Cd kg/d	Fe kg/d
Zn mg/L	1.000								
Pb mg/L	-0.209	1.000							
Cd mg/L	0.403	-0.378	1.000						
Fe mg/L	0.867	-0.167	0.385	1.000					
Discharge m3/s	-0.621	-0.151	-0.352	-0.342	1.000				
Zn kg/d	-0.196	-0.381	-0.181	0.104	0.787	1.000			
Pb kg/d	-0.327	0.818	-0.309	-0.126	0.061	-0.180	1.000		
Cd kg/d	0.112	-0.355	0.940	0.096	-0.280	-0.214	-0.291	1.000	
Fe kg/d	-0.144	-0.181	-0.194	0.297	0.675	0.873	0.052	-0.236	1.000

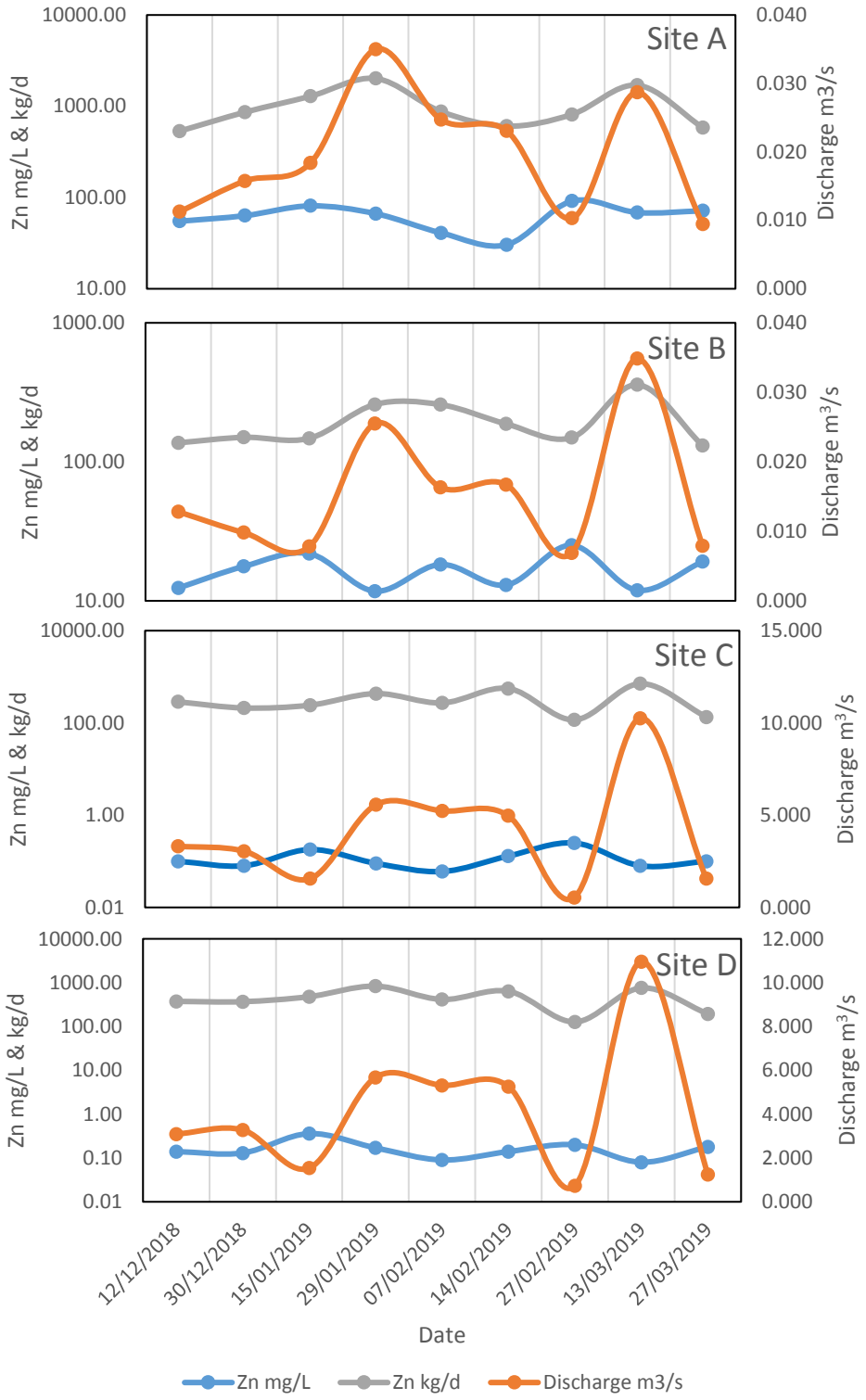

Figure 7.21. Unfiltered Zn concentration (mg/L), load relationship (kg/d) and discharge m^3/s at Cwm Rheidol mine based on sites A, B, C and D low resolution monitoring 03.12.18-28.03.19.

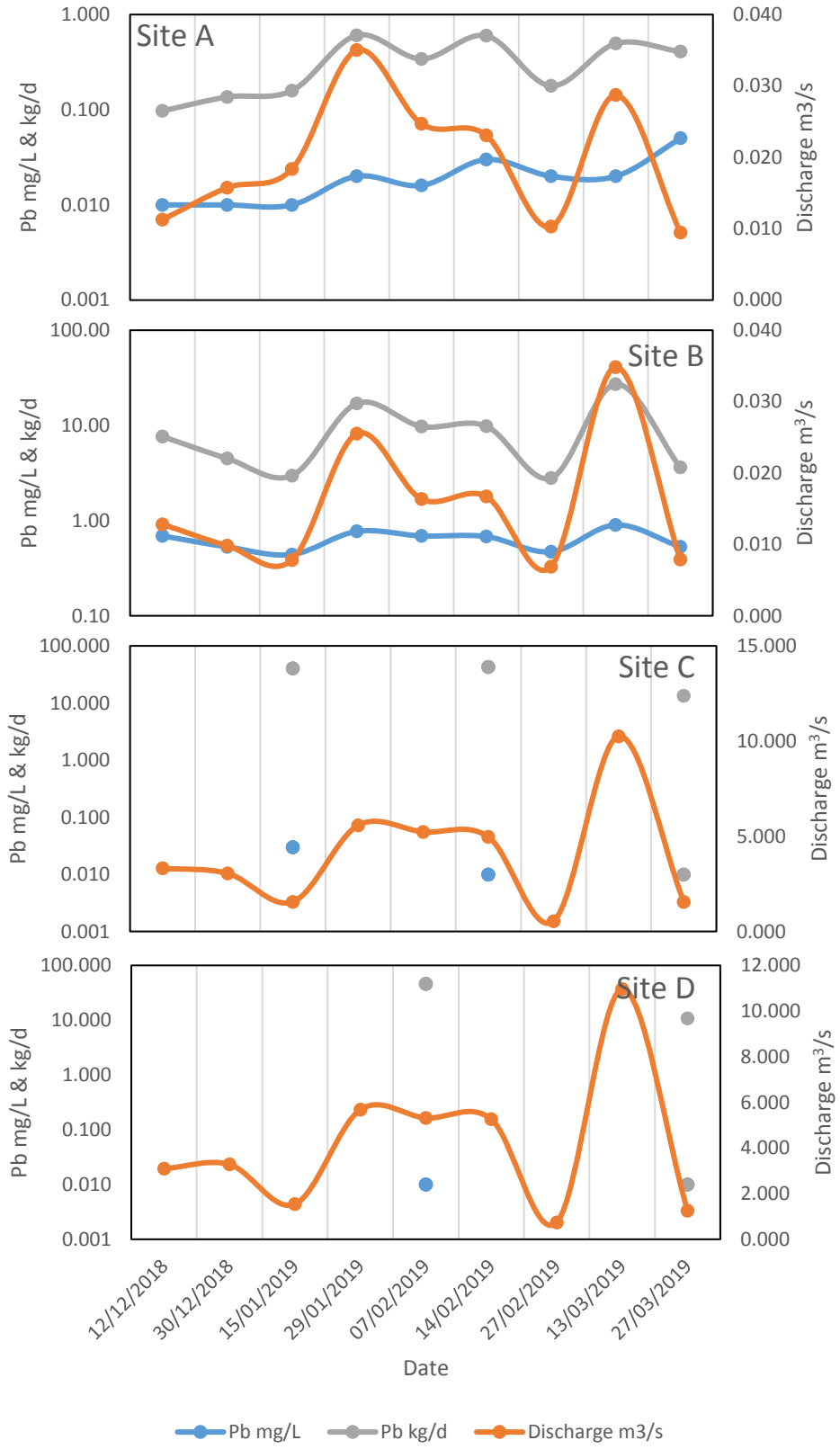

Figure 7.22. Unfiltered Pb concentration (mg/L), load relationship (kg/d) and discharge m^3/s at Cwm Rheidol mine based on sites A, B, C and D low resolution monitoring 03.12.18-28.03.19.

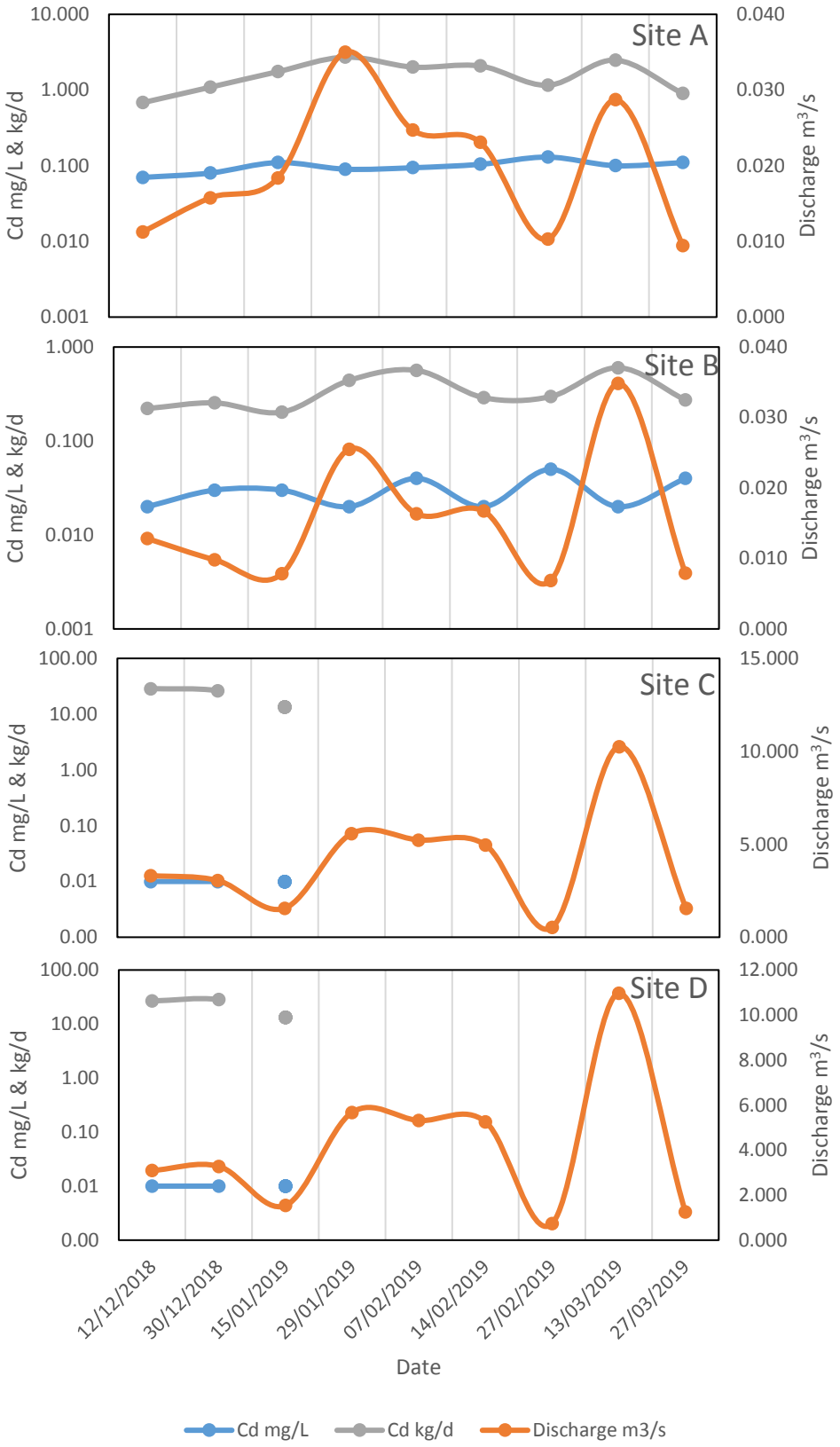

Figure 7.23. Unfiltered Cd concentration (mg/L), load relationship (kg/d) and discharge m^3/s at Cwm Rheidol mine based on sites A, B, C and D low resolution monitoring 03.12.18-28.03.19.

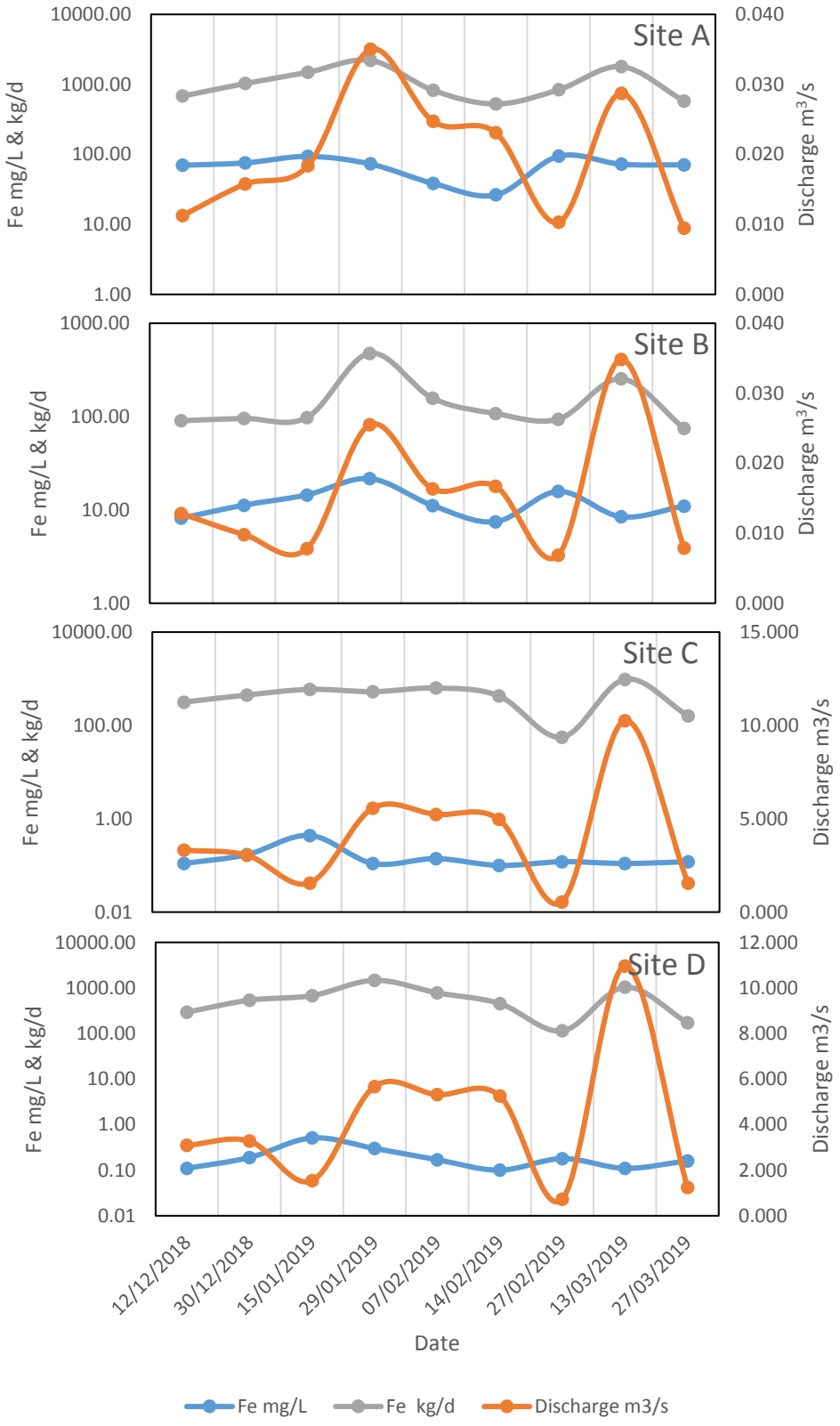

Figure 7.24. Unfiltered Fe concentration (mg/L), load relationship (kg/d) and discharge m^3/s at Cwm Rheidol mine based on sites A, B, C and D low resolution monitoring 03.12.18-28.03.19.

7.1.5 PHE speciation

During low resolution monitoring the dominant geochemical PHE species was analysed for each sample site, calculated as a mean values for the period of the study, speciation was calculated using pH and redox potential data, it was found that there was some variation between samples sites A and B, but despite this the PHE speciation remained the same at both sites (Figures 7.25, 7.26, 7.27 and 7.28). Sites C and D showed little spatial variation in speciation (Figures 7.25, 7.26, 7.27 and 7.28). The difference in sites C and D redox and pH with sites A and B, has an effect on the dominant species of Fe at sample sites A and B $Fe(SO_4)^{-}_2$ Is found and at sites C and D $FeSO_4$ is found. Cadmium dominant species was Cd_{2+} for all sample sites. The dominant species of Zn was Zn_{2+} and Pb was $PbSO_4$. The data shows that Zn and Cd are in solute forms for all sites showing no difference in speciation, this is due to their solubility at a range of pH (Jickells, 1997; Environment Agency Wales, 2002). Iron is shown to be present in the form of $Fe(SO_4)^{-}_2$ at the adit and filtration sites, in the River Rheidol Fe is present as $Fe_3(OH)_4(5^{+})$. This is due the change in pH and redox between mine and river sites, pH is increased and redox is reduced in the River Rheidol aiding precipitation and speciation of Fe (Gundersen and Steinnes, 2001; Environment Agency Wales, 2002; Lin, *et al.,* 2003; Bednar *et al.,* 2005).

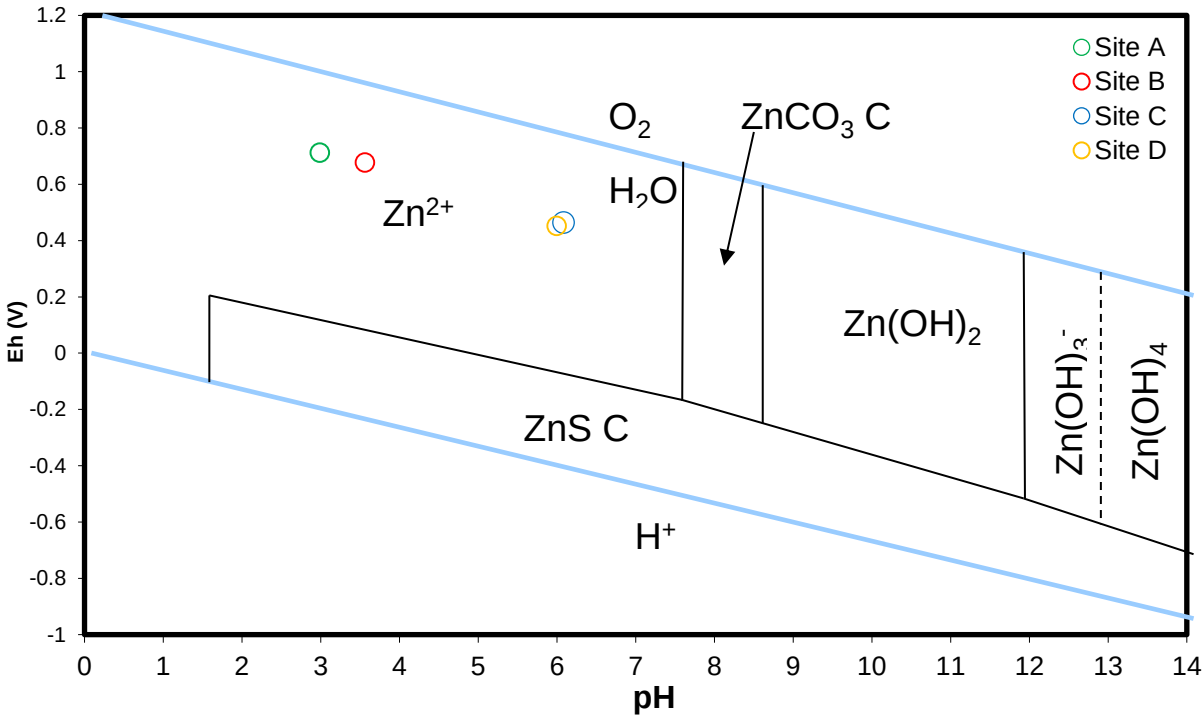

Figure 7.25. Speciation of Zn at Cwm Rheidol mine, sample sites A, B, C and D, based on mean pH and redox values from weekly low-resolution sampling. Adapted from (Garells and Christ,1965).

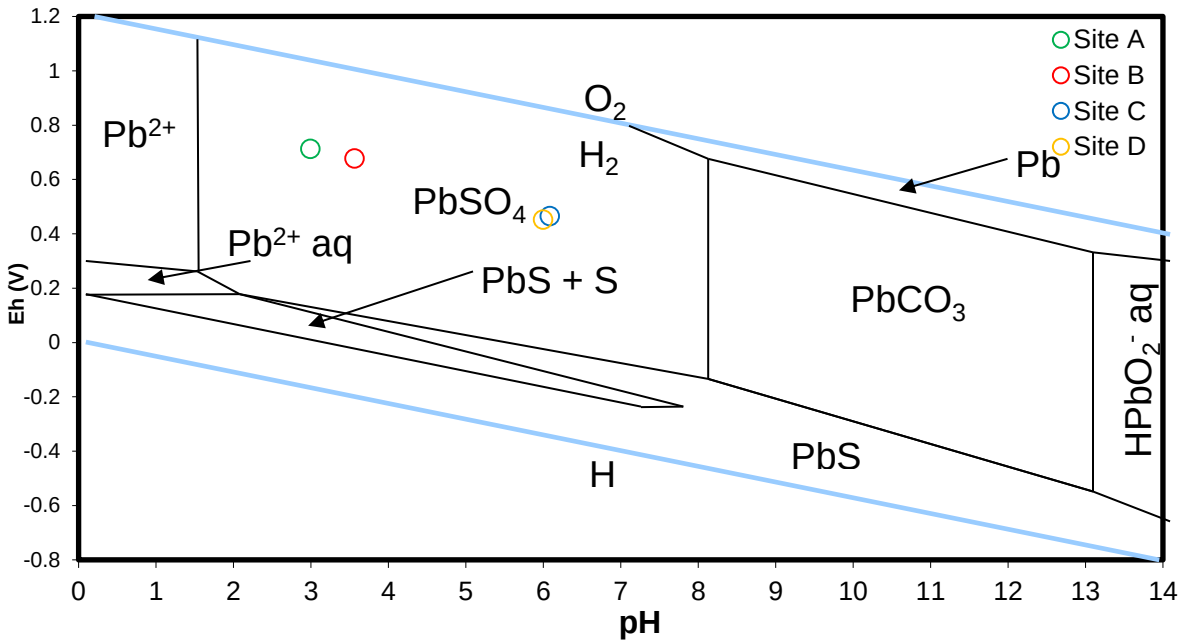

Diagram $FeCl^+$, T = 9.985 °C , P = 1.013 bars, a [main] = $10^{-.04925}$, a [H_2O] = 1, a [Ca^{++}] = $10^{-.186}$, a [Mg^{++}] = $10^{-.1752}$, a [Na^+] = $10^{-.04925}$, a [K^+] = $10^{-.0509}$, a [HCO_3^-] = $10^{-.04847}$, a [SO_4^{--}] = $10^{-.1981}$, a [Cl^-] = $10^{-.0509}$, a [Zn^{++}] = $10^{-.04925}$, a [Pb^{++}] = $10^{-.04925}$

Figure 7.26. Speciation of Pb at Cwm Rheidol mine, sample sites A, B, C and D, based on mean pH and redox values from weekly low-resolution sampling. Adapted from (Garells and Christ,1965).

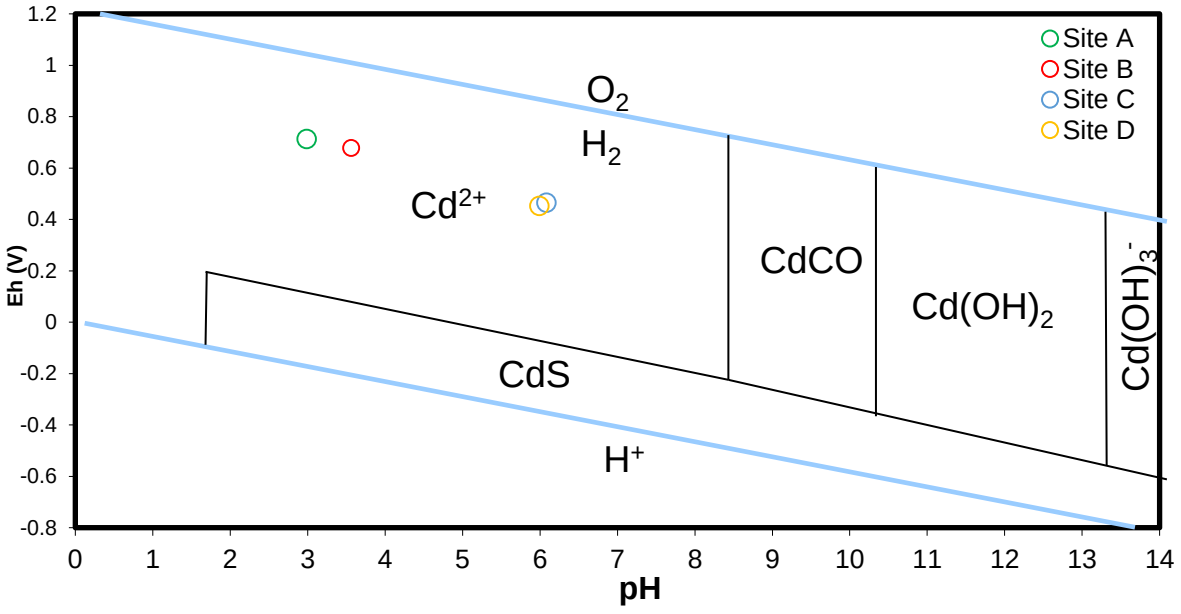

Diagram $FeCl^+$, T = 9.985 °C , P = 1.013 bars, a [main] = $10^{-.04925}$, a [H_2O] = 1, a [Ca^{++}] = $10^{-.186}$, a [Mg^{++}] = $10^{-.1752}$, a [Na^+] = $10^{-.04925}$, a [K^+] = $10^{-.0509}$, a [HCO_3^-] = $10^{-.04847}$, a [SO_4^{--}] = $10^{-.1981}$, a [Cl^-] = $10^{-.0509}$, a [Zn^{++}] = $10^{-.04925}$, a [Pb^{++}] = $10^{-.04925}$

Figure 7.27. Speciation of Cd at Cwm Rheidol mine, sample sites A, B, C and D, based on mean pH and redox values from weekly low-resolution sampling. Adapted from (Garells and Christ,1965).

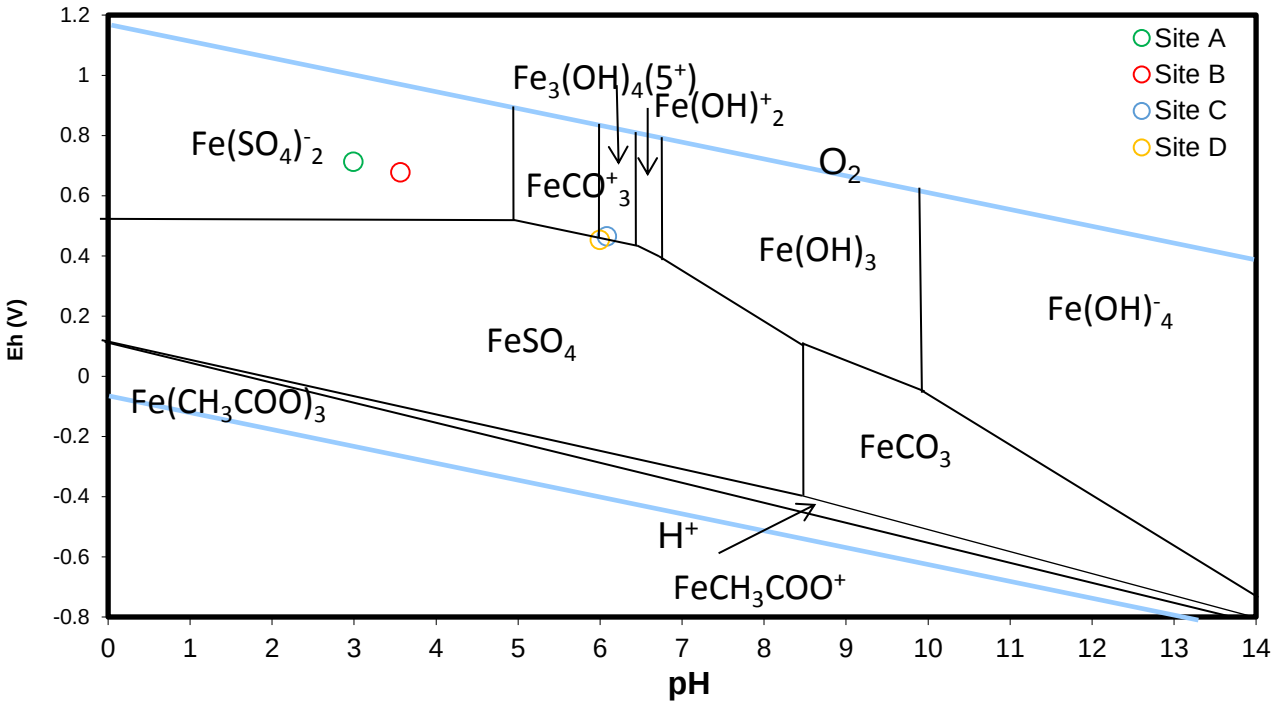

Diagram $FeCl^+$, T = 9.985 °C , P = 1.013 bars, a [main] = $10^{-.04925}$, a [H_2O] = 1, a [Ca^{++}] = $10^{-.186}$, a [Mg^{++}] = $10^{-.1752}$, a [Na^+] = $10^{-.04925}$, a [K^+] = $10^{-.0509}$, a [HCO_3^-] = $10^{-.04847}$, a [SO_4^{--}] = $10^{-.1981}$, a [Cl^-] = $10^{-.0509}$, a [Zn^{++}] = $10^{-.04925}$, a [Pb^{++}] = $10^{-.04925}$

Figure 7.28. Speciation of Fe at Cwm Rheidol mine, sample sites A, B, C and D, based on mean pH and redox values from weekly low-resolution sampling. Adapted from (Garells and Christ,1965).

7.1.6 Water origins

Anion and cation analysis were interpreted using trilinear plots to ascertain water quality at each sample site for Cwm Rheidol mine during the low-resolution weekly sampling (Figures 7.29, 7.30, 7.31 and 7.32). All Sample sites showed little temporal variation in water quality over the period of the study. Mean water quality at all samples sites was plotted (Figure 7.33), Sample sites A and B fall into the category for calcium sulphate rich waters, whereas sample sites C and D are bordering between calcium sulphate and sodium chloride rich waters. Sites A and B exhibit calcium sulphate rich waters the relatively high sulphate content of water from the mine can be accounted for by the dissolution of marcasite and pyrite, remaining in the adits of Cwm Rheidol, which would produce quantities sulphur in the form of sulphate (Fuge *et al.,* 1991). The high carbonate that accompanies the sulphur may be from dissolution of carbonate rich gangue, site B also demonstrates a similar geochemical facies to site A, there is a marginal increase in calcium at site B that may be accounted for the addition of limestone within the filter bed (Williams, 2014).

Site C and D demonstrate sodium chloride rich waters that, elevated sodium and potassium at sites C and D could be explained by upstream weathering and evaporate dissolution of silicate minerals and(or) atmospheric deposition (Pande *et al.,* 1994). Variation in sulphate at upstream site C is likely to be from groundwater inputs and overland flow of water from geogenically enriched strata (Bird *et al.,* 2014; Shea *et*

al., 2016; Di Bonito *et al.,* 2019) and exposed tailings proximal to the River Rheidol (Fuge *et al.,* 1991). At site D the controls of site C sulphate concentration apply with the addition of the mine water sulphate from site B that will contribute towards the sulphate of the river water at site D. Variation in sulphate in river water can be accounted for by variation of hydroclimatic variables controlling PHEs loads and fluxes inevitably also controlling the concentration of sulphate and loads.

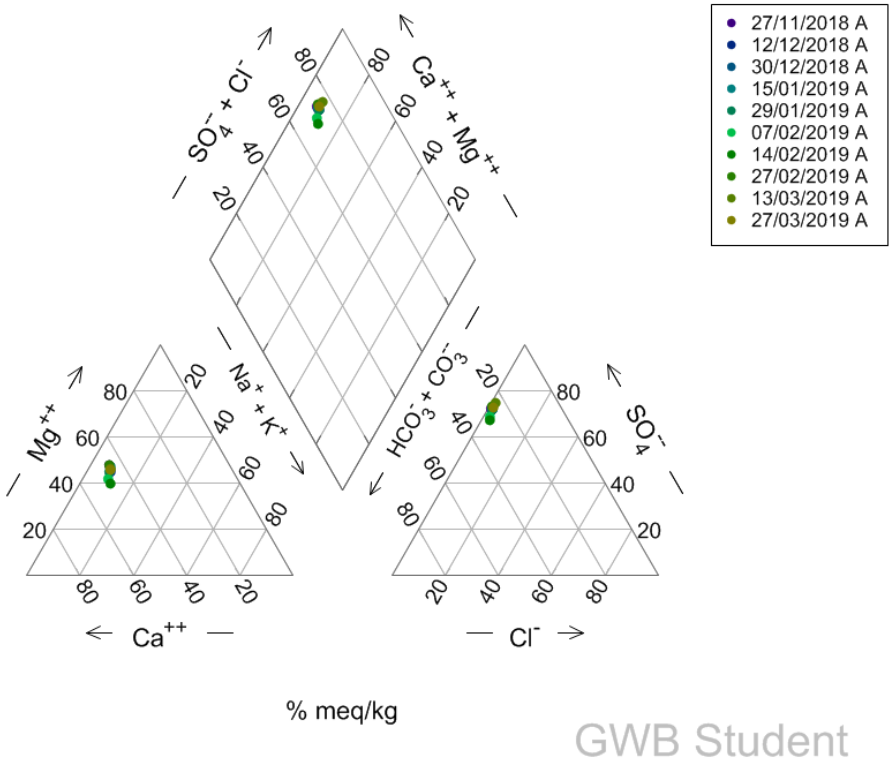

Figure 7.29. Water origins of low-resolution sampling carried out at Cwm Rheidol - 27.11.2018-28.03.2019. At site A adit drainage.

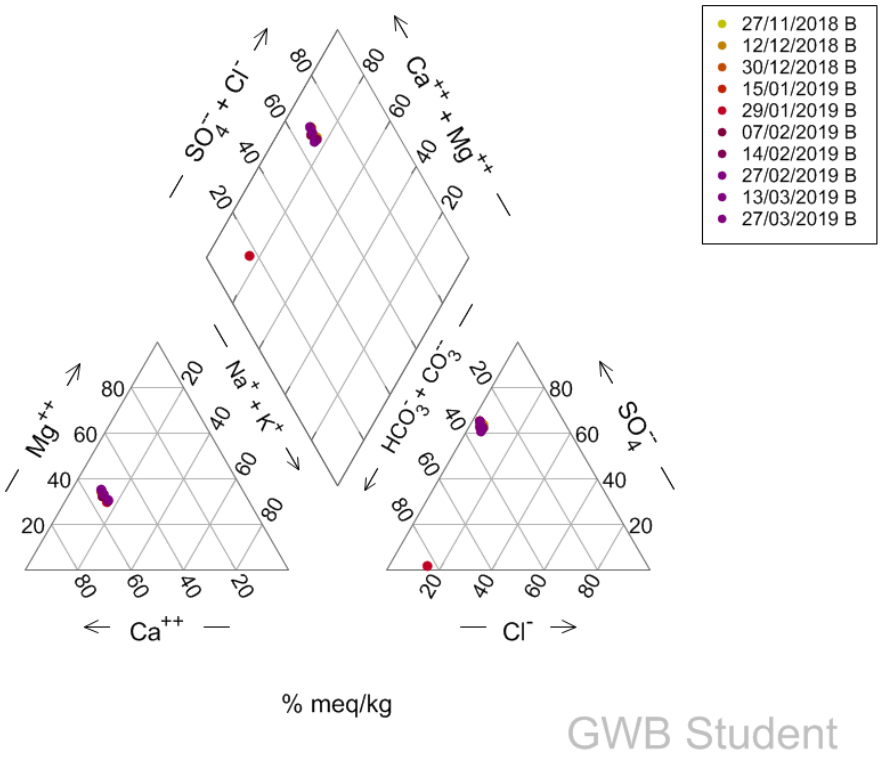

Figure 7.30. Water origins of low-resolution sampling carried out at Cwm Rheidol - 27.11.2018-28.03.2019. At site B filter drainage.

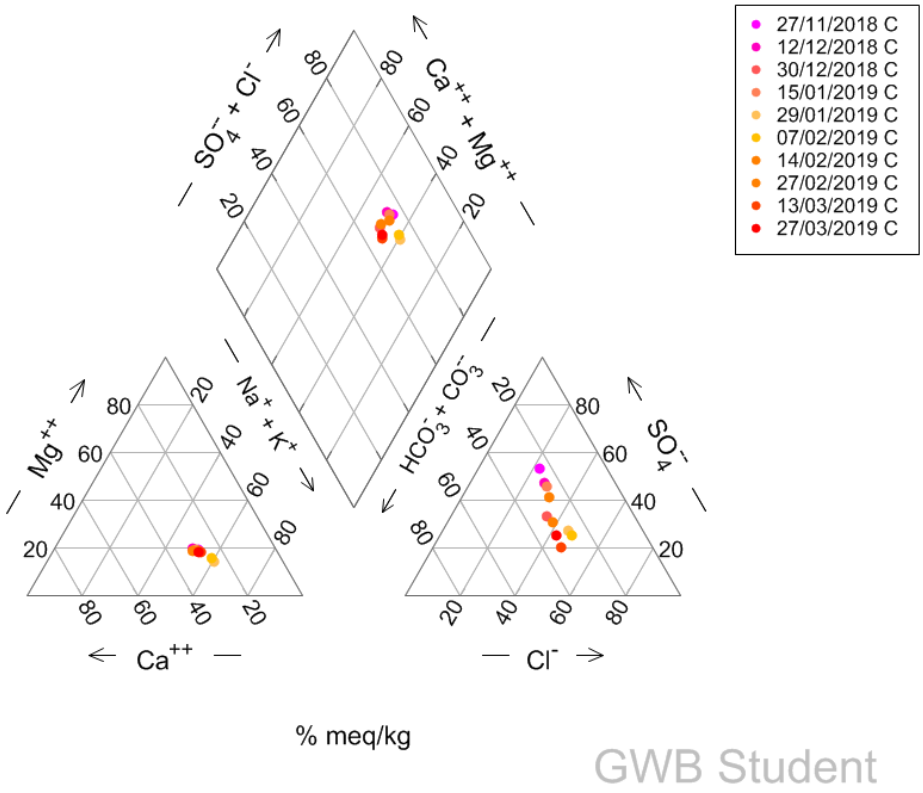

Figure 7.31. Water origins of low-resolution sampling carried out at Cwm Rheidol - 27.11.2018-28.03.2019. At site C control.

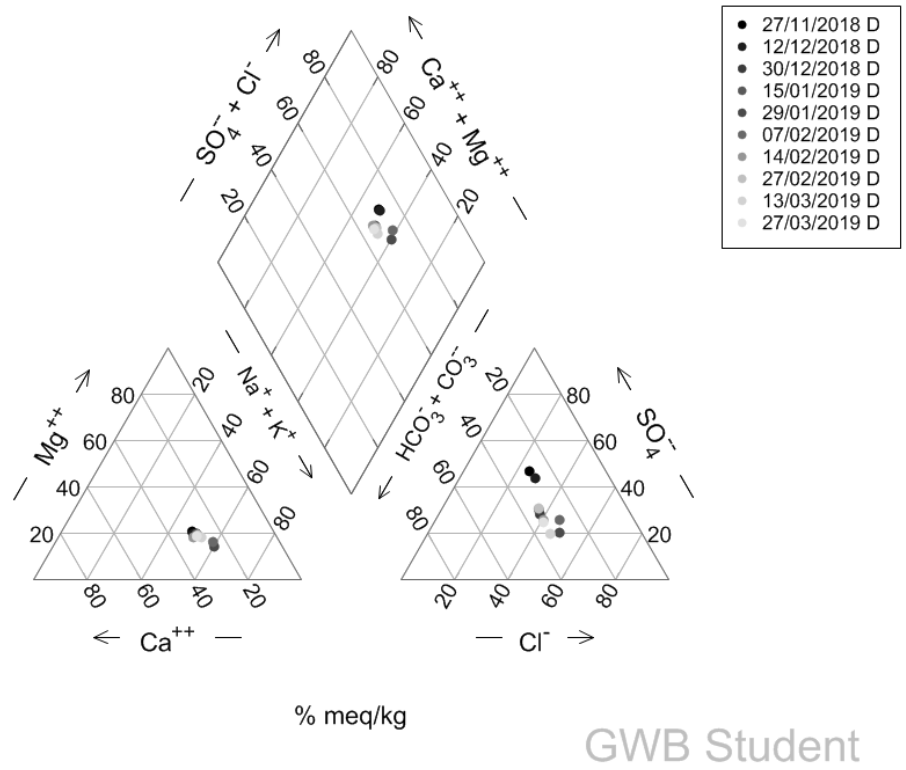

Figure 7.32. Water origins of low-resolution sampling carried out at Cwm Rheidol - 27.11.2018-28.03.2019. At site D downstream.

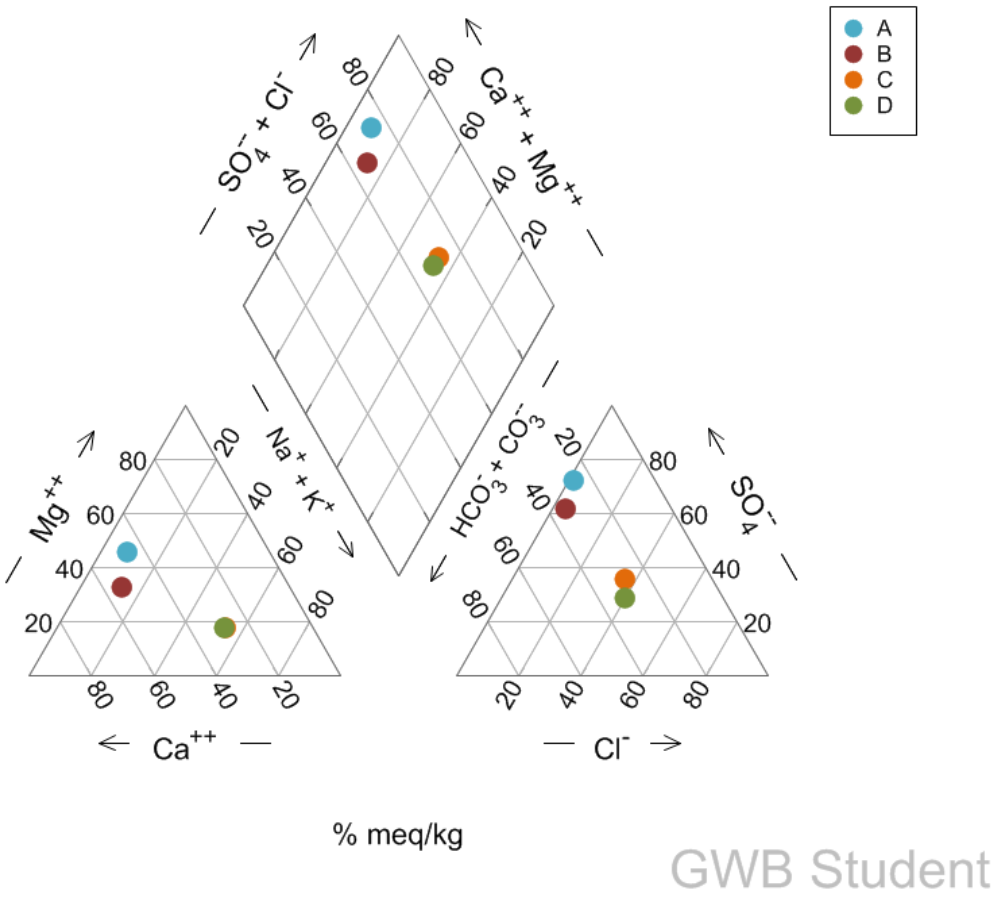

Figure 7.33. Mean water origins of low-resolution sampling carried out at Cwm Rheidol - 27.11.2018-28.03.2019. At sites A, B, C and D at Cwm Rheidol mine.

7.2 High-resolution monitoring – 07.02.19-14.02.19

7.2.1 Hydroclimatic and chemical monitoring

High-resolution monitoring of chemical and hydroclimatic variability was carried out at Cwm Rheidol mine, to assess and identify any relationships between hydroclimatic variability and changes in chemical parameters at sample sites A, B, C and D (Figure 7.34 and 7.35) pH EC, DO_2 demonstrated daily variability. Temperature and stage also demonstrated variation, temperature showed variation daily on a daily scale, stage showed variation over a period ~several days (Figure 7.35).

Temperature upstream has significant negative correlation with DO_2 upstream (Table 7.6). Stage upstream showed correlation with pH and EC (Table 7.6). Downstream temperature exhibited correlation DO_2 and turbidity, while stage exhibited negative correlations with EC and TDS. Independent samples T-tests on pH, EC and DO_2 between upstream and downstream sample sites exhibited significant difference $p < 0.05$. The data suggests that variation in temperature and stage act as a control on pH, EC and Temperature. The positive correlation of EC and stage may be due increases in stage flushing through oxidised mine tailings and accumulated PHEs in alluvial sediments being released from the river bed (Gundersen and Steinnes, 2001), this may also contribute to increases in turbidity that also exhibit a significant correlation with stage (table 7.6). The correlation between EC and temperature was also significant, but stage exemplified the strongest relationship with EC, suggesting that stage is the primary hydroclimatic control (Table 7.6).

Stage also showed significant ($p < 0.05$) correlation with turbidity, this confirms the temporal data, identifying that in times of increased discharge there is an increase in turbidity, the primary control on turbidity is temperature exhibiting a greater correlation than discharge, suggesting temperature to the primary control on temporal changes in turbidity. Data presented for high-resolution monitoring of chemical and hydroclimatic controls shows that hydroclimatic controls do effect chemical variables that are in turn controls on PHE concentrations and fluxes. Temperature correlates with chemical variable's demonstrating diurnal variation suggesting daily fluctuations of PHEs are controlled by temperature and stage.

Table 7.6. Pearson's r correlation of chemical and hydroclimatic variable during high-resolution monitoring 07.02.19-14.02.19.

	Temperature (°C) upstream	pH upstream	DO_2 mg/L upstream	EC (µS/cm) upstream	Stage (m) upstream	Temperature (°C) downstream	pH downstream	DO_2 mg/L downstream	EC (µS/cm) downstream	Stage (m) downstream	TDS (mg/L) downstream	Turbidity (NTU) downstream
Temperature (°C) upstream	1											
pH upstream	-0.516	1										
DO_2 mg/L upstream	-0.784	0.454	1									
EC (µS/cm) upstream	-0.162	0.157	0.250	1								
Stage (m) upstream	0.126	-0.528	0.126	0.254	1							
Temperature (°C) downstream	0.993	-0.529	-0.789	-0.140	0.122	1						
pH downstream	0.094	0.407	-0.381	0.108	-0.206	0.081	1					
DO_2 mg/L downstream	-0.322	0.474	0.655	0.110	-0.163	-0.322	-0.375	1				
EC (µS/cm) downstream	0.010	0.236	-0.360	-0.180	-0.573	0.016	0.260	0.031	1			
Stage (m) downstream	0.128	-0.544	0.126	0.253	0.997	0.125	-0.227	-0.172	-0.590	1		
TDS (mg/L) downstream	0.019	0.236	-0.364	-0.170	-0.576	0.025	0.265	0.031	0.999	-0.593	1	
Turbidity (NTU) downstream	-0.485	0.337	0.544	0.086	-0.319	-0.482	-0.399	0.396	-0.253	-0.301	-0.254	1

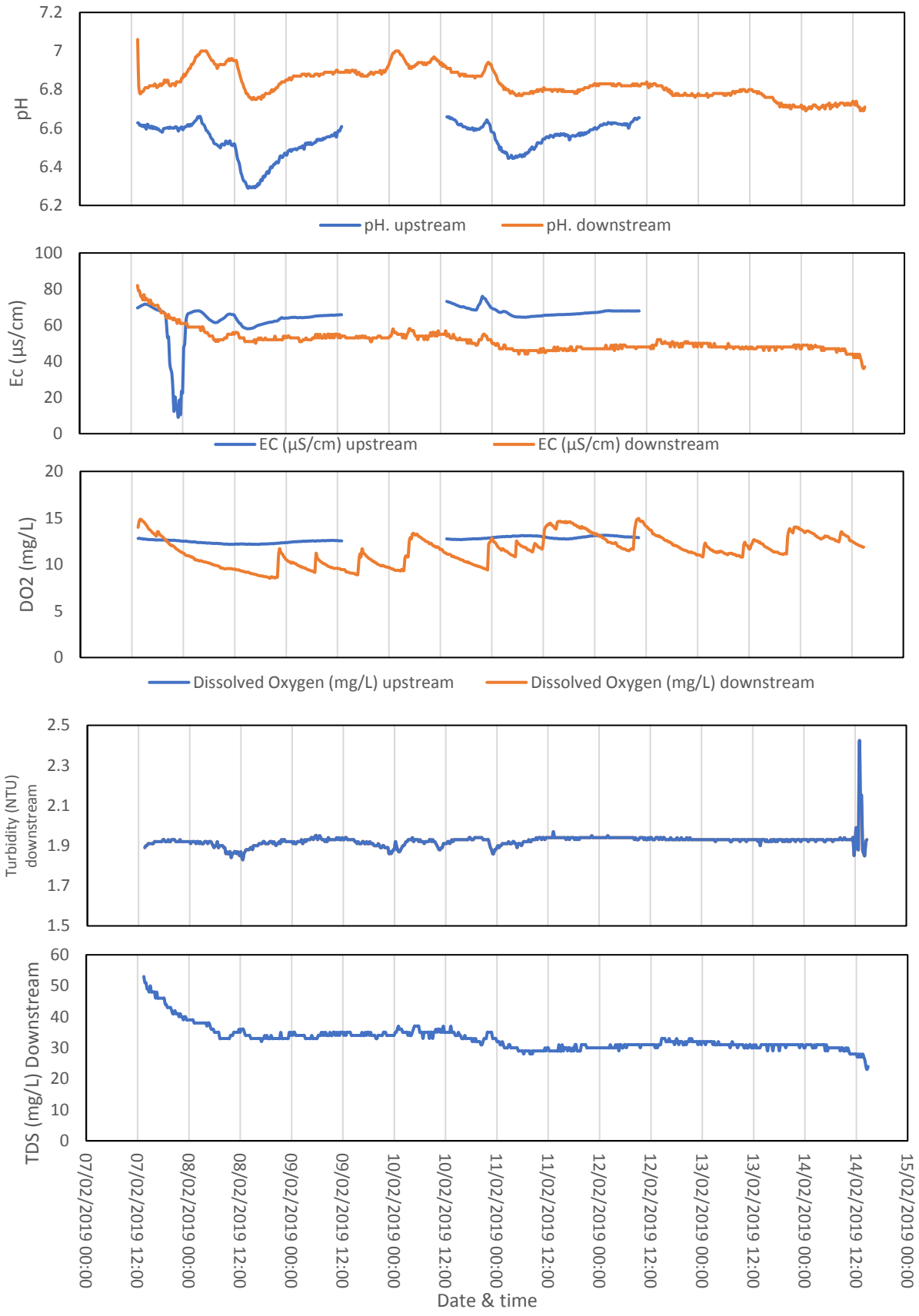

Figure 7.34. Chemical variability of high-resolution sampling carried out at Cwm Rheidol- 07.02.2019-14.02.2019.

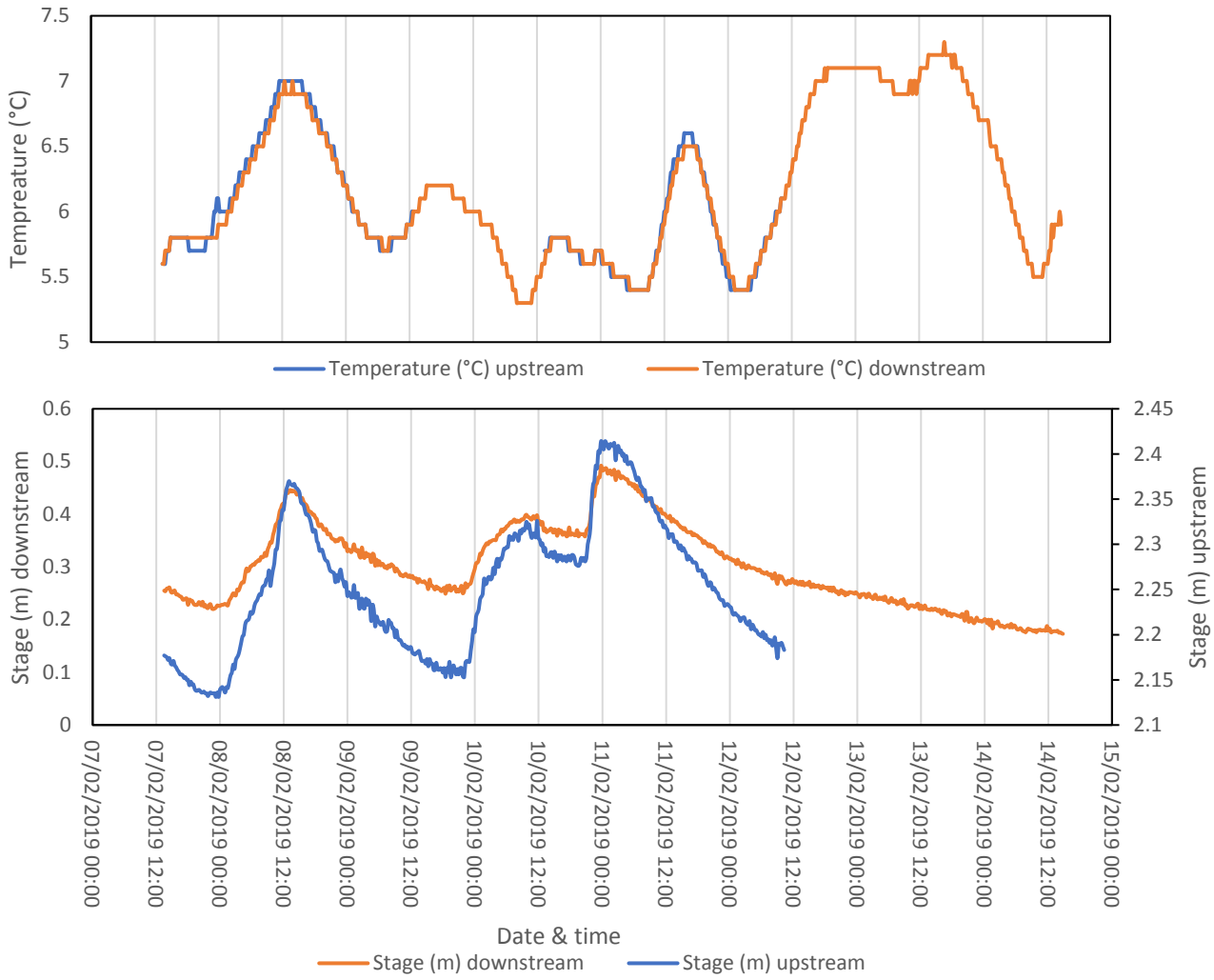

Figure 7.35. Hydroclimatic variability of high-resolution sampling carried out at Cwm Rheidol- 07.02.2019-14.02.2019.

Chapter 8 – Results & discussion 4

8.1 High-resolution vs low resolution data

Due to Zn being of primary concern at both mine sites this section has primarily concentrated on Zn, unfiltered Zn concentrations have been the focus of this section due to concentrations reflecting the total Zn contained within the fluvial system. Low resolution weekly monitoring of Zn has been compared to hourly high-resolution monitoring to identify differences in results from the differing monitoring regimes at Parc mine. Low resolution monitoring between 27.11.2018-28.03.2019 resulted in a variance of 1.39 mg/L for Zn and a mean concentration of 2.21 mg/L. 24-hour high-resolution monitoring between 01.02.2019-02.03.19 showed a variance of 0.58 mg/L and a mean of 2.7 mg/L. 24-hour monitoring has showed less variance than low resolution monitoring (Table 8.1 and Figure 8.1). This could be due to several factors that include, the hydroclimatic variables of stage and discharge demonstrating variance over periods of several days, which would not have been detected by 24-hour monitoring (Littlewood, 1995; Moore *et al.,* 1996; Jarvie *et al.,* 2000; Nimick *et al.,* 2007; Kimball *et al.,* 2010). The concentration of Zn may have been more stable during the 24-hour sampling period and observed variance may be due to less interference from other controlling factors that do not show diurnal variance such as discharge.

24-hour monitoring exemplifies an increased mean load in comparison to low resolution monitoring and shows an increase of 19.05%, this suggests that PHE concentrations estimated during low resolution may be underestimated leading to predicted loads of PHEs also being underestimated (Worrall *et al.,* 2013).

Table 8.1. Variation in water sampled unfiltered PHE concentrations at Parc Mine, weekly sampling carried out 27.11.18-280319 and hourly sampling carried out 01.03.19-02.03.19.

	Zn mg/l (Weekly)	Zn mg/l (hourly)
SD	0.50	0.20
Min	1.47	2.36
Max	2.86	2.94
Mean	2.21	2.73

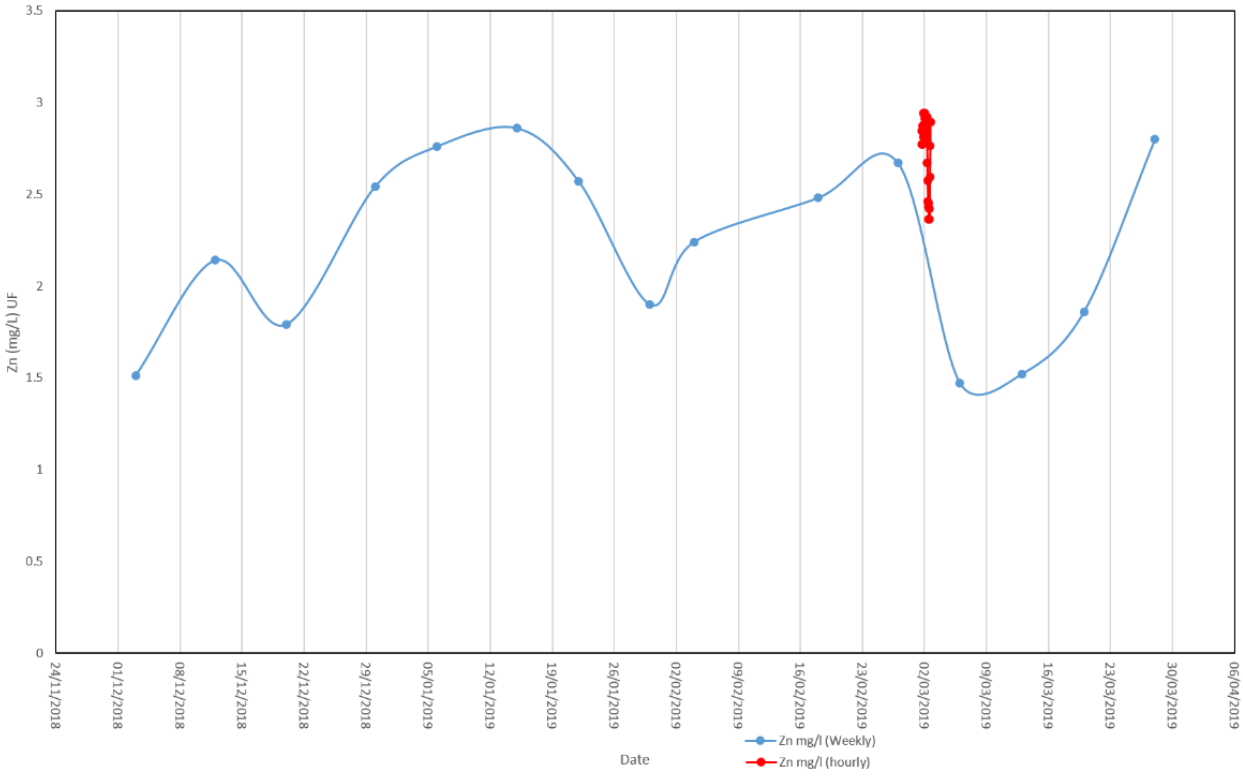

Figure 8.1. Weekly vs hourly sampling at Parc mine, weekly sampling was carried out 27.11.18-28.03.19 and hourly sampling was carried out 01.03.19-02.03.19.

The relationship between unfiltered Zn and pH at a low-resolution monitoring level (Figure 8.2) shows a significant ($p = < 0.05$) positive correlation ($r = 0.65$), this shows that over a low-resolution monitoring regime, 42% ($r^2 = 0.42$) of the variation in Zn concentrations can be explained by variation in pH (Figure 8.2). Figure 8.3 demonstrates the temporal trend of pH and unfiltered Zn concentrations at site D and it demonstrates the correlation seen in Figure 8.2. Low resolution monitoring demonstrates variance with no evidence of diel cycling (Figure 8.2).

The relationship between Zn and pH at a 24-hour high-resolution monitoring level (Figure 8.4) shows a negative significant ($p = <0.05$) negative correlation ($r = 0.76$), this shows that over a low-resolution monitoring regime, 58% ($r^2 = 0.58$) of the variation in Zn concentrations can be explained by variation in pH (Figure 8.4). Over a high-resolution monitoring regime, the trend of Zn concentration decreases coincides with increases in pH, figure 8.5 demonstrates the temporal trend of pH and unfiltered Zn concentrations at site D and it confirms the correlation seen in figure 8.4. 24-hour resolution monitoring demonstrates variance with evidence of diel cycling (Moore *et al.,* 1996; Nimick *et al.,* 2007). The data suggests that the increased resolution of monitoring has identified a differing relationship for pH and Zn concentration, this may be due to the resolution of the data showing less variance, possibly due to less interference from discharge which demonstrates variance over longer periods ~days (Worrall *et al.,* 2013).

The temporal trend that is shown in Figure 8.5 is evident of distinct diel cycling, it shows an increased Zn concentration during the night (18.00-06.00). The increased Zn concentration is demonstrated by an 0.269 mg/L increase (Figures 8.6, 8.7 and 8.8). Enrichment factors for PHEs during 24-hour monitoring clarify that Zn and Fe are enriched to an increased amount during the night and that Pb enrichment is greater during the day (Figures 8.9, 8.10 and 8.11). The increased concentration during the day for Pb may be due to increased discharge during the day, that increased the particulate load of the Pb, resulting in a higher Pb concentration being experienced during the day. Due to Pb being present in an insoluble form of Pb, PbSO. The increased concentrations of PHEs at night may be explained by the fall in pH during the night period (Figure 8.5). The decrease of pH levels during the night may be due to inactivity of photosynthesis during the night (Sullivan and Drever, 2001; Kimball *et al.,* 2010; Rudall and Jarvis, 2012). Photosynthetic processes act as a pH buffer during the day in fluvial systems (Rudall and Jarvis, 2012). The diurnal fluctuations in pH may also be due to diurnal temperature fluctuations, reflected in the river water that can affect pH levels (Moore *et al.,* 1996; Nagorski *et al.,* 2003).

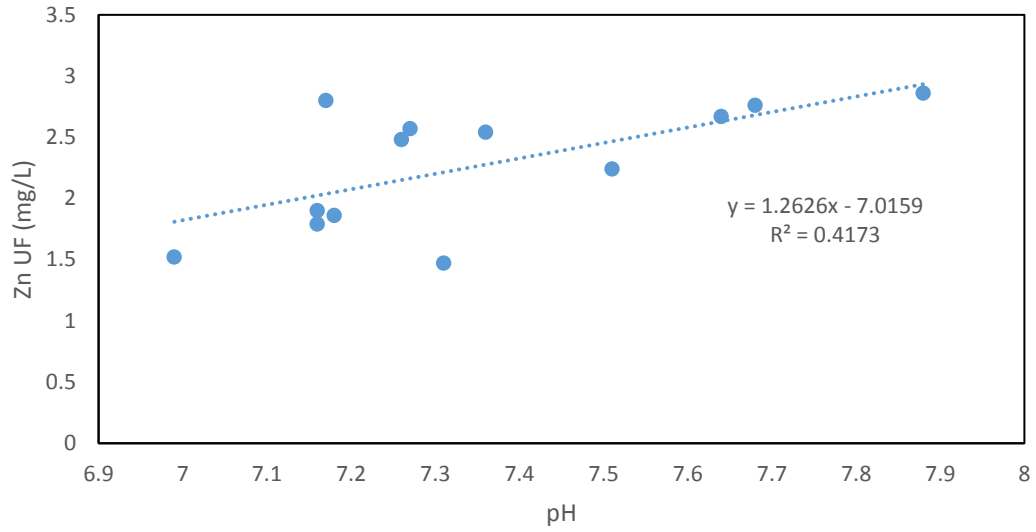

Figure 8.2 Zinc concentration and pH regression at Parc mine site D low resolution weekly monitoring.

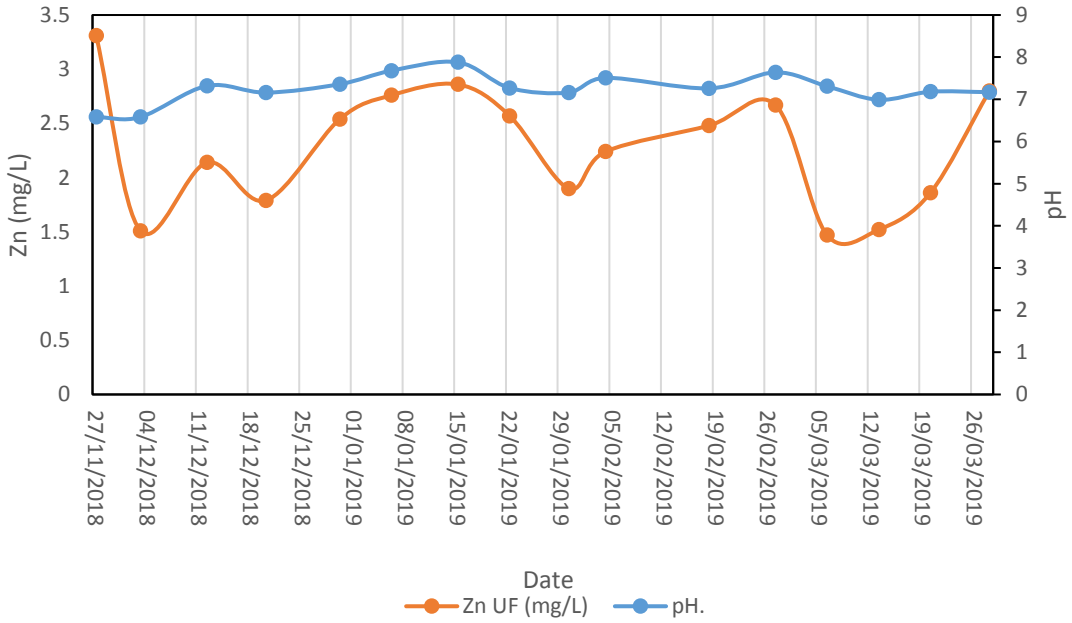

Figure 8.3. Zinc concentration and pH temporal relationship at Parc mine site D low resolution weekly monitoring.

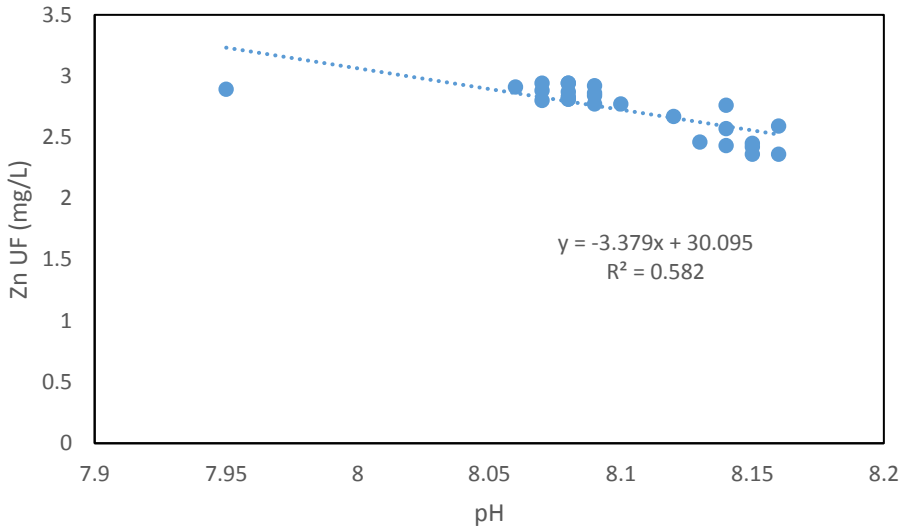

Figure 8.4. Zinc concentration and pH regression at Parc mine site D high-resolution 24-hour monitoring.

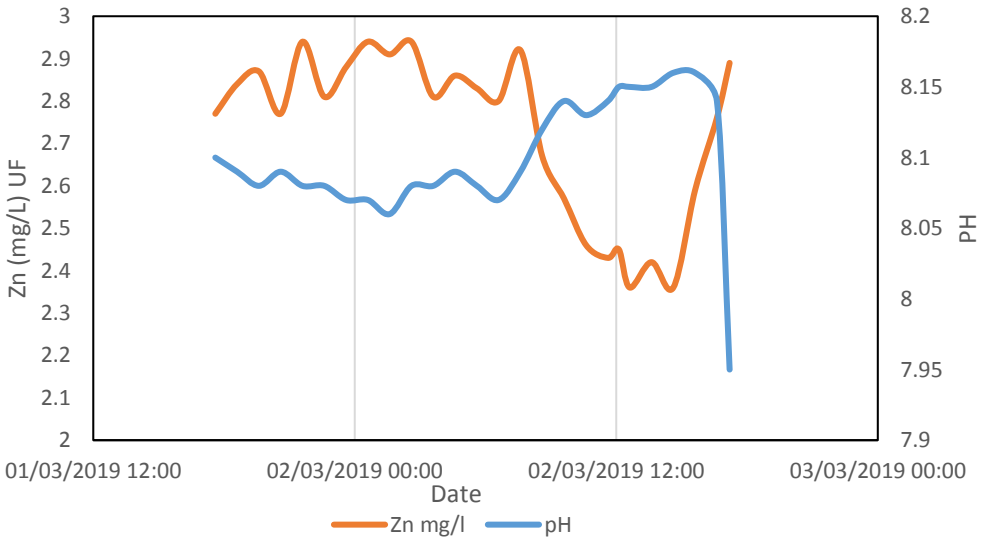

Figure 8.5. Zinc concentration and pH temporal relationship at Parc mine site D high-resolution 24-hour monitoring.

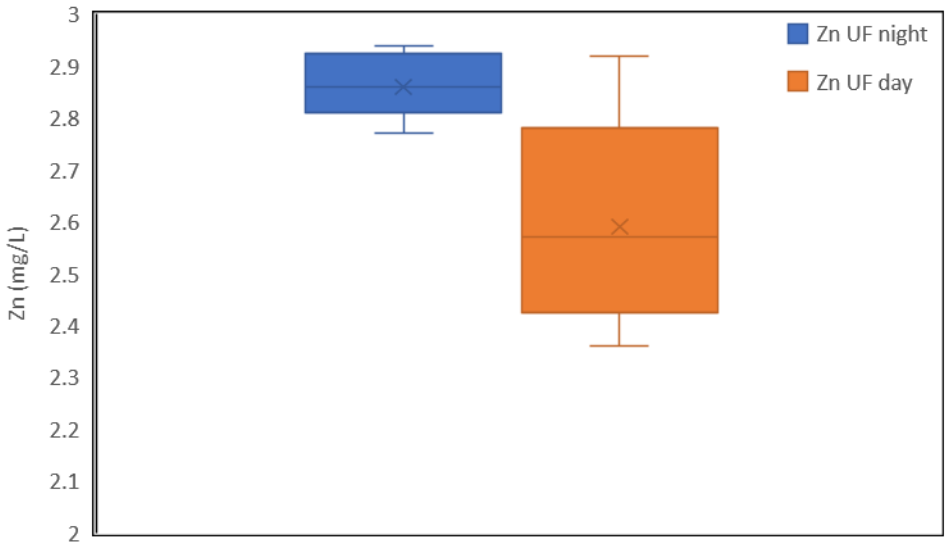

Figure 8.6. Zinc concentrations during day and night, at Parc mine site D, high-resolution 24-hour monitoring 01.03.19-02.03.19.

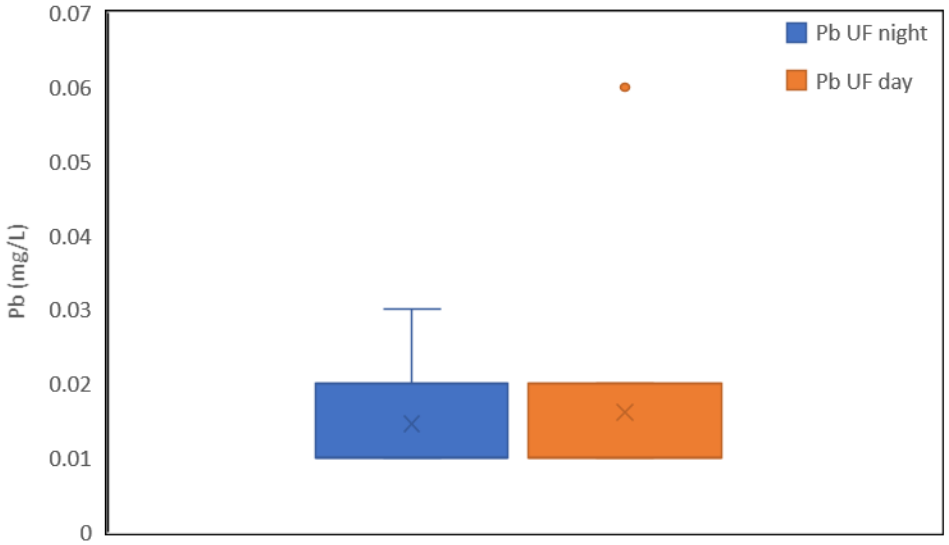

Figure 8.7. Lead concentrations during day and night, at Parc mine site D, high-resolution 24-hour monitoring 01.03.19-02.03.19.

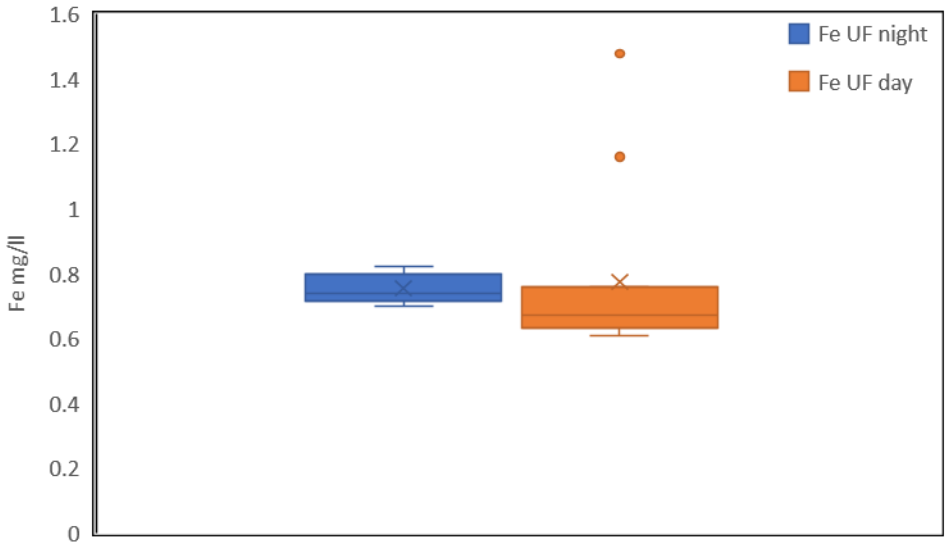

Figure 8.8. Iron concentrations during day and night, at Parc mine site D, high-resolution 24-hour monitoring 01.03.19-02.03.19.

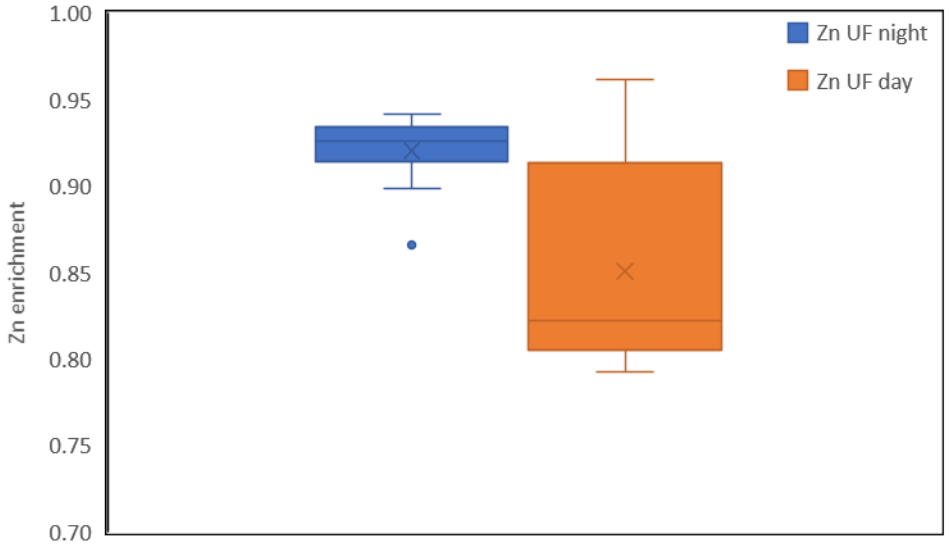

Figure 8.9. Zinc enrichment during day and night, at Parc mine site D, high-resolution 24-hour monitoring 01.03.19-02.03.19.

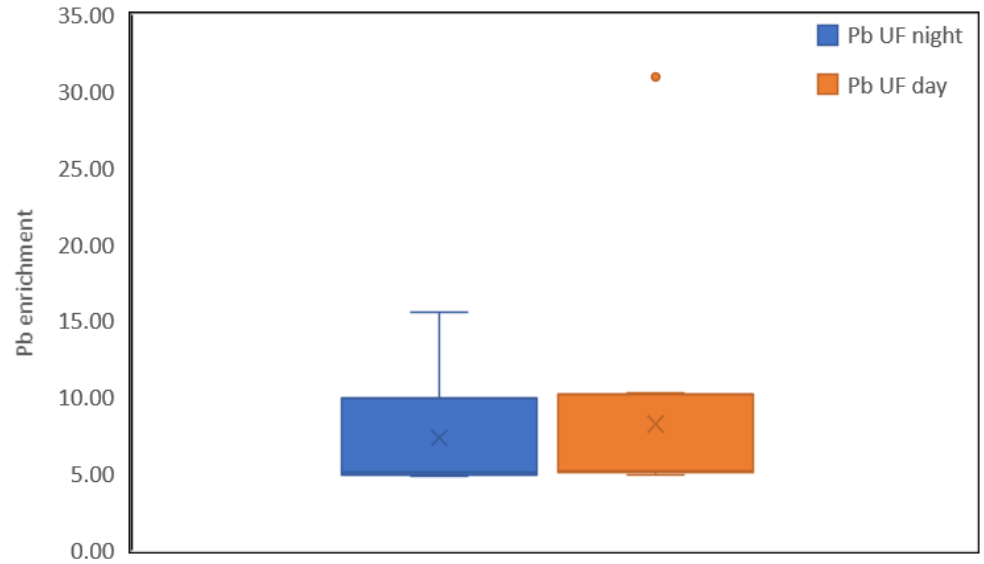

Figure 8.10. Lead enrichment during day and night, at Parc mine site D, high-resolution 24-hour monitoring 01.03.19-02.03.19.

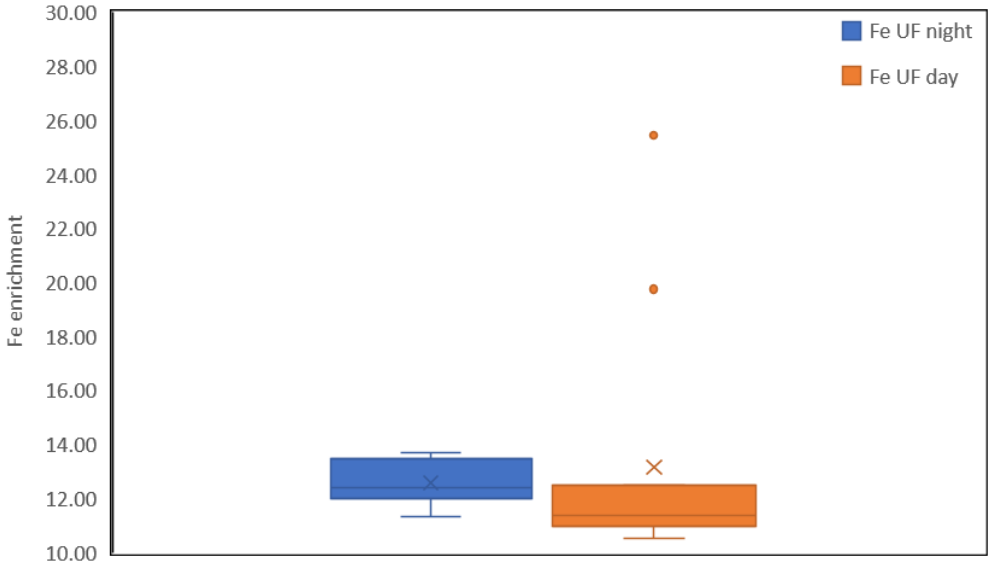

Figure 8.11. Iron enrichment during day and night, at Parc mine site D, high-resolution 24-hour monitoring 01.03.19-02.03.19.

8.2 Predicting PHE concentrations

Regression analysis of Zn and hydroclimatic variables has been examined to assess the potential of using hydroclimatic data to enable flux predictions (Figures 8.12-8.21). Previous research has looked at interpolating PHE concentrations, with results that do not reflect the true concentration present in the fluvial system in question (Littlewood, 1995; Worrall *et al.,* 2013). A regression equation that could predict PHE concentrations based on hydroclimatic data, would be highly beneficial and enable calculations of concentration at the same resolution as monitoring, without requiring the need for constant manual sampling, this means high volume PHE concentration datasets could be modelled using hydroclimatic data from remote monitoring stations.

Electrical conductivity yielded the strongest regression and was significant for both Parc mine at all sites and Cwm Rheidol mine sites A and B. Cwm Rheidol sites C and D demonstrate strongest regression with stage (Figure 8.22). EC demonstrated poor regression with unfiltered Zn at sites C and D (Figure 8.23). Zn variability in the River Rheidol (Sites C and D) is primarily controlled by hydroclimatic variability and sites A and B and all sites at Parc mine are primarily controlled by chemical variability, sites C and D at Cwm Rheidol differ in Zn variability controls due to significant dilution of adit waters from site B (Table 7.3). Monitoring of EC and stage will enable future concentration and load calculations based upon remote sensing of EC and stage enabling a high sampling frequency using water quality meters that will enable flux calculations that reflect the PHE load of the fluvial system in question (Worrall *et al.,* 2013). Previous research that has depended on low frequency data has resulted in underestimates of PHE load (Littlewood, 1995; Nagorski *et al.,* 2003; Kimball *et al.,* 2010; Worrall *et al.,* 2013). The underestimation of PHE load with low resolution sampling can be explained by the increased PHE concentration at night and or short-term flushing events which would have significant effect on the total load of PHEs within the fluvial system (Moore *et al.,* 1996; Nimick *et al.,* 2007).

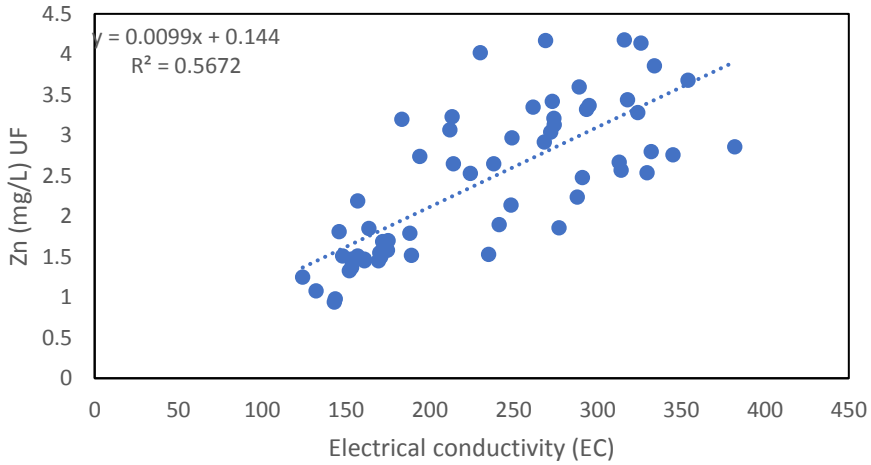

Figure 8.12. Regression of Zn concentration unfiltered (UF) and electrical conductivity (EC) exemplifying the equation for Zn concentration at Parc mine, based on data at sites A, B, C and D between 27.11.18-28.03.19.

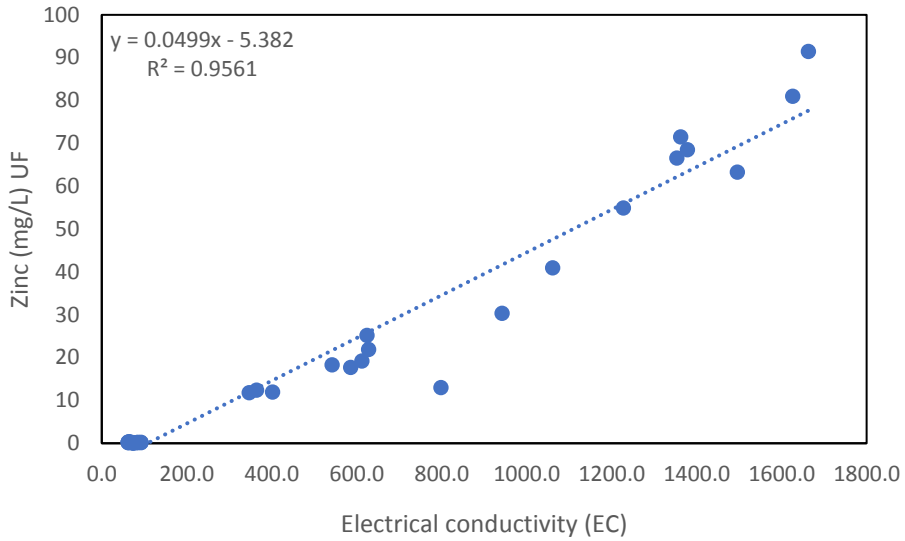

Figure 8.13. Regression of Zn concentration unfiltered (UF) and electrical conductivity (EC) exemplifying the equation for Zn concentration at Cwm Rheidol, based on data at sites A, B, C and D 27.11.18-28.03.19.

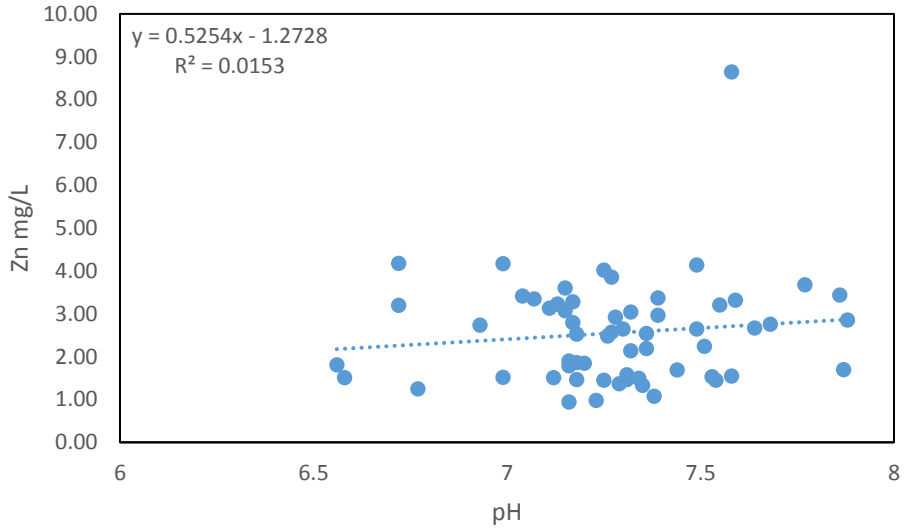

Figure 8.14. Zinc concentration and pH regression relationship for Parc mine sites based on data at sites A, B, C and D 27.11.18-28.03.19.

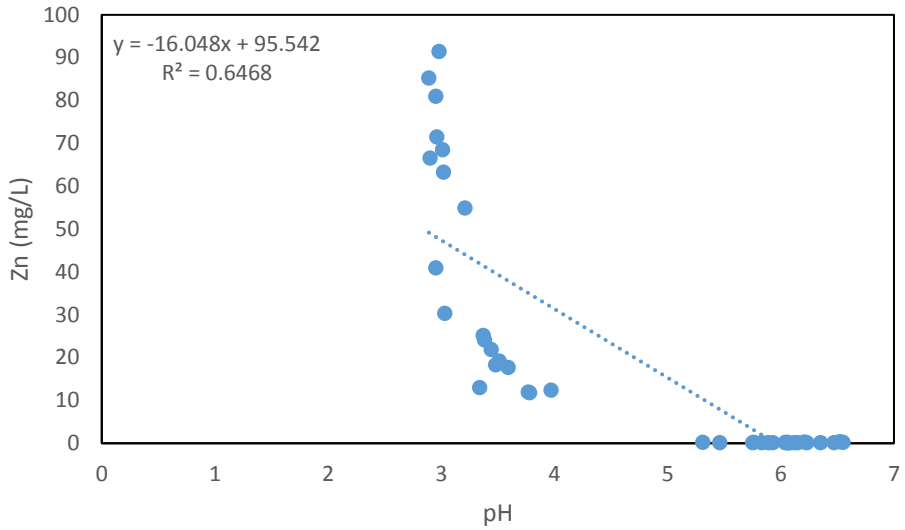

Figure 8.15. Zinc concentration and pH regression relationship for Cwm Rheidol mine sites based on data at sites A, B, C and D 27.11.18-28.03.19.

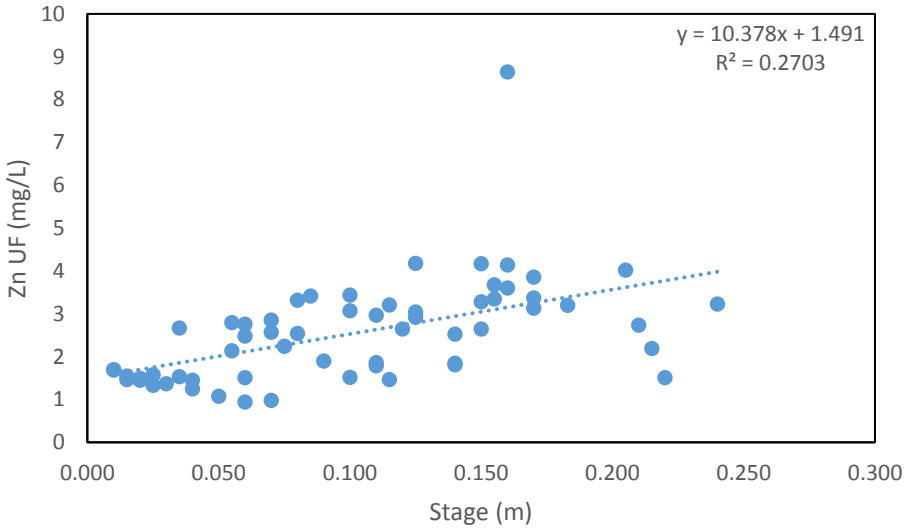

Figure 8.16. Zinc concentration and stage regression relationship for Parc mine sites based on data at sites A, B, C and D 27.11.18-28.03.19.

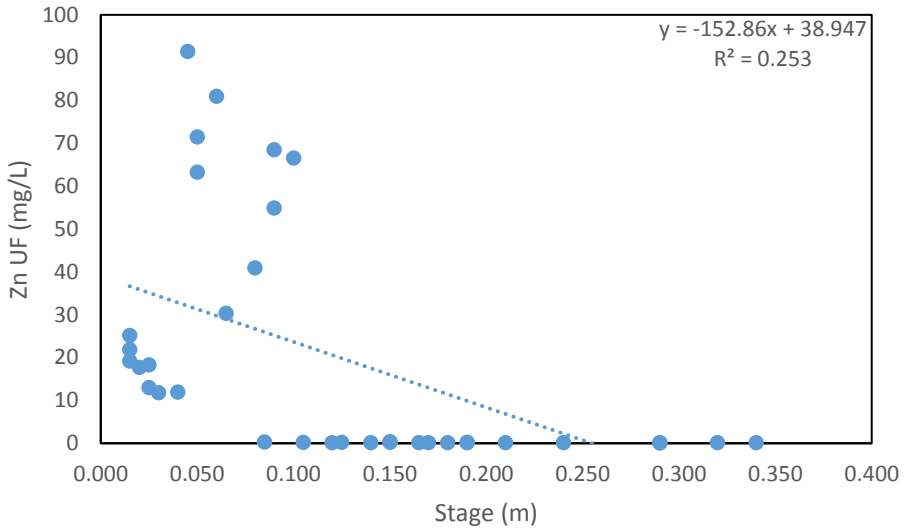

Figure 8.17. Zinc concentration and stage regression relationship at Cwm Rheidol mine sites based on data at sites A, B, C and D 27.11.18-28.03.19.

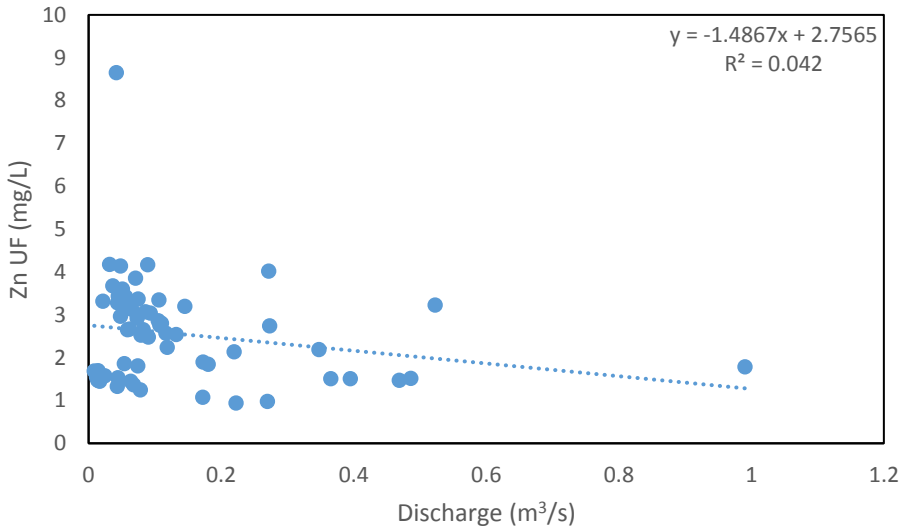

Figure 8.18. Zinc concentration and discharge regression relationship at Parc mine sites based on data at sites A, B, C and D 27.11.18-28.03.19.

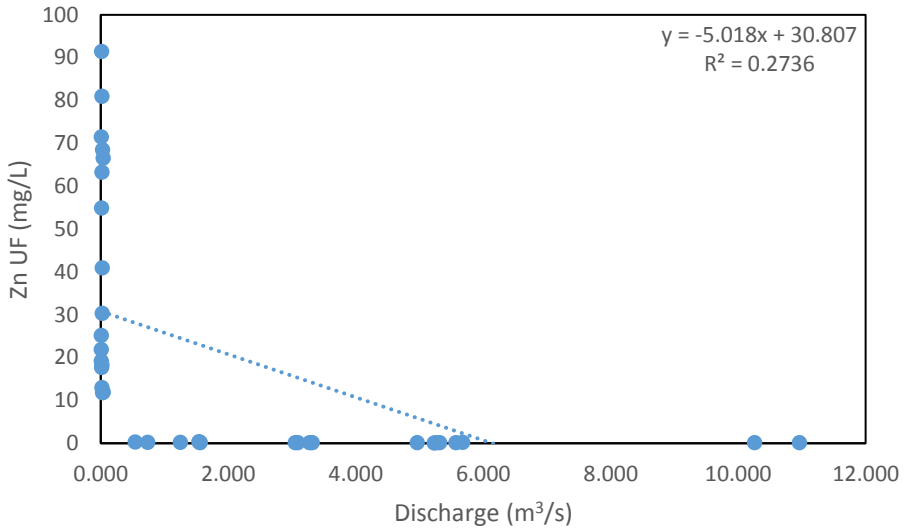

Figure 8.19. Zinc concentration and discharge regression relationship at Cwm Rheidol mine sites based on data at sites A, B, C and D 27.11.18-28.03.19.

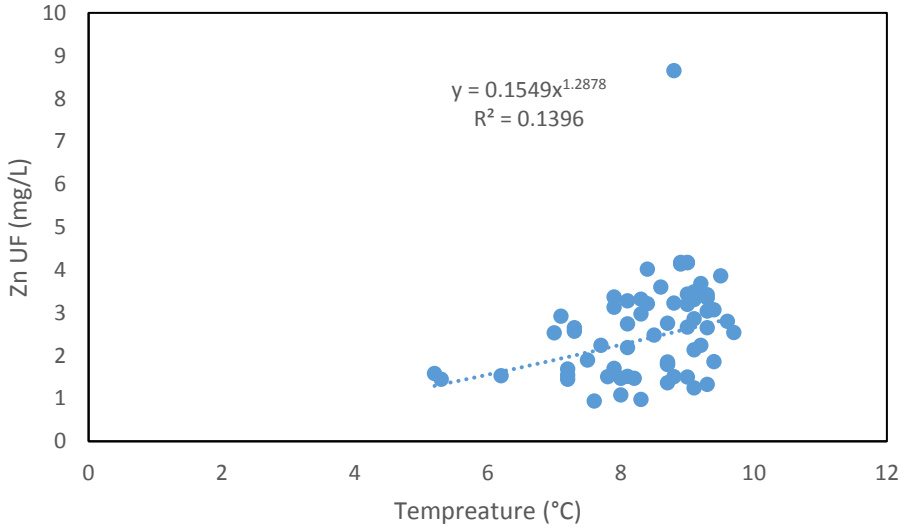

Figure 8.20. Zinc concentration and temperature regression relationship at Parc mine sites based on data at sites A, B, C and D 27.11.18-28.03.19.

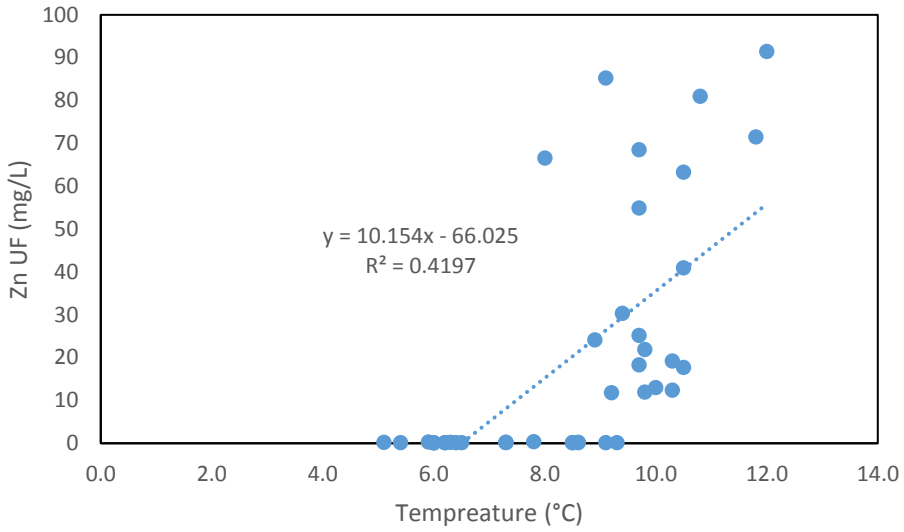

Figure 8.21. Zinc concentration and temperature regression relationship at Cwm Rheidol sites based on data at sites A, B, C and D 27.11.18-28.03.19.

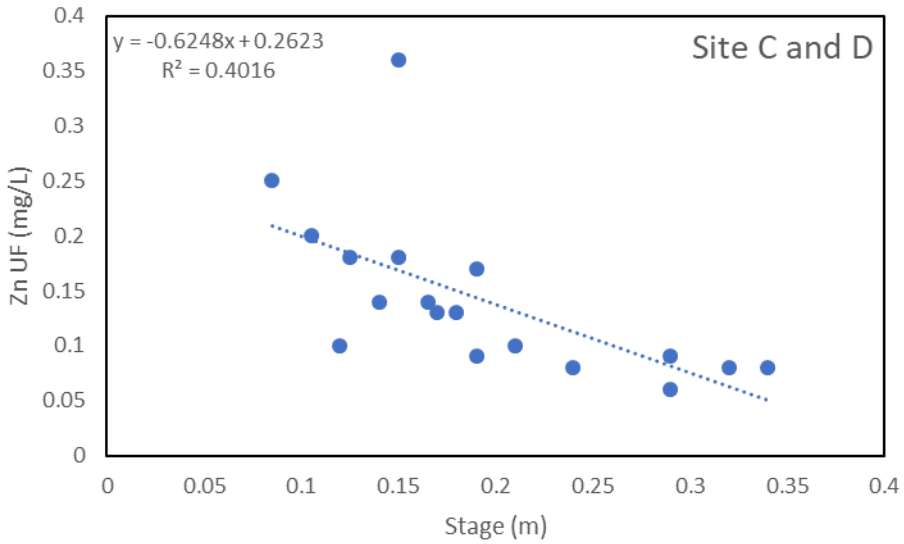

Figure 8.22. Zinc concentration and stage regression relationship at Cwm Rheidol sites based on data at sites C and D 27.11.18-28.03.19.

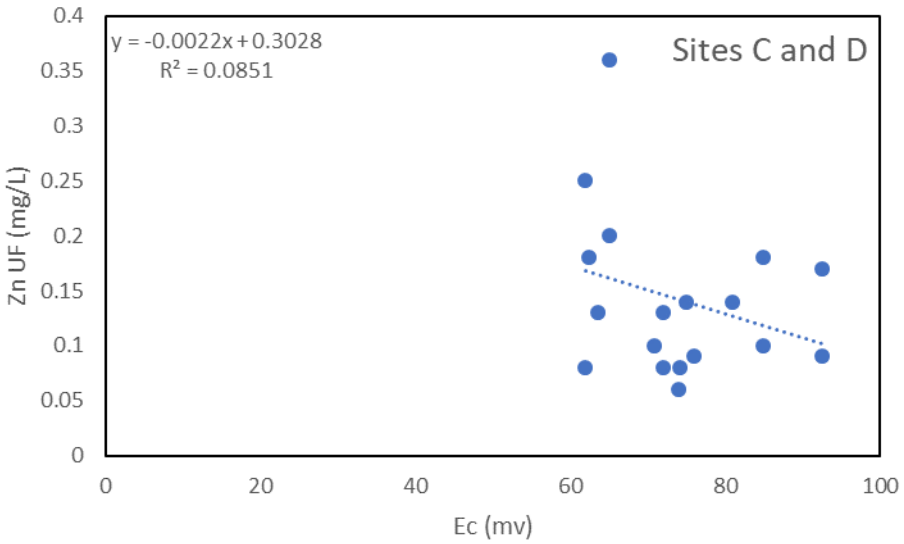

Figure 8.23. Zinc concentration and EC regression relationship at Cwm Rheidol sites based on data at sites C and D 27.111.8-28.03.19.

8.2.1 Testing PHE concentration predictions

To test the effectiveness of the predicted equations in response to temporal and spatial variability plots were produced for each site (Figures 8.24 and 8.25). Mean unfiltered Zn predicted and recorded concentrations demonstrated no significant difference ($p < 0.05$) for all sites at Cwm Rheidol and Parc mine, suggesting the prediction equations are a source of reliable high-resolution predictions for future monitoring. Site A and B at Cwm Rheidol showed significant difference from predicted Zn concentrations on two occasions. To eliminate deviations from recorded Zn concentrations further research looking at multiple regression would be required, multiple regression of pH, EC, temperature, stage and discharge at Cwm Rheidol accounts for 99% of Zn concentration variability, and this suggests a multi regression for predicted PHE concentration variability would be beneficial. At Parc mine 80% of variability can be accounted for by pH, EC, temperature, stage and discharge. This suggest that further research to identify other variables implicated in PHE variability is required to produce a robust multi regression for predicting PHE concentrations.

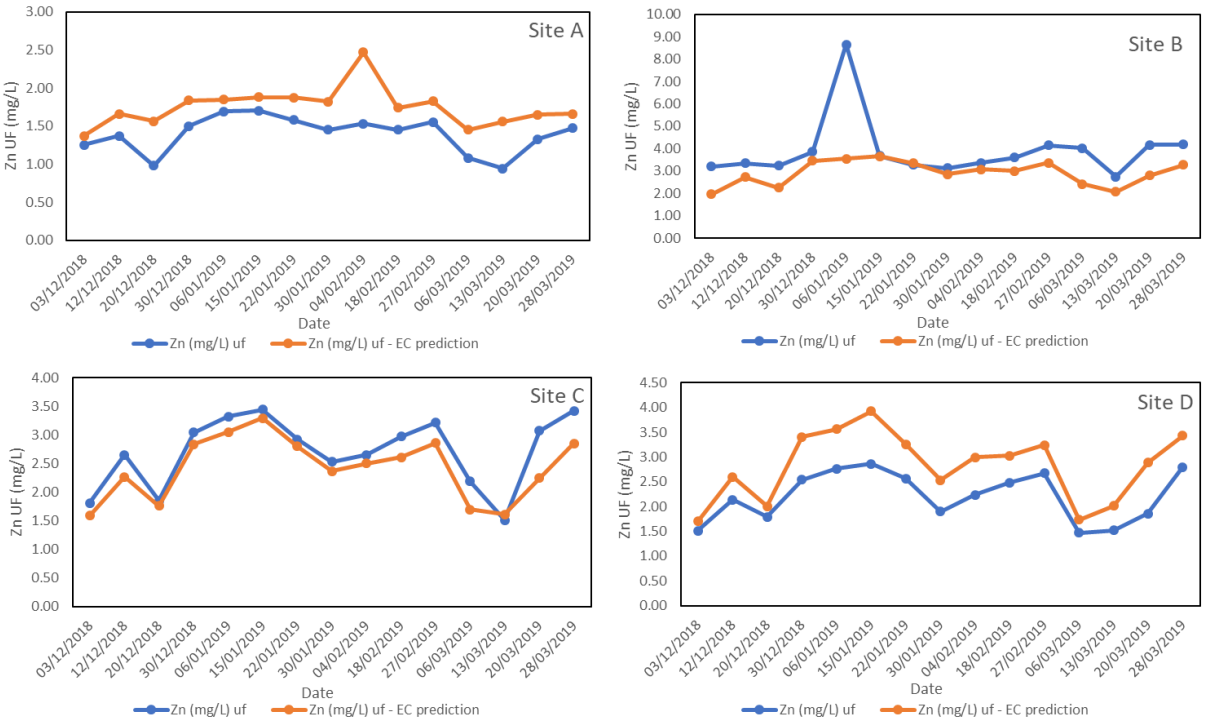

Figure 8.24. Zinc concentration and predicted Zn concentration relationship at Parc sites based on EC data at sites A, B, C and D 27.11.18-28.03.19.

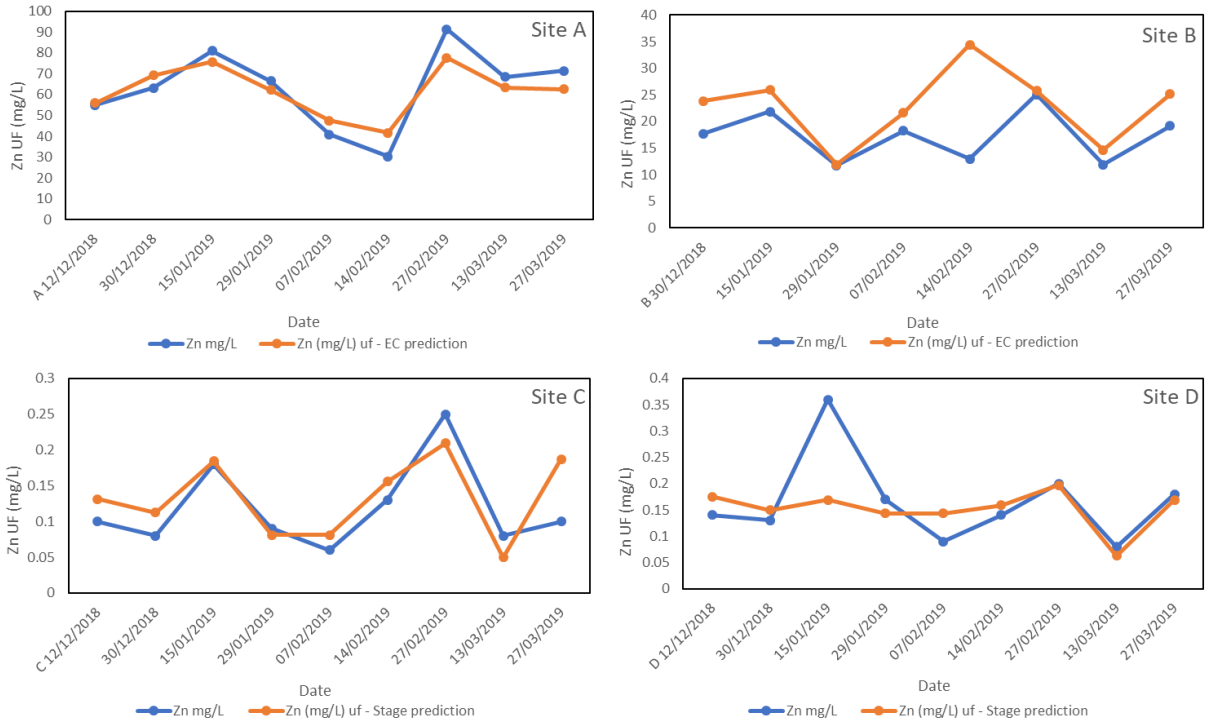

Figure 8.25. Zinc concentration and predicted Zn concentration relationship at Parc sites based on EC data at sites A and B, at sites C and D predictions based on stage data 27.11.18-28.03.19.

8.3 Effectiveness of the Cwm Rheidol passive filter

The effectiveness of the Cwm Rheidol filter bed has been analysed to examine temporal variation in the effectiveness of the filter bed and identify the primary hydroclimatic or chemical control that may alter the effectiveness of the filter bed. Regression analysis of the effectiveness of removal of Zn, Pb, Cd and Fe was carried out in relation to the hydroclimatic variables of discharge, Zn is exemplified (Figure 8.26 & 8.27). Percentage Zn removal demonstrates a significant ($p < 0.05$) correlation with discharge, suggesting increases in discharge increase the effectiveness of Zn removal. Lead, Cd and Fe % removal effectiveness did not show any significant correlation with discharge, this suggests that discharge does not have an effect on Pb, Cd and Fe removal. Temperature correlation with Zn showed poor insignificant correlation and suggests that temperature does not influence the effectiveness of the Cwm Rheidol filter bed.

The insignificant correlation of temperature and removal efficiency could be explained by sampling being carried out over winter months where previous research has found the filter to be less effective, due to increased discharge in winter months (Williams, 2014). To establish relationships of temperature and removal effectiveness, a long-term study encompassing seasonality would be required. The period and frequency of sampling may not have been sufficient to identify any trends (Littlewood, 1995). The significant ($p < 0.05$) correlation of Zn % reduction with discharge could also be explained by Zn being relatively soluble and is in solute Zn^{2+} form at the filter bed (Figure 7.25) (Jickells, 1997). Increases and decreases of Zn concentration in the filter bed could be due to dilution effects of dissolved Zn, increases in discharge act to reduce Zn concentrations by dilution, this would appear as a reduction in load due to the filter bed, but its primary control would be dilution (Fovet *et al.,* 2018).

Previous work has found increased discharge reduced residence times of PHEs in filter bed remediation systems reducing their effectiveness (Williams, 2014), evidence from this study has not found any significant results demonstrating this for this study. Iron demonstrated a negative correlation between discharge and removal percentage but was not significant and therefore cannot be concluded from this research (Figure 8.28). This may be due to inaccuracies in discharge monitoring due to logistical problems regarding monitoring of the filter bed discharge, the equipment used was impractical for relatively small water flow. Overall the filter temporally ranged in effectiveness between 72-83, 91-99, 57-81, 70-91 % for Zn, Pb, Cd and Fe respectively.

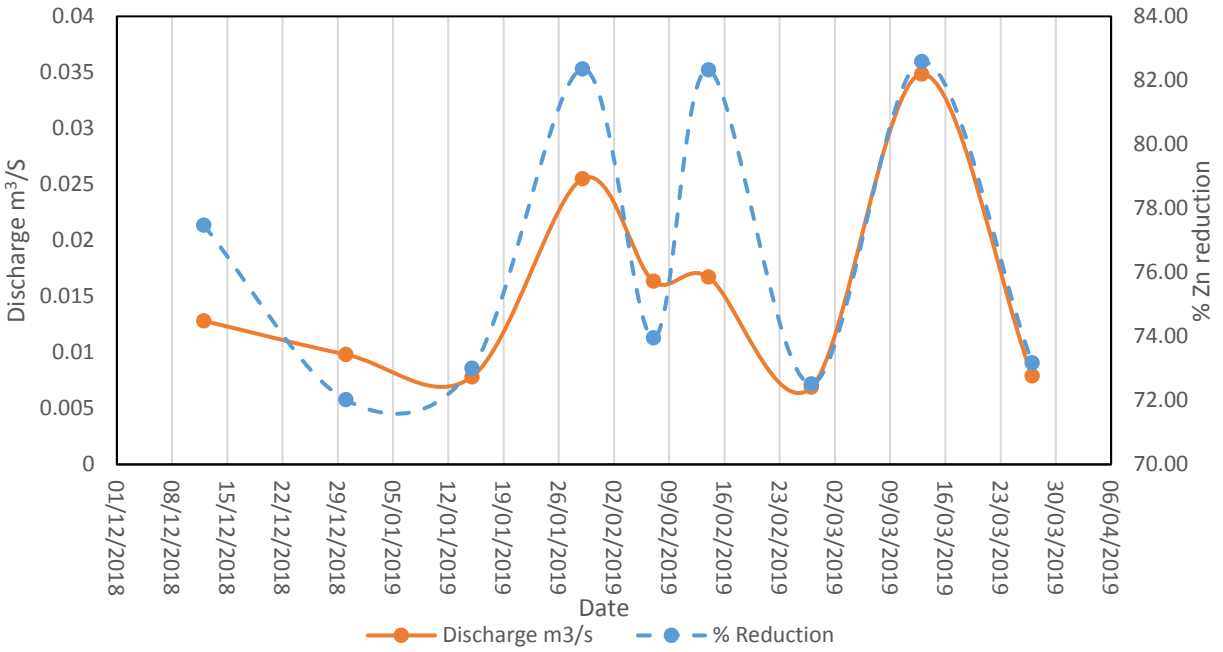

Figure 8.26. Comparison of Zn % reduction by filtration and discharge at Cwm Rheidol mine during low resolution monitoring 27.11.18-28.11.19.

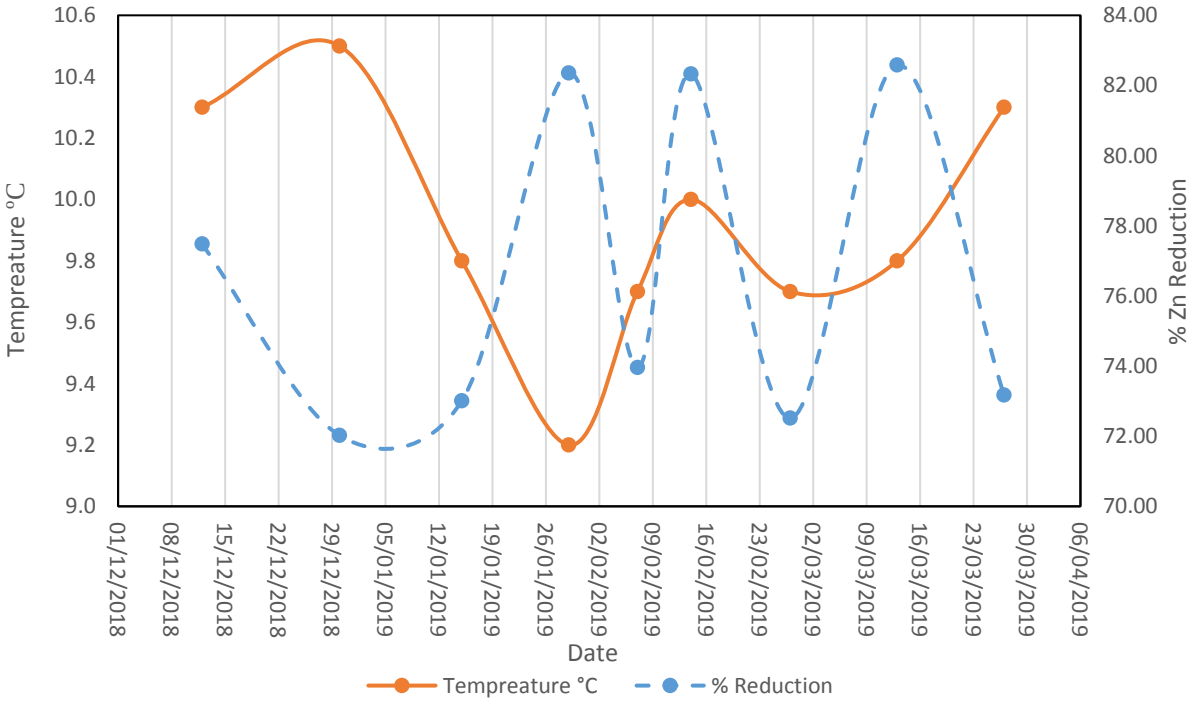

Figure 8.27. Comparison of Zn % reduction by filtration and temperature at Cwm Rheidol mine during low resolution monitoring 27.11.18-28.11.19.

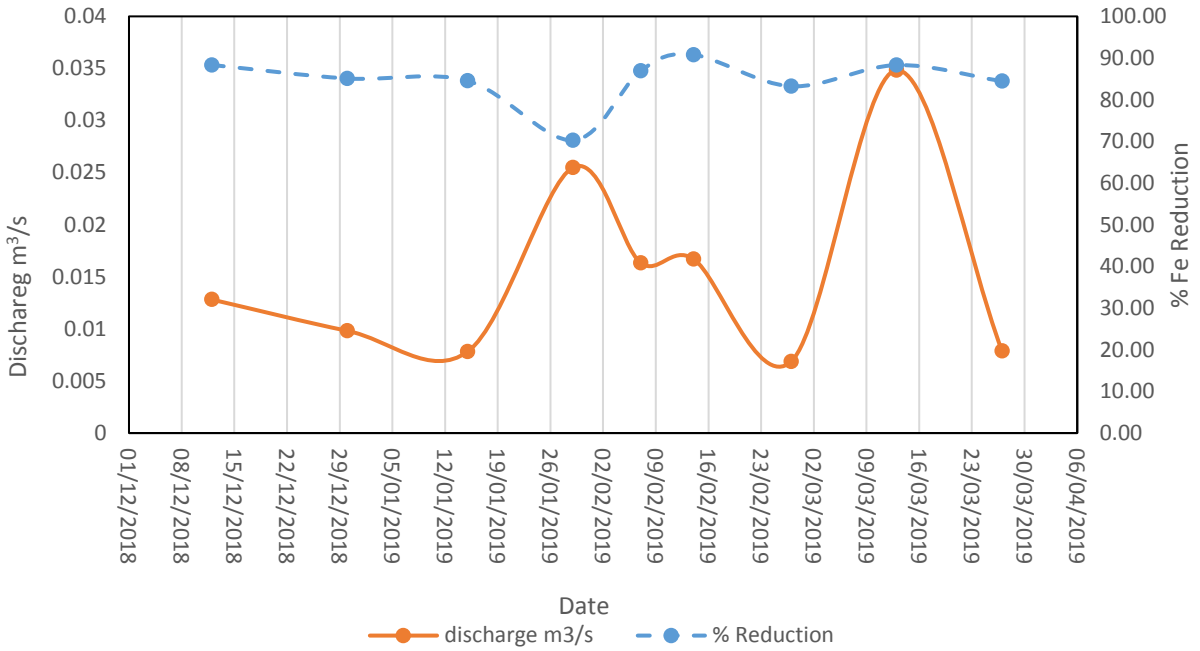

Figure 8.28. Comparison of Fe % reduction by filtration and discharge at Cwm Rheidol mine during low resolution monitoring 27.11.18-28.11.19.

8.4 Site contamination comparisons

Mine water remediation systems have become increasingly used and are potentially very effective, within the UK removal rates of up to 99.9% for Zn have been achieved (Table 8.2). Remediation schemes have the potential to reduce PHE loads to the fluvial environment and improve water quality. Cwm Rheidol filter bed demonstrates a 75.9% reduction that is comparable to removal rates at Wheal Jane mine, where a passive filter system is in place, in the form of anoxic limestone drain, whereas Cwm Rheidol is an oxic filter system, the systems are differing in the processes to remove PHEs, with oxic systems generally more effective (Chowdhury *et al.,* 2015). The removal rate currently demonstrated at Cwm Rheidol is reflective of previous research attained (Table 8.2), the trail filter bed has become less effective since its installation in 2011 where filter was found to be up to 100% effective, this study found the filtered had remained at a effectiveness similar to the mean effectiveness of the previous study by Williams (2014), that found Zn removal to have reached 69% by 2014. The previous study on the filter bed found the filter to be less effective during winter months with an effectiveness of 44% and 50% for 2011 and 2012 respectively. Similar systems to Cwm Rheidol at Force crag highlight the ineffectiveness of the Cwm Rheidol trail system. Although it is possible to reduce PHE concentrations and subsequently PHE loads by remediation, previous contamination that has precipitated and deposited in floodplains from mine waters still remains a risk for future flooding events, that are becoming increasingly frequent due to increased climate variability due to climate change (Boussen *et al.,* 2010; Bird, 2016; Hosseini *et al.,* 2017; Abraham *et al.,* 2018).

Recent trials of new technology in the form of sono-electrochemical precipitation have recently been trailed at Cwm Rheidol and Ystumtuen mines, the trail has proved a successful method to reduce PHE concentrations in mine waters, removal rates of Zn achieved 99.9% (Rose *et al.,* 2019). The remediation method allows for commercial recovery of PHEs, making the new remediation system an attractive prospect for remediation of PHE mine water. Feasibility studies are currently being carried out with a view to emplace the system at several sites in Wales (Rose *et al.,* 2019). Rose *et al.* (2019) suggests a system would require an electrical consumption of 32 KWh to achieve 99.5% removal of metals. Based upon scrap metal prices for Zn (£600/tonne) and Fe (£115/tonne) (LKM Recycling 2019), the two most abundant metals at Parc and Cwm Rheidol and an average electrical consumption cost of £0.1437 per KWh (UK Power 2019) this study has found that Cwm Rheidol could offset 67% of costs and Parc mine could offset 23% of energy costs. The data regarding feasibility from this study suggests that recovery of metals could not fully offset costs of remediation but is a more feasible option for Cwm Rheidol mine in comparison Park mine.

Contamination from Parc mine adit is relatively low in comparison to other adit sites identified by the WFD as requiring remediation and Cwm Rheidol demonstrates a relatively high concentration in comparison to other mines as requiring attention by the WFD (Table 8.3). Although Cwm Rheidol demonstrates relatively high concentrations of PHEs in waters draining the adit, it is Parc that demonstrates PHEs at a greater concentration in the fluvial system at downstream site D. The primary reason for this is the relative lack of dilution offered by the Nant Gwydir. Parc adit and the Nant Gwydir shows a dilution factor of

1.76 whereas Cwm Rheidol filter and the River Rheidol shows a dilution factor of 0.004. Due to dilution effects of adit mine waters with upstream waters, it is Parc that demonstrates the highest concentrations downstream of the two study sites. Although Parc mine demonstrates concentrations higher than Cwm Rheidol mine, the levels of PHE concentration are below the concentrations demonstrated at Force Crag circum neutral mine that has received remediation (Jarvis *et al.,* 2015).

The combined loads of Cwm Rheidol adit number 6 and 9, exemplify the highest concentrations from sites identified for concern by the WFD (Table 8.4). This suggests the Zn loads from adit site A are of particular concern due to excessive load demonstrated in comparison to other sites of concern. In addition, Parc mine exemplifies a PHE loads that are high in comparison to other mines based on Zn contamination from low resolution monitoring. 24-hour monitoring has identified an increased load in comparison to low resolution monitoring at Parc mine (Table 8.4), this likely to be a true reflection of PHE load due to the increased monitoring frequency (Worrall *et al.,* 2013). 24-hour monitoring of Parc mine exemplifying an increased PHE load (Table 8.4), suggests that estimates from low resolution monitoring of contaminated mine sites, which is generally the method of monitoring for previous studies (Gao and Bradshaw, 1995; Williams, 2014; Marsay, 2018), may be underestimates of the true PHE loads. Comparison to previous study data for adit concentrations showed differing concentrations gained in this study, this could be due to several factors including sampling location and sampling timing. Previous work has showed a variation in PHE concentrations at mine sites between differing seasons (Williams, 2014).

Table 8.2. Remediation effectiveness for Zn sites comparisons. Text in red indicates values obtained during this study.

Site	% Zn removal	Source
Bwlch, UK	98.5	(Perkins *et al.,* 2006; Bird, 2016)
Force Crag	97	(Jarvis *et al.,* 2015)
Wheal Jane	73*	(Whitehead *et al.,* 2005)
Cwm Rheidol	**75.9**	**This Study**
Cwm Rheidol	69	(Williams, 2014)
Cwm Rheidol	99.9	(Rose *et al.,* 2019)

Table 8.3. Site comparisons of PHE concentrations at adit and downstream river water samples, concentration (mg/L), - denotes results that are unattainable. Text in red indicates values obtained during this study.

		Adit water			**River water**			
Site	**Location**	**Zn**	**Pb**	**Cd**	**Zn**	**Pb**	**Cd**	**Source**
Parys mountain	North Wales	126.1	0.706	<0.01	-	-	-	(Marsay, 2018)
Abbey Consols	Western Wales	16.6	1.2	0.045	-	-	-	(Natural Resources Wales, 2016)
Force Crag	Cumbria	-	-	-	2.997	0.0436	0.01424	(Jarvis *et al.*, 2015)
Parc mine 24-hour	**North Wales**	**-**	**-**	**-**	**2.725**	**0.015**	**-**	**This study**
Frongoch	Western Wales	13.9	0.66	0.23	2.4	0.18	0.0006	(Natural Resources Wales, 2016)
Parc Mine	**North Wales**	**3.92**	**0.12**	**0.01**	**2.28**	**0.03**	**0.004**	**This study**
Parc Mine	**North Wales**	**2.17**	**0.27**	**-**	**1.55**	**0.29**	**0.73**	(Gao and Bradshaw, 1995)
Cwmystwyth	Western Wales	-	-	-	0.33	0.048	0.00064	(Natural Resources Wales, 2016)
Cwm Rheidol	**Western Wales**	**72.6**	**0.0216**	**0.101**	**0.17**	**0.002**	**0.004**	**This study**
Cwm Rheidol	Western Wales	92	0.76	0.15	-	-	-	(Williams, 2014)

Table 8.4. Site estimated PHE load comparisons (t/y), sites where data was unavailable are identifiable (-), * = using an anoxic lime-based filter, sites ranked by Zn load. Adapted from (Mayes *et al.,* 2010). Text in red indicates values obtained during this study.

Discharge	Location	Zn	Pb	Cd	Fe
Cwm Rheidol No. 6 and 9 adits (Combined)	**Western Wales**	**37.57**	**0.01**	**0.58**	**40.35**
County Adit	South West	34	0.07	0.06	140.8
Parc mine downstream (Nant Gwydyr) - 24hr	**North Wales**	**22.53**	**0.13**	**-**	**6.39**
Dyffryn Adda adit (joint level)	Western Wales	22.5	0.012	0.05	189
Cwm Rheidol downstream (River Rheidol)	**Western Wales**	**18.2**	**0.21**	**0.31**	**24.51**
Frongoch Stream	Western Wales	14.9	1.8	0.14	-
Cwm Rheidol No. 6 and 9 adits (Post filtration)	**Western Wales**	**14.84**	**0.33**	**0.12**	**14.5**
Parc mine downstream (Nant Gwydyr)	**North Wales**	**14.39**	**0.33**	**0.04**	**4.71**
Parc mine adit	**North Wales**	**13.87**	**0.7**	**0.04**	**7.57**
Frongoch Adit	Western Wales	10.5	11.8	-	-
Nant-y-Mwyn Lower Boat Adit	Western Wales	10	0.09	0.03	-
Pughs Adit	Western Wales	9.2	0.24	0.01	0.4
Milwr Tunnel	Dee	8.6	1.28	0.05	-
Meerbrook Sough	Humber	8.4	0.4	0.05	-
Caplecleugh	Northumbria	6.2	0.04	0.007	0.3
Kingside adit	Western Wales	5.2	0.4	0.02	-
Rispey Breakout	Northumbria	4.5	-	0.004	8.8
Bridford mine adit	South West	4.4	0.32	0.006	3
Wheal Maid Tailings Dam	South West	4.4	0.002	0.008	4.7
Dolcoath Adit	South West	4.3	0.009	0.009	37.9
Yatestoop Sough	Humber	3.9	0.11	0.04	-
Nent Force Level	Northumbria	2.6	0.02	0.006	0.11
Barney Craig	Northumbria	2.5	0.002	0.003	-
Gills Lower adit	Western Wales	2.5	0.21	0.006	-

8.5 Parameters for Suitable remediation

PHE remediation is a necessity to improve contaminated water quality and gain a good ecological status. Assuring that the correct remediation process is identified is necessary to ensure adequate removal of PHE to ensure improved water quality. Treatment of AMD such as cwm Rheidol mine drainage requires a treatment system that will raise the pH, lower PHE concentrations and salinity (Taylor, Pape and Murphy, 2005).

8.5.1 Cwm Rheidol

The data presented in Table 8.5 suggests that an active treatment system is required for Cwm Rheidol adit site A, it is suggested that acidity loads >150 kg/d are suited to active treatment systems (Taylor, Pape and Murphy, 2005). The limestone reaction bed at Cwm Rheidol has proven to remove PHEs but does not reach the maximum efficiency a remediation system can reach (Table 8.2). Due to set up and running costs of active treatment set up, a biological sulphate reducing remediation system would be recommend for site A due to the potential to subsidise costs by commercial recovery of PHEs (Taylor, Pape and Murphy, 2005). It may be possible to utilise the filter bed in place at cwm Rheidol with additional remediation at lower cost due to the improvement of water quality from the current filter bed, which has been identified as currently removing 75.9% of Zn. To remediate waters currently outflowing the filter bed at site B at Cwm Rheidol, a passive system is possible to be emplaced due to a mean load of $CaCO^3$ at site B is < 150 kg/d. An addition of a slag leach bed would raise the pH of the water draining site B >10 and in the process reduce PHEs by precipitation, due to insolubility at high pH (Jickells, 1997; Taylor, Pape and Murphy, 2005).

Estimation by Williams (2014) found that a 5000m^2 area would be required to produce a similar system to the current trail at Cwm Rheidol to fully remediate its mine waters, with the effectiveness remaining similar to previous research (Table 8.2), the estimation of the filter bed size required is still relevant. In light of this the recent trail of the sono-electrolysis system that proved more effective and would use less land area, with the potential of commercial recovery of PHEs seems to be a more viable option for future remediation at Cwm Rheidol (Rose *et al.,* 2019).

8.5.2 Parc mine

Parc mine is a site that demonstrates circum neutral drainage (Table 8.5). PHEs at sites of circum neutral drainage have been difficult to remediate (Nuttall and Younger, 2000b; Mayes *et al.,* 2009; Warrender, *et al.,* 2011; Jones *et al.,* 2013). Various methods have been proposed to remediate circum neutral waters including biofilms (Jones *et al.,* 2013; Jones *et al.,* 2015) and use of limestone beds as a way to marginally increase pH and enhance precipitation (Nuttall and Younger, 2000b).

Installation of a vertical flow pond remediation system has been emplaced at Force Crag mine, Northwest England. The system utilises bacterial sulphate reduction in a compost media (Jarvis *et al.,* 2015). The system has proven to be successful with removal rates of up to 99% achieved for Zn (Bailey, Gandy and Jarvis, 2016). The system has potential to reduce costs of remediation by recycling of sludge for commercial

gains. It is predicted recycling of waste could save ~£0.5m (Bailey, Gandy and Jarvis, 2016). Although remediation has taken place on Force Crag mine PHE concentrations still exceed those experienced at Parc mine (Table 8.3). This suggests that the expense of the system from set up ~£1.5M may not be considered a viable option considering the PHE concentrations are already lower at Parc than Force Crag mine. In light of this emplacement of a similar system at Parc mine could potentially eliminate PHE contamination, which would enable the area of Parc mine to gain a good ecological status as defined by the WFD (The Water Framework Directive, 2015). Previous research has looked at suitable reactive media for VFP systems and have found Fly-ash to be a suitable reactive media, removing Zn in 2 minutes from waters that demonstrate circum neutral drainage (Warrender and Pearce, 2007; Warrender 2009). The required remediation at Parc mine could be resolved by a VFP, with biological sulphate reduction with the use of Fly ash as a reactive media.

Table 8.5. Summary of key parameters for remediation.

	mean $CaCO^3$ mg/L	**mean $CaCO^3$ kg/d**	**mean Discharge L/s**	**pH range**
Parc adit site B (LR)	96.69	1041.17	124.63	6.43-7.77
Parc site C (LR)	76.98	751.36	112.97	6.44-7.86
Parc downstream site D (LR)	94.40	1955.95	239.81	6.58-7.88
Parc downstream site D (HR)	112.67	2557.17	262.69	8-8.2
Cwm Rheidol adit site A (LR)	216.57	367.15	19.62	2.89-3.21
Cwm Rheidol site B (LR)	91.62	121.93	15.40	3.34-3.97
Cwm Rheidol downstream site D (LR)	11.02	3925.73	4122.93	5.31-6.52

Chapter 9 – Further Discussion

9.1 Extent of contamination

The extent of contamination for Parc and Cwm Rheidol mines is primarily from Zn and Cd. The Conwy and Rheidol catchments are failing standards for good ecological status defined by the WFD due Zn and Cd contamination (The Water Framework Directive, 2015). Cd contamination is linked with the Zn contamination, Cd is a natural impurity that occurs within Zn, it is evident from the studies at Parc and Cwm Rheidol that Zn and Cd are both present (Foulds *et al.,* 2014). Zinc and Cd are naturally found in solute forms, due to their solubility at a range of pH, this has been found at Parc and Cwm Rheidol mines where Zn and Cd have been found primarily in solute forms of Zn_{2+} and Cd_{2+}. Pb and Fe exemplify increased particulate loads, with 93.1% of Pb and 95.1% of Fe at Parc mine >0.45µ and 17.7% of Fe >0.45µ at Cwm Rheidol, this is likely to be due to their relative insolubility, it is likely that they are in particulate form due to oxidation as mine water encounters the atmosphere and it is confirmed by their speciation Pb is present in the form PbSO and Fe is present in the form $Fe(OH)_3$ at Parc mine and $Fe(SO_4)^-_2$, $FeSO_4$ and $PbSO_4$ at Cwm Rheidol mine. Generally particulate loads increased downstream of adit sites. PHE loads and concentrations of solute loads generally decrease downstream, data for Parc and Cwm Rheidol mines exemplifies this, sample sites downstream of the adits at both sites reduce in concentration (Bourg, 1988; Macklin and Klimek, 1992). Due to changes in water chemistry downstream of the mining sites due to localised changes in topography, geology and dilution which aid speciation and coprecipitation depositing PHEs in the channel that are remobilised during periods of peak discharge (Bourg, 1988; Macklin and Klimek, 1992). Although Fe levels are below WFD guidelines at downstream sites, Fe shows the greatest enrichment from control sites at downstream sites for Parc mine with enrichment of 12.87 and at Cwm Rheidol Zn exhibits an enrichment of 1.87 and Fe of 1.43. Zn is the primary concern at downstream sites where it still exceeds WFD guidelines of 0.0129 mg/L and 0.015 mg/L for Parc and Cwm Rheidol respectively with concentrations 2.54 mg/L and 0.21 mg/L.

Of the sites examined in this study Cwm Rheidol adits number 6 and 9 combined Zn load is in excess of all other sites including County Adit, Dyffryn Adda adit, Frongoch Stream and adit, Milwr Tunnel and Kingside adit. Parc mine Adit demonstrated Zn concentrations relatively low in comparison to Cwm Rheidol and Parys mountain adits, in light of this Parc mine Zn load was in excess of sites such as Frongoch Adit and Milwr Tunnel. The study has shown how monitoring resolution can alter how the extent contamination is perceived, sampling at high-resolution encompassing day and night-time PHE concentrations can result in an increased load of PHEs (Moore *et al.,* 1996; Nimick *et al.,* 2007; Kimball *et al.,* 2010). This is demonstrated at Parc mine where mean night Zn concentrations were exhibiting a 0.269 mg/L increase. The study has found that increased monitoring frequency may lead to identification further downstream of concentrations above guidelines that only occur at night, this can aid identification of adequate remediation systems.

The study has found that solute PHEs are primarily controlled by chemical variability at both sites, which is primarily controlled by temperature and local environment. Particulate loads are primarily controlled by changes in flow and discharge, increases in discharge can increase particulate loads, remobilising PHEs deposited in the fluvial system and thus reducing water quality. Dilution plays a key role in the concentrations of solute PHEs, dilution can effectively reduce concentrations of solute loads at sites downstream of mine adits (Sullivan and Drever, 2001). Increases in discharge may increase solute concentrations from adit sites due to seasonal and juvenile acidity (Gzyl and Banks, 2007). Downstream PHE concentrations are resultant of a combination of geogenic and anthropogenic point sources. Dilution at Cwm Rheidol has a significant effect on the mine waters entering the river Rheidol effectively reducing them to levels below guidelines for Pb and Fe and Reducing Zn and Cd levels significantly due to a dilution of 0.004. At Parc mine the opposite occurs, the Nant Gwydyr is contaminated with a greater volume of discharge from the adit than the discharge flowing from the upstream site A with a dilution of 1.76 which has a significant effect raising the PHEs concentrations of the Nant Gwydyr downstream of the adit site B. This has implications explained by load and concentration at the study sites, Parc exemplifies the greatest downstream site PHE concentrations of the studies, explained by the dilution at Parc mine. Cwm Rheidol even though it exhibits the lower PHE concentrations at its downstream site it demonstrates the greater PHE loads at the downstream sites of the study due to its increased discharge compared to Parc mine.

9.2 PHEs load variability and water quality

From the data analysed for this study it can be said that PHEs loads vary temporally primarily due to hydroclimatic controls, increased discharge has the potential reduce solute PHE concentrations and increase particulate loads. Temporal changes in discharge result in changes in PHE concentration and therefore PHE load resulting in a varied water quality. Temperature has the capability affect PHE load changes on a daily basis, indirectly by having an effect on chemical parameters that ultimately control short term temporal changes in loads and water quality.

Spatial variation in PHEs loads is evident. For example, maximum mean unfiltered PHE loads are generally experienced at the adit 102.93, 0.03, 1.58 and 110.54 kg/d for Zn, Pb, Cd and Fe at Cwm Rheidol and 37.99, 1.93, 0.10 and 20.74 kg/d for Zn, Pb, Cd and Fe at Parc mine. PHE loads then generally decrease downstream of the adit to the lowest reach of each study (Site D) 49.86, 0.57, 0.85 and 67.16 kg/d for Zn, Pb, Cd and Fe at Cwm Rheidol and 39.41, 0.90, 0.11 and 12.92 kg/d for Zn, Pb, Cd and Fe at Parc mine, likely due to dilution and precipitation and sorption, incorporating PHEs in alluvial sediments. Temporal changes in discharge result in a varied PHE unfiltered concentration output at the adits at Parc mine from 2.74-8.65, 0.04-0.3, 0.01-0.02 and 0.73-9.27 mg/L for Zn, Pb, Cd and Fe and at Cwm Rheidol mine varied from 30.34-91.39, 0.01-0.05, 0.07-0.13 and 26.32-114.99 mg/L respectively. Increases in PHEs during increased discharge is likely to be due to flushing of mine juvenile acidity. Increased discharge has the potential to remobilize contaminated alluvial sediments. This suggests that generally downstream of mine adits there is an

improvement in water quality, but this can be distorted by increases in discharge remobilizing PHE contaminated sediments reducing downstream water quality in times of increased discharge.

Cd demonstrated relationships for load of a similar nature to Pb and Fe, with increased particulate loads and present in insoluble forms. Previous work by Foulds *et al.* (2014) had found Cd to act in a similar nature to Zn. This highlights that the controls on PHEs, speciation, spatial and temporal variation is of a complex nature encompassing multiple variables, some of which have been monitored during this study but further research to identify more controls affecting PHE variability is required.

The remediation system at Cwm Rheidol demonstrates a temporally varied effectiveness ranging from 72-83, 91-99, 57-81, 70-91 % for Zn, Pb, Cd and Fe respectively. The remediation system shows variation in its effectiveness, partly due to changes in discharge resulting in a temporally varied loads being discharged from remediation system with a maximum load of 201.22, 2.71, 2.72 and 220.24 kg/d and a minimum load 13.70, 0.06, 0.02 and 9.03 kg/d for Zn, Cd, Pb and Fe respectively. Emplacement of the correct remediation system is necessary to ensure, continued effectiveness over long temporal periods ~months-years. To ensure the correct remediation system is emplaced, high-resolution monitoring of PHE concentrations is required to identify increased PHE loads that may not be identified by low resolution monitoring resulting in inadequate remediation systems being used. The use of monitoring systems to produce predicted PHEs based upon hydroclimatic variables is possible to gain high-resolution monitoring of PHEs without the requirement of manual sampling.

9.3 Hydroclimatic effects on PHEs and water quality

The study found temperature affects chemical variability resulting in variability of PHEs concentrations, loads and water quality. Increases in temperature have been found to reduce pH, when pH reduction takes place increases in PHE concentrations occur, this will inevitably reduce water quality, this was found at both sites. Hydroclimatic monitoring identified temperature can result in changes in dissolved oxygen, temperature increases reduce the availability of dissolved oxygen, which can have negative effects for aquatic life (The Water Framework Directive, 2015). The studies demonstrated temperature increases which can increase redox potential which has been found to facilitate increased oxidation rates, leading to increased PHE precipitation, lowering water quality by increasing turbidity and particulate loads of PHEs. Correlation analysis found that temperature affects chemical variability and thus PHE loads, increases in temperature generally increase PHE loads and concentrations. Temperature demonstrates a diurnal variation, altering chemical properties on a daily basis, resulting in diel cycling of PHE concentrations and water quality (Moore *et al.,* 1996; Nimick *et al.,* 2007).

The studies at both sites Parc and Cwm Rheidol mines found stage and discharge demonstrate variability ~days to months due to changes in rainfall and temperature that occur seasonally. Discharge increases can reduce EC values and increase pH, resulting in dilution of PHEs lowering PHE solute concentration. Increases in discharge can also remobilize previously deposited PHEs which would reduce

water quality by increasing PHE concentration and turbidity. Increased discharge has the potential to increase dissolved oxygen levels. Discharge demonstrates variability over longer temporal period than temperature, due to hydroclimatic variability such as rainfall and storms (Macdonald *et al.,* 2010), short term high-resolution monitoring would not identify these trends. Discharge is the primary control on particulate loads.

Increased discharge has the capability to increase or decrease PHE loads dependent upon there speciation. Solute loads generally decrease where increased dilution take place. This evident for Zn in the Cwm Rheidol filter bed that demonstrated a significant ($p < 0.05$) correlation with discharge. Particulate loads from remediation increase during periods of increased discharge that result in an increased flow velocity reducing residence time within the filter reducing its effectiveness and transporting an increased particulate PHE load, this was found to be the case for Fe at Cwm Rheidol, but it did not yield any significant correlation. Increases in discharge reduce the effectiveness of remediation for particulate loads but dilutes solute loads, reducing their concentration. Overall increases in discharge in passive remediation systems reduces their effectiveness and results in a reduced water quality in general but this was not evident at Cwm Rheidol possibly due to dilution effects of the mine water outweighing the reduced effectiveness from the increased discharge.

Changes in mine water chemistry resulting from variation in hydroclimatic controls influence redox and pH that control speciation conditions for PHEs. Ultimately speciation is controlled by pH and redox potential defined by localised changes in environment such as changes in localised geology and topography. Observed speciation of PHEs is resultant of the local environment and temporal variation in hydroclimatic controls on pH and redox potential. Speciation is ultimately controlled by the source of water, at Parc mine a limestone geology generates a circum neutral pH and demonstrates high pH, at Cwm Rheidol the volcanic geology and substantial pyrite deposits that have weathered result in an acidic mine drainage which has led to increased redox potential and decreased pH. Water from mine adits is typical of low pH and high redox at AMD sites such as Cwm Rheidol, circum neutral sites such as Parc are pH buffered but adit waters still exhibit increases in redox potential. Water at circum neutral mines sites demonstrates water that can be categorized as calcium carbonate rich, AMD sites demonstrate water with sulphur rich origin. Hydroclimatic factors are direct controls on fluvial chemistry variability and resultant PHEs loads and thus water quality. Spatial variability of PHE concentrations and loads is primarily a result of local mineralisation distribution and subsequent release and deposition of PHEs by outflows of ground and fluvial waters.

9.4 Limitations

There are several limitations for the study that could have improved the research. A comparative 24-hour study for cwm Rheidol filter bed and upstream and downstream sites would have enabled identification of any diel cycles present within the filter bed or River Rheidol. For hourly PHE monitoring at Parc mine a longer period than 24 hours for hourly monitoring, preferably 3-5 days of monitoring would have confirmed

any diel cycles present. The reason for not carrying out hourly monitoring at Cwm Rheidol or a longer period at Parc mine was due to expense and health and safety carrying out the monitoring on my own. Data below quantification limits is questionable, Pb data with the exception for site B at Cwm Rheidol, is below the quantification limit (LOQ) of 0.04 mg/L. Further research would benefit from improved detection limits for PHE analysis, improving the software to report to more than three significant figures would give more informed concentrations of PHEs. To improve quantifiable limits of PHEs a system of analysis with improved accuracy and precision would be required, such as ICP-MS (Pearce, 1991). Upstream and downstream monitoring at Parc mine on 28.02.19-06.3.19 and Cwm Rheidol 07.02.19-14.0219 used electrodes of differing brands making results less comparable, even though they were fully calibrated with the same buffers. Ensuring electrodes of detection for differing sites is necessary for fully comparable results. The long-term low-resolution study was over a period of 4 months during winter, monitoring over a year would demonstrate a greater variability due to seasonality that was not detected during this study. At Cwm Rheidol monitoring of the adits No. 6 and 9 was of their combined discharge, previous studies had analysed them individually, analysis of the adits separately would have made this study's results comparable with previous studies of adit No.6 and No.9s concentrations.

Chapter 10 - Conclusions and recommendations

10.1 Conclusions

This study has found Zn and Cd to be of greatest concern at both Parc and Cwm Rheidol mine sites. At Parc mine Zn reached a maximum concentration of 8.65 mg/L and a mean load of 14.39 t/y leaving the site. At Parc mine Cd reached a maximum concentration of 0.02 mg/L and a mean load of 0.04 t/y leaving the site. At Cwm Rheidol mine Zn reached a maximum concentration of 91.39 mg/L with a mean load of 18.2 t/y leaving the site. At Cwm Rheidol mine Cd reached a maximum concentration of 0.13 mg/L with a mean load of 0.31 t/y leaving the site. Both sites are failing water quality standards defined by the WFD for Zn and Cd. PHEs above WFD guidelines for a good ecological status have the potential to be detrimental to Aquatic life and habitats (The Water Framework Directive, 2015).

The WFD identified Cwm Rheidol as a site for concern, requiring urgent remediation and identified Parc mine as a site for further research, not requiring urgent remediation (Environment Agency Wales, 2002). This study found that it is Parc mine that demonstrates the maximum concentrations of PHEs at downstream sites. Despite this it is Cwm Rheidol that demonstrates the greatest PHE loads downstream, due to the increased volume of discharge at the downstream site. Although Parc mine demonstrates the maximum downstream concentrations of PHEs they are lower than concentrations of Force Crag mine, Western England that has been subject to a full-scale passive remediation system (Jarvis *et al.,* 2015). This suggests that WFD was correct to identify Parc as not requiring urgent remediation. Cwm Rheidol mine does require urgent remediation of its adits, but downstream concentrations of PHEs are of a lesser concern than Parc mine. Revision of contaminated sites for concern by the WFD is required (The Water Framework Directive, 2015).

Hydroclimatic controls affect the temporal variability of water quality, directly and indirectly by altering PHE concentrations, a key factor for water quality (The Water Framework Directive, 2015). Hydroclimatic factors directly affect water quality variability by controlling chemical parameters that include pH, EC, DO_2, Eh. turbidity and TDS. Chemical properties of fluvial systems govern PHE concentrations and loads that are key to water quality.

The resolution of monitoring PHEs can alter load estimations. Hourly high-resolution monitoring at Parc mine identified increase load of 36.1 % in comparison to low resolution monitoring techniques for Zn. High-resolution, hourly monitoring of PHEs can identify daily periods of increased and reduced PHE concentration. Low resolution monitoring would effectively miss diurnal changes in PHE concentration. Previous studies utilizing low resolution monitoring techniques may have underestimated PHE loads at contaminated sites (Gao and Bradshaw, 1995; Williams, 2014). This study demonstrates techniques to enable

PHE concentration and load calculations based upon regression analysis of remote monitoring of hydroclimatic variability, resulting high resolution monitoring of PHEs, this has implications for remediation, due to identification increased PHE loads. A remediation system must be identified that can manage increased PHE loads at night -time periods, use of this remote monitoring and regression technique would be beneficial for remediation at future sites. Further research to develop this would be highly beneficial.

The Cwm Rheidol filter bed influences water quality, this study found it removes 75.9, 69.3 and 81.5% of Zn, Cd and Fe concentrations respectively. Increases in discharge have the potential to reduce the filters effectiveness in reducing particulate loads but appears to improve the effectiveness at reducing solute loads via dilution. Comparison to the other remediation systems in the UK has shown there is potential for 99% PHE removal at Cwm Rheidol.

Ultimately both sites demonstrate that the loads and concentrations of PHEs vary temporal and spatially and are controlled by a complex series of factors that include chemical and hydroclimatic controls. Chemical and hydroclimatic variables monitored in this study have accounted for up to 80% of the PHE variability demonstrated, further research to identify other variables in PHE spatial and temporal variability would be highly beneficial.

10.2 Recommendations

To gain effective future remediation at Parc mine, a passive vertical flow pond encompassing a fly ash or a bacterial sulphate reduction media system would be most suitable to ensure efficient remediation of up to 99%. Fly ash having potential to remediate PHE concentrations within 2 minutes would be a suitable media to manage periods of increased discharge. For Cwm Rheidol a biological sulphate reducing system would be suitable due to lower running cost than active systems, however a sono-electrochemical system has the potential to remediate 99.5% of PHEs, the running costs of which can be partially subsidised by commercial recovery PHEs from the remediated sludge produced.

The future increased variability of hydroclimatic factors due to climate change is of concern to remediation systems (Anawar, 2013; Foulds *et al.,* 2014; Hosseini *et al.,* 2017). Further research to identify controls not identified in this study would be beneficial to enable more accurate load and concentration predictions. Increased future flooding has the potential to reduce the effectiveness of passive remediation systems, this would reduce water quality in previously remediated remediation systems. Future increased flooding also has the potential to remobilize particulate PHEs thus reducing water quality, by increasing PHE concentration and turbidity.

References

Abraham, J., Dowling, K. and Florentine, S. (2018) 'Assessment of potentially toxic metal contamination in the soils of a legacy mine site in Central Victoria, Australia', *Chemosphere; Chemosphere,* 192, pp. 122-132. doi: 10.1016/j.chemosphere.2017.10.150.

Ackova, D.G. (2018) 'Heavy metals and their general toxicity on plants', *Plant Science Today,* 5(1), pp. 14-18. doi: 10.14719/pst.2018.5.1.355.

Adams, T.D. (1963) 'The Geology of the Dinas Cwm-Rheidol Hydroelectric Tunnel', *Geological Magazine; Geol.Mag.,* 100(4), pp. 371-378. doi: 10.1017/S0016756800056119.

Anawar, H.M. (2013) 'Impact of climate change on acid mine drainage generation and contaminant transport in water ecosystems of semi-arid and arid mining areas', *Physics and chemistry of the earth.,* 58-60, pp. 13-21. doi: doi/10.1016/j.pce.2013.04.002.

Andersen, C.B. (2001) 'The Problem of Sample Contamination in a Fluvial Geochemistry Research Experience for Undergraduates', *Journal of Geoscience Education,* 49(4), pp. 351-357. doi: 10.5408/1089-9995-49.4.351.

Antoniadis, V., Shaheen, S.M., Boersch, J., Frohne, T., Du Laing, G. and Rinklebe, J. (2017) 'Bioavailability and risk assessment of potentially toxic elements in garden edible vegetables and soils around a highly contaminated former mining area in Germany', *Journal of environmental management,* 186, pp. 192-201. doi: 10.1016/j.jenvman.2016.04.036.

Bailey, M.T., Gandy, C.J. and Jarvis, A.P. (2016) *Reducing life-cycle costs of passive mine water treatment by recovery of metals from treatment wastes.* Leipzig. January 2016. Newcastle University, UK: School of Civil Engineering and Geosciences, pp. 1255.

Basu, A. (2008) *Alkalinity (As of CaCO3 to As of HCO3-): Practical guide on unit conversion – Coal Geology and Mining: Consulting Services.* Available at: http://www.coalgeology.com/alkalinity-as-of-caco3-to-as-of-hco3-practical-guide-on-unit-conversion/34/ (Accessed: Jul 23, 2019).

Bearcock, J., Palumbo-Roe, B., Banks, V. and Klinck, B. (2010) *The hydrochemistry of Frongoch Mine, mid Wales* British Geological Survey.

Bednar, A.J., Garbarino, J.R., Ranville, J.F. and Wildeman, T.R. (2005) 'Effects of iron on arsenic speciation and redox chemistry in acid mine water', *Journal of Geochemical Exploration,* 85(2), pp. 55-62. doi: //doi.org/10.1016/j.gexplo.2004.10.001.

Bern, C.R., Walton-Day, K. and Naftz, D. (2019) 'Improved enrichment factor calculations through principal component analysis: Examples from soils near breccia pipe uranium mines, Arizona, USA', *Environmental Pollution; Environmental Pollution,* 248, pp. 90-100. doi: 10.1016/j.envpol.2019.01.122.

Bhat, S.A., Meraj, G., Yaseen, S. and Pandit, A.K. (2014) 'Statistical Assessment of Water Quality Parameters for Pollution Source Identification in Sukhnag Stream: An Inflow Stream of Lake Wular (Ramsar Site), Kashmir Himalaya', *Journal of Ecosystems,* 2014, pp. 1-18. doi: 10.1155/2014/898054.

Bikundia, D.S. and Mohan, D. (2014) 'Major ion chemistry of the ground water at the Khoda Village, Ghaziabad, India', *Sustainability of Water Quality and Ecology,* 3-4, pp. 133-150. doi: 10.1016/j.swaqe.2014.12.001.

Bini, C. and Wahsha, M. (2014) 'Potentially Harmful Elements and Human Health', in Bini, C. and Bech, J. (eds.) *PHEs, Environment and Human Health: Potentially harmful elements in the environment and the impact on human health* Dordrecht: Springer Netherlands, pp. 401-463.

Bird, G. (2016) 'The influence of the scale of mining activity and mine site remediation on the contamination legacy of historical metal mining activity', *Environmental Science and Pollution Research,* 23(23), pp. 23456–23466.

Bird, G., Bell, H. and Perkins, W. (2014) 'Arsenic within the secondary environment resulting from geogenic inputs, Harlech Dome, United Kingdom', *Environmental Earth Sciences,* 72(9), pp. 3521-3530. doi: 10.1007/s12665-014-3261-2.

Bird, G., Macklin, M.G., Brewer, P.A., Zaharia, S., Balteanu, D., Driga, B. and Serban, M. (2009) 'Heavy metals in potable groundwater of mining-affected river catchments, northwestern Romania', *Environmental Geochemistry and Health,* 31(6), pp. 741. doi: 10.1007/s10653-009-9259-0.

Bourg, A.C.M. (1988) 'Metals in Aquatic and Terrestrial Systems: Sorption, Speciation, and Mobilization', in Salomons, W. and Förstner, U. (eds.) *Chemistry and Biology of Solid Waste: Dredged Material and Mine Tailings* Berlin, Heidelberg: Springer Berlin Heidelberg, pp. 3-32.

Boussen, S., Sebei, A., Soubrand-Colin, M., Bril, H., Chaabani, F. and Abdeljaouad, S. (2010) 'Mobilization of lead-zinc rich particles from mine tailings in northern Tunisia by aeolian and run-off processes', *Bulletin de la Societe Geologique de France,* 181(5), pp. 459-471. doi: 10.2113/gssgfbull.181.5.459.

Boyd, C. (2015) *Water quality: An introduction.* 1st edn. New York: Springer Science & business Media.

Brodie, R.S., Baskaran, S., Ransley, T. and Spring, J. (2009) 'Seepage meter: progressing a simple method of directly measuring water flow between surface water and groundwater systems', *Australian Journal of Earth Sciences,* 56(1), pp. 3-11. doi: 10.1080/08120090802541879.

Brooks, B.W., Valenti, T.W., Cook-Lindsay, B.A., Forbes, M.G., Doyle, R.D., Scott, J.T. and Stanley, J.K. (2010) 'Influence of Climate Change on Reservoir Water Quality Assessment and Management Effects of Reduced Inflows on Diel Ph and Site-Specific Contaminant Hazards', *Climate: Global Change and Local Adaptation,* , pp. 491-522. doi: 10.1007/978-94-007-1770-1_26.

Brown, K.P. and Hosseinipour, E.Z. (1991) 'Modeling Speciation, Transport and Transformation of Metals from Mine Wastes', *Ecological Modelling,* 57(1-2), pp. 65-89. doi: 10.1016/0304-3800(91)90055-6.

Burnham, D. (2007) *Volcanoes of the Eastern Sierra Nevada: Geology and natural heritage of the long valley caldera.* Available at: http://www.indiana.edu/~sierra/papers/2007/burnham.html (Accessed: 12/03/19).

Camm, G.S. and Hosking, K.F.G. (1985) 'Stanniferous placer development on an evolving landsurface with special reference to placers near St Austell, Cornwall', 142, pp. 803-813. doi: 10.1144/gsjgs.142.5.0803.

Cao, X., Chen, Y., Wang, X. and Deng, X. (2001) 'Effects of redox potential and pH value on the release of rare earth elements from soil', *Chemosphere,* 44(4), pp. 655-661. doi: //doi.org/10.1016/S0045-6535(00)00492-6.

Carvalho, F.P. (2017) 'Mining industry and sustainable development: time for change', *Food and Energy Security,* 6(2), pp. 61-77. doi: 10.1002/fes3.109.

Charlesworth, S.M., Foster, I.D.L. and Charlesworth, S.M. (1996) 'Heavy metals in the hydrological cycle: Trends and explanation', *Hydrological Processes,* 10(2), pp. 227-261. doi: AID-HYP357>3.0.CO; 2-X.

Chowdhury, R.A., Dibyendu, S. and Rupali, D. (2015) 'Remediation of Acid Mine Drainage-Impacted Water', *Current Pollution Reports,* 1(3), pp. 131-141. doi: 10.1007/s40726-015-0011-3.

Chowdhury, S., Mazumder, M.A.J., Al-Attas, O. and Husain, T. (2016) 'Heavy metals in drinking water: Occurrences, implications, and future needs in developing countries', *The science of the total environment.,* 569, pp. 476-488. doi: doi/10.1016/j.scitotenv.2016.06.166.

Clarke, F.W. (1924) *The data of geochemistry.* Washington, D.C.: U.S. Government Printing Office. Available at: http://pubs.er.usgs.gov/publication/b770 (Accessed: 26/02/19).

Clements, W.H. (1994) 'Benthic Invertebrate Community Responses to Heavy-Metals in the Upper Arkansas River Basin, Colorado', *Journal of the North American Benthological Society,* 13(1), pp. 30-44. doi: 10.2307/1467263.

Cooper, D.C., Rollin, K.E., Colman, T., Davies, J. and Wilson, D. (2000) *Potential for mesothermal gold and VMS deposits in the Lower Palaeozoic Welsh Basin.* British Geological Survey. Available at: http://pubs.bgs.ac.uk/publications.html?pubID=B06261 (Accessed: 10/12/18).

Corella, J.P., Saiz-Lopez, A., Sierra, M.J., Mata, M.P., Millán, R., Morellón, M., Cuevas, C.A., Moreno, A. and Valero-Garcés, B.L. (2018) 'Trace metal enrichment during the Industrial Period recorded across an altitudinal transect in the Southern Central Pyrenees', *Science of the Total Environment,* 645, pp. 761-773. doi: 10.1016/j.scitotenv.2018.07.160.

Davies, A.A., Perkins, W.F. and Bowell, R.J. (2016) 'Geochemical assessment of mine waste cover performance post reclamation at Parc mine, North Wales', *Geochemistry-Exploration Environment Analysis,* 16(2), pp. 127-136. doi: 10.1144/geochem2014-320.

Davies, B. (1987) 'Consequences of environmental contamination by lead mining in Wales', *Hydrobiologia; The International Journal of Aquatic Sciences,* 149(1), pp. 213-220. doi: 10.1007/BF00048662.

Di Bonito, M., Albanese, S., Zuzolo, D., Lima, A., Thiombane, M. and De Vivo, B. (2019) 'Geogenic versus anthropogenic behaviour and geochemical footprint of Al, Na, K and P in the Campania region (Southern Italy) soils through compositional data analysis and enrichment factor', *Geoderma,* 335, pp. 12-26. doi: doi/10.1016/j.geoderma.2018.08.008.

Diederichs, K. and Karplus, P.A. (1997) 'Improved R-factors for diffraction data analysis in macromolecular crystallography', *Nature structural biology,* 4(4), pp. 269-275. doi: 10.1038/nsb0497-269.

Dvorak, D.H., Hedin, R.S., Edenborn, H.M. and McIntire, P.E. (1992) 'Treatment of metal-contaminated water using bacterial sulfate reduction: Results from pilot-scale reactors', *Biotechnology and bioengineering,* 40(5), pp. 609-616. doi: 10.1002/bit.260400508.

Dybowska, A., Farago, M., Valsami-Jones, E. and Thornton, I. (2006) 'Remediation strategies for historical mining and smelting sites', *Science Progress,* 89, pp. 71-138. doi: 10.3184/003685006783238344.

Ediagbonya, T. (2015) 'Identification and Quantification of Heavy Metals, Anions and Coliforms in Water bodies using Enrichment Factors', *Environ Anal Chem,* 2, pp. 146. doi: 10.4172/2380-2391.1000146.

Edwards, P. and Potter, H. (2007) *The Cwm Rheidol metal mines remediation project - phase 1.* Proceedings of the International Mine Water Association Symposium: Water in Mining Environments. May 27-31 2007. Cagliari, Italy: pp. 181.

Elderfield, H., Hepworth, A., Edwards, P.N. and Holliday, L.M. (1979) 'Zinc in the Conwy River and estuary', *Estuarine and Coastal Marine Science,* 9(4), pp. 403-422. doi: //doi.org/10.1016/0302-3524(79)90014-8.

Environment Agency Wales (2002) *Metal Mine Strategy for Wales.* Available at: https://www.naturalresources.wales/media/680181/metal-mines-strategy-for-wales-2.pdf (Accessed: 01/10/2018).

Erickson, M.L., Malenda, H.F. and Berquist, E.C. (2018) 'How or When Samples Are Collected Affects Measured Arsenic Concentration in New Drinking Water Wells', *Groundwater,* 56(6), pp. 921-933. doi: 10.1111/gwat.12643.

Evans, A.M. (1987) *Introduction to ore geology.* United States: Blackwell Scientific Publications, Inc.

Evans, P.R. and Murshudov, G.N. (2013) 'How good are my data and what is the resolution?', *Acta Crystallographica Section D,* 69(7), pp. 1204-1214.

Foulds, S.A., Brewer, P.A., Macklin, M.G., Haresign, W., Betson, R.E. and Rassner, S.M.E. (2014) 'Flood-related contamination in catchments affected by historical metal mining: An unexpected and emerging hazard of climate change', *Science of the Total Environment,* 476-477, pp. 165-180. doi: 10.1016/j.scitotenv.2013.12.079.

Fovet, O., Humbert, G., Dupas, R., Gascuel-Odoux, C., Gruau, G., Jaffrezic, A., Thelusma, G., Faucheux, M., Gilliet, N., Hamon, Y. and Grimaldi, C. (2018) 'Seasonal variability of stream water quality response to storm events captured using high-frequency and multi-parameter data', *Journal of Hydrology,* 559, pp. 282-293. doi: //doi.org/10.1016/j.jhydrol.2018.02.040.

Fuge, R., Laidlaw, I., Perkins, W. and Rogers, K. (1991) 'The influence of acidic mine and spoil drainage on water quality in the mid-Wales area', *Environmental Geochemistry and Health; Official Journal of the Society for Environmental Geochemistry and Health,* 13(2), pp. 70-75. doi: 10.1007/BF01734297.

Galuszka, A. and Migaszewski, Z. (2011) 'Geochemical background - an environmental perspective', *Mineralogia,* 42(1), pp. 7. doi: 10.2478/v10002-011-0002-y.

Gao, Y. and Bradshaw, A.D. (1995) 'The containment of toxic wastes: II. Metal movement in leachate and drainage at Parc lead-zinc mine, North Wales', *Environmental Pollution,* 90(3), pp. 379-382. doi: 10.1016/0269-7491(95)00011-F.

Garells, R.M. and Christ, C.L. (1965) 'Solutions, minerals and equilibria' New York: Harper and Row, pp. 450.

Gleeson, S., Wilkinson, J., Stuart, F.M. and Banks, D.A. (2001) 'The origin and evolution of base metal mineralising brines and hydrothermal fluids, South Cornwall, UK', *Geochimica et Cosmochimica Acta,* 65(13), pp. 2067-2079. doi: 10.1016/S0016-7037(01)00579-8.

Golden software (2018) *What is a piper plot (trilinear diagram)?* Available at: http://support.goldensoftware.com/hc/en-us/articles/115003101648-What-is-a-piper-plot-trilinear-diagram- (Accessed: Apr 2, 2019).

Guan, J., Yan, B., Wang, L., Zhu, H. and Cheng, L. (2016) 'Variation in Total Dissolved Iron Output and Iron Species During Extreme Rainfall Events', *Clean-Soil Air Water,* 44(6), pp. 624-630. doi: 10.1002/clen.201400573.

Gundersen, P. and Steinnes, E. (2001) 'Influence of temporal variations in river discharge, pH, alkalinity and Ca on the speciation and concentration of heavy metals in some mining polluted rivers', *Aquatic Geochemistry,* 7(3), pp. 173-193. doi: 1012927809602.

Gzyl, G. and Banks, D. (2007) 'Verification of the "first flush" phenomenon in mine water from coal mines in the Upper Silesian Coal Basin, Poland', *Journal of contaminant hydrology,* 92(1-2), pp. 66-86. doi: 10.1016/j.jconhyd.2006.12.001.

Haggerty, R., Bottrell, S.H., Cliff, R.A. and Rex, D.C. (1995) 'Constraints on the Age and Genesis of the Llanrwst and Llanfair-Talhaiarn Orefields, North Wales from K-Ar and Rb-Sr Studies', *Geological Magazine,* 132(4), pp. 387-398. doi: 10.1017/S0016756800021452.

Haggerty, R., Cliff, R. and Bottrell, S. (1996) 'Pb-isotope evidence for the timing of episodic mineralization in the Llanrwst and Llanfair-Talhaiarn orefields, North Wales', *Mineralium Deposita; International Journal of Geology, Mineralogy and Geochemistry of Mineral Deposits,* 31(1), pp. 93-97. doi: 10.1007/BF00225399.

Haggerty, R. and Bottrell, S.H. (1997) 'The genesis of the Llanrwst and Llanfair veinfields, North Wales: evidence from fluid inclusions and stable isotopes', *Geological Magazine,* 134(2), pp. 249-260. doi: 10.1017/S0016756897006729.

Hakanson, L. (1980) 'An Ecological Risk Index for Aquatic Pollution-Control - a Sedimentological Approach', *Water research,* 14(8), pp. 975-1001. doi: 10.1016/0043-1354(80)90143-8.

Hartland, A., Fairchild, I.J., Lead, J.R., Borsato, A., Baker, A., Frisia, S. and Baalousha, M. (2012) 'From soil to cave: Transport of trace metals by natural organic matter in karst dripwaters', *Chemical Geology,* 304, pp. 68-82. doi: 10.1016/j.chemgeo.2012.01.032.

He Xuwen, Fang Zengqiang, Wang Yuxiang, Jia Mengyao, Song Junying, Wang Qifan and Hu Maoguan (2015) 'Study on Leaching Characteristics and Bio-availability of Heavy Metals in Soil of the Lead and Zinc Mine', *Proceedings of the 2015 International Conference on Mechatronics, Electronic, Industrial and Control Engineering,* 8, pp. 1597-1600.

Hernández-Mena, L., Murillo-Tovar, M., Ramírez-Muñíz, M., Colunga-Urbina, E., de la Garza-Rodríguez, I. and Saldarriaga-Noreña, H. (2011) 'Enrichment Factor and Profiles of Elemental Composition of PM 2.5 in the City of Guadalajara, Mexico', *Bulletin of Environmental Contamination & Toxicology,* 87(5), pp. 545-550. doi: 10.1007/s00128-011-0369-x.

Hosseini, N., Johnston, J. and Lindenschmidt, K. (2017) 'Impacts of Climate Change on the Water Quality of a Regulated Prairie River', *Water,* 9(3), pp. 199. doi: 10.3390/w9030199.

Hu, X., Lin, B. and Gao, F. (2018) 'Enhanced biotreatment of acid mine drainage in the presence of zero-valent iron and zero-valent copper', *Journal of Water Reuse and Desalination,* 8(4), pp. 447-454. doi: 10.2166/wrd.2018.014.

Hu, Z. and Gao, S. (2008) 'Upper crustal abundances of trace elements: A revision and update', *Chemical Geology,* 253(3), pp. 205-221. doi: //doi.org/10.1016/j.chemgeo.2008.05.010.

Jarsjö, J., Chalov, S., Pietroń, J., Alekseenko, A. and Thorslund, J. (2017) 'Patterns of soil contamination, erosion and river loading of metals in a gold mining region of northern Mongolia', *Regional Environmental Change,* 17(7), pp. 1991-2005. doi: 10.1007/s10113-017-1169-6.

Jarvie, H.P., Oguchi, T. and Neal, C. (2000) 'Pollution regimes and variability in river water quality across the Humber catchment: interrogation and mapping of an extensive and highly heterogeneous spatial dataset', *Science of The Total Environment,* 251-252, pp. 27-43. doi: //doi.org/10.1016/S0048-9697(00)00412-5.

Jarvis, A., Gandy, C., Bailey, M., Davis, J., Orme, P., Malley, J., Potter, H. and Moorhouse, A. (2015) *Metal Removal and Secondary Contamination in a Passive Metal Mine Drainage Treatment System.* April 21-24. Santiago, Chile: Gecamin, pp. 1.

Jickells, T. (1997) 'Atmospheric inputs of some chemical species to the North Sea', *Deutsche Hydrografische Zeitschrift,* 49(2), pp. 111-118. doi: 10.1007/BF02764027.

Johnston, D. (2002) *A metal mines strategy for Wales.* Available at: https://www.imwa.info/docs/imwa_2004/IMWA2004_03_Johnston.pdf (Accessed: 01/10/2018).

Johnston, D., Potter, H., Jones, C., Rolley, S., Watson, I. and Pritchard, J. (2008) *Abandoned mines and the water environment.* Bristol: Environment Agency. Available at: https://assets.publishing.service.gov.uk/government/uploads/system/uploads/attachment_data/file/291482/LIT_8879_df7d5c.pdf (Accessed: 01/10/2018).

Jones, A., Rogerson, M., Greenway, G. and Mayes, W.M. (2015) 'Zinc Uptake from Circumneutral Mine Drainage in Freshwater Biofilms: New Insights from In Vitro Experiments', *Mine Water and the Environment,* 34(3), pp. 295-307. doi: 10.1007/s10230-015-0325-9.

Jones, A., Rogerson, M., Greenway, G. and Mayes, W.M. (2013) *Controls on zinc uptake from circum-neutral mine drainage in freshwater biofilms.* Golden County, USA. 2013. pp. 383.

Karuppannan, S. and Kawo, N.S. (2018) 'Groundwater quality assessment using water quality index and GIS technique in Modjo River Basin, central Ethiopia', *Journal of African earth sciences.,* 147, pp. 300-311. doi: doi/10.1016/j.jafrearsci.2018.06.034.

Kim, Y.T., Yoon, H., Yoon, C. and Woo, N.C. (2007) 'An assessment of sampling, preservation, and analytical procedures for arsenic speciation in potentially contaminated waters', *Environmental Geochemistry and Health,* 29(4), pp. 337-346. doi: 10.1007/s10653-007-9091-3.

Kimball, B.A., Runkel, R.L. and Walton-Day, K. (2007a) 'Principal locations of metal loading from flood-plain tailings, lower Silver Creek, Utah, April 2004', U.S. Geological Survey Scientific Investigations Report 2007–5248, pp. 33.

Kimball, B.A., Runkel, R.L. and Walton-Day, K. (2010) 'An approach to quantify sources, seasonal change, and biogeochemical processes affecting metal loading in streams: Facilitating decisions for remediation of mine drainage', *Applied Geochemistry,* 25(5), pp. 728-740. doi: 10.1016/j.apgeochem.2010.02.005.

Kimball, B., A., Runkel, R., L and Walton-Day, K. (2007b) 'Quantification of Metal Loading by Tracer Injection and Synoptic Sampling, 1996–2000', *U.S. Geological Survey Professional Paper,* (1651), pp. 417-495.

Lane, S.N., Tarras-Wahlberg, N. and Lane, S.N. (2003) 'Suspended sediment yield and metal contamination in a river catchment affected by El Niño events and gold mining activities: the Puyango river basin, southern Ecuador', *Hydrological Processes,* 17(15), pp. 3101-3123. doi: doi/10.1002/hyp.1297.

Law, J. (2018) *Water Framework Directive*, 9th edn Oxford University Press.

Lawler, D.M., Petts, G.E., Foster, I.D.L. and Harper, S. (2006) 'Turbidity dynamics during spring storm events in an urban headwater river system: The Upper Tame, West Midlands, UK', *Science of the Total Environment,* 360(1), pp. 109-126. doi: 10.1016/j.scitotenv.2005.08.032.

Leduc, L. (1994) 'The chemolithotrophic bacterium Thiobacillus ferrooxidans', *FEMS microbiology reviews.,* 14(2), pp. 103-119.

Lee, G., Bigham, J.M. and Faure, G. (2002) 'Removal of trace metals by coprecipitation with Fe, Al and Mn from natural waters contaminated with acid mine drainage in the Ducktown Mining District, Tennessee', *Applied Geochemistry,* 17(5), pp. 569-581. doi: //doi.org/10.1016/S0883-2927(01)00125-1.

Likuku, S., Mmolawa, K. and Gaboutloeloe, G. (2013) 'Assessment of heavy metal enrichment and degree of contamination around the copper-nickel mine in the Selebi Phikwe Region, Eastern Botswana', *Environ Ecol Res,* 1, pp. 32-40.

Lim, M., Han, G., Ahn, J., You, K. and Kim, H. (2009) 'Leachability of Arsenic and Heavy Metals from Mine Tailings of Abandoned Metal Mines', *International Journal of Environmental Research and Public Health,* 6(11), pp. 2865-2879. doi: 10.3390/ijerph6112865.

Lin, J.G., Chen, S.Y. and Su, C.R. (2003) 'Assessment of sediment toxicity by metal speciation in different particle-size fractions of river sediment', *Water science and technology: a journal of the International Association on Water Pollution Research.,* 47(7-8), pp. 233-241.

Lin, J., Zhang, S., Liu, D., Yu, Z., Zhang, L., Cui, J., Xie, K., Li, T. and Fu, C. (2018) 'Mobility and potential risk of sediment-associated heavy metal fractions under continuous drought-rewetting cycles', *Science of the Total Environment,* 625, pp. 79-86. doi: 10.1016/j.scitotenv.2017.12.167.

Littlewood, I.G. (1995) 'Hydrological regimes, sampling strategies, and assessment of errors in mass load estimates for United Kingdom rivers', *Environment International,* 21(2), pp. 211-220. doi: //doi.org/10.1016/0160-4120(95)00011-9.

LKM Recycling (2019) Scrap Metal Prices UK - Current Scrap Metal Prices. Available at: https://www.lkm.org.uk/scrap-metal-prices-uk/ (Accessed: Nov 3, 2019).

Macdonald, N., Phillips, I.D. and Mayle, G. (2010) 'Spatial and temporal variability of flood seasonality in Wales', *Hydrological Processes,* 24(13), pp. 1806-1820. doi: 10.1002/hyp.7618.

Macklin, M.G. and Klimek, K. (1992) 'Dispersal, Storage and Transformation of Metal-Contaminated Alluvium in the Upper Vistula Basin, Southwest Poland', *Applied Geography,* 12(1), pp. 7-30. doi: 10.1016/0143-6228(92)90023-G.

Macklin, M.G. and Lewin, J. (1989) 'Sediment Transfer and Transformation of an Alluvial Valley Floor - the River South Tyne, Northumbria, Uk', *Earth Surface Processes and Landforms,* 14(3), pp. 233-246. doi: 10.1002/esp.3290140305.

Macklin, M.G., Ridgway, J., Passmore, D.G. and Rumsby, B.T. (1994) 'The use of overbank sediment for geochemical mapping and contamination assessment: results from selected English and Welsh floodplains', *Applied Geochemistry,* 9(6), pp. 689-700. doi: //doi.org/10.1016/0883-2927(94)90028-0.

Macpherson, G.L. and Towsend, M.A. (1998) *Water Chemistry and sustainable yield.* Kansas: Kansas Geological Survey. Available at: http://www.kgs.ku.edu/Publications/Bulletins/239/Macpherson/gifs/5_macpherson.pdf (Accessed: 21/01/2019).

Madej, M.A. (2005) 'The role of organic matter in sediment budgets in forested terrain', *Sediment Budgets 2,* 292, pp. 9-15.

Majumdar, D. (2003) 'The Blue Baby Syndrome', *Resonance,* 8(10), pp. 20-30. doi: 10.1007/BF02840703.

Marinho Reis, A.P., Cave, M., Sousa, A.J., Wragg, J., Rangel, M.J., Oliveira, A.R., Patinha, C., Rocha, F., Orsiere, T. and Noack, Y. (2018) 'Lead and zinc concentrations in household dust and toenails of the residents (Estarreja, Portugal): a source-pathway-fate model', *Environmental Science: Processes & Impacts,* 20(9), pp. 1210-1225. doi: 10.1039/c8em00211h.

Marsay, N. (2018) 'Is the Remediation at Parys Mountain Successfully Reducing Acid Mine Drainage?', *Journal of environmental protection,* 9, pp. 540-553. doi: 10.4236/jep.2018.95034.

Martin, R., Dowling, K., Pearce, D., Florentine, S., Bennett, J. and Stopic, A. (2016) 'Size-dependent characterisation of historical gold mine wastes to examine human pathways of exposure to arsenic and other potentially toxic elements', *Environmental Geochemistry and Health; Official Journal of the Society for Environmental Geochemistry and Health,* 38(5), pp. 1097-1114. doi: 10.1007/s10653-015-9775-z.

Mativenga, P.T., Marnewick, A., Mhlongo, S., Mativenga, P.T. and Marnewick, A. (2018) 'Water quality in a mining and water-stressed region', *Journal of cleaner production.,* 171, pp. 446-456. doi: doi/10.1016/j.jclepro.2017.10.030.

Matschullat, J., Ottenstein, R. and Reimann, C. (2000) 'Geochemical background - can we calculate it?', *Environmental Geology,* 39(9), pp. 990-1000. doi: 10.1007/s002549900084.

Mayes, W.M., Potter, H.A.B. and Jarvis, A.P. (2010) 'Inventory of aquatic contaminant flux arising from historical metal mining in England and Wales', *Science of The Total Environment,* 408(17), pp. 3576-3583. doi: //doi.org/10.1016/j.scitotenv.2010.04.021.

Mayes, W.M., Potter, H.A.B. and Jarvis, A.P. (2009) 'Novel approach to zinc removal from circum-neutral mine waters using pelletised recovered hydrous ferric oxide', *Journal of hazardous materials,* 162(1), pp. 512-520. doi: 10.1016/j.jhazmat.2008.05.078.

Michalski, R. (2018) 'Ion Chromatography Applications in Wastewater Analysis', 5, pp. 16. doi: 10.3390/separations5010016.

Milton, A., Johnson, M.S. and Cook, J.A. (2002) 'Lead within ecosystems on metalliferous mine tailings in Wales and Ireland', *The Science of the total environment,* 299(1-3), pp. 177. doi: 10.1016/S0048-9697(02)00253-X.

Moncur, M.C., Ptacek, C.J., Hayashi, M., Blowes, D.W. and Birks, S.J. (2014) 'Seasonal cycling and mass-loading of dissolved metals and sulfate discharging from an abandoned mine site in northern Canada', *Applied Geochemistry,* 41, pp. 176-188. doi: 10.1016/j.apgeochem.2013.12.007.

Moore, J.N., Brick, C.M. and Moore, J.N. (1996) 'Diel Variation of Trace Metals in the Upper Clark Fork River, Montana', *Environmental science & technology.,* 30(6), pp. 1953-1960. doi: doi/10.1021/es9506465.

Morgan, S.A., Matthews, Z.N., Morgan, P.G. and Stanley, P. (2017) 'Removal of Iron from Dyffryn Adda, Parys Mountain, N. Wales, UK using Sono-electrochemistry (Electrolysis with assisted Power Ultrasound)', *Minewater and circular Economy,* 2, pp. 1228-1236.

Muhammad, S.N., Kusin, F.M. and Madzin, Z. (2018) 'Coupled physicochemical and bacterial reduction mechanisms for passive remediation of sulfate- and metal-rich acid mine drainage', *International Journal of Environmental Science and Technology,* 15(11), pp. 2325-2336. doi: 10.1007/s13762-017-1594-6.

Nagorski, S.A., Moore, J.N., McKinnon, T.E. and Smith, D.B. (2003) 'Scale-dependent temporal variations in stream water geochemistry', *Environmental science & technology,* 37(5), pp. 859-864. doi: 10.1021/es025983+.

Nancucheo, I., Bitencourt, J.A.P., Sahoo, P.K., Alves, J.O., Siqueira, J.O. and Oliveira, G. (2017) 'Recent Developments for Remediating Acidic Mine Waters Using Sulfidogenic Bacteria', *BioMed Research International,* 2017. doi: 10.1155/2017/7256582.

Natural Resources Wales (2016) *Addressing the impacts from abandoned Metal Mines*.

Natural Resources Wales (2013) *Metal Mines Strategy for Wales*.

Neal, C., Sleep, D., Vincent, C., Scholefield, P. and Rowland, P. (2011) 'Chemical Quality Status of Rivers for the Water Framework Directive: A Case Study of Toxic Metals in North West England', *Water.,* 3(2), pp. 649-666. doi: doi/10.3390/w3020650.

Nimick, D.A., Gammons, C.H., Wanty, R.B., Chapin, T.P., Nimick, D.A., Gammons, C.H. and Wanty, R.B. (2007) 'Diel Cycling of Zinc in a Stream Impacted by Acid Rock Drainage: Initial Results from a New in situ Zn Analyzer', *Environmental monitoring and assessment,* 133(1-3), pp. 161-167. doi: doi/10.1007/s10661-006-9569-y.

Nriagu, J.O. (1988) 'A silent epidemic of environmental metal poisoning?', *Environmental Pollution,* 50(1), pp. 139-161. doi: //doi.org/10.1016/0269-7491(88)90189-3.

Nriagu, J.O. (1979) 'Global inventory of natural and anthropogenic emissions of trace metals to the atmosphere', *Nature,* 279, pp. 409.

Nriagu, J.O. (1996) 'A history of global metal pollution', *Science,* 272(5259), pp. 223-224. doi: 10.1126/science.272.5259.223.

Nuttall, C.A. and Younger, P.L. (2000a) 'Zinc removal from hard, circum-neutral mine waters using a novel closed-bed limestone reactor', *Water research,* 34(4), pp. 1262-1268. doi: 10.1016/S0043-1354(99)00252-3.

Nuttall, C.A. and Younger, P.L. (2000b) 'Zinc removal from hard, circum-neutral mine waters using a novel closed-bed limestone reactor', *Water Research,* 34(4), pp. 1262-1268. doi: //doi.org/10.1016/S0043-1354(99)00252-3.

Palmer, J.P. (2006) *Dealing with Water Issues in Abandoned Metalliferous Mine Reclamation in the United Kingdom.* Brisbane. November 14-16. pp. 1.

Palumbo-Roe, B. and Colman, T. (2010) *The nature of waste associated with closed mines in England and Wales* British Geological Survey.

Pande, K., Sarin, M.M., Trivedi, J.R., Krishnaswami, S. and Sharma, K.K. (1994) *The Indus river system (India-Pakistan): Major-ion chemistry, uranium and strontium isotopes*.

Pearce, F.M. (1991) 'The use of ICP-MS for the analysis of natural waters and an evaluation of sampling techniques', *Environmental Geochemistry and Health,* 13(2), pp. 50-55. doi: 10.1007/BF01734294.

Perkins, W., Hartley, S., Pearce, N., Dinelli, E., Edyvean, R. and Sandlands, L. (2006) 'Bioadsorption in remediation of metal mine drainage: The use of dealginated seaweed in the BIOMAN project', *Geochimica Et Cosmochimica Acta - Geochim cosmochim acta,* 70. doi: 10.1016/j.gca.2006.06.1427.

Pettersson, C., Håkansson, K., Karlsson, S. and Allard, B. (1993) 'Metal speciation in a humic surface water system polluted by acidic leachates from a mine deposit in Sweden', *Water research,* 27(5), pp. 863-871. doi: doi/10.1016/0043-1354(93)90151-7.

Pettine, M., Camusso, M., Martinotti, W., Marchetti, R., Passino, R. and Queirazza, G. (1994) 'Soluble and particulate metals in the Po River: Factors affecting concentrations and partitioning', *Science of The Total Environment,* 145(3), pp. 243-265. doi: //doi.org/10.1016/0048-9697(94)90118-X.

Pizarro, J., Vergara, P.M., Rodriguez, J.A. and Valenzuela, A.M. (2010) 'Heavy metals in northern Chilean rivers: Spatial variation and temporal trends', *Journal of hazardous materials,* 181(1-3), pp. 747-754. doi: 10.1016/j.jhazmat.2010.05.076.

Portier, K.M. (2001) 'Statistical issues in assessing anthropogenic background for arsenic', *Environmental Forensics,* 2(2), pp. 155-160. doi: 10.1006/enfo.2001.0051.

Potter, H.A.B., Jarvis, A.P., Mayes, W.M., Potter, H.A.B. and Jarvis, A.P. (2013) 'Riverine Flux of Metals from Historically Mined Orefields in England and Wales', *Water, air, and soil pollution.,* 224(2). doi: doi/10.1007/s11270-012-1425-9.

Pozo-Antonio, S., Puente-Luna, I., Lagüela-López, S. and Veiga-Ríos, M. (2014) 'Techniques to correct and prevent acid mine drainage: A review', *DYNA,* 81(186), pp. 73-80. doi: 10.15446/dyna.v81n186.38436.

Ptacek, C.J., Hayashi, M., Blowes, D.W., Birks, S.J., Moncur, M.C., Ptacek, C.J., Blowes, D.W. and Birks, S.J. (2014) 'Seasonal cycling and mass-loading of dissolved metals and sulfate discharging from an abandoned mine site in northern Canada', *Applied geochemistry journal of the International Association of Geochemistry and Cosmochemistry.,* 41, pp. 176-188. doi: doi/10.1016/j.apgeochem.2013.12.007.

Rao, S.M. and Mamatha, P. (2004) 'Water quality in sustainable water management', *Current science,* 87(7), pp. 942-947.

Reimann, C., Ayras, M., Chekushin, V., Bogatyrev, I., Boyd, R., Caritat, P., Dutter, R., Finne, T.E., Halleraker, J.H., Jaeger, O., Kashulina, G., Lehto, O., Niskavaara, H., Pavlov, V.K., Raisanen, M.L., Strand, T. and Volden, T. (1998) *Geochemical analysis of soil in the central Barents Region.* Trondheim: Pangaea.

Reimann, C. and de Caritat, P. (2005) 'Distinguishing between natural and anthropogenic sources for elements in the environment: regional geochemical surveys versus enrichment factors', *Science of the Total Environment,* 337(1), pp. 91-107. doi: 10.1016/j.scitotenv.2004.06.011.

Reimann, C. and de Caritat, P. (2000) 'Intrinsic Flaws of Element Enrichment Factors (EFs) in Environmental Geochemistry', *Environmental science & technology.,* 34(24), pp. 5084-5091. doi: doi/10.1021/es001339o.

Reimann, C. and Garrett, R.G. (2005) 'Geochemical background—concept and reality', *The science of the total environment.,* 350(1-3), pp. 12-27. doi: doi/10.1016/j.scitotenv.2005.01.047.

Rico, M., Benito, G., Salgueiro, A.R., Díez-Herrero, A. and Pereira, H.G. (2008) 'Reported tailings dam failures: A review of the European incidents in the worldwide context', *Journal of hazardous materials,* 152(2), pp. 846-852. doi: 10.1016/j.jhazmat.2007.07.050.

Rivera, M.B., Giráldez, M.I. and Fernández-Caliani, J.C. (2016) 'Assessing the environmental availability of heavy metals in geogenically contaminated soils of the Sierra de Aracena Natural Park (SW Spain). Is there a health risk?', *Science of the Total Environment,* 560-561, pp. 254-265. doi: 10.1016/j.scitotenv.2016.04.029.

Rose, S.A., Matthews, Z.N., Morgan, G., Bullen, C. and Stanley, P. (2019) *Sono-electrochemistry (Electrolysis with assisted Power Ultrasound) Treatment Trials of discharges from Cwm Rheidol – Ystumtuen mines, Ceredigion, Mid Wales, UK.* Prem. July 2019. Russia: Perm Federal Research Centre of the Ural Branch of RAS, pp. 750.

Rudall, S. and Jarvis, A.P. (2012) 'Diurnal fluctuation of zinc concentration in metal polluted rivers and its potential impact on water quality and flux estimates', *Water Science and Technology,* 65(1), pp. 164-170. doi: 10.2166/wst.2011.834.

Salgado, P., Melin, V., Cantreras, D., Moreno, Y. and Mansilla, H.D. (2013) 'Fenton reaction driven by iron ligands', *Journal of the Chilean Chemical Society,* 58(4), pp. 2096-2101. doi: 10.4067/S0717-97072013000400043.

Schälchli, U. (1992) 'The clogging of coarse gravel river beds by fine sediment', *Hydrobiologia,* 235(1), pp. 189-197. doi: 10.1007/BF00026211.

Shea, B., Capistrano, C. and Lee, W. (2016) 'Geogenic metal mobility in a coastal inlet impacted by cannery discharge, Magdalena Bay, Baja California Sur, Mexico', *Marine pollution bulletin; Marine pollution bulletin,* 109(1), pp. 495-506. doi: 10.1016/j.marpolbul.2016.05.014.

Sheppard, S.M.F. (1977) 'The Cornubian batholith, SW England: D/H and $^{18}O/^{16}O$ studies of kaolinite and other alteration minerals', *Journal of the Geological Society,* 133(6), pp. 573. doi: 10.1144/gsjgs.133.6.0573.

Shooter, D. (1976) 'Aqueous environmental chemistry of metals', *AIChE Journal,* 22(1), pp. 202. doi: 10.1002/aic.690220136.

Shu, J. and Bradshaw, A.D. (1995) 'The containment of toxic wastes: I. Long term metal movement in soils over a covered metalliferous waste heap at Parc lead-zinc mine, North Wales', *Environmental pollution,* 90(3), pp. 371-377. doi: doi/10.1016/0269-7491(95)00010-O.

Sierra, C., Álvarez Saiz, J. and Gallego, J. (2013) 'Nanofiltration of Acid Mine Drainage in an Abandoned Mercury Mining Area', *Water, Air, & Soil Pollution,* 224(10), pp. 1-12. doi: 10.1007/s11270-013-1734-7.

Simpson, P.R., Breward, N., Flight, D.M.A., Lister, T.R., Cook, J.M., Smith, B. and Hall, G.E.M. (1996) 'High-resolution regional hydrogeochemical baseline mapping of stream water of Wales, the Welsh borders and West Midlands region', *Applied Geochemistry,* 11(5), pp. 621, IN-632, IN1. doi: 10.1016/S0883-2927(96)00001-7.

Singer, M.B., Aalto, R., James, L.A., Kilham, N.E., Higson, J.L. and Ghoshal, S. (2013) 'Enduring legacy of a toxic fan via episodic redistribution of California gold mining debris', *Proceedings of the National Academy of Sciences of the United States of America,* 110(46), pp. 18436. doi: 10.1073/pnas.1302295110.

Skinner, B.J. and Porter, S.C. (2007) *Physical geology.* New York: John Wiley & Sons.

SKM (2011) *Contaminated Land Remedial Works at Henwaith Settlement Ponds, Parys Mountain, Amlwch, Anglesey*.

Spectro (2014) *Analysis of Drinking water by ICP-OES with Axial Plasma Observation.* Germany: SPECTRO Analytical Instruments GmbH. Available at: https://www.spectro.com/landingpages/analysis-of-drinking-water-by-icp-oes-with-axial-plasma-observation (Accessed: 23.07.19).

Srivastava, N.K. and Majumder, C.B. (2008) 'Novel biofiltration methods for the treatment of heavy metals from industrial wastewater', *Journal of hazardous materials,* 151(1), pp. 1-8. doi: 10.1016/j.jhazmat.2007.09.101.

Sullivan, A.B. and Drever, J.I. (2001) 'Spatiotemporal variability in stream chemistry in a high-elevation catchment affected by mine drainage', *Journal of Hydrology,* 252(1-4), pp. 237-250. doi: 10.1016/S0022-1694(01)00458-9.

Taylor, J., Pape, S. and Murphy, N. (2005) *A Summary of Passive and Active Treatment Technologies for Acid and Metalliferous Drainage (AMD).* Fremantle, Western Australia. August 2015.

The Water Framework Directive (2015) *(Standards and Classification) Directions (England and Wales)*.

Tuovinen, H., Pelkonen, M., Lempinen, J., Pohjolainen, E., Read, D., Solatie, D. and Lehto, J. (2018) 'Behaviour of Metals during Bioheap Leaching at the Talvivaara Mine, Finland', *Geosciences,* 8(2), pp. UNSP 66. doi: 10.3390/geosciences8020066.

UK Power (2019) Compare Energy Prices Per kWh | Gas & Electric Per Unit | UKPower. Available at: https://www.ukpower.co.uk/home_energy/tariffs-per-unit-kwh (Accessed: Nov 3, 2019).

Vega, F.A. and Weng, L. (2013) 'Speciation of heavy metals in River Rhine', *Water Research,* 47(1), pp. 363-372. doi: //doi-org.ezproxy.bangor.ac.uk/10.1016/j.watres.2012.10.012.

Vepraskas, M.J. (2002) *Redox Potential Measurements*.

Walsh, C.T., Sandstead, H.H., Prasad, A.S., Newberne, P.M. and Fraker, P.J. (1994) 'Zinc - Health-Effects and Research Priorities for the 1990s', *Environmental health perspectives,* 102, pp. 5-46. doi: 10.2307/3431820.

Wang, K., Yang, P., Hudson-Edwards, K., Lyu, W., Yang, C. and Jing, X. (2018) 'Integration of DSM and SPH to Model Tailings Dam Failure Run-Out Slurry Routing Across 3D Real Terrain', *Water,* 10(8). doi: 10.3390/w10081087.

Wang, Q.R., Kim, D., Dionysiou, D.D., Sorial, G.A. and Timberlake, D. (2004) 'Sources and remediation for mercury contamination in aquatic systems - a literature review', *Environmental Pollution,* 131(2), pp. 323-336. doi: 10.1016/j.envpol.2004.01.010.

Warrender, R., Pearce, N., Perkins, W., Florence, K., Brown, A., Sapsford, D., Bowell, R. and Dey, M. (2011) 'Field Trials of Low-cost Reactive Media for the Passive Treatment of Circum-neutral Metal Mine Drainage in Mid-Wales, UK', *Mine Water and the Environment; Journal of the International Mine Water Association (IMWA),* 30(2), pp. 82-89. doi: 10.1007/s10230-011-0150-8.

Warrender, R. and Pearce, N. (2007) *Remediation of circum-neutral, low-iron waters by permeable reactive media.* Cagliari, Italy. May 2007.

Warrender, R. (2009) *Remediation of circum-neutral metal mine drainage using laboratory-scale permeable reactive barriers*.

Whalley, C., Hursthouse, A., Rowlatt, S., Iqbal-Zahid, P., Vaughan, H. and Durant, R. (1999) 'Chromium speciation in natural waters draining contaminated land, Glasgow, U.K', *Water, air, and soil pollution,* 112(3), pp. 389-405. doi: 1005017506227.

Whitehead, P., Cosby Jr, B. and Prior, H. (2005) 'The Wheal Jane wetlands model for bioremediation of acid mine drainage', *The Science of the total environment,* 338, pp. 125-35. doi: 10.1016/j.scitotenv.2004.09.012.

Williams, T. (2014) *Cwm Rheidol pilot-scale minewater treatment system progress report.* Available at: https://onedrive.live.com/?authkey=%21ADNpttzTzfOeGGY&cid=AFAE6166C10D306D&id=AFAE6166C10D306D%2166465&parId=AFAE6166C10D306D%2166442&o=OneUp (Accessed: 15/10/2018).

World Health Organization (2011) *Guidelines for Drinking-water Quality & nbsp;* Malta: Gutenberg. Available at: http://apps.who.int/iris/bitstream/handle/10665/44584/9789241548151_eng.pdf;jsessionid=31A2EBEE921325A6E59209C6E8AF97BA?sequence=1 (Accessed: 17/01/19).

Worrall, F., Howden, N.J.K. and Burt, T.P. (2013) 'Assessment of sample frequency bias and precision in fluvial flux calculations – An improved low bias estimation method', *Journal of Hydrology,* 503, pp. 101-110. doi: //doi.org/10.1016/j.jhydrol.2013.08.048.

Yi, Y., Yang, Z. and Zhang, S. (2011) 'Ecological risk assessment of heavy metals in sediment and human health risk assessment of heavy metals in fishes in the middle and lower reaches of the Yangtze River basin', *Environmental Pollution,* 159(10), pp. 2575-2585. doi: 10.1016/j.envpol.2011.06.011.

Younger, P.L. (1997) 'The longevity of minewater pollution: A basis for decision-making', *Science of the Total Environment,* 194, pp. 457-466. doi: 10.1016/S0048-9697(96)05383-1.

Younger, P. and Potter, H.A.B. (2012) *Parys in Springtime: Hazard Management and Steps Towards Remediation of the UK's Most Polluted Acidic Mine Discharge.* 9th International Conference on Acid Rock Drainage (ICARD). May 2012. Ottawa, Canada.

Zalasiewicz, J., Williams, M., Steffen, W. and Crutzen, P. (2010) 'The New World of the Anthropocene', *Environmental science & technology,* 44(7), pp. 2228-2231. doi: 10.1021/es903118j.

Zheng, S., Zheng, X. and Chen, C. (2012) 'Leaching Behaviour of Heavy Metals and Transformation of Their Speciation in Polluted Soil Receiving Simulated Acid Rain', *PLOS ONE,* 7(11), pp. e49664. doi: //doi.org/10.1371/journal.pone.0049664.

Zhu, D., Schwab, A.P. and Banks, M.K. (1999) 'Heavy metal leaching from mine tailings as affected by plants', *Journal of environmental quality,* 28(6), pp. 1727-1732. doi: 10.2134/jeq1999.00472425002800060006x.

Appendix A

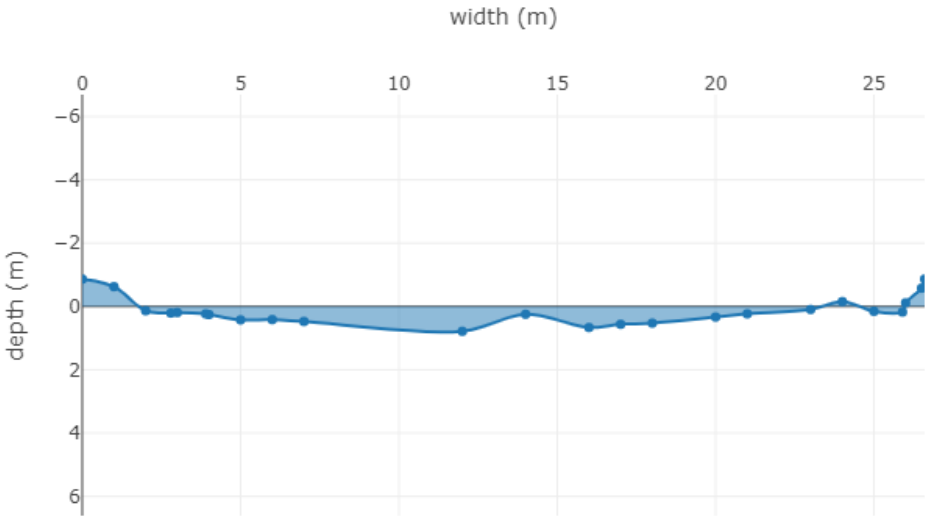

Cross sectional area: 9.48 m²
Wetted perimeter: 22.82 m
Hydraulic radius: 0.42

Appendix A.1.1 Example cross section at Cwm Rheidol 12/12/18 site C, for generalized discharge calculations

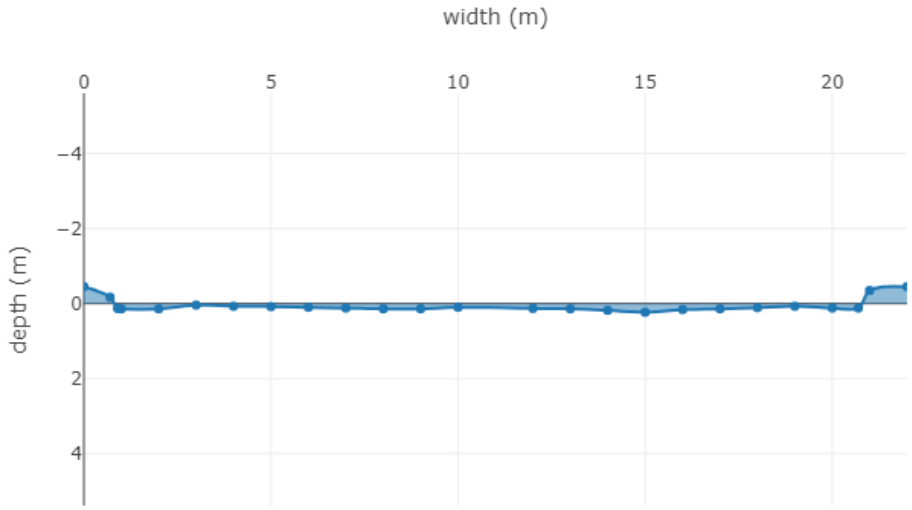

Cross sectional area: 2.43 m²
Wetted perimeter: 19.43 m
Hydraulic radius: 0.13

Appendix A.1.2 Example cross section at Cwm Rheidol 12/12/18 site D, for generalized discharge calculations.

Appendix A.2 Example methods available for anion analysis of waste waters (Michalski, 2018).

Method Number	Method Name	Analytes	Method of Detection
ISO Methods (https://www.iso.org/standards.html, accessed 10 September 2017)			
ISO 10304-2	Water Quality—Determination of Dissolved Anions by Liquid Chromatography of Ions. Part 2: Determination of Bromide, Chloride, Nitrate, Nitrite, Orthophosphate and Sulfate in Waste Waters	Br^-, Cl^-, NO_3^-, NO_2^- PO_4^{3-}, SO_4^{2-}	Conductivity or UV (200–215 nm)
ISO 10304-3	Water Quality—Determination of Dissolved Anions by Liquid Chromatography of Ions Part 3: Determination of Chromate, Iodide, Sulfite, Thiocyanate, and Thiosulfate	CrO_4^{2-}, I^-, SO_3^{2-}, SCN^-, $S_2O_3^{2-}$	Conductivity or UV (λ = 205 nm–220 nm); Amperometry (0.7 V–1.1 V)
ISO 14911	Water Quality—Determination of Dissolved Li^+, Na^+, NH_4^+, K^+, Mn^{2+}, Ca^{2+}, Mg^{2+}, Sr^{2+} and Ba^{2+} Using Ion Chromatography Method	Li^+, Na^+, NH_4^+, K^+, Mn^{2+}, Ca^{2+}, Mg^{2+}, Sr^{2+}, Ba^{2+}	Conductivity
US EPA Methods (https://www.epa.gov/ accessed 5 September 2017)			
300.0	Determination of Inorganic Anions by Ion Chromatography	F^-, Br^-, Cl^-, NO_3^-, NO_2^-, PO_4^{3-}, SO_4^{2-}	Conductivity
200.10	Determination of Trace Elements in Marine Waters by On-Line Chelation Preconcentration and Inductively-Coupled Plasma—Mass Spectrometry	Cd^{2+}, Co^{2+}, Cu^{2+}, Pb^{2+}, Ni^{2+}, VO^{2+}, VO_2^{2+}, UO_2^{2+}	UV-VIS, ICP-MS
200.13	Determination of Trace Elements in Marine Waters by Off-Line Chelation Preconcentration with Graphite Furnace Atomic Absorption	Cd^{2+}, Co^{2+}, Cu^{2+}, Pb^{2+}, Ni^{2+}	UV-VIS, ICP-MS
300.7	Dissolved Sodium, Ammonium, Potassium, Magnesium, and Calcium in Wet Deposition by Chemically Suppressed Ion Chromatography	Na^+, NH_4^+, K^+, Mg^{2+}, Ca^{2+}	Conductivity
ASTM Methods (https://www.astm.org/ accessed 11 September 2017)			
D 4327-97	Standard Test Method for Anions in Water by Suppressed Ion Chromatography	F^-, Br^-, Cl^-, NO_3^-, NO_2^-, PO_4^{3-}, SO_4^{2-}	Conductivity
D19.05.03.23	Standard Test Method for Determination of Inorganic Cations and Ammonia in Water and Waste water by Ion Chromatography	Li^+, Na^+, NH_4^+, K^+, Mg^{2+}, Ca^{2+}	Conductivity
D 6919-03	Standard Test Method for Determination of Dissolved Alkali and Alkaline Earth Cations and Ammonium in Water and Waste water by Ion Chromatography	Li^+, Na^+, NH_4^+, K^+, Mg^{2+}, Ca^{2+}	Conductivity
UOP 959-98	Ammonium Determination in Aqueous Solutions by Ion Chromatography	NH_4^+	Conductivity
NIOSH Methods (https://www.cdc.gov/niosh/docs/2003-154/default.html accessed 15 September 2017)			
7405	Alkali Metals Cations Li^+, Na^+, K^+	Li^+, Na^+, K^+	Conductivity
7605	Chromium Hexavalent by Ion Chromatography	CrO_4^{2-}	UV-VIS (540 nm)

Appendix A.3 Wavelength, LOD and LOQ of elements achieved utilising Spectro Arcos ICP-OES.

Element	Wavelength	LOD mg/l	LOQ mg/l
Ca high	**315.887**	**0.002**	**0.01**
Ca low	**317.933**	**0.002**	**0.01**
Cd high	**228.802**	**0.002**	**0.01**
Cd low	**214.438**	**0.001**	**0.01**
Fe high	**259.941**	**0.01**	**0.03**
Fe low	**238.204**	**0.01**	**0.01**
Mg high	**285.213**	**0.002**	**0.01**
Mg low	**280.27**	**0.002**	**0.01**
Pb high	**220.353**	**0.16**	**0.56**
Pb low	**220.353**	**0.01**	**0.04**
Zn high	**202.613**	**0.004**	**0.01**
Zn low	**213.856**	**0.004**	**0.01**

Appendix A.4.1 Standards for specific pollutants. Adapted from The Water Framework Directive (Standards and Classification) Directions (England and Wales) 2015 (The Water Framework Directive, 2015).

Standards[i] for specific pollutants				
Substance	*Dissolved concentration (µg/l)*			
	Fresh water		*Salt water*	
	Column 1	*Column 2*	*Column 3*	*Column 4*
	Long term (Mean)	*Short term (95 percentile)*	*Long term (Mean)*	*Short term (95 percentile)*
Unionised ammonia (as nitrogen)			21	
Arsenic[ii]	50		25	
Benzyl butyl phthalate[iii]	7.5	51	0.75	10
Carbendazim	0.15	0.7		
Chlorine[iv][v]	2	5		10
Chlorothalonil	0.035	1.2		
Chromium(III)[vi]	4.7	32		
Chromium(VI)[vii]	3.4		0.6	32
Copper [viii], [ix], [x]	1µg/l bioavailable		3.76 µg/l dissolved, where DOC ≤ 1mg/l 3.76 + (2.677 x ((DOC/2) – 0.5)) µg/l dissolved, where DOC > 1mg/l	
Cyanide[xi]	1	5	1	5
Cypermethrin[xii], [xiii]	0.0001	0.0004	0.0001	0.0004
Diazinon[xiv]	0.01	0.02	0.01	0.26
2, 4 Dichlorophenol	4.2	140	0.42	6
2, 4 Dichlorophenoxyacetic acid (2, 4 D[xv]	0.3	1.3	0.3	1.3
3, 4 Dichloroaniline	0.2	5.4	0.2	5.4
Dimethoate[xvi]	0.48	4.0	0.48	4.0
Glyphosate	196	398	196	398
Iron	1000		1000	
Linuron[xvii]	0.5	0.9	0.5	0.9
Manganese[xviii]	123 bioavailable			
Mecoprop[xix]	18	187	18	187
Methiocarb	0.01	0.77		
Pendimethalin	0.3	0.58		
Permethrin	0.001	0.01	0.0002	0.001
Phenol[xx]	7.7	46	7.7	46
Tetrachloroethane	140	1848		
Triclosan	0.1	0.28	0.1	0.28
Toluene	74	380	74	370
Zinc[xxi], [xxii]	10.9 bioavailable plus Ambient Background Concentration (µg/l) dissolved		6.8 dissolved plus Ambient Background Concentration (µg/l)	

Appendix A.4.2 WFD Zn standards for additional ambient background concentrations that combine with the SFSP value for Zn. Adapted from The Water Framework Directive (Standards and Classification) Directions (England and Wales) 2015 (The Water Framework Directive, 2015).

Ambient Background Concentrations[i] for dissolved zinc in freshwaters in England and Wales	
Catchment/Group of catchments[ii]	*ABC (µg/l)*
Tyne	4.8
Tees	4.1
Ouse, Humber	2.9
Nene	4.0
Great Ouse	3.1
River Stour	3.0
Blackwater/Chelmer	3.6
Lee	3.3
Thames	2.0
Test	2.0
Avon/Hants	3.1
Exe	1.4
Dart	1.7
Clywd/Conwy	2.0
Dee	2.9
Eden	1.2
Anglesey	3.0
Tamar	2.9
Fal	5.8
Camel	7.1
Tone/Parrett	3.3
Frome, Bristol Avon	2.3
Wye	2.0
Usk	2.2
Taff	2.8
Neath	2.8
Loughar	3.9
Tywi	2.0
Teifi	2.5
Rheidol/Ystwyth	4.1
Dovey	3.2
Glaslyn	2.6
All other freshwaters not listed above	1.4

Appendix A.4.3 Environmental quality standards (EQS) of priority pollutants. Annual average (AA) and maximum allowance controls (MAC) are expressed. Adapted from The Water Framework Directive (Standards and Classification) Directions (England and Wales) 2015 (The Water Framework Directive, 2015).

Table 1: Environmental quality standards for priority substances and other pollutants used to clarify chemical status

No	*Name of substance*	*CAS number*[1]	*Date*	*AA-EQS*[2] *Inland surface waters* [4] *(µg/l)*	*AA-EQS*[2] *Other surface waters (µg/l)*	*MAC-EQS*[3] *Inland surface waters*[4] *(µg/l)*	*MAC-EQS*[3] *Other surface waters (µg/l)*	*EQS Biota*[5] *(µg/kg)*
				Column 1	Column 2	Column 3	Column 4	Column 5
1	Alachlor	15972-60-8		0.3	0.3	0.7	0.7	
2	Anthracene	120-12-7		0.1	0.1	0.1	0.1	
3	Atrazine	1912-24-9		0.6	0.6	2.0	2.0	
4	Benzene	71-43-2		10	8	50	50	
5	Brominated diphenylethers[6]	32534-81-9				0.14	0.014	0.0085
6	Cadmium and its compounds[7] (depending on water hardness classes)	7440-43-9		≤ 0.08 (Class 1) 0.08 (Class 2) 0.09 (Class 3) 0.15 (Class 4) 0,25 (Class 5)	0.2	≤ 0.45 (Class 1) 0.45 (Class 2) 0.6 (Class 3) 0.9 (Class 4) 1,5 (Class 5)		
6a	Carbon-tetrachloride[8]	56-23-5		12	12	not applicable	not applicable	
7	C10-13 Chloroalkanes[9]	85535-84-8		0.4	0.4	1.4	1.4	
8	Chlorfenvinphos	470-90-6		0.1	0.1	0.3	0.3	
9	Chlorpyrifos (Chlorpyrifosethyl)	2921-88-2		0.03	0.03	0.1	0.1	
9a	Cyclodiene pesticides: Aldrin[8] Dieldrin[8] Endrin[8] Isodrin[8]	309-00-2 60-57-1 72-20-8 465-73-6		Σ = 0.01	Σ = 0.005	not applicable	not applicable	
9b	DDT total[8], [10]	not applicable		0.025	0.025	not applicable	not applicable	
	para-para-DDT[8]	50-29-3		0.01	0.01	not applicable	not applicable	
10	1.2-Dichloroethane	107-06-2		10	10	not applicable	not applicable	
11	Dichloromethane	75-09-2		20	20	not applicable	not applicable	
12	Di(2-ethylhexyl)-phthalate (DEHP)	117-81-7		1.3	1.3	not applicable	not applicable	
13	Diuron	330-54-1		0.2	0.2	1.8	1.8	
14	Endosulfan	115-29-7		0.005	0.0005	0.01	0.004	
15	Fluoranthene	206-44-0		0.0063	0.0063	0.12	0.12	30
16	Hexachloro-benzene	118-74-1				0.05	0.05	10
17	Hexachloro-butadiene	87-68-3				0.6	0.6	55
18	Hexachloro-cyclohexane	608-73-1		0.02	0.002	0.04	0.02	
19	Isoproturon	34123-59-6		0.3	0.3	1.0	1.0	
20	Lead and its compounds	7439-92-1		1.2[11]	1.3	14	14	
21	Mercury and its compounds	7439-97-6				0.07	0.07	20
22	Naphthalene	91-20-3		2	2	130	130	
23	Nickel and its compounds	7440-02-0		4[11]	8.6	34	34	
24	Nonylphenols. (4-Nonylphenol)	84852-15-3		0.3	0.3	2.0	2.0	
25	Octylphenols ((4-(1,1′, 3,3′-tetramethylbutyl) -phenol))	140-66-9		0.1	0.01	not applicable	not applicable	
26	Pentachloro-benzene	608-93-5		0.007	0.0007	not applicable	not applicable	
27	Pentachloro-phenol	87-86-5		0.4	0.4	1	1	
28	Polyaromatic hydrocarbons (PAH)	Not applicable		not applicable	not applicable	not applicable	not applicable	
	Benzo(a)pyrene	50-32-8		1.7×10^{-4}	1.7×10^{-4}	0.27	0.027	5

Appendix A.4.4 WFD guidelines for site class of CD dependent upon $CaCo^3$. Adapted from The Water Framework Directive (Standards and Classification) Directions (England and Wales) 2015 (The Water Framework Directive, 2015).

cd	ug/l													
< 0.45 (Class 1) 0.45 (Class 2) 0.6 (Class 3) 0.9 (Class 4) 1.5 (Class 5)														
(Class 1: < 40 mg CaCO3/l, Class 2: 40 to < 50 mg CaCO3/l, Class 3: 50 to < 100 mg CaCO3/l, Class 4: 100 to < 200 mg CaCO3/l and Class 5: ≥ 200 mg CaCO3/l)														
	site	class	ug	mg		site	class	ug	mg					
Cwm Rheidol	a	5	1.5	0.0015	Parc mine	a	2	0.45	0.00045	0.0009				
	b	4	0.9	0.0009		b	3	0.6	0.0006					
	c	1	0.45	0.00045		c	3	0.6	0.0006					
	d	1	0.45	0.00045		d	3	0.6	0.0006					
Mean	A, B, D	4		Mean	B, C, D	3								

Appendix A.5 Example of The Geochemist workbench® SpecE8 output for Anion and Cation activity values.

Temperature	=	10.0 C
Pressure	=	1.013 bars
Ionic strength	=	0.013172 molal
Charge imbalance	=	-0.004220 eq/kg (-28.12% error)
Activity of water	=	0.999990
Solvent mass	=	1.0000 kg
Solution mass	=	1.0007 kg
Mineral mass	=	0.00000 kg
Solution density	=	1.023 g/cm3
Solution viscosity	=	0.013 poise
Chlorinity	=	0.000271 molal
Dissolved solids	=	700 mg/kg sol'n
Elect. Conductivity	=	790.15 uS/cm (or umho/cm)
Hardness	=	183.72 mg/kg sol'n as CaCO3
Water type	=	Ca-SO4
Bulk volume	=	978. cm3
Fluid volume	=	978. cm3

Mineral volume	=	0.000 cm3
Inert volume	=	0.000 cm3
Porosity	=	100. %
Permeability	=	98.7 cm2

Aqueous species	molality	mg/kg sol'n	act. coef.	Log act.
SO4--	0.003200	307.2	0.6337	-2.6929
HCO3-	0.002947	179.7	0.8944	-2.5790
Ca++	0.0007680	30.76	0.6517	-3.3006
Mg++	0.0006919	16.80	0.6680	-3.3352
Zn++	0.0005069	33.12	0.6517	-3.4810
Fe++	0.0004931	27.52	0.6517	-3.4930
Na+	0.0003867	8.884	0.8928	-3.4619
Cl-	0.0002696	9.550	0.8894	-3.6203
CaSO4	0.0001951	26.54	1.0000	-3.7098
MgSO4	0.0001451	17.45	1.0000	-3.8383
ZnSO4	0.0001161	18.73	1.0000	-3.9351
FeSO4	0.0001021	15.50	1.0000	-3.9910
FeHCO3+	2.813e-05	3.285	0.8928	-4.6000
K+	2.380e-05	0.9301	0.8894	-4.6743
CaHCO3+	2.236e-05	2.259	0.8966	-4.6978
MgHCO3+	1.329e-05	1.133	0.8928	-4.9259
NaSO4-	3.585e-06	0.4265	0.8928	-5.4948
NaHCO3	1.657e-06	0.1391	1.0000	-5.7807
Pb++	1.634e-06	0.3382	0.6384	-5.9818
CaCl+	9.449e-07	0.07132	0.8928	-6.0739
KSO4-	3.289e-07	0.04443	0.8928	-6.5321
MgCl+	2.248e-07	0.01343	0.8928	-6.6974
ZnCl+	1.325e-07	0.01335	0.8928	-6.9270
FeCl+	1.093e-07	0.009976	0.8928	-7.0105
PbCl+	1.101e-08	0.002669	0.8928	-8.0076
NaCl	1.476e-09	8.618e-05	1.0000	-8.8310

KCl	1.045e-10	7.787e-06	1.0000	-9.9808
ZnCl2	4.081e-11	5.557e-06	1.0000	-10.3893
FeCl2	1.242e-11	1.573e-06	1.0000	-10.9060
PbCl2	3.425e-12	9.520e-07	1.0000	-11.4653
ZnCl3-	8.087e-15	1.388e-09	0.8928	-14.1415
PbCl3-	6.801e-16	2.131e-10	0.8928	-15.2166
ZnCl4--	1.096e-18	2.269e-13	0.6337	-18.1584
PbCl4--	1.028e-19	3.587e-14	0.6337	-19.1859

Mineral saturation states

	log Q/K		log Q/K
Anglesite	-0.7127	MgSO4(c)	-11.8571
Gypsum	-1.5291	Bloedite	-13.3813
Anhydrite	-1.8567	Kainite	-14.2914
Bassanite	-2.4898	Antarcticite	-14.5866
CaSO4^1/2H2O(bet	-2.6775	Bischofite	-15.2465
Melanterite	-3.6818	CaCl2^4H2O	-15.5122
Epsomite	-4.1282	MgCl2^4H2O	-18.4291
Hexahydrite	-4.4713	CaCl2^2H2O	-19.0375
Pentahydrite	-4.7930	CaCl2^H2O	-19.2431
Leonhardtite	-5.3830	Lawrencite	-20.5327
Kieserite	-6.3685	Hydrophilite	-23.0857
Kalicinite	-7.0446	Carnallite	-23.2384
Mirabilite	-7.8270	MgCl2^2H2O	-24.3052
Halite	-8.6273	MgCl2^H2O	-27.9095
Sylvite	-9.0804	KMgCl3^2H2O	-33.6929
Thenardite	-9.3725	Chloromagnesite	-34.0325
FeSO4(c)	-9.4657	KMgCl3	-41.5158
Arcanite	-10.0958	Tachyhydrite	-49.8800

Partial Gases	press. (bar)	fugacity	fug. coef.	log fug.

Steam	0.01294	0.01207	0.9326	-1.9183

Original basis	In fluid total moles	Sorbed moles	Sorbed mg/kg	Kd moles	Kd mg/kg
H2O	55.5	55.5		9.99e+05	
Ca++	0.000986	0.000986		39.5	
Cl-	0.000271	0.000271		9.60	
Fe++	0.000623	0.000623		34.8	
HCO3-	0.00301	0.00301		184	
K+	2.41e-05	2.41e-05		0.943	
Mg++	0.000850	0.000850		20.7	
Na+	0.000392	0.000392		9.00	
Pb++	1.64e-06	1.64e-06		0.341	
SO4--	0.00376	0.00376		361	
Zn++	0.000623	0.000623		40.7	

Elemental composition	In fluid total moles	Sorbed moles	Sorbed mg/kg	Kd moles	Kd mg/kg
Calcium	0.0009863	0.0009863		39.50	
Carbon	0.003013	0.003013		36.16	
Chlorine	0.0002710	0.0002710		9.600	
Hydrogen	11.0	111.0		1.118e+05	
Iron	0.0006235	0.0006235		34.79	
Lead	1.645e-06	1.645e-06		0.3405	
Magnesium	0.0008505	0.0008505		20.66	
Oxygen	55.53	55.53		8.879e+05	
Potassium	2.413e-05	2.413e-05		0.9429	
Sodium	0.0003919	0.0003919		9.004	
Sulphur	0.003763	0.003763		120.6	
Zinc	0.0006232	0.0006232		40.71	

Appendix B

Appendix B.1 - List of abbreviations

Water Framework directive – WFD

Metal mines strategy for Wales – MMSW

Natural Resources Wales – NRW

Potentially harmful elements – PHE

Maximum allowance control – MAC

Standard for specific pollutant – SFSP

Copper – Cu

Gold – Au

Silver - Ag

Lead - Pb

Zinc - Zn

Iron - Fe

Cadmium –Cd

F – Filtered (0.45µ)

UF - Unfiltered